

**DESIGN AND SYNTHESIS OF NATURAL PRODUCT ANALOGS
OF STEVIOSIDE AND SYNTHETIC ANALOGS OF RETINOIC
ACID**

A DISSERTATION
SUBMITTED TO THE FACULTY OF THE GRADUATE SCHOOL
OF THE UNIVERSITY OF MINNESOTA
BY

TRINH AMY DOAN HOLTH

IN PARTIAL FULFILLMENT OF THE REQUIREMENTS
FOR THE DEGREE OF
DOCTOR OF PHILOSOPHY

GUNDA I. GEORG

JANUARY 2018

© Trinh A. D. Holth 2018

Acknowledgements

First and foremost, I am grateful to God for giving me the perseverance to chase my ambitions.

Second, I am deeply indebted to Dr. Gunda Georg for allowing me the opportunity to work in her laboratory over the past decade. Her support and mentorship will always be appreciated as well as her encouragement to follow my career paths. I am thankful to her for everything she has taught me during my undergraduate research and graduate education. Thank you, GIG!

I would like to acknowledge my graduate faculty committee: Dr. Rodney Johnson, Dr. Barry Finzel, and Dr. Mark Distefano for their professional support, academic instruction, and guidance. I would also like to thank Dr. Yusuf Abul-Hajj and Dr. Michael Walters for their professional support and friendship during my graduate career.

There are also many former members of the Georg research group that I would like to give a special acknowledgement. Dr. Oliver E. Hutt, Dr. Karen Beckman, Dr. Matthew Leighty, Dr. Christopher Schneider, Dr. Xingxian (Wayne) Gu, Dr. Brandon Turunen, Dr. Jared Spletstoser, Dr. Jack Greiner, and Dr. Micah Niphakis, thank you for your help during my undergraduate research experience at the University of Kansas and encouragement as I made the decision to attend graduate school at the University of Minnesota. I also like to thank Dr. Mary Smart, Dr. Rebecca Cuellar, Mary Crosson, Sara Wajeesh, Dr. Shameem Syeda, Dr. Leigh Allen and other Georg research group members, especially Dr. Narsi Cheryala and Jill Kyzer (Team RAR!), and staff for their support, friendship, and guidance.

To the best fellow graduate student friends who fought the good fight with me: Dr. Susanna Emond, Dr. Aaron Teitelbaum, Dr. Amber Onorato, Dr. Hailey Gahlon, Dr.

Kathryn Peitsch, and Dr. Kathryn Nelson, thank you! Thanks to the other graduate students and researchers for making my graduate school experience a studious, fun, exciting, and worthwhile experience. And a big thank you to the University of Minnesota Department of Medicinal Chemistry for financial support, personal assistance, and encouragement through my graduate career!

Lastly, I would like to thank my outside support team. To my parents, Luan T. Doan and Sau T. Truong, thank you for being my inspiration. To my siblings/great friends (Tim, Tram, Viet, Nam, Chi, Suong, Julia, David, Dani Sue, Valerie, Katie, Traci, Valone, Jan), thank you for your unwavering encouragement! It has truly helped me through this crazy endeavor.

Last but certainly not least, I want to thank my husband, Daniel Holth, for making Minnesota my new home away from home. You are my rock and my favorite person to journey life with!

Dedication

I dedicate this dissertation to my son, David Hieu Holth. May you dream big, work hard to achieve greatness, and be a kind gentleman through it all.

Abstract

Part I

Stevioside is a natural product from the *Stevia rebaudiana* Bertoni plant native to South America. It is one of the major steviol glycosides, with rebaudioside A as the other main natural product, isolated from the *Stevia* plant and comprises 5 – 22% by weight from the dried plant leaves. These natural products are commercially sold as natural sweeteners with reports of being 200 to 300 times sweeter than table sugar. Steviol glycosides are made up of a tetracyclic diterpene, also called *ent*-kaurene, core structure attached to varying sugar chains at the A ring carboxyl group or C-ring hydroxyl group; Stevioside contains three glucose molecules while rebaudioside A contains four glucose molecules. The stevioside diterpene serves as novel template for analog development and exploration because there are numerous directions to diversify the different rings, mainly the A, C and D rings, within the molecule. Stevioside undergoes enzymatic or basic hydrolysis to form the steviol acid, which rearranges to the isosteviol acid under acidic conditions via a Wagner-Meerwein methyl shift of the bridging carbon. These two diterpenes were further explored via a diversity-oriented synthetic approach to yield other diterpene scaffolds from which compound libraries were synthesized in order to explore novel chemical space. Testing of the libraries demonstrate initial activity in several biological assays, thus proving that the *ent*-kaurene core scaffold is a viable starting point to elicit biological activity and for therapeutic development.

Part II

Through the efforts by the National Institutes of Health, research is being conducted to develop non-hormonal reversible male contraceptive agents. Current forms of male contraception include a temporary barrier by means of condoms or permanent surgical sterilization. Their unpopularity and the unmet need for something more tolerable have led to the development of non-hormonal male contraceptive agents targeting the retinoic acid receptor alpha (RAR α) nuclear receptor. Previous research has shown that RAR α disrupts spermatogenesis during mitosis and the administration of RAR agonists to Vitamin A deficient mice, which is similar to RAR α gene knockout mice, reversed infertility effects. Given these promising results, we designed and synthesized retinoids for the development of RAR α antagonists. Four compounds were produced and assayed for activity in RAR α as well as selectivity against RAR beta (RAR β) and RAR gamma (RAR γ).

Table of Contents

Acknowledgements	i
Dedication	iii
Abstract	iv
Table of Contents	vi
List of Tables	x
List of Figures	xi
List of Schemes	xii
List of Charts	xiv
List of Abbreviations	xv

Part I- Stevioside Library Development

Chapter 1. Design and Synthesis of Diterpene Scaffolds from Stevioside	1
A. Background of Stevioside, Steviol, and Isosteviol	1
1. Biosynthesis of <i>ent</i> -Kaurene Diterpene and Stevioside	1
2. Biological Evaluation of Stevioside and Its Metabolites	8
B. Rationale for Developing <i>ent</i> -Kaurene Scaffolds	9
1. Pilot Scale Libraries Initiative	9
2. Natural Products and Steviol-Related Compounds	11
C. Design of Diterpene Scaffolds with Diversity-Oriented Synthesis (DOS)	15
1. Background on DOS and Its Utilities	15
2. Introduction of Scaffolds	16
3. Synthesis of DOS Scaffolds	18

vi

Chapter 2. Exploring the Beckmann Rearrangement Reaction	20
A. Background of the Beckmann Reaction	20
1. Lactam Formation from Beckmann Rearrangement	20
2. Nitrile Formation from Beckmann Fragmentation	25
3. Photo-Beckmann Rearrangement	27
B. Oxime Reactions of Steviol and Isosteviol	29
Chapter 3. Design and Synthesis of Small Molecule Libraries from the Stevioside Diterpene Scaffolds	35
A. Synthesis of Mono-functional Small Molecule Libraries	35
1. Initial Amide Validation Array	36
2. Amide Libraries	38
3. Ether and Amine Libraries	39
B. Synthesis of Bifunctional Small Molecular Libraries	41
1. Rationale for Bifunctional Libraries	41
2. Synthesis of Bifunctional Libraries	42
C. Evaluation of Steviol- and Isosteviol-Derived Libraries	43
1. Biological Activity of Steviol and Isosteviol Library of Analogs	43
2. Computational Comparison with Commercial Libraries	50
D. Concluding Remarks	55
Chapter 4. Experimental Data	56
A. General Methods	56
B. DOS Scaffolds	57
C. Oxime Reaction Compounds	64

D. Mono- and Bi-functional Library Compounds	75
Part II- Retinoic Acid Receptor Alpha Antagonist Development for Male	
Contraception	
Chapter 5. Design and Synthesis of Retinoids for Non-Hormonal Male	
Contraceptive Development	98
A. Contraception Background	98
1. Unintended Pregnancies and Unmet Need for Contraception	98
2. Current Forms of Male Contraception	100
3. Areas of Focus for Non-Hormonal Male Contraceptive Development	102
B. Retinoic Acid Receptor Alpha (RAR α)	103
1. Implications in Male Contraception	105
2. Previous Agonist and Antagonist Development	107
C. Design of Retinoids	110
D. Computational Modeling of Retinoids	114
E. Synthesis of Retinoids	118
1. BMS Triazole Derivatives	118
2. ER Derivatives	122
F. Biological Screening of Retinoids	124
1. Binding Assay	125
2. Luciferase Reporter Activity Assay	128
G. Concluding Remarks	132
Chapter 6. Experimental Data	134

CUMULATIVE REFERENCES	150
APPENDICES	179

List of Tables

Table I-1. Activity of steviol and isosteviol analogs	44
Table II-1. The number of pregnancies and percent distribution in 2008	99
Table II-2. Pharmacology of known RAR α antagonist and pan-antagonist	109
Table II-3. Commercially available retinoids	111
Table II-4. Docking scores for proposed retinoids plus II-5	115

List of Figures

Figure I-1. <i>Stevia rebaudiana</i> Bertoni plant	1
Figure I-2. Stevia sweetening agents	2
Figure I-3. Biosynthesis of steviol glycoside	4
Figure I-4.* All new approved drugs from 1981 until 2014	12
Figure I-5.* Chemical space analysis of compounds from a) combinatorial chemistry b) natural products, and c) drugs	13
Figure I-6. Structures of steviol-related natural products	14
Figure I-7. Amines I-78a-z for library synthesis	38
Figure I-8. Alkyl halide compounds for library synthesis	40
Figure I-9. Other steviol and isosteviol derivatives submitted to the MSLMR	44
Figure II-1.* The process of spermatogenesis	101
Figure II-2. Structures of all- <i>trans</i> retinoic a, 9- <i>cis</i> RA, and vitamin A	104
Figure II-3. Normal spermatogenesis in healthy vs vitamin A deficient mice	106
Figure II-4. BMS compounds	108
Figure II-5. 1dkf protein structure with proposed docked compounds	115
Figure II-6. Binding energies for proposed compounds	117
Figure II-7. ER-50891 (II-52)	122
Figure II-8. ITC data for II-1	126
Figure II-9. ITC data for II-2	127
Figure II-10. Concentration map of the activity plate.	129
Figure II-11. Map of activity plate assay results of BMS retinoids	130
Figure II-12. Antagonistic assay of BMS RAR analogs	131

*reprinted with permission from publisher

List of Schemes

Scheme I-1. Biosynthesis of steviol via the MEP pathway	3
Scheme I-2. Hydrolysis of stevioside (I-8)	6
Scheme I-3. Biosynthesis of stevioside (I-8) and rebaudioside A (I-2)	7
Scheme I-4. Outline for the PSL	10
Scheme I-5. DOS approach to the <i>ent</i> -kaurene scaffold of steviol (I-23) by D-ring modifications	17
Scheme I-6. Hydrolysis of stevioside	18
Scheme I-7. Steviol DOS products	18
Scheme I-8. Synthesis of isosteviol DOS products	19
Scheme I-9. General Beckmann rearrangement reaction	21
Scheme I-10. Mechanism for Beckmann rearrangement reaction	22
Scheme I-11. <i>E</i> - vs <i>Z</i> - oxime isomer	23
Scheme I-12. Examples of retention of stereochemistry during the Beckmann Rearrangement	24
Scheme I-13. Proposed self-initiation mechanism for Beckmann rearrangement reaction	25
Scheme I-14. Beckmann fragmentation reaction	26
Scheme I-15. Mechanism of Beckmann fragmentation reaction	26
Scheme I-16. Photo-Beckmann reaction	27
Scheme I-17. Mechanism of oxaziridine in Photo-Beckmann rearrangement	28
Scheme I-18. Synthesis of steviol oxime I-67 and isosteviol oxime I-37	29
Scheme I-19. Beckmann rearrangement of oxime I-37	30
Scheme I-20. Beckmann Fragmentation of isosteviol oxime I-37	31
Scheme I-21. Beckmann fragmentation of steviol oxime I-67	32
Scheme I-22. Cyclic products from the isosteviol Beckmann fragmentation product (I-35)	33
Scheme I-23. Proposed mechanisms for the formation of cyclic products	33
Scheme I-24. Photo-Beckmann of isosteviol ester I-73	34
Scheme I-25. Validation array for steviol (I-23) and isosteviol (I-25) by solution phase (A) and solid phase synthesis (B)	37
Scheme I-26. Amide Libraries I-79 , I-80 , I-82 , I-84 , and I-86	39
Scheme I-27. Synthesis of ether and amine libraries	41
Scheme I-28. Synthesis of a bifunctional library from amide I-90a	43
Scheme II-1. Formation of different tetralin linkers	112
Scheme II-2. Quinoline linkers via boronic acid II-13	113
Scheme II-3. Triazole products from azide II-14 and alkyne II-15	114

Scheme II-4. Synthesis of triazole II-37	118
Scheme II-5. Towards the synthesis of triazole II-24	119
Scheme II-6. Towards the synthesis of quinoline II-27	121
Scheme II-7. Synthesis of quinoline analog II-29	122
Scheme II-8. Towards the synthesis of ER analogs	123
Scheme II-9. Developing quinoline analogs for hydrophobic pocket exploration	124
Scheme II-10. General process for INDIGO activity assay	128

List of Charts

Chart I-1. Comparison of cLogP values	52
Chart I-2. Comparison of Fsp3 value	53
Chart I-3. Comparison of the number stereocenters per molecule	54
Chart I-4. Pairwise similarity coefficients for I-23 and I-25 library compounds (full chart in APPENDICES)	55
Chart II-1. Existing contraceptive methods in the developing and develop regions in the world	100

List of Abbreviations

Ac	Acetyl
AcCl	Acetyl Chloride
Ar	Aryl
Bn	Benzyl (C ₆ H ₅ CH ₂ -)
°C	Degrees Celsius
Calcd	Calculated
CYP	Cytochrome P450
DBU	1,8-Diazabicyclo[5.4.0]undec-7-ene
DCM	Dichloromethane
DIBALH	Diisobutylaluminum Hydride
DIPEA	Diisopropylethylamine
DMAP	4-Dimethylaminopyridine
DMB	2,4-Dimethoxybenzyl
DMF	Dimethylformamide
DMP	Dess-Martin Periodinate
DMSO	Dimethylsulfoxide
equiv	Equivalent
TEA	Triethylamine
EtOAc	Ethyl Acetate
HMPA	Hexamethylphosphoramide
HRMS	High Resolution Mass Spectrometry
IC ₅₀	50% inhibitory concentration
IR	Infrared Radiation
<i>J</i>	Coupling Constant (NMR)
K _d	Dissociation Constant
LCMS or LC/MS	Liquid Chromatography-Mass Spectrometry
LRMS	Low-Resolution Mass Spectrometry
Me	Methyl
MeI	Methyl Iodide
MeOH	Methanol
mp	Melting Point
MTBE	Methyl Tert-Butyl Ether
MS	Molecular Sieves
NMR	Nuclear Magnetic Resonance
PPh ₃	Triphenylphosphine
<i>p</i> TSOH or <i>p</i> TSA	<i>p</i> -Toluenesulfonic acid
py	Pyridine
<i>i</i> -Pr or <i>i</i> Pr	Isopropyl
R _f	Ratio to Front
RT or <i>rt</i>	Room or Ambient Temperature
<i>t</i> _{1/2}	Half-Life Time
TBAI	Tetrabutyl Ammonium Iodide
TFA	Trifluoroacetic Acid
THF	Tetrahydrofuran

TLC
TMS

Thin Layer Chromatography
Trimethylsilyl

PART I- STEVIOSIDE LIBRARY DEVELOPMENT

Chapter 1. Design and Synthesis of Diterpene Scaffolds from Stevioside

A. Background of Stevioside, Steviol, and Isosteviol

For centuries, the indigenous people of South America have been using the ka'a he'ê plant, meaning "sweet herb," for its sweetening power and potential medicinal aspects.^{1,2} After introduction to European settlers and continued use by both natives and



Figure I-1. *Stevia rebaudiana* Bertoni plant.

non-natives, the plant has become scientifically known as *Stevia rebaudiana* Bertoni and commonly called "stevia" (Figure I-1).³ The plant was named by Italian-Swiss botanist Moises Santiago de Bertoni, when he first gained a sample in 1887.⁴ He at first named it *Eupatorium rebaudianum* after Paraguayan chemist Ovidio Rebaudi,⁵ but then later corrected the genus as *Stevia*, after the Spanish botanist Pedro Jaime Esteve,

who first researched the plants in a territory of Paraguay.⁶ While the *Stevia* genus contains over 230 species, *S. rebaudiana* has been the only plant observed to contain sweetening agents.⁷ Eight natural products isolated from the *S. rebaudiana* Bertoni leaf tissues were identified with sweetening properties: dulcoside A (**I-1**), rebaudiosides A-E (**I-2:I-6**),

steviolbioside (**I-7**), and stevioside (**I-8**) (Figure I-2).⁸ The four main sweeteners are rebaudioside A (**I-2**), rebaudioside C (**I-4**), dulcoside A (**I-1**), and stevioside (**I-8**).⁹

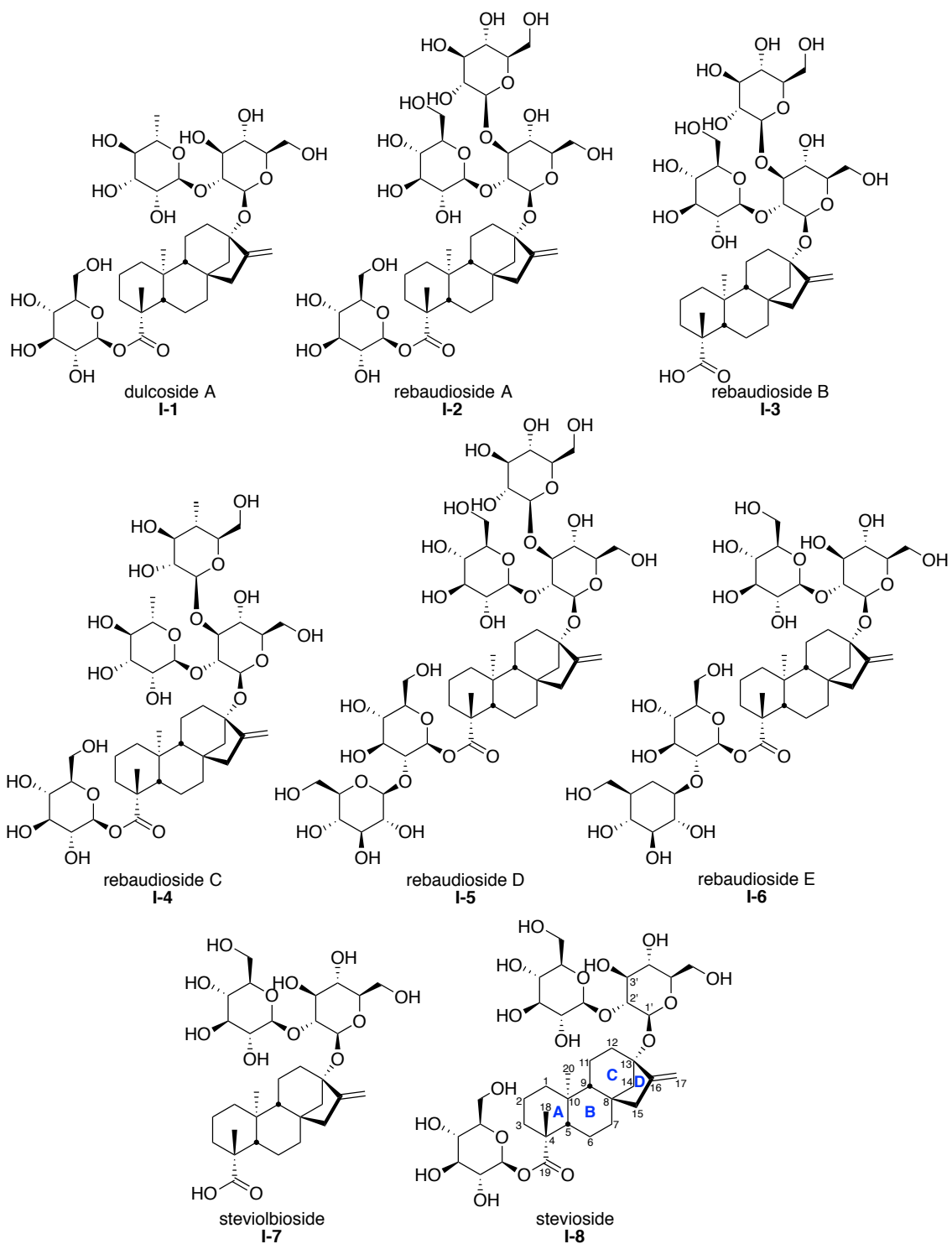
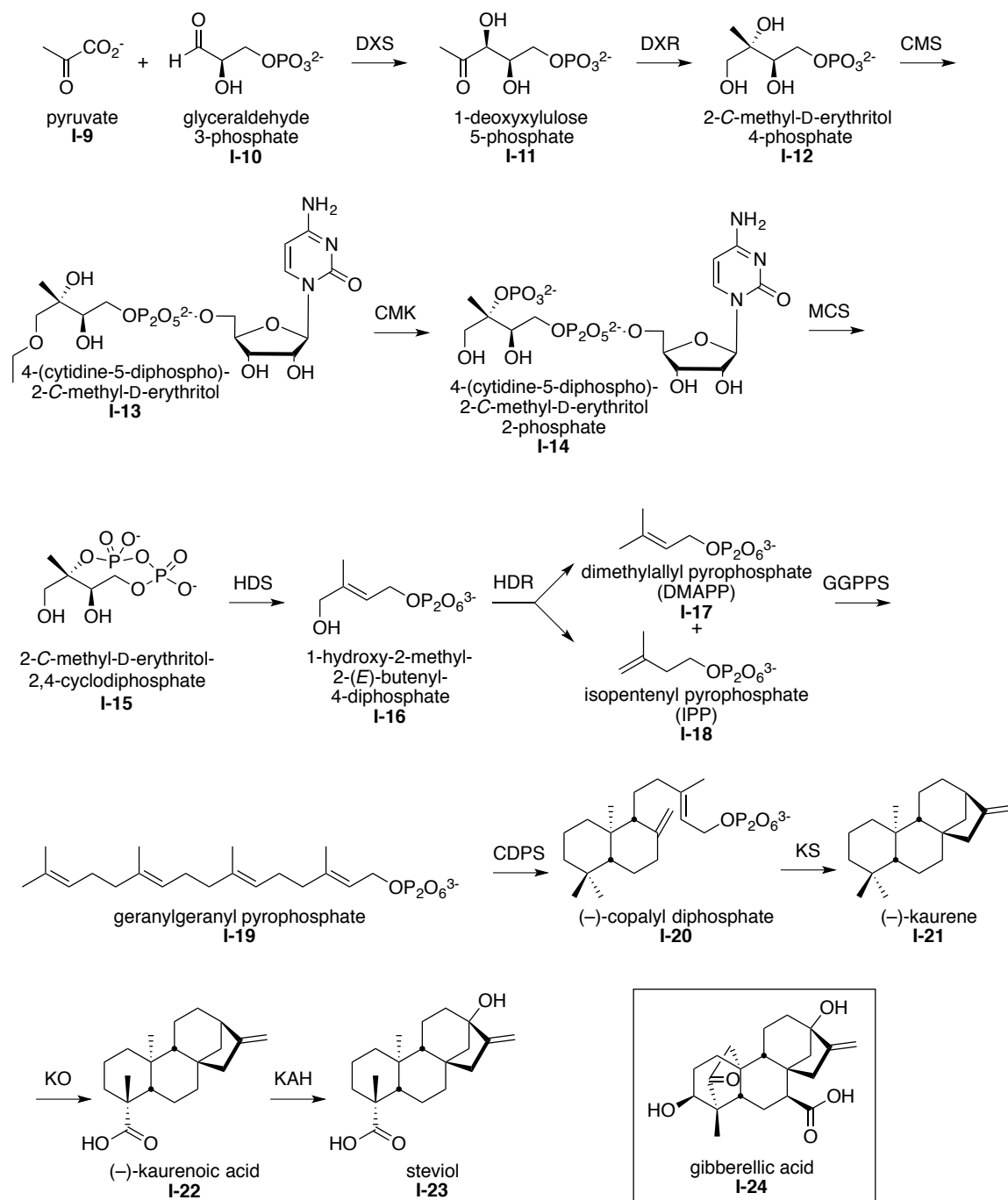


Figure I-2. Stevia sweetening agents.

These compounds are classified as *ent*-kaurene glycosides or steviol glycosides, because they all contain that same kaurenoid precursor. The *ent*-kaurene core is formed by the methylerythritol 4-phosphate (MEP) pathway (Scheme I-1).¹⁰



Scheme I-1. Biosynthesis of steviol via the MEP pathway.

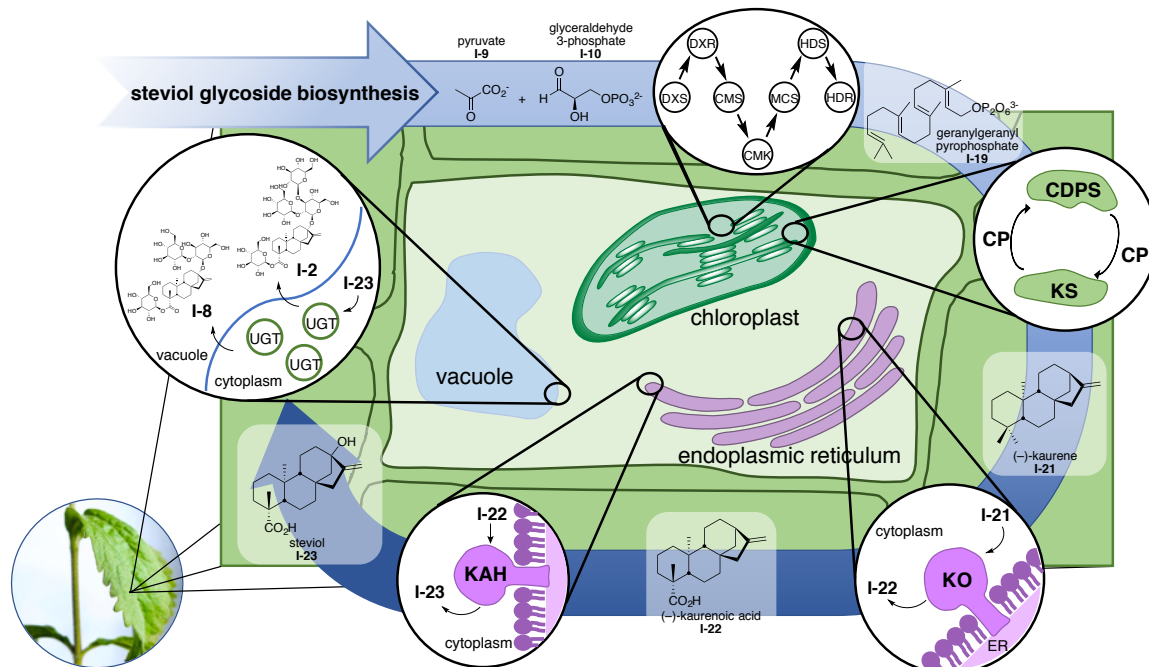
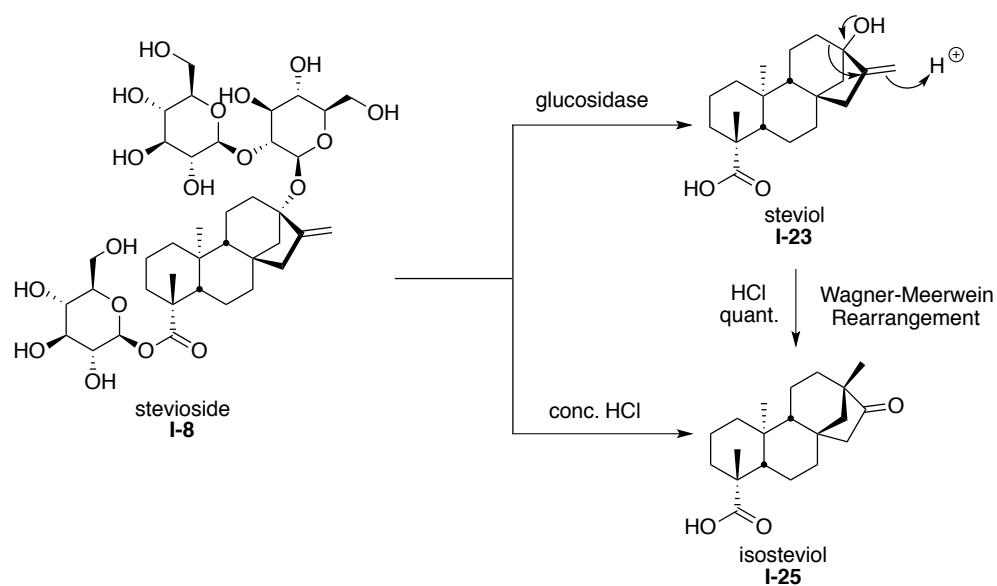


Figure I-3. Biosynthesis of steviol glycoside.¹⁰

This pathway begins with pyruvate **I-9** and glyceraldehyde 3-phosphate **I-10** in the chloroplasts of the plant cells. From these two common, biosynthetic compounds, deoxyxyulose-5-phosphate (**I-11**, DXP) is generated with the DXP synthase (DXS). DXP can be used for further production of vitamin B1¹¹ or isoprenoids as with the MEP pathway. With DXP reductase (DXR), the DXP chain is rearranged to form 2-*C*-methyl-D-erythritol 4-phosphate (**I-12**, MEP).¹² From **I-12**, 4-diphosphocytidyl-2-*C*-methyl-D-erythritol synthase (CMS) produces 4-(cytidine-5-diphospho)-2-*C*-methyl-D-erythritol (**I-13**), then 4-diphosphocytidyl-2-*C*-methyl-D-erythritol kinase (CMK) yields 4-(cytidine-5-diphospho)-2-*C*-methyl-D-erythritol-2-phosphate (**I-14**). From there, 2-*C*-methyl-D-erythritol-2,4-cyclodiphosphate (**I-15**) is generated with 4-diphosphocytidyl-2-*C*-methyl-D-erythritol 2,4-cyclodiphosphate synthase (MCS). The next two steps of the synthesis are not well characterized, but essentially, intermediate **I-15** is converted to 1-hydroxy-2-methyl-2-(*E*)-butenyl-4-diphosphate (**I-16**) with 1-hydroxy-2-methyl-2-(*E*)-butenyl 4-

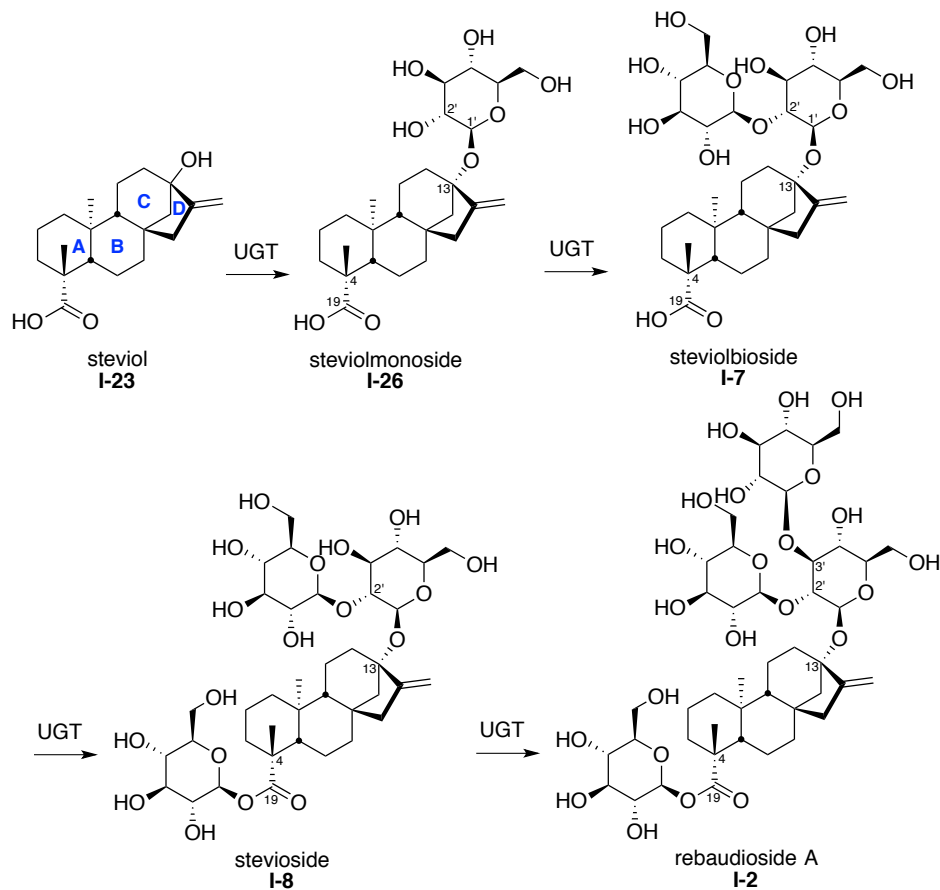
diphosphate synthase (HDS) and then reduced by 1-hydroxy-2-methyl-2(*E*)-butenyl 4-diphosphate reductase (HDR) to provide the MEP pathway products: dimethylallyl pyrophosphate (**I-17**, DMAPP) and its isomer isopentyl pyrophosphate (**I-18**, IPP).¹³ DMAPP **I-17** and IPP **I-18** advance to diterpene synthesis starting with the conversion to geranylgeranyl pyrophosphate (**I-19**, GGPP) by GGPP synthase (GGPPS) and three successive condensation steps.¹⁴ Next, copalyl diphosphate (**I-20**, CDP) is made from CDP synthase (CDPS) and then, kaurene synthase produces (–)-kaurene (**I-21**, or *ent*-kaurene) via an ionization dependent cyclization step.¹⁰ Interestingly, GGDP, CDP, and kaurene synthases also play crucial roles in the gibberellic acid biosynthetic pathway and low concentrations of gibberellic acid are found in *Stevia* plant tissues.¹⁵ However, further research is ongoing to determine the special organization of these enzymes and how they divert the synthesis of steviol glycosides from gibberellic acid (**I-24**, GA).¹⁶

Next in the steviol glycoside biosynthesis, the kaurene **I-21** is oxidized to kaurenoic acid (**I-22**) by the p450 mono-oxygenase kaurene oxidase (KO). The KO enzyme is also found in the GA biosynthetic pathway and is highly expressed in the same tissues as CDP and kaurene synthases, but the oxidation step has been shown to occur in the endoplasmic reticulum not chloroplasts (Figure I-3).¹⁶ Acid **I-22** is then hydroxylated by kaurenoic acid 13-hydroxylase (KAH) at C-13 to give the steviol diterpene **I-23** (Scheme I-1).¹⁷ The hydroxylation step by KAH is completely separate and different from the GA biosynthetic pathway, marking the divergence of steviol glycoside formation from the gibberellic acid pathway.¹⁸ Additionally, acid treatment of **I-23** will give its isomeric diterpene isosteviol **I-25** via a Wagner-Meerwein rearrangement (Scheme I-2).¹⁹ This alternative structure of steviol **I-23** will be further explored within this chapter.



Scheme I-2. Hydrolysis of stevioside (**I-8**).

Finally, a series of glycosyltransferases append glucose residues onto the aglycone **I-23** to form stevioside (**I-8**).²⁰ Like with the acid treatment of steviol **I-23**, isosteviol **I-25** can be directly synthesized from **I-8** via acid hydrolysis (Scheme I-2).¹⁹ The first glycosylation occurs at the C-13 hydroxyl of steviol **I-23** to yield steviolmonoside **I-26**,



Scheme I-3. Biosynthesis of stevioside (**I-8**) and rebaudioside A (**I-2**).

followed by another glucose addition to the 13-*O*-glucose at the C-2' of the first glucose on the C-13 end of the steviolmonoside molecule by a UDP-glycosyltransferase (UGT) to give steviolbioside (**I-7**) (Scheme I-3 and Figure I-2). Lastly, the C-19 hydroxyl of the A-ring of **I-7** is glycosylated to generate the desired stevioside (**I-8**). Upon another glycosyl transfer on the C-13 end of **I-8**, rebaudioside A (**I-2**) is produced; stevioside (**I-8**) and rebaudioside A (**I-2**) are the most prominent natural products of the major steviol glycosides isolated from *S. rebaudiana* Bertoni plant.²¹ They make up to 20% of the dry leaf weight of the *Stevia* plant.²²

2. Biological evaluation of stevioside and its metabolites

These diterpene natural products were isolated from the leaves in 1931 and found to be at least 300 times sweeter than sucrose, or table sugar.²³ Specifically, stevioside (**I-8**), which contains one glucose molecule at the C-4 carboxyl end of the A-ring and another two glucose molecules at the C-13 hydroxyl end of the C-ring, has been shown to be 150-250 times sweeter than sucrose.²⁴ Rebaudioside A (**I-2**), which contains four glucose molecules: one at the C-4 carboxyl end and three at the C-13 hydroxyl end, is 200-300 times more sweet.²⁴ Due to its sweetness from the steviol glycosides, the stevia plant has become commercially sold as a food additive and non-caloric natural sweetener, after being used as such for centuries by the indigenous Guarani natives in South America.²⁵ Moreover, the steviol glycosides and their aglycone structures from the stevia plant have been extensively reviewed for their pharmacological effects,²⁵⁻³¹ including glucoregulation for diabetes mellitus treatment,³² anti-hypertensive activity for blood pressure regulation,³³ anti-tumor effects for cancer therapy,³⁴ anti-microbial effects,³⁵ anti-diarrheal or anti-rotavirus capabilities for treatment of gastrointestinal problems,³⁶ renal function regulation for kidney disease treatment,³⁷ antiviral activity,³⁸ antifungal properties,³⁹ anti-HIV research,⁴⁰ hepatoprotective effects,⁴¹ immunomodulatory, and anti-inflammatory effects.⁴² Most of these aforementioned studies were performed on mice or rats with ongoing research being conducted for the full effect of stevioside or its metabolites in the human body.^{43, 44}

A study of the metabolism of rebaudioside A (**I-2**) and stevioside (**I-8**) from extracts of *S. rebaudiana* plants containing either 85% w/w **I-8** or 90% w/w **I-2** was performed on eleven healthy human subjects and found no levels of either **I-2** or **I-8** in the fecal

analysis.⁴⁵ A separate human metabolism study of ten healthy human subjects given 250mg stevioside (**I-8**) capsules for 3 times daily for a period of 3 days did not detect any amounts of stevioside in the blood, urine, or fecal collections examined.⁴⁶ Both of these two human studies did find steviol in the stool collections and determined that it was not further degraded. Instead, the human microflora had completely hydrolyzed the steviol glycosides down to the aglycone steviol (**I-23**) metabolite. Moreover, Geuns *et al.* showed that the Caco-2 cell line absorbed steviol but not stevioside.⁴⁷ Blood samples taken from the healthy subjects did not identify stevioside (**I-8**), the aglycone steviol (**I-23**), or any other possible steviol metabolites in the blood. Urine analysis from the study by Geuns *et al.* revealed the presence of steviol glucuronide as the major metabolized product.⁴⁶ These two studies suggest that stevioside and rebaudioside A are completely metabolized in the colon to steviol, which is then absorbed and glucuronidated in the liver for eventual urine excretion.

Given the increased interest in stevioside (**I-8**) and its metabolites for biological activity evaluation, we determined that this natural product was an excellent source and starting place for our compound library development.

B. Rationale for Developing *ent*-Kaurene Scaffolds

1. Pilot Scale Libraries Initiative

Under the Pilot Scale Libraries Initiative, our goal was to synthesize and submit compounds to become part of the NIH Molecular Libraries Small Molecule Repository (MLSMR) and to be evaluated in the NIH-funded Molecular Libraries Screening Center Network (MLPCN) centers.⁴⁸ The MLPCN is a consortium of centers around the United States that perform high throughput screening assays with the library of over 300,000 small

molecules from the MLSMR and the information from these activities are deposited on to the PubChem public database.⁴⁹

Stevioside (**I-8**), a widely used natural sweetener, was chosen for library development for several reasons. First, natural products isolated from plant, marine, and microbial sources are excellent leads for library generation. They are a source of varied molecular structure and continue to be an excellent resource for probing and discovering new therapeutic agents. Therefore, probing biological systems with natural products or natural product-like compounds remains fertile ground to uncover novel lead structures of biomedical significance. Second, carbon skeletons of the complexity of the steviol glycoside natural product cannot be readily accessed via total synthesis. This library project had a unique opportunity to explore the potential of stevioside (**I-8**), which is already produced commercially worldwide through extraction of *Stevia rebaudiana*.⁵⁰ The Pilot Scale Libraries project is part of the NIH Molecular Libraries Initiative. The purpose of this work is to synthesize molecules that explore sparsely populated chemical space and then submit them to the MLSMR. The MLSMR is part of the MLPCN and once they are submitted, any screening information will be made available on PubChem, an online database that stores all publicly available structural and biological data, (Scheme I-4).⁴⁹



Scheme I-4. Outline for the PSL.

Unlike many other natural products, stevioside (**I-8**) is readily available in kilogram quantities and can be easily hydrolyzed to provide two scaffolds: steviol (**I-23**) and isosteviol (**I-25**) ideally suited for the development of natural product-derived combinatorial libraries. Library synthesis for these structures is facilitated by the extensive work already published for steviol glycoside chemistry, and chemical transformations that lead to different types of scaffolds are well known.⁵¹⁻⁵³ Since stevioside (**I-8**), steviol (**I-23**), isosteviol (**I-25**), and related natural products such as gibberellic acid derivatives possess a variety of biological activities, we hypothesized that stevioside-derived libraries could provide promising opportunities to generate hits in screening campaigns.^{28, 54-56}

2. Natural Products and Steviol-Related Compounds

Natural products can serve as excellent scaffolds for chemical library development due to their inherent structural diversity and complexity, as compared to synthetic products.⁵⁷ In addition, natural products have been shown to occupy areas of chemical space that are generally not well covered by synthetic compounds.^{58,59} Furthermore, natural products, their analogs, and natural product-inspired bioactive compounds have been sources of new drugs over many decades. In a report by Newman *et al.*, over 40% of the 1562 approved drugs from 1981 to 2014 are either natural products, mimic natural products, are derived from natural products, or are synthesized from a natural product (Figure I-4).⁶⁰ Therefore, natural products provide a solid platform for the discovery of biologically active small molecules.⁶¹ It has been suggested that because natural products are molded by protein domains, their shape is more likely to be complementary to other protein domains.⁶²

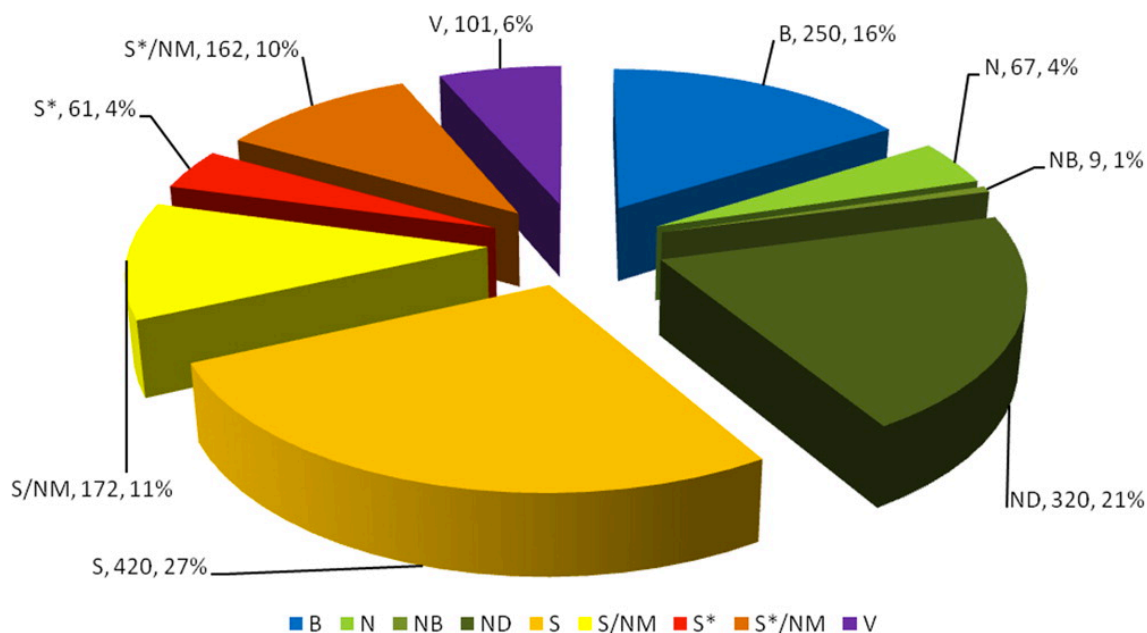


Figure I-4. All new approved drugs from 1981 until 2014.⁶⁰

“B”: Biological, usually a large (>50 residues) peptide or protein either isolated from an organism/cell line or produced by biotechnological means in a surrogate host; “N”: Natural product, unmodified in structure, though might be semi- or totally synthetic; “NB”: Natural product “botanical drug” (in general these have been recently approved); “ND”: Derived from a natural product and is usually a semisynthetic modification; “S”: Totally synthetic drug, often found by random screening/modification of an existing agent; “S*”: Made by total synthesis, but the pharmacophore is/was from a natural product; “V”: Vaccine; “NM”: Natural product mimic

Additionally, natural products also occupy a large area of chemical space. Chemical space, or multi-dimensional descriptor space, is like a map of the area a molecule occupies. Since it is so vast, chemical space is a region defined by a particular choice of descriptors and limits placed on them. Dobson *et al.* compare the molecular diversity of compounds from combinatorial chemistry, natural products, and drugs (Figure I-5).⁶³ From the parameters shown, there is still a large amount of “space” or white areas that are not speckled with data.

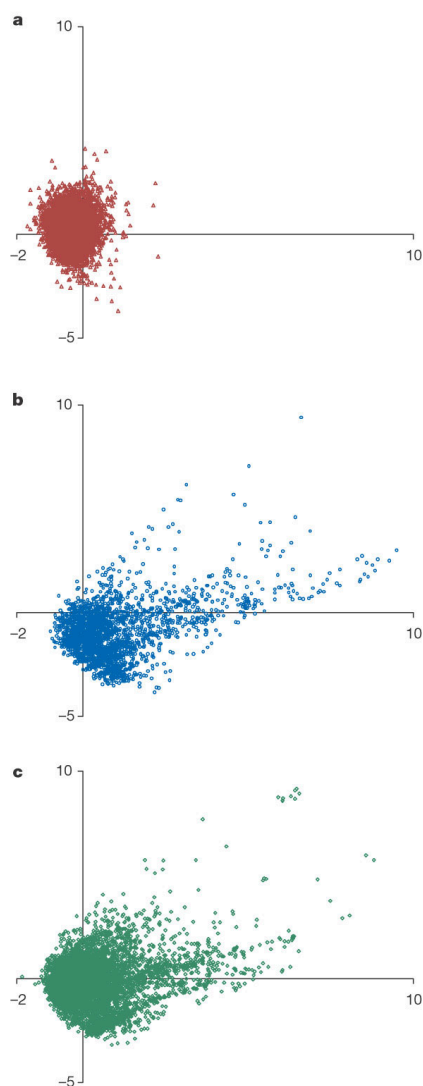


Figure I-5. Chemical space analysis of compounds from a) combinatorial chemistry b) natural products, and c) drugs.^{63, 64}

Two major issues associated with the development of high-value information-rich small molecule libraries are achieving skeletal diversity⁶⁵⁻⁶⁷ and mining areas of biologically relevant chemical space.⁶⁴ Because nature can impart chemical diversity in many different areas of chemical space, cheminformatics research for drug discovery aims to chart out these areas and explore their potential.⁶⁸ Additionally, Larsson *et al.* introduced ChemGPSNP,⁶⁹ a tool for exploring chemical diversity that identifies volumes of chemical space related to particular biological activities and tracks changes in chemical properties

that have been used for natural product drug development.^{70, 71} Other more recent cheminformatics tools have been developed to assess chemical space and diversity.⁷² With these tools in mind, developing small molecule libraries that are novel and valuable is possible. Stevioside (**I-8**), as mentioned earlier, is easily and readily available and its biosynthetic intermediates could also be used for divergent template development.

Potentially, the steviol glycoside scaffold could provide access to templates representative of the large and diverse family of diterpenes derived from the methylerythritol 4-phosphate pathway¹⁰ and subsequent metabolic processes. Representative diterpenes from this family include platensimycin (**I-27**), and triptolide (**I-28**), labdane (**I-29**) with antibiotic,⁷³ anticancer,⁷⁴ and neuroprotective properties,⁷⁵ respectively (Figure I-6).

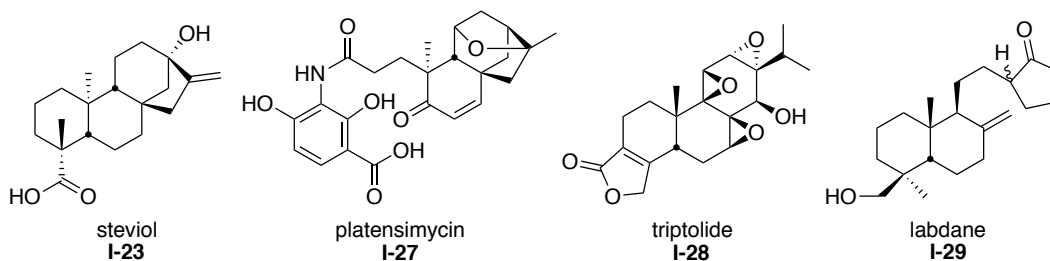


Figure I-6. Structures of steviol-related natural products.

These compounds have attracted much attention from the synthetic community and therefore a large amount of literature has been produced over the last eight decades pertaining to the synthesis⁷⁶⁻⁸¹ and structural modification of stevioside⁸²⁻⁸⁴ and structurally-related diterpenes.⁸⁵⁻⁸⁷ Moreover, studies have revealed that steviol (**I-23**) and isosteviol (**I-25**) have exhibited pharmacological activities,²⁸ thus, we will unlock their potential by making these molecules as the initial scaffolds for our library.

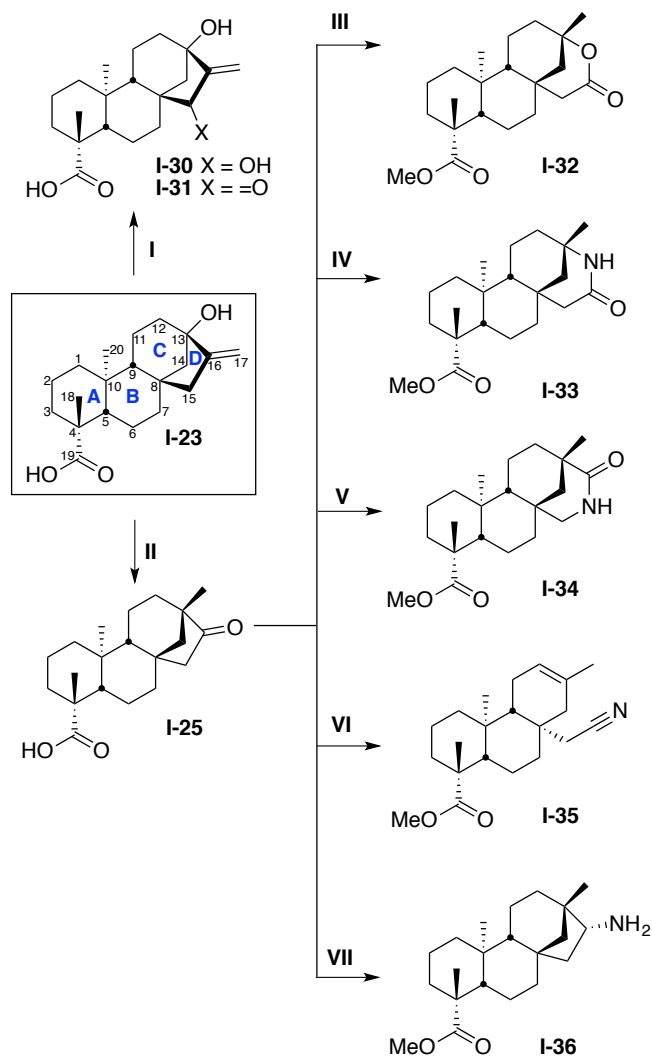
C. Design of Diterpene Scaffolds with Diversity-Oriented Synthesis

1. Background on DOS and its utilities

In order to create functional diverse small-molecule libraries that occupy novel areas of chemical space, a synthetic approach was introduced by Schreiber *et al.* called diversity-oriented synthesis.⁸⁸ It is an efficient approach to design and develop multiple small molecules that populate structurally diverse areas of chemical space. “Diversity-oriented synthesis involves the deliberate, simultaneous, and efficient synthesis of more than one target compound in a diversity-driven approach to answer a complex problem.”⁸⁹ This method provides rapid access to known and previously ‘un-tapped’ regions of bioactive chemical space to yield complex compound libraries for biological screening.⁹⁰ In contrast to target-oriented synthesis (TOS), which focuses on the synthesis of structural analogs in a dense region of chemical space, DOS explores a broad area of chemical space that features compounds with different skeletal and stereochemical moieties.⁹¹ Furthermore, while Fragment-based Drug Design (FBDD) focuses on the synthesis of a small library of compounds or fragments with high structural diversity, DOS is able to achieve a library with both high structural diversity and molecular complexity through a series of parallel reactions.⁹² Through DOS, it is possible to create libraries of compounds from a single building block (scaffold) or collections of compounds from structurally similar scaffolds. To generate compounds that are structurally diverse, complex, and have natural product-like properties, we chose to work with stevioside (**I-8**) to provide numerous, different scaffolds from its core skeleton, the *ent*-kaurene.

2. Introduction of Scaffolds

Scheme I-5 illustrates several approaches that can be taken. Path I involves an allylic oxidation of the C-17 methylene of steviol to furnish diol **I-30**, which can be further oxidized to the C-15 ketone analog **I-31**. For path II, the Wagner-Meerwein rearrangement, as discussed above, is achieved with hydrochloric acid to yield isosteviol (**I-25**). From isosteviol, several different scaffolds can be generated after one or two synthetic steps. Through route III, a Baeyer-Villiger oxidation of isosteviol (**I-25**) produces lactone **I-32**. Formation of an oxime and subsequent Beckmann rearrangement (path IV) yields lactam **I-33**, and photo-Beckman rearrangement leads to the corresponding amide regioisomer **I-34** (path V). As shown for path VI, the Beckman fragmentation product, nitrile **I-35**, can also be obtained with a slight change to reaction conditions. Optimized protocols for isosteviol oxime formation, Beckman rearrangement and Beckmann fragmentation have all been reported by us.⁵¹ In addition to forming novel scaffolds, the functional groups in the molecules can be easily modified for library synthesis.⁵³ Reductive amination of isosteviol (**I-25**) via route VII yields amine **I-36**.^{93,94} Other obvious modifications involve the carboxylic acid moiety of the A-ring, which can be reduced to the corresponding aldehyde, alcohol, or methyl group. The carboxylic acid can also be converted to an acid chloride or activated ester for amide bond formation, which will be discussed later in this section. Additionally, formation of the acid chloride from the C-4 carboxylic acid and subsequent acyl azide can lead to a Curtius rearrangement toward the formation of a 4-amine analog.⁹⁵ The double bond of steviol can be transformed to a hydroxymethyl group or an epoxide, and ozonolysis of the double bond provides the corresponding ketone.⁵³

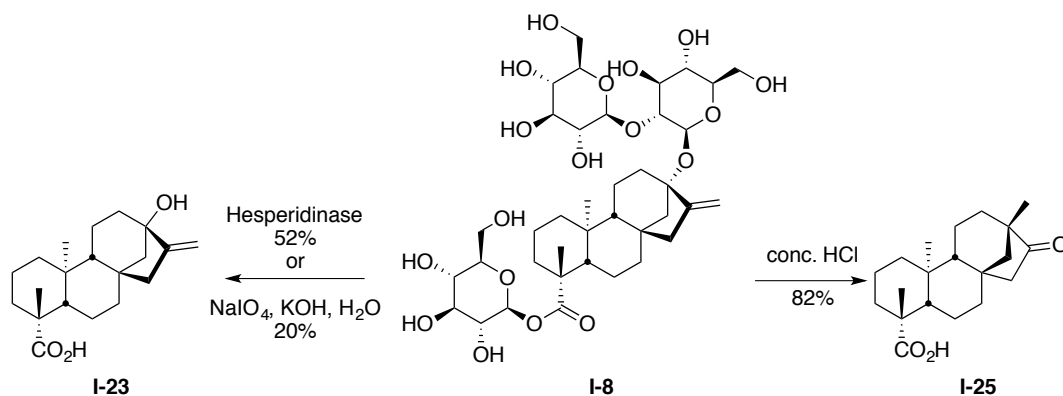


Scheme I-5. DOS approach to the *ent*-kaurene scaffold of steviol (**I-23**) by D-ring modifications.

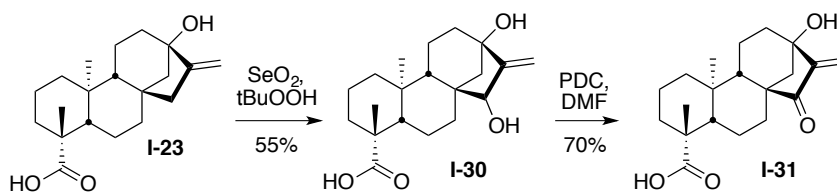
We focused on steviol (**I-23**) and D-ring modified compounds **I-25**, **I-33**, **I-35**, and **I-36** as the scaffolds for library development. We also describe the synthesis of several pilot scale libraries, their evaluation in multiple high throughput screens and an *in silico* analysis of the chemical and drug-like properties of the compounds prepared in this study.

3. Synthesis of DOS Scaffolds

Enzymatic hydrolysis of stevioside under well-known reaction conditions provided steviol (**I-23**) in good yield. Basic hydrolysis also provided steviol (**I-23**) in low yield while acid hydrolysis gave isosteviol (**I-25**) in good yield (Scheme I-6).^{21, 96}

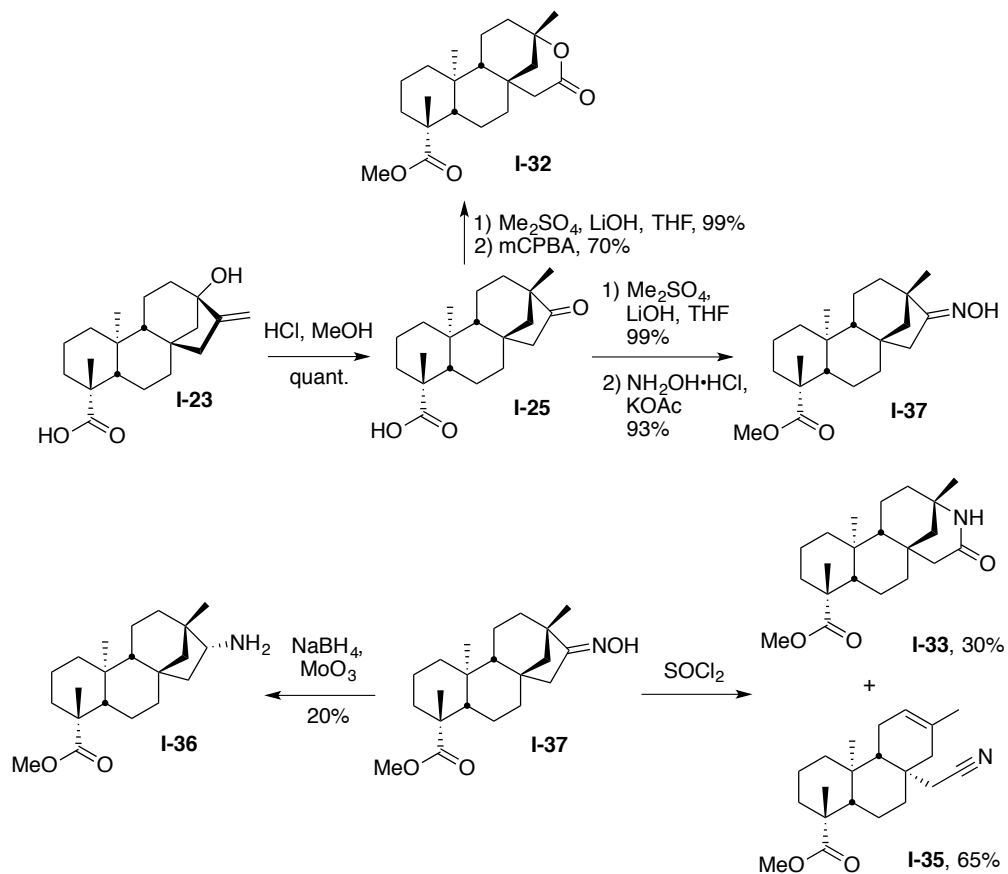


From the steviol scaffold, an allylic oxidation with selenium (IV) dioxide afforded the diol **I-30** in good yield (Scheme I-7).⁹⁷ This Riley oxidation step is an excellent way to introduce a hydroxyl moiety into the allylic position of the methylene group.⁹⁸ Then, a PDC oxidation of the secondary hydroxyl afforded ketone **I-31**.⁹⁹



When treated with hydrochloric acid, steviol generated the isomerized product, isosteviol (**I-25**), in quantitative yield (Scheme I-8). Isosteviol has a variety of DOS routes

to produce other interesting scaffolds for library development. With *m*CPBA, isosteviol (**I-25**) undergoes a Baeyer-Villiger oxidation to give lactone **I-32** (Scheme 1-8).¹⁰⁰



Scheme I-8. Synthesis of isosteviol DOS products.

Isosteviol can also be converted to oxime **I-37** with hydroxyl amine under basic conditions in excellent yield. The oxime intermediate can also be reduced with sodium borohydride and molybdenum trioxide to give amine **I-36**.¹⁰¹ Additionally, treatment of oxime **I-37** with thionyl chloride affords both the Beckmann rearrangement lactam product **I-33** as well as the Beckmann fragmentation nitrile product **I-35**. The freshness of the thionyl chloride can affect the yields of the Beckman reaction products with a significantly decreased lactam **I-**

33 yield if fresh reagent is not used. The chemistry of the Beckmann reaction and its reaction products are described in the next section.^{51, 102}

Chapter 2. Exploring the Beckmann Rearrangement Reaction

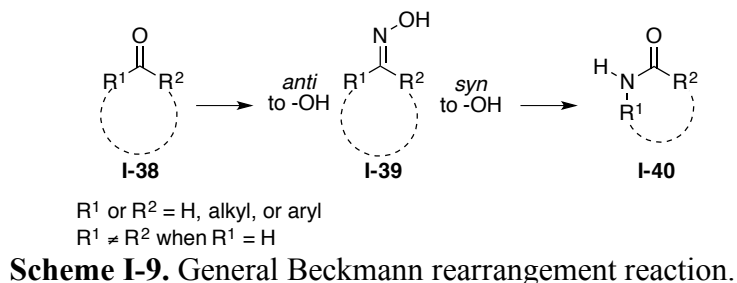
A. Background of the Beckmann Reaction

Since its discovery in 1886 by Ernst Beckmann,¹⁰³ the eponymous rearrangement reaction has been a useful tool in organic synthesis to incorporate a nitrogen atom into a molecule. This is typically achieved by a modification of a ketone or aldehyde via oxime formation. The Beckmann rearrangement reaction is an important method to convert oximes in open chain and cyclic systems to the corresponding amides and lactams. Additionally, a Beckmann fragmentation can instead occur during the rearrangement process to form a nitrile group from the initial oxime. The Beckmann reactions have been extensively reviewed because of their versatility and wide synthetic scope.¹⁰⁴⁻¹⁰⁹ Given their utility and significance in synthetic organic chemistry, our group employed this reaction to uncover new steviol and isosteviol scaffolds. This chapter contains sections of a review that we previously published in the book *Molecular Rearrangements in Organic Synthesis*.^{102, 110}

1. Lactam Formation from the Beckmann Rearrangement

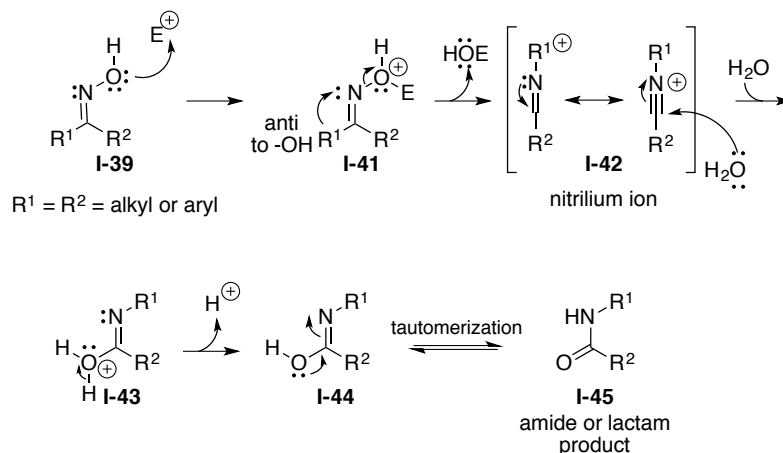
The Beckmann rearrangement is the most recognized of the Beckmann reactions and generally describes the conversion of a ketone or aldehyde **I-38** to an oxime **I-39** (Scheme I-9). Oxime **I-39**, under acidic and dehydrating conditions, rearranges to an amide **I-40**. This conversion occurs with the carbon bond *anti* to the oxime hydroxyl group

migrating to the nitrogen. Moreover, the Beckmann rearrangement of aldoximes (where R¹ or R² = H) produces primary amides via hydrogen migration in a non-stereospecific manner. Acyclic ketoximes produce the corresponding secondary amide groups, while cyclic ketoximes yield the lactam moieties (Scheme I-9).



Conventionally, the Beckmann reaction requires a strong acid to initiate the rearrangement reaction; however, there have been reports of milder, greener, and non-acidic conditions for this transformation including: Lewis acids, solid catalysts,^{105, 111} ionic liquids,¹¹² and organocatalysts.¹¹³ Activation of the oxime intermediate **I-39** begins by transforming the *N*-hydroxyl group of the oxime into a better leaving group by reaction with an acid or formation of an ester or an ether. As shown in Scheme I-10, the oxime hydroxyl of **I-39** is converted into a better leaving group with an electrophile, subsequently forming the oxonium intermediate **I-41**. Next in the Beckmann rearrangement, the nitrilium ion **I-42** is formed. This is achieved when the leaving group departs and the substituent situated *anti* to the nitrogen-oxygen (N-O) bond of **I-41** migrates to the nitrogen atom.¹⁰⁶

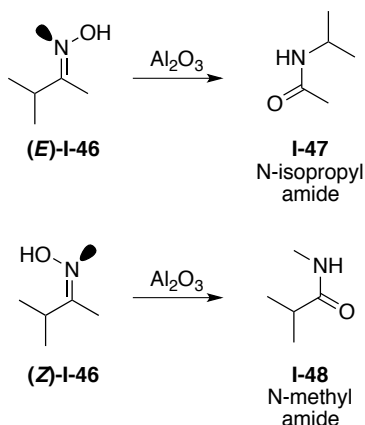
This process maximizes the antiperiplanar electron delocalization of the carbon-carbon (C-C) σ orbital to the antibonding σ^* orbital of the N-O bond.¹¹⁴



Scheme I-10. Mechanism for Beckmann rearrangement reaction.

Subsequently, the nitrilium ion **I-42** reacts with a nucleophile, such as water, to form intermediate **I-43**. This intermediate is deprotonated to furnish imidic acid **I-44**, which then tautomerizes to yield amide **I-45** (Scheme I-10). In fact, the oxime **I-39** can exist in two different and distinct isomers: the *E* or *anti* isomer and the *Z* or *syn* isomer (Scheme I-11). The (*E*)-isomer **I-46** rearranges to give the *N*-isopropylamide **I-47** upon treatment with aluminum oxide, while the (*Z*)-oxime isomer **I-46** yields the *N*-methylamide **I-48** under

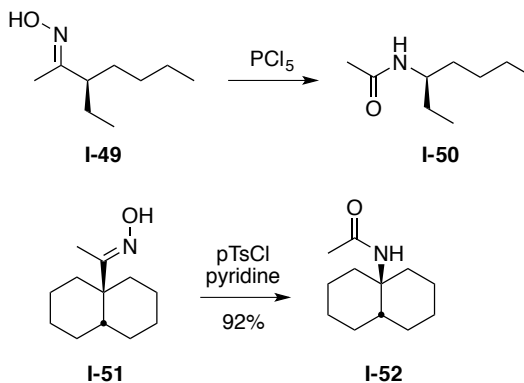
the same normal Beckmann reaction conditions.¹¹⁵ In some cases, the interconversion of the two distinct isomers takes place. This type of non-stereospecific conversions explains



Scheme I-11. *E*- vs *Z*- oxime isomer.

the different products observed, particularly under acidic conditions and in protic solvents.¹¹⁶ When both alkyl groups are able to migrate, the more bulky group forms the amide in greater proportion.¹⁰⁵

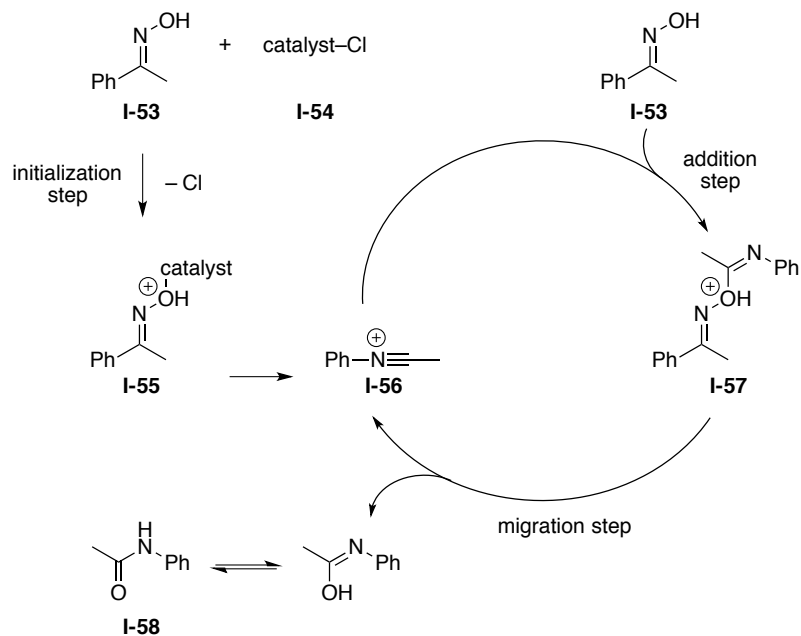
Kenyon *et al.* investigated the stereochemical course of the Beckmann reaction by studying the optically active (*R,E*)-3-ethylheptan-2-one oxime **I-49** and its conversion to the corresponding amide **I-50** (Scheme I-12).¹¹⁷ They treated the dextrorotatory oxime **I-49** with phosphorus pentachloride to afford the dextrorotatory amide product **I-50**.¹¹⁸ Then, they compared the optical activity of the amide product **I-50** with its corresponding *dl*-amide and determined that the asymmetry of the migrating group was preserved.



Scheme I-12. Examples of retention of stereochemistry during the Beckmann Rearrangement.

Likewise, experiments by Hill *et al.* showed the same retention of stereochemistry of the Beckmann rearrangement on a system with a trisubstituted-stereogenic carbon (Scheme I-12).¹¹⁹ They treated *cis*-decalin oxime **I-51** with *p*-toluenesulfonic acid chloride in pyridine to produce *cis*-amide **I-52** in very good yield. These examples confirm that the Beckmann rearrangement reaction proceeds in an intramolecular fashion with retention of configuration of the migrating group.¹²⁰

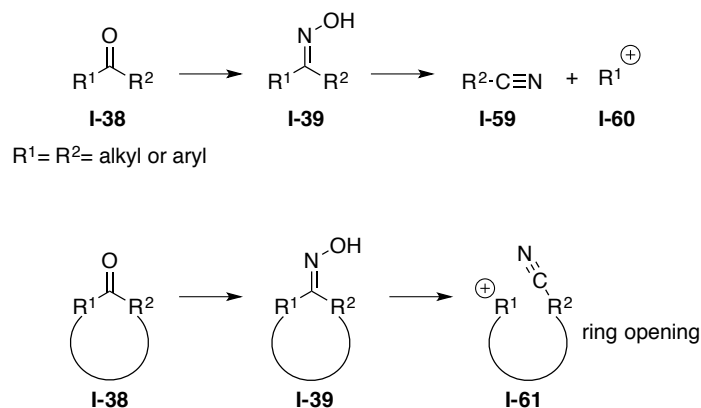
Subsequently, Ericksson and colleagues used DFT calculations to show that in the case of certain organo-mediated Beckmann rearrangements, a self-propagating mechanism is energetically-favored over other mechanisms (Scheme I-13).¹²¹ In their proposal, the chloride reagent **I-54** only initiates the reaction with oxime **I-53** rather than actually catalyzing the reaction.¹²² In the initialization step oxime **I-53** reacts with chloride **I-54** to yield oxime complex **I-55**, which then forms nitrilium ion **I-56**. Next, an addition of another oxime **I-53** to nitrilium ion **I-56** forms a dimer-like structure **I-57**. Intermediate **I-57** then undergoes the phenyl migration to produce the rearrangement product **I-58** while simultaneously regenerating the phenyl-nitrilium ion **I-56**.



Scheme I-13. Proposed self-initiation mechanism for Beckmann rearrangement reaction.

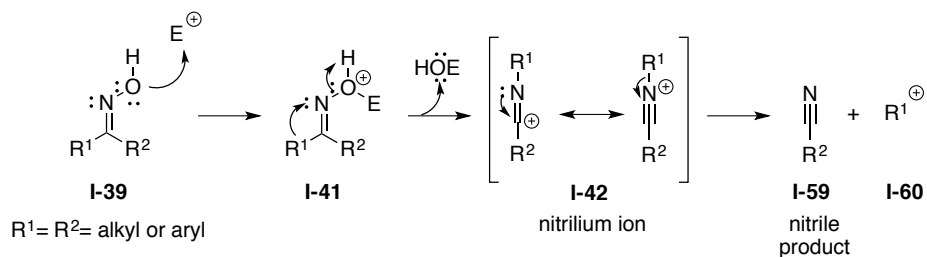
2. Nitrile Formation from the Beckmann Fragmentation

First discovered by Wallach in 1889, the Beckmann reaction can also form a nitrile product instead of the amide by a Beckmann fragmentation reaction. Sometimes called the abnormal or second-order Beckmann rearrangement, or Beckmann fission, this reaction begins like the Beckmann rearrangement reaction with oximes **I-39** derived from linear or cyclic ketones **I-38** (Scheme I-14). The fragmentation occurs when the C-C α bond breaks after shifting to the nitrogen atom, this results in the formation of a nitrile product **I-59** and carbocation intermediate **I-60** (Scheme I-14). In a cyclic system, the fragmentation sequence causes the cyclic oxime ring **I-39** to open and generate the non-cyclic nitrile product **I-61**.



Scheme I-14. Beckmann fragmentation reaction.

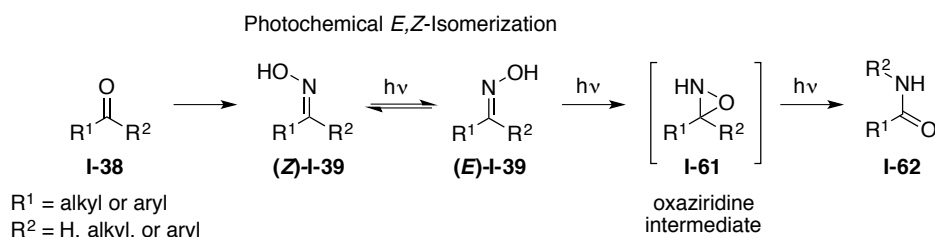
In general, the fragmentation reaction can take place when the hydroxyl group of an oxime is *anti* to a group that can stabilize a positive charge, such as a quaternary carbon or a heteroatom. The process begins with the addition of an electrophile to activate oxime **I-39** (Scheme I-15). From here, the oxonium ion **I-41** is formed and then nitrilium ion **I-42**. Next, **I-42** converts into nitrile **I-59** and carbocation **I-60**. Whether Beckmann rearrangement or fragmentation takes place is wholly dependent on the exact reaction conditions employed, such as using light radiation for promoting the photo-Beckmann rearrangement.



Scheme I-15. Mechanism of Beckmann fragmentation reaction.

3. Photo-Beckmann Rearrangement

In 1963, De Mayo *et al.* observed a different product from the direct irradiation of aldoxime **I-39**.¹²³ The aldoxime derived from ketone **I-38** forms an oxaziridine intermediate **I-61** before conversion to amide **I-62** (Scheme I-16). This photochemical reaction proceeds through an intramolecular oxygen migration and is commonly considered a photo-Beckmann rearrangement reaction.¹²⁴ Ogata and coworkers later determined the exact mechanism for this photochemical reaction through studies with ¹⁸O-labeled oximes.¹²⁵ Also, the photochemical Beckmann rearrangement is not accompanied by the corresponding alpha-fission to produce nitrile products, like in the Beckmann fragmentation reaction. Instead, the photo-Beckmann reaction is a method to produce the regioisomeric amide product **I-62** (Scheme I-16).

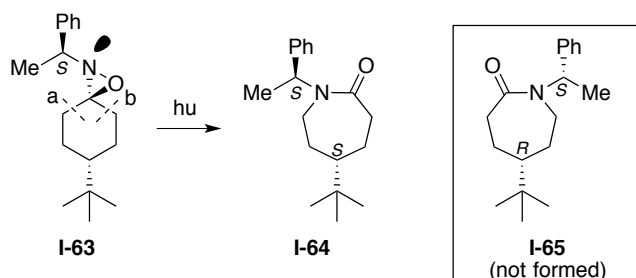


Scheme I-16. Photo-Beckmann reaction.

Traditional acid-catalyzed Beckmann reactions typically show the migration of the carbon bond *anti* to the hydroxyl group of the oxime. Whereas in the photo-Beckmann reaction, stereoelectronic control dictates that the group *anti* to the lone pair of the oxaziridine is the one that migrates to the nitrogen atom. Only empirical evidence of this transformation exists; it suggests that the photo-Beckmann rearrangement reaction involves the photochemical *E,Z*-isomerization of oxime **I-39** (Scheme I-16).¹²⁶ The work

of Suginome *et al.* for the photo-Beckmann reaction shows the transformations of the excited singlet *E*- and *Z*-oximes **I-39** into oxaziridine intermediate **I-61** before the molecule is reorganized to the resulting amide **I-62** in a fully concerted manner.

Lattes and coworkers studied oxaziridine **I-63** in which both bonds adjacent to the oxaziridine ring are chemically equivalent which rules out a possible steric influence of neighboring groups (Scheme I-17).¹²⁷ X-ray analysis and NMR spectroscopy of **I-63** and its reaction product after irradiation of the oxaziridine, determined the formation of lactam **I-64**. Their work also concluded that the position of the nitrogen lone pair is *anti* to bond “a.” Thus, oxaziridine **I-63** generated amide **I-64** by breaking bond “a” and not bond “b” and lactam **I-65** did not form.

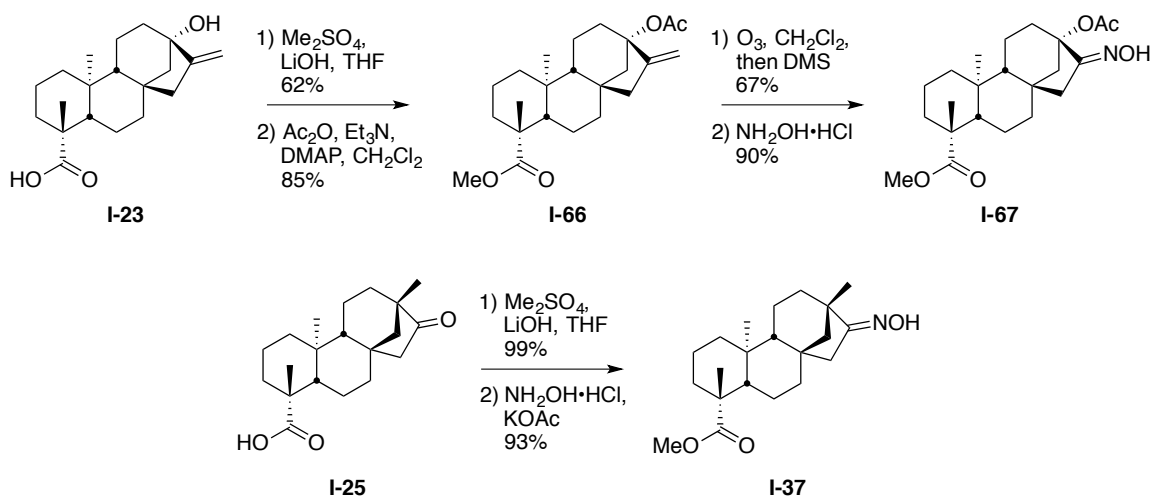


Scheme I-17. Mechanism of oxaziridine in photo-Beckmann rearrangement.

The interesting outcomes of the possible Beckmann reactions encouraged us to look into this existing research further when developing scaffolds around steviol and isosteviol. The next section covers our published work with oximes reactions of these aglycones.⁵¹

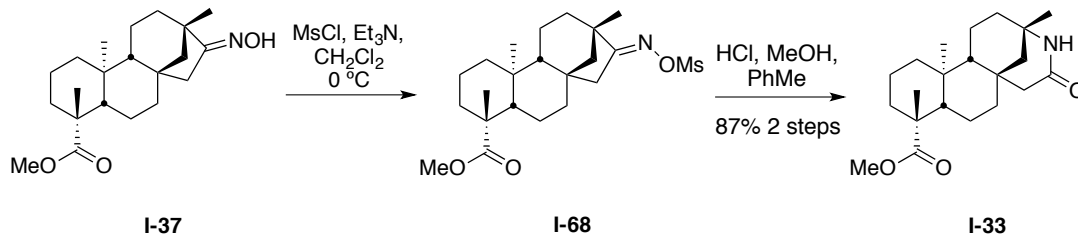
B. Oxime Reactions of Steviol and Isosteviol

The following examples show the versatility of the Beckmann reaction in the formation of novel structures by exploring the *ent*-kaurene skeleton of stevioside (**I-8**). Our group initially applied a diversity-oriented approach to synthesize multiple templates from steviol (**I-23**) and isosteviol (**I-25**), but continued to explore various reaction routes from two of those scaffolds: the steviol and isosteviol oximes, **I-67** and **I-37**, respectively (Scheme I-18).⁵¹ To synthesize the steviol oxime, the acid and the hydroxyl moieties were protected to ease the handling of the compounds and the reaction products. First, esterification with dimethyl sulfate followed by acetylation of the C-13 hydroxyl gave intermediate ester **I-66** in good yields for both reactions. Next, ozonolysis of the methylene produced a ketone that was then treated with hydroxylamine to generate the steviol oxime **I-67**. Isosteviol oxime **I-37** was produced by esterification of the C-4 acid followed by oxime formation of the C-16 ketone. From these oximes, multiple scaffolds were prepared from Beckmann rearrangement, Beckmann fragmentation, and photo-Beckmann reactions.



Scheme I-18. Synthesis of steviol oxime **I-67** and isosteviol oxime **I-37**.

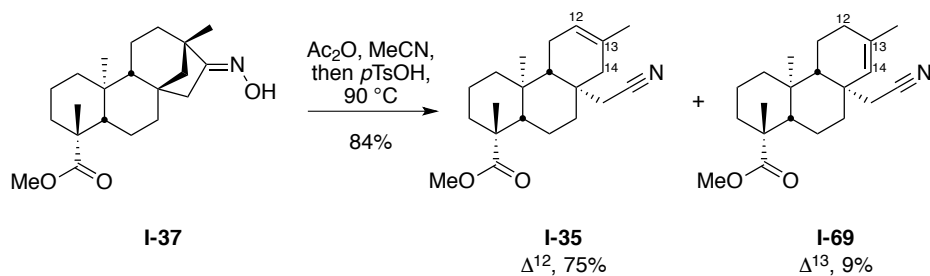
From isosteviol oxime **I-37**, we initially observed the Beckmann rearrangement and fragmentation products (Scheme I-8). When **I-37** was treated with thionyl chloride, an almost 1:2 mixture of the lactam and nitrile products, respectively, was observed. We then tried to change reaction conditions to selectively engender either the Beckmann rearrangement product or the Beckmann fragmentation product in a series of trials (and errors). First, oxime **I-37** was treated with mesyl chloride to produce the mesylated-oxime intermediate **I-68** (Scheme I-23). Then, under acidic conditions made with hydrochloric acid, lactam **I-33**, the Beckmann rearrangement product, was obtained as the sole product, thus shutting out the Beckmann fragmentation pathway.⁵¹ This idea was developed from studying the work of White *et al.* during their morphine synthesis. They formed a brosylated oxime intermediate in acetic acid to provide the desired lactam, whereas the



Scheme I-19. Beckmann rearrangement of oxime **I-37**.

reaction of the corresponding oxime under acidic conditions did not yield any lactam product.¹²⁸ Despite being relatively hindered, this amide lends itself well to alkylation and was useful in the development of small-molecule libraries of lactam derivatives, *vide supra*.

Previously, Coates *et al.* reported a Beckmann fragmentation reaction using TsCl in DMF, but this delivered a 2:1 mixture of the alkenes that required a difficult separation.¹²⁹ With this problem in mind, we investigated the suitability of this fragmentation pathway for further library production (Scheme I-20). In our hands, a selective Beckmann fragmentation was achieved by reaction of isosteviol oxime **I-37** with acetic anhydride in acetonitrile, followed by treatment with *p*TsOH in acetonitrile at 90 °C. This reaction with *p*-toluenesulfonic acid cleanly delivered the $\Delta^{12}:\Delta^{13}$ olefinic nitriles **I-35** and **I-69** in an 8:1 ratio, respectively, in 84% yield. Through a single crystallization

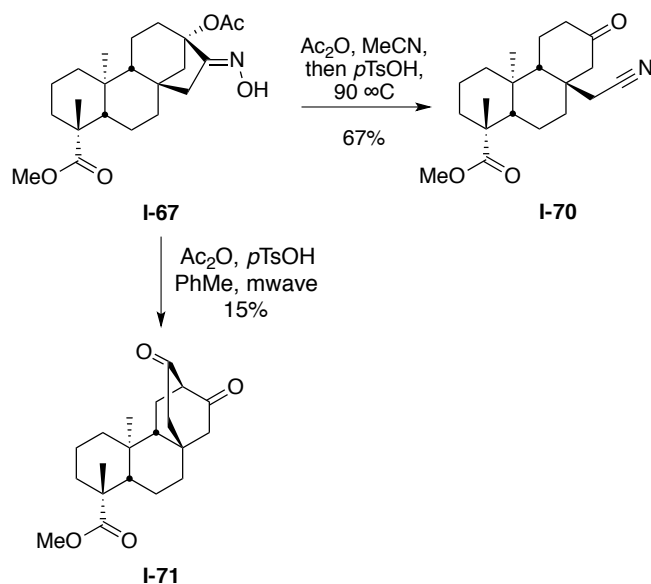


Scheme I-20. Beckmann Fragmentation of isosteviol oxime **I-37**.

with dichloromethane and ethyl acetate, this mixture could be enriched to 20:1 in favor of the Δ^{12} -nitrile product **I-35**. The more robust 2-step procedure perhaps proceeds *via* a tetrahedral intermediate in a similar fashion to that described by White *et al.*, in which the less sterically crowded anti-stereoisomer favors the migration of the bridgehead carbon in the lactam formation.¹³⁰ The Beckmann fragmentation reaction is well documented for systems with a quaternary carbon.¹³¹

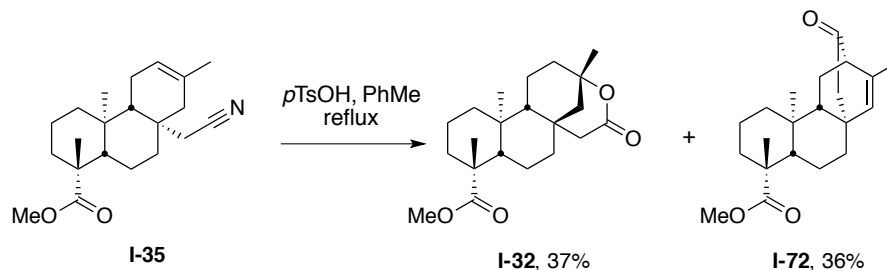
Likewise, we repeated the Beckmann fragmentation reaction with the steviol oxime intermediate **I-67** (Scheme I-21). Upon reaction with acetic anhydride and *p*-toluenesulfonic acid in acetonitrile at 90 °C, the steviol oxime **I-67** exclusively formed

nitrile **I-70**, as expected, in 67% yield. However, when the solvent is changed, the reaction product was completely unexpected. With vigorous heating in toluene, we observed a bicyclo[2.2.2]octane product **I-71**. We determined that the oxime **I-67** undergoes a Thorpe-Ziegler-type cyclization process to afford the octane diketone **I-71**.⁵¹ These experiments suggest that the reaction outcomes are partly determined by the character of the oxime leaving groups. Good leaving groups such as sulfonates promote Beckmann rearrangement pathway, whereas poorer leaving groups such as the acetates promote the Beckmann fragmentation route.



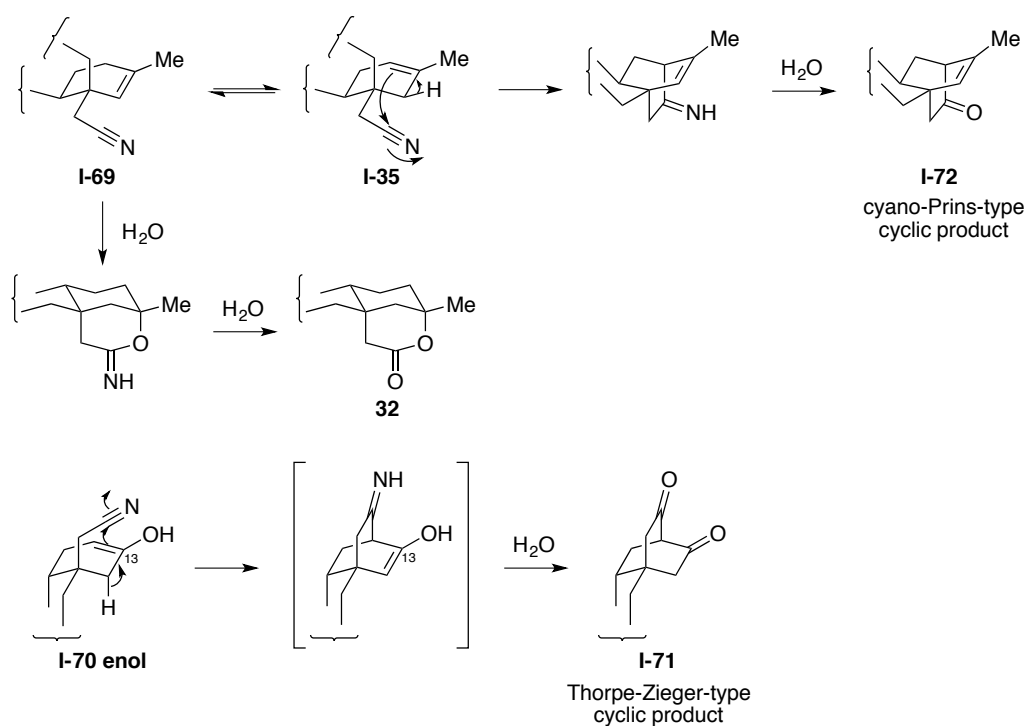
Scheme I-21. Beckmann fragmentation of steviol oxime **I-67**.

Additionally, when the isosteviol oxime **I-37** was subjected to the same reaction conditions as the steviol oxime **I-67** Beckmann fragmentation sequence in an effort to favor the Δ^{12} -nitrile **I-35**, this unexpectedly led to the formation of lactone **I-32** and another bicyclo[2.2.2]octane **I-72** in an almost 1:1 ratio of products in 73% yield (Scheme I-22).



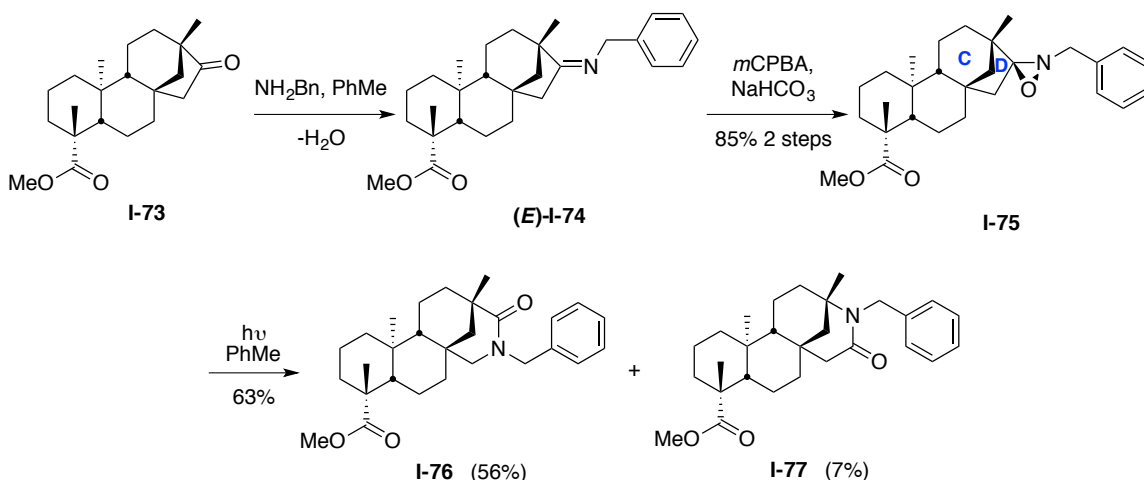
Scheme I-22. Cyclic products from the isosteviol Beckmann fragmentation product **I-35**.

The lactone **I-32** product has been previously observed, *vide supra*, while the cyclic ketone **I-72** product is novel to this work. We conclude that the formation of **I-72** was the result of a cyano-Prins-type cyclization to generate the ketone product.⁵¹ We have proposed the following scheme to show mechanistically how the formations of the cyclic products are possible (Scheme I-23).



Scheme I-23. Proposed mechanisms for the formation of cyclic products.

In our exploration of the Beckmann reaction products of the steviol and isosteviol scaffolds, we also explored the photo-Beckmann rearrangement reaction (Scheme I-24).¹³² This work was initially done to verify the isosteviol lactam **I-32** product. We first converted isosteviol **I-25** to its ester **I-73**. From there, the isosteviol ester **I-73** was heated in the presence of benzylamine under dehydrating conditions to afford imine **I-74**.¹³³ Then, to generate the oxaziridine ring for irradiation, the imine **I-74** was epoxidized with *m*-chloroperoxybenzoic acid to provide oxaziridine **I-75**.



Scheme I-24. Photo-Beckmann of isosteviol ester **I-73**.

Notably, the oxidation occurred exclusively at the *exo* face of the CD-rings. The structure of the oxaziridine was not independently confirmed until we were able to compare the photo-Beckmann lactam product **I-76** with its regioisomeric lactam **I-77** from the photolysis step (Scheme I-24). Equipped with a photochemical immersion well reactor and a 254 nm mercury lamp,¹³⁴ we were able to generate a flow reaction and regioselectively deliver the expected photo-Beckmann lactam **I-76** in 56% yield and the minor regioisomer

I-77 in 7% yield. The minor product **I-77** can also be obtained by synthesizing alkylated lactam libraries of amide **I-33**, (*vide infra*, Scheme I-26). For the Beckmann rearrangement, the bond that migrates is the one that is *anti* to the lone pair on nitrogen,¹³⁵ however, the outcome of the photo-Beckmann is also stereoelectronically defined. That is to say, the stereoelectronic effect of the oxaziridine ring is able to promote the migration of the N-O bond antiperiplanar to the nitrogen lone pair. Formation of minor regioisomer **I-77** is a result from the *exo*-oxaziridine derived from the other imine isomer, (**Z**)-**I-74** (not shown). As stated earlier, the isolation of the lactam **I-76** helped confirm the assignment of the *E*-imine **I-74**.

Chapter 3. Design and Synthesis of Small Molecule Libraries from the Stevioside

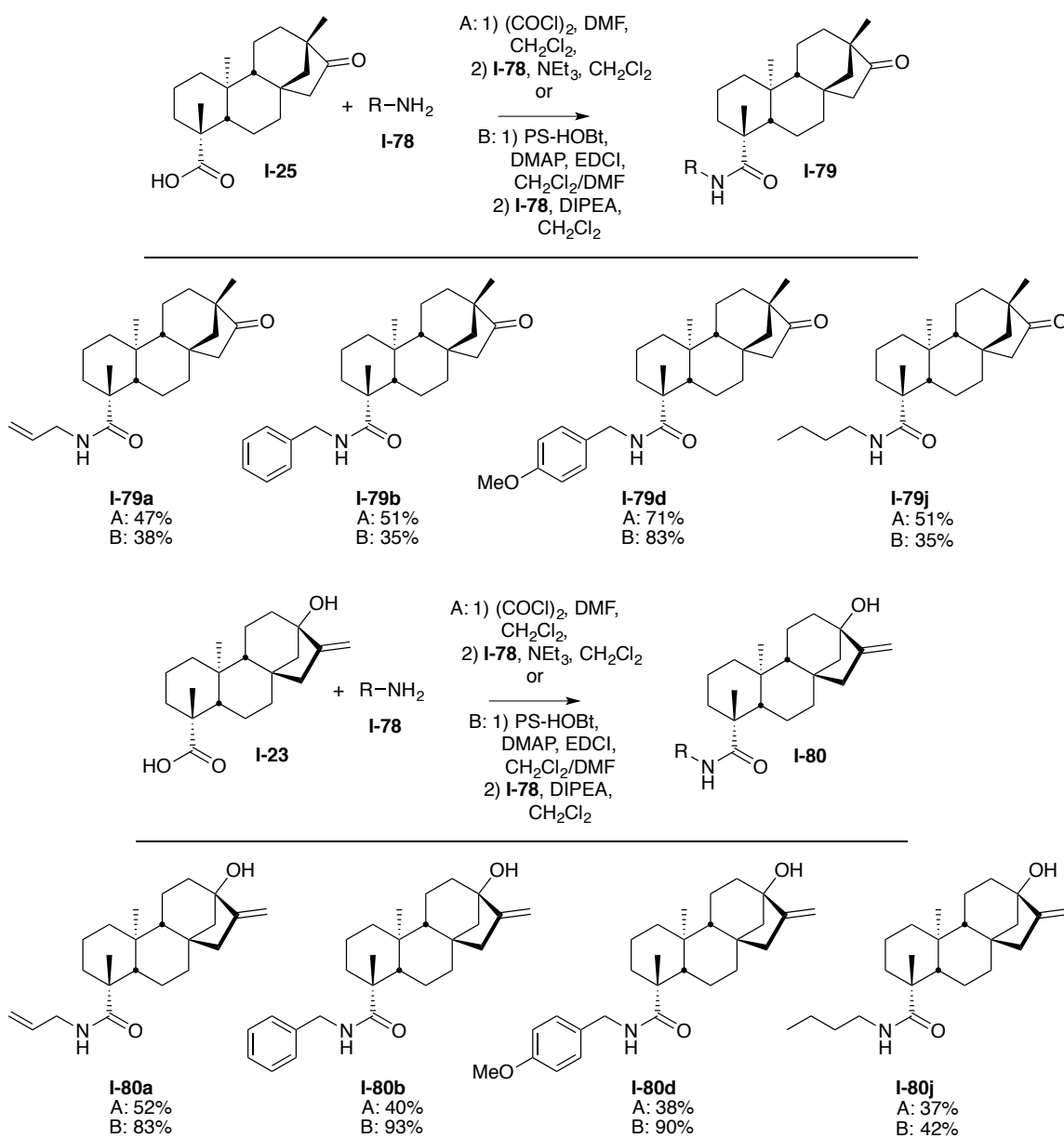
Diterpene Scaffolds

A. Synthesis of Mono-functional Small Molecule Libraries

Steviol and isosteviol serve as scaffolds for library development with reactions aimed at transforming the carboxylic acid moiety of the A-ring in both compounds to amides. Additionally, formation of the oxime intermediate **I-37** from the C-16 ketone of isosteviol was crucial in providing lactam **I-33**, nitrile **I-35**, and amine **I-36** (Scheme I-8). Each of these transformations yielded reaction products that can be further used for library synthesis through amide formation. Another route enlisted explores the D-ring of the *ent*-kaurene core skeleton. D-ring modifications from alkylation of the hydroxyl or amino moieties can further create diverse compounds to explore chemical space.

1. Initial Amide Validation Array

With the steviol aglycones in hand, we set out to prepare a small molecule library using these scaffolds. Validation arrays were set up for the steviol (**I-23**) and isosteviol (**I-25**) molecules for amide bond formation utilizing both solution and solid phase chemistry to provide amides **I-79** and **I-80** (Scheme I-25). These reactions were carried out to compare product yields, ease of work-up, and purity of products. For the solution phase chemistry, steviol (**I-23**) and isosteviol (**I-25**) was converted to the corresponding acid chloride by reaction with oxalyl chloride and then reacted with amines **I-78a**, **b**, **d**, and **j** (Figure I-7) to furnish amides **I-79a**, **b**, **d**, and **j** and **I-80a**, **b**, **d**, and **j**. For the second array, we used polymer-bound 1-hydroxybenzotriazole (HOBt), a reagent that reacts with the acid moiety to form a reactive ester intermediate. Isosteviol was loaded on to the polymer by using the coupling reagent EDCI in the presence of DMAP. The polymer bound activated ester was purified by several washes and then reacted with amines **I-78a**, **b**, **d**, and **j** to form the corresponding amides **I-79a**, **b**, **d**, and **j** and **I-80a**, **b**, **d**, and **j**. Use of the amine as the limiting reagent in this reaction assures high purity of the resulting amide reaction products.



Scheme I-25. Validation array for steviol (**I-23**) and isosteviol (**I-25**) by solution phase (A) and solid phase synthesis (B).

With the solution-phase method we encountered unanticipated problems with solubility during the purification process and NMR analysis showed only 25 to 50 percent conversion of most of the compounds. Eventually, this method was abandoned for an easier solid phase

chemistry approach to obtain multiple compounds in parallel with much easier work up and purification conditions. After careful analysis and comparison of both the solution and solid phase approaches, we decided to carry out a polymer-supported parallel synthesis for the synthesis of our libraries. The resin-bound synthesis approach allowed for a simple filtration to obtain the final products in high purity.

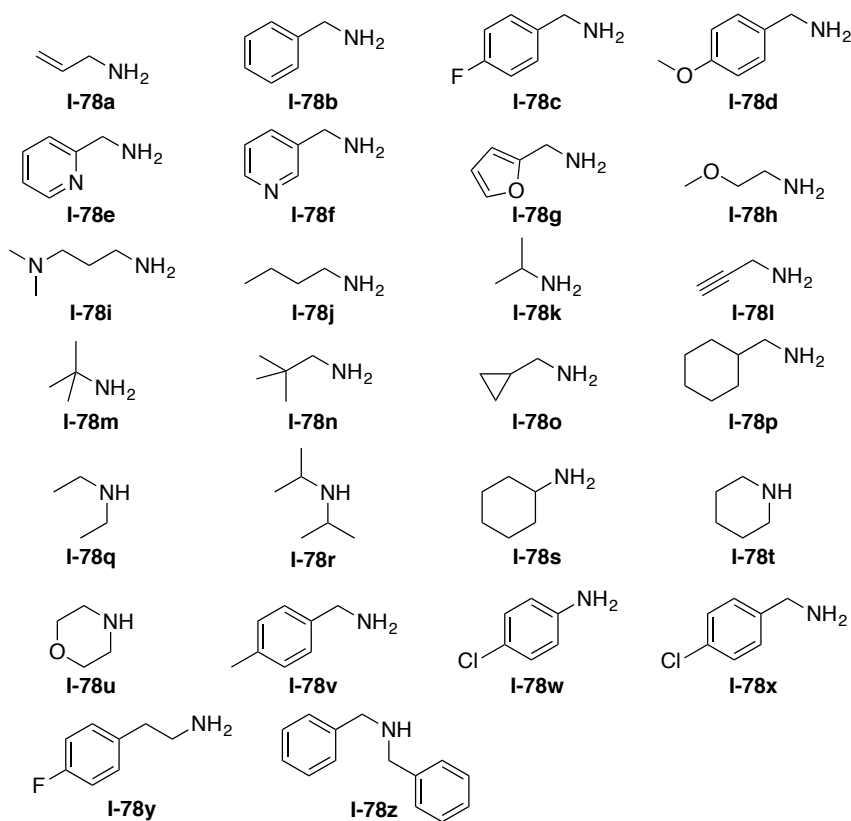
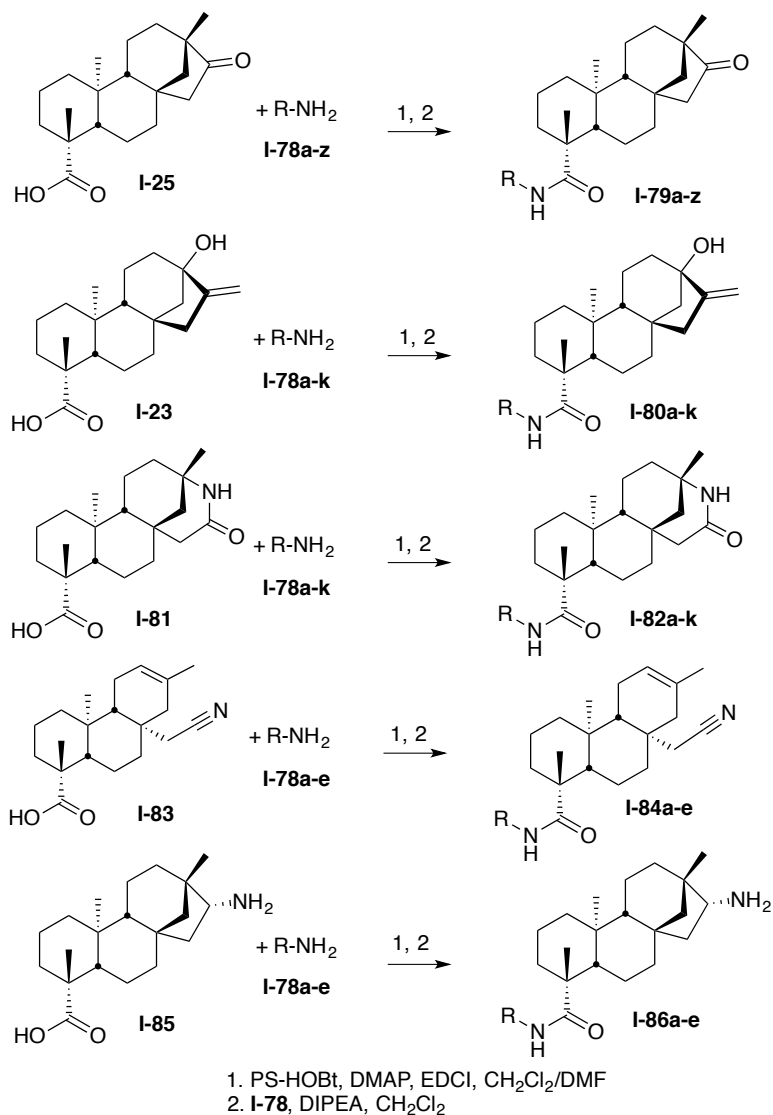


Figure I-7. Amines **I-78a-z** for library synthesis.

2. Amide Libraries

Using parallel solid phase synthesis, we then prepared small libraries from steviol (**I-23**), isosteviol (**I-25**), lactam **I-33**, nitrile **I-35** and amine **I-36** with amines **I-78** (Scheme

I-26). A selection of diverse primary amines was used in the library production (Figure I-7). This work produced almost 60 compounds of diverse amide libraries for evaluation.



Scheme I-26. Amide Libraries I-79, I-80, I-82, I-84, and I-86.

3. Ether and Amine Libraries

After modifying the carboxylic acid moiety on the A ring, modifications of the C and D rings were explored through alkylation of the hydroxyl group of steviol, reduction

of the ketone of isosteviol, and alkylation of the D-ring lactam (Scheme I-27). A small set of alkyl halides were used for the synthesis of alkylated products (Figure I-8).

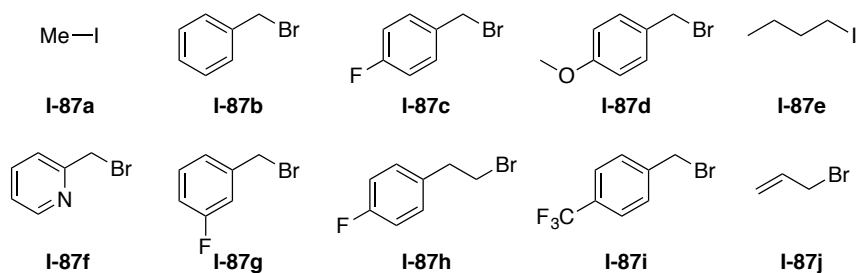
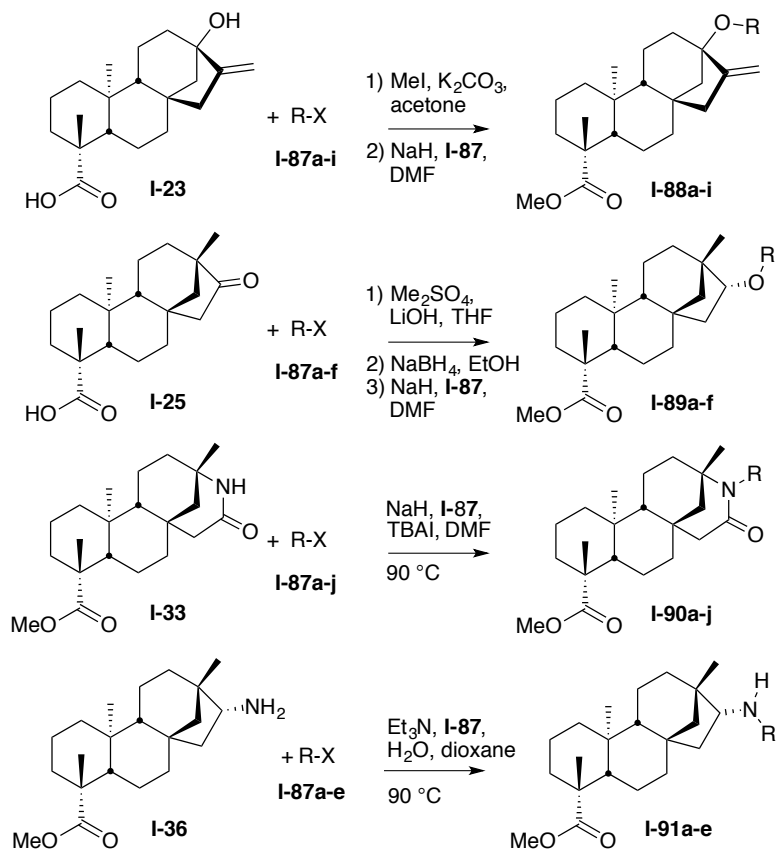


Figure I-8. Alkyl halide compounds for library synthesis.

We first converted the acid functionalities of scaffolds **I-23**, **I-25**, **I-33**, **I-35**, and **I-36** to the corresponding methyl esters. Reacting the hydroxyl group of the steviol methyl ester with alkylating agents **I-87a-i** provided ethers **I-88a-i** (Scheme I-27). The C-16 ketone group of the isosteviol methyl ester was reduced with sodium borohydride to yield the corresponding secondary alcohol, which then was alkylated with **I-87a-f** to provide ethers **I-89a-f**.¹³⁶ *N*-Alkylated lactams **I-90a-j** were obtained by reaction of lactam **I-33** with **I-87a-j**, while *N*-alkylated amines **I-91a-e** were generated from reacting amine **I-36** with **I-87a-e**. The alkylation reactions for steviol, isosteviol, and lactam **I-33** were carried out with sodium hydride, because a strong base was necessary to facilitate the removal of the hydroxyl proton for ether formation and amide proton for lactam alkylation. This route created a 30-membered library of *O*- and *N*-alkylated reaction products.



Scheme I-27. Synthesis of ether and amine libraries.

B. Synthesis of Bifunctional Small Molecular Libraries

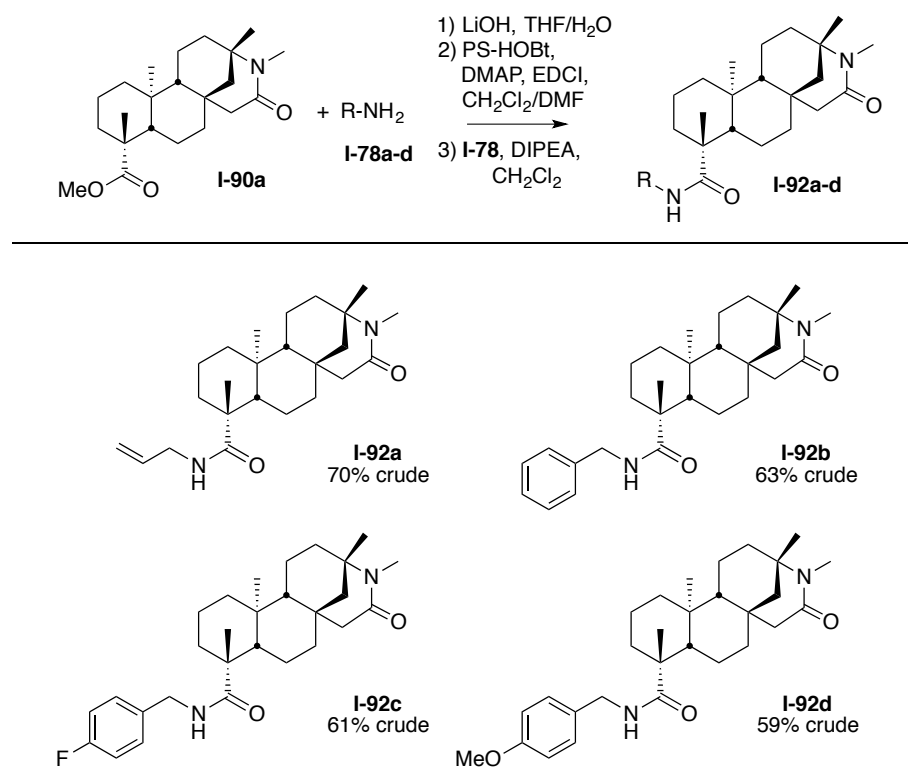
1. Rationale for Bifunctional Libraries

In the drug development and chemical biology disciplines, achieving binding between a target and a small molecule that is generating a biological effect is the starting point that drives further structure-activity exploration. In order to enhance biological activity, often more than one functional group is added to the molecule to form a bi- or multi-functional molecule. A bifunctional molecule can interact either with one protein or with two protein molecules simultaneously. In some instances, a molecule that consists of two protein-binding groups can be connected via a linker.¹³⁷ While most linker regions

consist of cleavable groups¹³⁸ or drug molecules,¹³⁹ there have been molecules with a natural product in the linker region.¹⁴⁰ In the synthesis of our bifunctional libraries, the *ent*-kaurene will essentially serve as the linker with functional groups flanking either end of the scaffold. In addition, drug-like combinatorial libraries can be generated from combinations of “natural product-like” scaffolds and “drug-like” functional groups.¹⁴¹ As noted by Corson *et al.*, having two functional groups that can potentially bind is better than one, especially in terms of increasing activity.¹³⁷ Here, we attempted to expand the potential of biological activity of our compounds by generating bifunctional molecules.

2. Synthesis of Bifunctional Libraries

Bifunctional libraries can be prepared using alkylated products **I-87** through **I-90** and synthesizing their respective amides. Scheme I-28 shows a representative example of one such library: the reaction of *N*-methyl amide analog **I-90a** from previous library synthesis, *vide supra*, with amines **I-78a-d**. First, we hydrolyzed the ester to expose the carboxylic acid for amide production. Then, standard amide formation with polymer-supported chemistry, *vide supra*, generated bifunctional *N*-methyl lactam amides **I-92a-d**.



Scheme I-28. Synthesis of a bifunctional library from amide **I-50a**.

C. Evaluation of Steviol- and Isosteviol-Derived Libraries

1. Biological Activity of Steviol and Isosteviol Library of Analogs

Compounds were then submitted to the NIH Molecular Libraries Small Molecule Repository for biological evaluation.⁴⁸ Through PubChem mining, we were able to visualize the activity of our compounds. Table I-1 below provides a listing of compounds that were evaluated in over 50 assays by the Molecular Libraries Screening Center Network so far. Several library members, including previously submitted compounds **I-37**, **I-66**, **I-67**, and **I-93** (Figure I-9) that displayed single digit or double digit micromolar inhibition of target proteins are displayed.

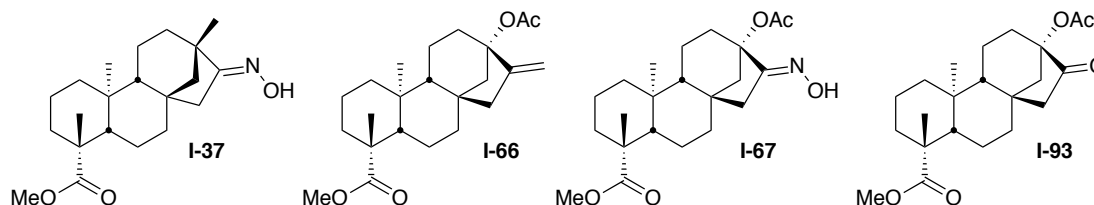
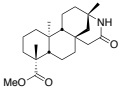
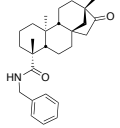


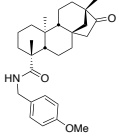
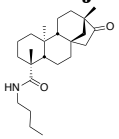
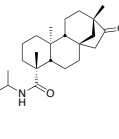
Figure I-9. Other steviol and isosteviol derivatives submitted to the MSLMR.

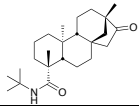
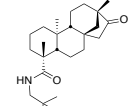
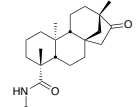
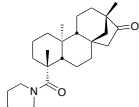
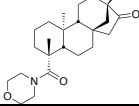
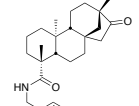
Table I-1 shows current PubChem data on submitted compounds that have been tested by the MSLMR.^{142, 143} The compounds were tested in a variety of assays to determine their bioactivity and identified as a chemical probe, active, inactive, inconclusive, or unspecified in the experiments. The table below only displays compounds that were found to be “active” in primary screens or “active” with concentration data in confirmatory assays. Compounds that were found inactive, inconclusive, or unspecified from the bioactivity results, which make up a majority of the available screening data, are not listed. Typically, initial or primary screens were performed first to determine whether or not a compound is active, followed by confirmatory screens to determine the concentration of the compound in the activity screen.

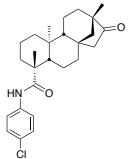
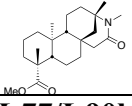
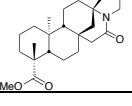
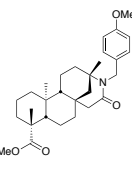
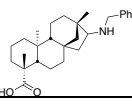
Table I-1. Activity of Steviol and Isosteviol Analogs

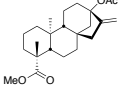
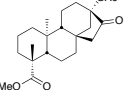
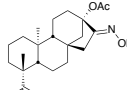
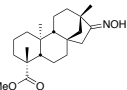
Compound	PubChem ID	Assay ID	BioAssay	Activity (if given)	
				Assay Type	Result or Value (μM)
I-23 	9905087	602438	uHTS identification of modulators of interaction between CendR and NRP-1 using Fluorescence Polarization assay	Primary screen	active
I-25 	42601320	652104	qHTS of TDP-43 inhibitors	Confirmatory screen	IC ₅₀ ^A 19.953

<p>I-33</p> 	42601318	720706	HTS for bacterial rRNA inhibitors measured in microorganism-based system	Primary screen	active
<p>I-79b</p> 	42601330	540271	<i>In vivo</i> -based yeast HTS to detect compounds rescuing yeast growth/survival of Plasmodium Falciparum HSP40-mediated toxicity measured in whole organism system	Confirmatory screen	AbsAC ^C 1.427
		686978	qHTS for inhibitors of human TDP1: qHTS in cells in absence of CPT	Confirmatory screen	EC ₅₀ 18.356
		652041	Cell-based secondary assay to test the inhibitory activity of small molecule on Plasmodium falciparum (HB3 strain) survival in red blood cells measured in cell-based system	Confirmatory screen	AbsAC 21.72
		652047	Cell-based secondary assay to test the inhibitory activity of small molecule on Plasmodium falciparum (3D7 strain) survival in red blood cells measured in cell-based system	Confirmatory screen	AbsAC 30.22
		2825	uHTS Luminescent assay for identification of inhibitors of NALP3 in yeast	Primary screen	active
		435006	Single concentration confirmation of uHTS for the identification of inhibitors of NALP3 in yeast using a luminescent assay	Primary screen	active
		504582	<i>In vivo</i> -based yeast HTS to detect compounds rescuing yeast growth/survival of Plasmodium Falciparum HSP40-mediated toxicity measured in whole organism system	Primary screen	active
I-79d	42601335	624417	qHTS of GLP-1 Receptor Inverse Agonists	Confirmatory screen	EC ₅₀ 10

		624466	Fluorescence-based cell-based primary HTS assay to identify antagonists of human TAAR1	Primary screen	active
		2825	uHTS Luminescent assay for identification of inhibitors of NALP3 in yeast	Primary screen	active
		504582	<i>In vivo</i> -based yeast HTS to detect compounds rescuing yeast growth/survival of Plasmodium Falciparum HSP40-mediated toxicity measured in whole organism system	Primary screen	active
<p>I-79j</p> 	42601331	488784	Single concentration confirmation of inhibitors of NALP3 in yeast using Caspase-1-ASC counter screen	Primary screen	active
		2685	qHTS Assay for Lipid Storage Modulators in Drosophila S3 Cells	Confirmatory screen	EC ₅₀ 0.651
		2825	uHTS Luminescent assay for identification of inhibitors of NALP3 in yeast	Primary screen	active
		463195	uHTS identification of small molecule inhibitors of tim10 yeast via a luminescent assay	Primary screen	active
		435006	Single concentration confirmation of uHTS for the identification of inhibitors of NALP3 in yeast using a luminescent assay	Primary screen	active
		488794	Single concentration confirmation of uHTS for the identification of inhibitors of NALP3 in yeast using a luminescent assay-retest	Primary screen	active
<p>I-79k</p> 	42601329	2825	uHTS Luminescent assay for identification of inhibitors of NALP3 in yeast	Primary screen	active
		488784	Single concentration confirmation of inhibitors of NALP3 in yeast using Caspase-1-ASC counter screen	Primary screen	active

		488794	Single concentration confirmation of uHTS for the identification of inhibitors of NALP3 in yeast using a luminescent assay-retest	Primary screen	active
I-79m 	42601326	2825	uHTS Luminescent assay for identification of inhibitors of NALP3 in yeast	Primary screen	active
I-79n 	42601334	686978	qHTS for inhibitors of human TDP1: qHTS in cells in absence of CPT	Confirmatory screen	EC ₅₀ 23.109
I-79s 	42601327	686978	qHTS for inhibitors of human TDP1: qHTS in cells in absence of CPT	Confirmatory screen	EC ₅₀ 23.109
		686979	qHTS for inhibitors of human TDP1: qHTS in cells in absence of CPT	Confirmatory screen	EC ₅₀ 18.356
		602438	uHTS identification of modulators of interactions between CendR and NRP-1 using Fluorescence Polarization assay	Primary screen	active
I-79t 	42601332	602123	Fluorescence polarization-based primary biochemical HTS assay to identify inhibitors of E. coli DNA-binding ATP-dependent protease La (eLon)	Primary screen	active
		624169	Luminescence-based cell-based primary HTS assay to identify agonists of the mouse HTR2A	Primary screen	active
I-79u 	42601333	652048	qHTS of D3 Dopamine Receptor Agonist	Primary screen	active
		652051	qHTS of D3 Dopamine Receptor Potentiators	Primary screen	active
I-79v 	42601336	504582	<i>In vivo</i> -based yeast HTS to detect compounds rescuing yeast growth/survival of Plasmodium Falciparum HSP40-mediated toxicity measured in whole organism system	Primary screen	active

I-79w 	42601328	602438	uHTS identification of modulators of interactions between CendR and NRP-1 using Fluorescence Polarization assay	Primary screen	active
I-90a 	42601319	-	Inconclusive data in 7 assays and inactive in 417 assays	Primary screen	inactive
I-77/I-90b 	53299290	-	N/A	N/A	N/A
I-90c 	42601337	624132	Shn3: Dual-Go Shn3RL cells measured in cell-based system	Confirmatory screen	AC ₅₀ ^D 10.58
		624133	Schnurri-3 Inhibitors: specific inducers of adult bone formation measured in cell-based system	Confirmatory screen	AC ₅₀ 8.16
		504832	Primary qHTS for delayed death inhibitors of the malarial parasite plastid, 48 hr incubation	Confirmatory screen	IC ₅₀ 1.651
		504834	Primary qHTS for delayed death inhibitors of the malarial parasite plastid, 96 h incubation	Confirmatory screen	IC ₅₀ 1.472
		504444	Nrf2 qHTS screen for inhibitors	Confirmatory screen	IC ₅₀ 14.581
		651820	qHTS assay for inhibitors of Hepatitis C Virus	Confirmatory screen	IC ₅₀ 12.589
		686978	qHTS for inhibitors of human TDP1: qHTS in cells in absence of CPT	Confirmatory screen	EC ₅₀ 6.513
		686979	qHTS for inhibitors of human TDP1: qHTS in cells in absence of CPT	Confirmatory screen	EC ₅₀ 11.582
		743417	Schnurri-3 Inhibitors: specific inducers of adult bone formation measured in cell-based system	Confirmatory screen	AC ₅₀ 8.16
I-91b 	42601325	686978	qHTS for inhibitors of human TDP1: qHTS in cells in absence of CPT	Confirmatory screen	EC ₅₀ 20.596

I-66 	42601321	588850	uHTS identification of cystic fibrosis induced NFkB inhibitors in a fluorescence assay	Primary screen	active
		686979	qHTS for inhibitors of human TDP1: qHTS in cells in absence of CPT	Confirmatory screen	EC ₅₀ 18.356
		602438	uHTS identification of modulators of interactions between CendR and NRP-1 using Fluorescence Polarization assay	Primary screen	active
I-93 	42601322	686979	qHTS for inhibitors of human TDP1: qHTS in cells in absence of CPT	Confirmatory screen	EC ₅₀ 20.596
		624466	Fluorescence-based cell-based primary HTS assay to identify antagonists of human TAAR1	Primary screen	active
I-67 	42601323	686978	qHTS for inhibitors of human TDP1: qHTS in cells in absence of CPT	Confirmatory screen	EC ₅₀ 16.360
		686979	qHTS for inhibitors of human TDP1: qHTS in cells in absence of CPT	Confirmatory screen	EC ₅₀ 16.360
I-37 	42601324	686978	qHTS of inhibitors of human TDP1: qHTS in cells in absence of CPT	Confirmatory screen	EC ₅₀ ^B 20.596
		463212	uHTS identification of small molecule inhibitors of tim23-1 yeast via a luminescent assay	Primary screen	active
		463218	Single concentration confirmation of small molecule inhibitors of tim23-1 yeast via a luminescent assay	Primary screen	active

^AIC₅₀= concentration of an inhibitor required for 50% inhibition of maximum control response;

^BEC₅₀= concentration of an agonist required to produce 50% maximum (effective) response;

^CAbsAC= Absolute active concentration with compounds below 10 μM to be considered active hits;

^DAC₅₀= concentration required to elicit a 50% response in an *in vitro* assay

Our small molecule libraries showed activity in numerous assays with a variety of protein targets, including neuropilin-1 (NRP-1), tyrosyl-DNA phosphodiesterase 1

(TDP1), NACHT, Leucine-rich repeat, Pyrin domain-containing-3 (NALP3), hepatitis C virus (HCV), glucagon-like peptide-1 (GLP1), or lipid storage modulators. NRP-1 is a protein receptor for vascular endothelial growth factor; it plays a role in angiogenesis and is being studied for its role in tumor growth progression for anticancer research.^{144, 145} The TDP1 enzyme is also investigated for its anticancer development through its mechanism of DNA repair and treatment for spinocerebellar ataxia, which is caused by a TDP1 mutation.¹⁴⁶ Furthermore, many of our compounds showed activity in an assay for NALP3, a protein that is involved in the inflammatory process of the human innate immune system.¹⁴⁷ Primary screens for inhibitors of the NALP3 protein can provide potential starting points for anti-inflammatory therapeutic development.¹⁴⁸ Lactam **I-50c** showed low micromolar activity in a confirmatory inhibitor assay for HCV (Table I-1). Current treatments for HCV infections are costly and poorly accessible, and there is an unmet need to develop a detection method to diagnose those who are infected.¹⁴⁹ Recently, Lin *et al.* created a 33 ureido- and amide-substituted steviol analogs, similar to amide products **I-40a-k** of steviol (**I-23**), to study their inhibitory effects against the Hepatitis B Virus (HBV), which similar to HCV infections can lead to liver cirrhosis and cancer.⁹⁵ Their work demonstrates the importance of using natural products and their analogs as sources for therapeutic research as well as implies the potential for isosteviol analogs to be further investigated in HBV drug development. Finally, both GLP1 and lipid storage modulators have been instrumental in diabetes and anti-obesity research.^{150, 151} Our compounds showed at least 10 micromolar activity in confirmatory assays for these proteins (Table I-1).

2. Computational Comparison with Commercial Libraries

Additionally, we sought to determine the potential utility of the compounds by measuring parameters beyond the Lipinski's "rule of five."¹⁵² Walters and coworkers previously analyzed over 415,000 molecules reported in the *Journal of Medicinal Chemistry* from 1959 to 2009.¹⁵³ In their investigation, they identified eight important properties for all the drugs or drug-like molecules to be molecular weight (MW), cLogP, total polar surface area (TPSA), rotatable bonds, hydrogen bond donors (HBD), hydrogen bond acceptors (HBA), complexity, and fraction of sp^3 carbons (Fsp3). From this information, Hergenrother and coworkers established the importance for compounds to have higher Fsp3 values, from 0 to 1, and lower cLogP values, lower than 5 units, in order to be developed into drugs.¹⁵⁴ The Fsp3 value pertains to the number of sp^3 -hybridized carbon atoms in a compound divided by the sum of carbon atoms and this value can indicate lower melting points as well as enhanced aqueous solubility.¹⁵⁵ They calculated four main parameters: Fsp3, cLogP, number of stereocenters, and Tanimoto similarity coefficients of their compounds compared to a 150,000-member ChemBridge collection. In our case, we compared our library to the ChemBridge CombiSet and the Maybridge Diversity Set of compounds, which contain 30,000 and about 54,000 compounds, respectively. We expected this would offer insight in to the diversity of our libraries relative to two commercially-available libraries.

Similarly, our group employed the Pipeline Pilot software to calculate ALogP values,¹⁵⁶ the number of stereocenters, and the Fsp3 ratio.¹⁵⁷ While our compounds have an average cLogP of 4.69, the compounds investigated by Hergenrother *et al.* had an average cLogP of 2.90 (Chart I-1).¹⁵⁴

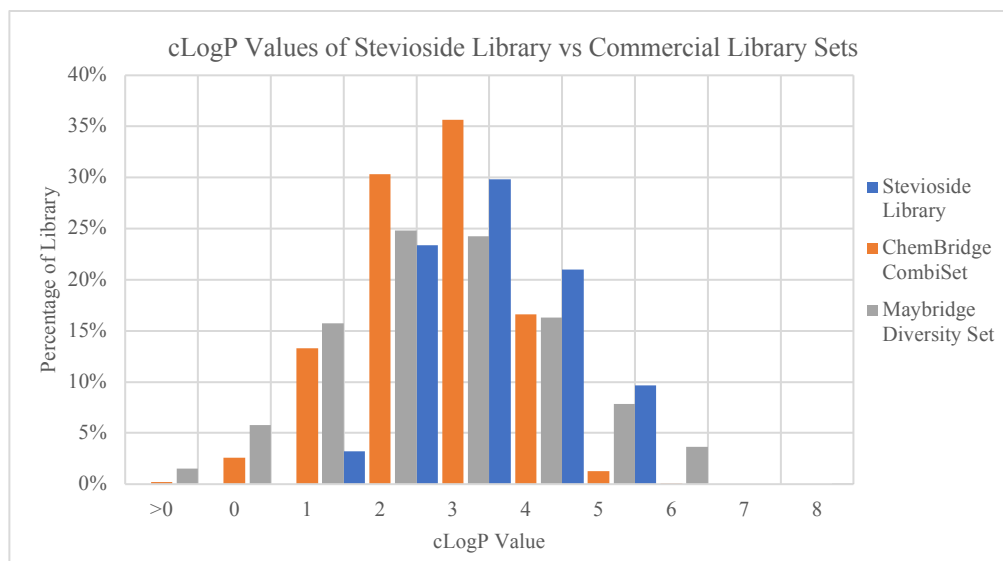


Chart I-1. Comparison of cLogP values.

The ChemBridge and MayBridge library sets that we chose for comparison have an average cLogP value of 3.11 and 3.04, respectively. With such a lipophilic core scaffold, we endeavored to create less lipophilic compounds by adding various substituents and hydrophilic groups that would lower cLogP values. Our Fsp3 calculations yielded an average of 0.79, while the ChemBridge and MayBridge libraries have average Fsp3 values of 0.45 and 0.22, respectively (Chart I-2).

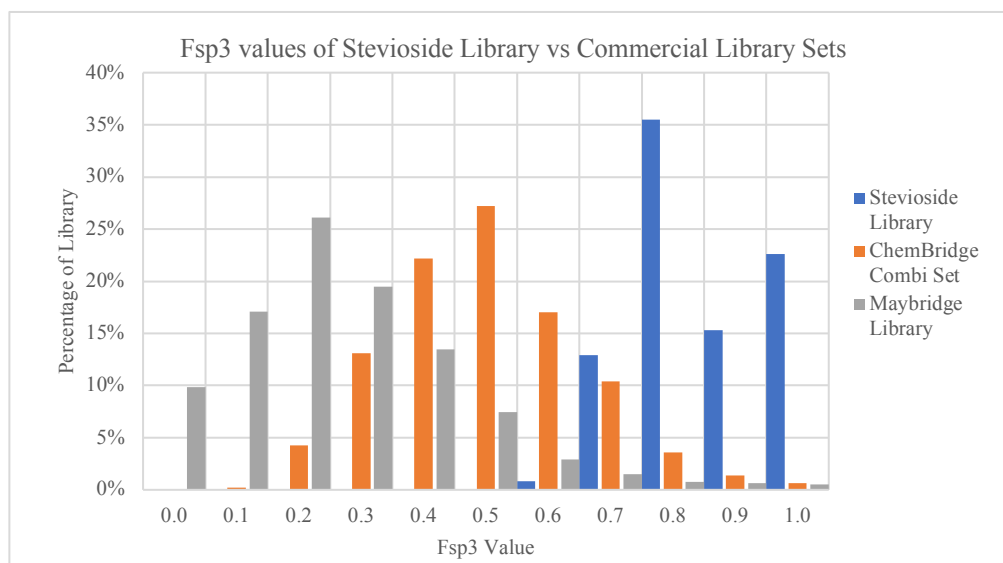


Chart I-2. Comparison of Fsp3 values.

The number of stereocenters in a compound can correlate to its structural complexity; on average, the structures in our compound library contained six stereocenters, while the ChemBridge and Maybridge libraries both have zero averages. Interestingly, Hergenrother's library of compounds had an average of 5.17 stereocenters (Chart I-3).¹⁵⁴ The majority of the compounds in the commercial libraries contain aromatic rings and aryl group substitutions to account for their lack of stereocenters.

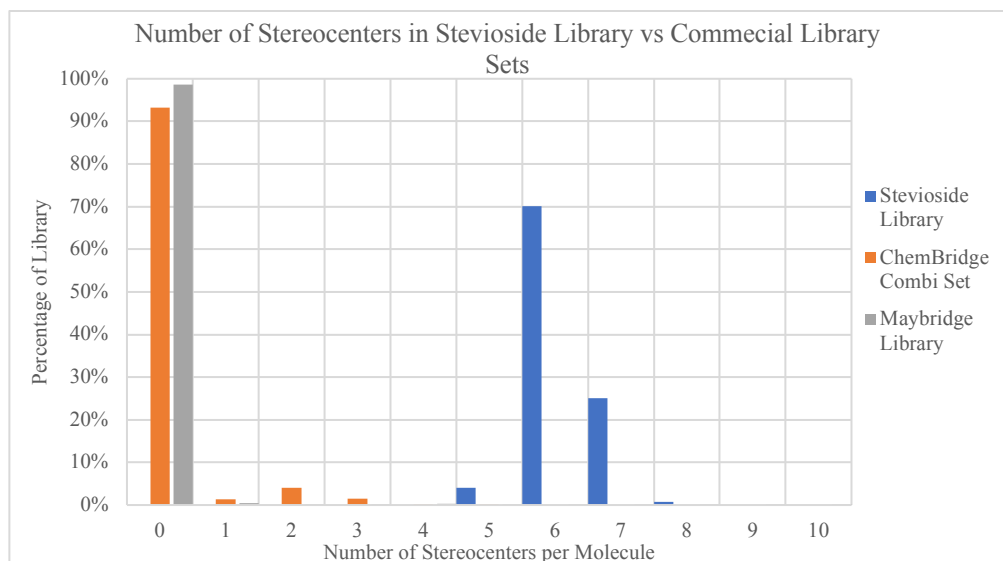


Chart I-3. Comparison of the number stereocenters per molecule.

Our compounds as well as those in the compound library of Hergenrother's group appear to be more structurally complex with a greater number of stereocenters because they are natural product analogs. ChemBridge and Maybridge compound libraries contain compounds with no or few stereocenters. This is perhaps because less complex molecules are relatively easier to synthesize.¹⁵⁸

Furthermore, similarity coefficients were generated (Tanimoto, ECFP₄) to determine the structural similarity between the compounds in our libraries. These values are graphed in a matrix format in Chart 1 to allow visualization of the pairwise similarity of the compounds. That is an intersection of a column and a row contains the calculated similarity between the compounds in the row and column. Low scores (blue) indicate a relatively high level of difference between the structures, while high scores (red) indicate very similar ($0.700 < \text{ratio} < 1.00$) or the identical structure (coefficient = 1.00) when a compound is compared to itself. Low (blue) pairwise similarity is desired in a diverse library. The calculated average similarity between compounds in the library was 0.44.

Over half, or 63%, of the complete steviol and isosteviol analog library compounds had similarities below 0.44, represented in Chart 1 as indicated by the blue cells in Chart 1.

Cmpd	24	25	11{1}	10{1}	13{1}	11{5}	10{5}	13{5}	19{2}	17{2}	15{2}	20{3}	20{5}	21{3}	21{5}	22{3}	22{5}	23{1}	26	27	8	5	7	2	1
24	1.000	0.792	0.456	0.406	0.389	0.403	0.346	0.333	0.677	0.329	0.262	0.444	0.463	0.472	0.507	0.438	0.456	0.384	0.737	0.567	0.525	0.576	0.420	0.443	0.525
25	0.792	1.000	0.380	0.455	0.394	0.338	0.405	0.354	0.561	0.333	0.265	0.451	0.470	0.500	0.538	0.444	0.463	0.389	0.750	0.576	0.534	0.614	0.426	0.526	0.435
11{1}	0.456	0.380	1.000	0.695	0.661	0.657	0.440	0.423	0.427	0.425	0.346	0.321	0.329	0.346	0.368	0.333	0.342	0.651	0.378	0.406	0.348	0.391	0.295	0.444	0.691
10{1}	0.406	0.455	0.695	1.000	0.712	0.453	0.631	0.453	0.382	0.437	0.354	0.329	0.338	0.372	0.397	0.342	0.351	0.700	0.370	0.462	0.358	0.424	0.303	0.648	0.444
13{1}	0.389	0.394	0.661	0.712	1.000	0.436	0.453	0.647	0.367	0.419	0.341	0.317	0.325	0.358	0.382	0.329	0.338	0.667	0.355	0.380	0.343	0.644	0.291	0.438	0.424
11{5}	0.403	0.338	0.657	0.453	0.436	1.000	0.721	0.690	0.450	0.487	0.405	0.318	0.294	0.341	0.329	0.345	0.306	0.430	0.337	0.359	0.308	0.346	0.279	0.389	0.594
10{5}	0.346	0.405	0.440	0.631	0.453	0.721	1.000	0.746	0.395	0.507	0.420	0.329	0.305	0.369	0.358	0.357	0.317	0.447	0.333	0.411	0.320	0.378	0.289	0.565	0.375
13{5}	0.333	0.354	0.423	0.453	0.647	0.690	0.746	1.000	0.381	0.487	0.405	0.318	0.294	0.356	0.345	0.345	0.306	0.430	0.321	0.342	0.308	0.567	0.279	0.389	0.360
19{2}	0.677	0.561	0.427	0.382	0.367	0.450	0.395	0.381	1.000	0.434	0.357	0.514	0.432	0.500	0.473	0.468	0.427	0.363	0.529	0.500	0.463	0.507	0.413	0.391	0.463
17{2}	0.329	0.333	0.425	0.437	0.419	0.487	0.507	0.487	0.434	1.000	0.521	0.453	0.411	0.354	0.325	0.507	0.425	0.413	0.316	0.338	0.583	0.342	0.288	0.368	0.357
15{2}	0.262	0.265	0.346	0.354	0.341	0.405	0.420	0.405	0.357	0.521	1.000	0.281	0.241	0.289	0.261	0.322	0.253	0.337	0.253	0.268	0.250	0.272	0.662	0.289	0.282
20{3}	0.444	0.451	0.321	0.329	0.317	0.318	0.329	0.318	0.514	0.453	0.281	1.000	0.656	0.583	0.434	0.712	0.529	0.313	0.427	0.457	0.581	0.464	0.395	0.352	0.342
20{5}	0.463	0.470	0.329	0.338	0.325	0.294	0.305	0.294	0.432	0.411	0.241	0.656	1.000	0.421	0.537	0.529	0.683	0.321	0.443	0.477	0.643	0.484	0.389	0.364	0.353
21{3}	0.472	0.500	0.346	0.372	0.358	0.341	0.369	0.356	0.500	0.354	0.289	0.583	0.421	1.000	0.682	0.575	0.416	0.461	0.453	0.486	0.449	0.515	0.403	0.400	0.370
21{5}	0.507	0.538	0.368	0.397	0.382	0.329	0.358	0.345	0.473	0.325	0.261	0.434	0.537	0.682	1.000	0.429	0.529	0.493	0.486	0.523	0.484	0.556	0.411	0.431	0.397
22{3}	0.438	0.444	0.333	0.342	0.329	0.345	0.357	0.345	0.468	0.507	0.322	0.712	0.529	0.575	0.429	1.000	0.662	0.325	0.421	0.451	0.571	0.457	0.390	0.347	0.338
22{5}	0.456	0.463	0.342	0.351	0.338	0.306	0.317	0.306	0.427	0.425	0.253	0.529	0.683	0.416	0.529	0.662	1.000	0.333	0.437	0.470	0.632	0.477	0.384	0.358	0.348
23{1}	0.384	0.389	0.651	0.700	0.667	0.430	0.447	0.430	0.363	0.413	0.337	0.313	0.321	0.461	0.493	0.325	0.333	1.000	0.351	0.375	0.338	0.400	0.288	0.431	0.418
26	0.737	0.750	0.378	0.370	0.355	0.337	0.333	0.321	0.529	0.316	0.253	0.427	0.443	0.453	0.486	0.421	0.437	0.351	1.000	0.732	0.500	0.548	0.403	0.444	0.431
27	0.567	0.576	0.406	0.462	0.380	0.359	0.411	0.342	0.500	0.338	0.268	0.457	0.477	0.486	0.523	0.451	0.470	0.375	0.732	1.000	0.544	0.596	0.433	0.564	0.467
8	0.525	0.534	0.348	0.358	0.343	0.308	0.320	0.308	0.463	0.583	0.250	0.581	0.643	0.449	0.484	0.571	0.632	0.338	0.500	0.544	1.000	0.554	0.415	0.414	0.400
5	0.576	0.614	0.391	0.424	0.644	0.346	0.378	0.567	0.507	0.342	0.272	0.464	0.484	0.515	0.556	0.457	0.477	0.400	0.548	0.596	0.554	1.000	0.439	0.491	0.450
7	0.420	0.426	0.295	0.303	0.291	0.279	0.289	0.279	0.413	0.288	0.662	0.395	0.389	0.403	0.411	0.390	0.384	0.288	0.403	0.433	0.415	0.439	1.000	0.324	0.314
2	0.443	0.526	0.444	0.648	0.438	0.389	0.565	0.389	0.391	0.368	0.289	0.352	0.364	0.400	0.431	0.347	0.358	0.431	0.444	0.564	0.414	0.491	0.324	1.000	0.640
1	0.525	0.435	0.691	0.444	0.424	0.594	0.375	0.360	0.463	0.357	0.282	0.342	0.353	0.370	0.397	0.338	0.348	0.418	0.431	0.467	0.400	0.450	0.314	0.640	1.000

Chart I-4. A representative chart of the pairwise similarity for the steviol and isosteviol library compounds described herein. Red indicates similarity coefficient of 1.0 (identical) and Blue indicates pairwise structural comparison with similarities less than the average pairwise similarity for the entire library.^a

^aA full chart is available in the Appendix A.

D. Concluding Remarks

In conclusion, we have designed and synthesized a number of diverse and novel scaffolds from the stevioside aglycones: steviol **I-23** and isosteviol **I-25**. This research was aimed at eliciting potential biological activity from the modified *ent*-kaurene core given the precedence of natural products exhibiting pharmacological properties that can be used for drug discovery. We have shown different approaches in library development from many different templates as well as explored the synthesis of multiple structures derived from the Beckmann reaction pathways. The submitted compounds from our libraries that have been

tested, demonstrate initial activity in a variety of different assays, thus proving the *ent*-kaurene core scaffold is a viable starting point to elicit biological activity and for therapeutic development.

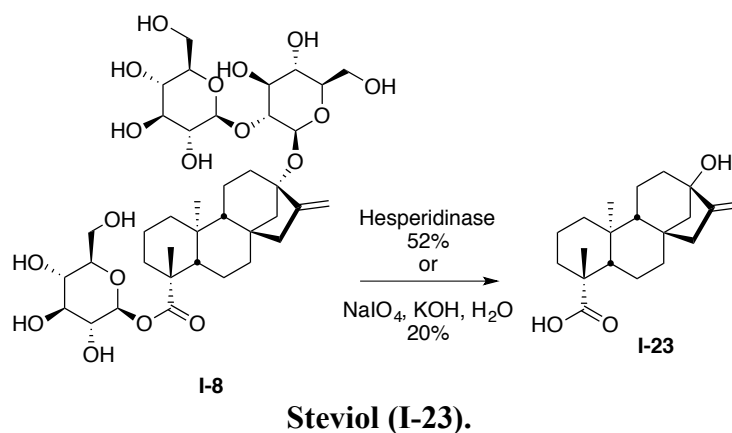
Chapter 4. Experimental Data

A. General Methods

Unless otherwise stated, reactions were carried out open to air with reagent grade solvents without purification. Tetrahydrofuran (THF), toluene, diethyl ether (Et₂O), and dichloromethane (CH₂Cl₂ or DCM) were purified by passage through a bed of activated alumina. Purification of reaction products was carried out by flash column chromatography using silica gel 60 (230-400 mesh). Analytical thin layer chromatography (TLC) was performed on 0.25 mm silica gel 60-F plates. Visualization was accomplished with UV light and cerium molybdate stain followed by heating. Infrared spectra (IR) were reported on NaCl or KBr plates using a FT-IR spectrometer. High-resolution mass spectral data were acquired utilizing the electrospray ionization technique. Optical rotations were measured using a polarimeter. ¹H NMR spectra were recorded at ambient temperature at 400 MHz and are reported in ppm using a solvent as an internal standard (CDCl₃ at 7.26 ppm or CD₃OD at 3.31 ppm). Proton-decoupled ¹³C NMR spectra were recorded at 100 MHz and are reported in ppm using a solvent as an internal standard (CDCl₃ at 77.16 ppm). The data are reported as follows: chemical shift on the δ scale, multiplicity (b = broad, s = singlet, d = doublet, t = triplet, q = quartet, m = multiplet), coupling constants (Hz), and integration. Melting points were determined with Electrothermal Digital Mel-Temp 3.0 melting point apparatus. High-resolution mass spectra were recorded with electron-spray

ionization (ESI) or electron ionization (EI) with a Bruker BioTOF II ESI/TOF-MS instrument, while low-resolution mass spectra were recorded with a CombiFlash Rf+ PurIon instrument.

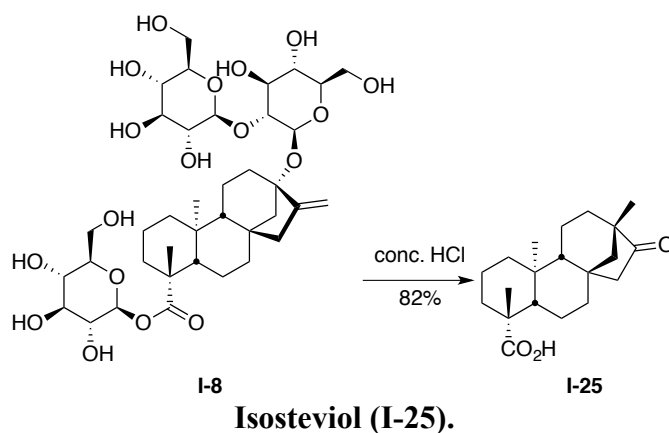
B. DOS Scaffolds



Enzymatic route: To a 2 L round-bottomed flask containing stevioside (**I-23**) (100 g, 124 mM) in citrate-phosphate buffer (1 L, pH 4) was added hesperidinase enzyme from *Aspergillus niger* (330 g, 100 units).¹⁵⁹ The reaction was allowed to stir at 50 °C for a week, at which time TLC analysis indicated that the starting material was consumed. The precipitate was collected by filtration in a Buchner flask to yield 30 g of crude steviol (**1**) as a colorless powder. The crude compound was then dissolved in ethanol (50 mL) and allowed to crystallize overnight to give steviol (**I-23**, 21 g, 52%).

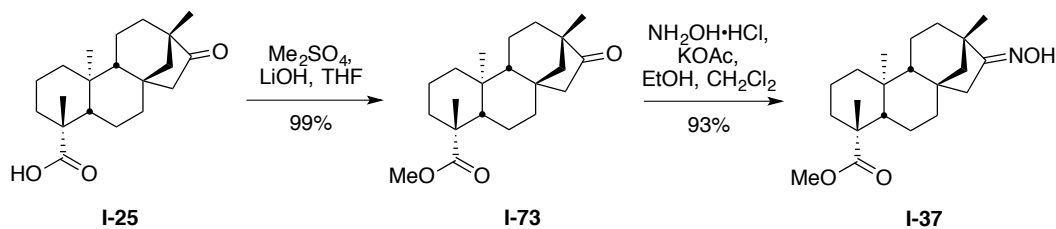
Non-enzymatic route: To a solution of stevioside (10.0 g, 12.4 mmol) in 200 mL of deionized water was added NaIO₄ (7.98 g, 37.3 mmol). The mixture was stirred overnight at 0 °C (Cryocool apparatus). Then, KOH (6.95 g, 124 mmol) was added slowly to the resulting solution, which was subsequently refluxed for another 2 h. The resulting solution

was cooled, acidified with acetic acid to a pH of 3–4, and extracted with EtOAc. The combined extracts were washed with distilled water and brine, dried over MgSO₄, and concentrated *in vacuo* to give the crude product, which was then purified by flash chromatography with 25% EtOAc:Hex to give 790 mg of steviol (**I-23**) in 20% yield. mp 203–208 °C (Lit 206–207 °C),¹⁶⁰ ¹H NMR (400 MHz, CDCl₃): δ 4.83 (d, *J* = 66.2 Hz, 2H), 2.17 – 1.97 (m, 4H), 1.93 – 1.76 (m, 3H), 1.76 – 1.63 (m, 3H), 1.59 – 1.44 (m, 3H), 1.37 (td, *J* = 13.3, 3.9 Hz, 2H), 1.26 – 1.21 (m, 1H), 1.17 (s, 3H), 1.04 – 0.91 (m, 3H), 0.89 (s, 3H), 0.76 (td, *J* = 13.1, 3.8 Hz, 1H); ¹³C NMR (101 MHz, CDCl₃) δ 183.2, 155.7, 103.0, 80.3, 56.8, 53.8, 47.4, 46.9, 43.6, 41.7, 41.2, 40.5, 39.5, 39.3, 37.7, 28.8, 21.8, 20.4, 19.0, 15.4. HRMS (ESI) (*m/z*): [M+Na]⁺ calcd for C₂₀H₃₀O₃Na 341.2087, found 341.2080; [α]_D²³ –63.8° (*c* 1.00, CHCl₃).



To a 3L 3-necked round-bottomed flask, mounted on a heating mantle, was added stevioside (**I-8**) (201 g, 250.0 mmol) and MeOH (1 L) at ambient temperature. Upon dissolution of the stevioside, concentrated HCl (75 mL) was added carefully. A reflux condenser was fitted to the flask and the temperature slowly increased until reflux. After 2

h the heating mantle was turned off and the reaction allowed to cool to room temperature overnight. The methanolic solution was then poured with care into a 5 L Erlenmeyer flask (fitted with a mechanical stirrer) of stirring water (3 L). After stirring for 30 minutes, the precipitate was collected by filtration in a 200 mm diameter Buchner flask. The flask was left under vacuum overnight to dry the precipitate to yield 75 g of crude isosteviol as an off-white powder. The crude compound was then dissolved in ethanol (400 mL) and allowed to crystallized overnight to give isosteviol (**I-6**) as colorless crystals (65 g, 82 %): $R_f = 0.6$ (Hex:EtOAc 2:1); mp 230-232 °C (Lit 230-231 °C);¹⁶¹ ^1H NMR (400 MHz, CDCl_3): δ 11.66 (br s, 1 H), 2.63 (dd, $J = 18.7, 3.7$ Hz, 1H), 2.14 (d, $J = 13.3$ Hz, 1H), 1.87 (dd, $J = 13.9, 1.9$ Hz, 1H), 1.81 (d, $J = 18.7$ Hz, 2H), 1.73 (d, $J = 12.9$ Hz, 2H), 1.65 (ddd, $J = 26.4, 14.2, 5.0$ Hz, 3H), 1.55 (dd, $J = 11.6, 2.5$ Hz, 1H), 1.34-1.51 (m, 4H), 1.24 (s, 3H), 1.18 (ddd, $J = 14.0, 12.1, 4.7$ Hz, 3H), 0.98-1.06 (m, 1H), 0.97 (s, 3H), 0.90 (td, $J = 13.2, 13.1, 4.1$ Hz, 1H), 0.76 (s, 3H); ^{13}C NMR (100 MHz, CDCl_3): δ 222.8, 183.9, 57.0, 54.7, 54.3, 48.7, 48.4, 43.7, 41.4, 39.7, 39.5, 38.2, 37.6, 37.3, 28.9, 21.6, 20.3, 19.8, 18.8, 13.3; IR (film) 2957, 1736, 1693, 1455, 1108 cm^{-1} ; HRMS (ESI) (m/z): $[\text{M}+\text{Na}]^+$ calcd for $\text{C}_{20}\text{H}_{30}\text{O}_3\text{Na}$ 341.2087, found 341.2080; $[\alpha]_D^{23} -89.1^\circ$ (c 1.00, CHCl_3).



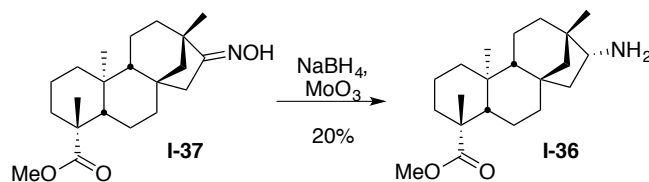
(4*R*,4*aS*,6*aR*,9*S*,11*aR*,11*bS*)-Methyl 4,9,11*b*-Trimethyl-8-oxotetradecahydro-6*a*,9-methanocyclohepta[*a*]naphthalene-4-carboxylate (I-73**).**

(4*R*,4*aS*,6*aR*,9*S*,11*aR*,11*bS*,*E*)-Methyl 8-(Hydroxyimino)-4,9,11*b*-trimethyl-tetradecahydro-6*a*,9-methanocyclohepta[*a*]naphthalene-4-carboxylate (I-37**).**

To a flame-dried 500 mL round-bottomed flask was added isosteviol (**I-25**, 20 g, 63 mmol) and dry THF (120 mL). Upon dissolution, LiOH•H₂O (2.9 g, 68 mmol) was added and the reaction stirred for 1 h at room temperature under an atmosphere of nitrogen. Me₂SO₄ (6.5 mL, 69 mmol) was slowly added, then a reflux condenser was fitted to the flask and the temperature was raised to 80 °C for 18 h. The colorless precipitate was then recovered through filtration. The cake was washed repeatedly with Et₂O and then concentrated *in vacuo* to furnish methyl ester **I-73** (18.3 g, 88%). The reaction was quenched with 10% NaOH and then washed with brine and dried over MgSO₄. Filtration and removal of the solvent under reduced pressure afforded an additional 2.2 g (11%) of ester **I-73**: R_f = 0.3 (Hex:EtOAc 9:1); mp 200-202 °C (Lit 202-203 °C)¹; ¹H NMR (400 MHz, CDCl₃): δ 3.63 (s, 3H), 2.62 (dd, *J* = 18.6, 3.8 Hz, 1H), 2.18 (d, *J* = 13.3 Hz, 1H), 1.89 (dd, *J* = 13.6, 2.9 Hz, 1H), 1.74-1.85 (m, 2H), 1.57-1.74 (m, 5H), 1.52 (ddd, *J* = 17.8, 12.5, 3.3 Hz, 2H), 1.33-1.45 (m, 3H), 1.19-1.30 (m, 2H), 1.19 (s, 3H), 1.10-1.16 (m, 1H), 0.99-1.06 (m, 1H), 0.97 (s, 3H), 0.92 (dd, *J* = 13.2, 4.2 Hz, 1H), 0.68 (s, 3H); ¹³C NMR (100 MHz, CDCl₃): δ 222.4, 177.8, 57.0, 54.7, 54.3, 51.2, 48.7, 48.5, 48.4, 43.8, 41.5, 39.8, 39.4, 37.9, 37.3, 28.8, 21.7, 20.3, 19.9, 18.9, 13.2; IR (film) 2952, 1744, 1720, 1452, 1240, 1175, 1153 cm⁻¹; HRMS (ESI) (*m/z*): [M+Na]⁺ calcd for C₂₁H₃₂O₃Na 355.2244; found 355.2234; [α]_D²³ -82.2 (*c* 1.00, CHCl₃); reported [α]_D²⁵ -69.0° (*c* 1.02, CHCl₃).

To a 1 L round-bottomed flask was added **I-73** (18 g, 55 mmol), EtOH (250 mL), CH₂Cl₂ (150 mL), NH₂OH•HCl (10.6 g, 165 mmol) and KOAc (16.2 g, 165 mmol). The mixture was heated to 50 °C for 1 h after which time TLC analysis indicated the starting material was consumed. The mixture was then filtered and the solvent was removed under reduced

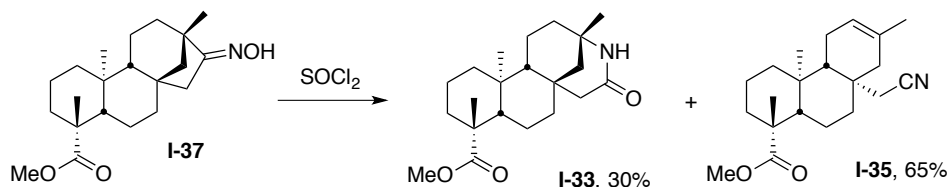
pressure. The colorless residue was taken up in CH₂Cl₂ (200 mL). The organic layer wash then washed with 10% HCl (100 mL), 1M NaOH (100 mL), and brine (100 mL). The aqueous layers were then re-extracted with CH₂Cl₂ (200 mL) and the combined organic layers dried over MgSO₄ and filtered. The solvent was then removed under reduced pressure and the residue chromatographed on silica gel (Hex:EtOAc 9:1 → 4:1) to yield oxime **I-37** (18 g, 93%): *R_f* = 0.2 (Hex:EtOAc 4:1); mp 154-156 °C (Lit 153-155 °C);³ ¹H NMR (400 MHz, CDCl₃): δ 7.42 (br s, 1H), 3.63 (s, 3H), 2.96 (dd, *J* = 18.6, 3.2 Hz, 1H), 2.17 (d, *J* = 13.5 Hz, 1H), 1.97 (d, *J* = 18.6 Hz, 1H), 1.54-1.89 (m, 8H), 1.38-1.47 (m, 4H), 1.19-1.31 (m, 2H), 1.18 (s, 3H), 1.10 (d, *J* = 3.3 Hz, 3H), 1.07 (t, *J* = 3.3, 3.3 Hz, 1H) 1.00 (td, *J* = 13.5, 13.4, 4.2 Hz, 1H), 0.88 (td, *J* = 13.2, 13.1, 4.2 Hz, 1H), 0.74 (s, 3H); ¹³C NMR (100 MHz, CDCl₃): δ 178.0, 170.4, 57.1, 56.3, 54.9, 51.2, 43.8, 43.8, 40.9, 40.3, 39.9, 39.5, 38.05, 38.00, 36.8, 28.7, 22.1, 21.7, 20.4, 18.9, 13.1; IR (film) 3292, 2948, 1724, 1453, 1235, 1153, 930, 737 cm⁻¹; HRMS (ESI) (*m/z*): [M+Na]⁺ calcd for C₂₁H₃₃NO₃Na 370.2353; found 370.2338; [α]_D²³ -57.1° (*c* 1.00, CHCl₃).



Methyl (4*R*,4*aS*,6*aR*,9*S*,11*aR*,11*bS*)-8-Amino-4,9,11b-trimethyltetradecahydro-6*a*,9-methanocyclohepta [*α*]naphthalene-4-carboxylate (I-36).

To a solution of oxime ester **I-37** (348 mg, 1.00 mmol, 1.0 equiv) in MeOH, cooled to 0 °C (ice bath), was added sodium borohydride (189 mg, 5.00 mmol, 5.0 equiv) then molybdenum (VI) oxide (216 mg, 1.50 mmol, 1.5 equiv). The reaction was stirred at

room temperature overnight. The next day the reaction was filtered, and then the solvent was evaporated. The resulting residue was treated with aqueous KOH (20%) and extracted with CH₂Cl₂. The combined organic layers were washed with brine, dried with MgSO₄, and then concentrated *in vacuo*. Column chromatography with 5% MeOH/CH₂Cl₂ provided amine **I-36** in 20% yield. mp 255-258 °C; ¹H NMR (400 MHz, CDCl₃): 3.60 (s, 3H), 3.12 (dd, *J* = 10.8, 6.6 Hz, 1H), 2.95 – 2.78 (m, 1H), 2.13 (d, *J* = 13.3 Hz, 1H), 1.87 – 1.50 (m, 10H), 1.40 – 1.28 (m, 4H), 1.24 (s, 1H), 1.14 (s, 3H), 1.11 – 1.02 (m, 2H), 1.00 (s, 3H), 0.99 – 0.95 (m, 1H), 0.87 – 0.79 (m, 2H), 0.72 (s, 3H). ¹³C NMR (125 MHz, CDCl₃): 178.2, 59.8, 57.1, 56.2, 55.7, 51.3, 49.8, 43.9, 42.6, 41.3, 41.3, 39.9, 39.2, 38.2, 33.2, 28.9, 24.7, 21.8, 20.3, 18.9, 13.0. HRMS (ESI) (*m/z*): [M+H]⁺ calcd for C₂₁H₃₆NO₂ 334.2746, found 334.2747; [α]_D²³ –95.3° (*c* 0.468, EtOH).



(3*S*,6*aR*,8*aR*,9*R*,12*aR*,12*bR*)-Methyl 3,12*a*-Dimethyl-5-oxotetradecahydro-1*H*-3,6*a*-methanonaphtho[2,1-*d*]azocine-9-carboxylate (I-33) and 1*R*,4*aR*,4*bR*,8*aR*,10*aR*)-Methyl 8*a*-(Cyanomethyl)-4*a*,7-dimethyl-1,2,3,4,4*a*,4*b*,5,8,8*a*,9,10,10*a*-dodecahydrophenanthrene-1-carboxylate (I-35).

To a 500 mL flame-dried round-bottomed flask of oxime **I-37** (10.0 g, 28.8 mmol) in chloroform (200 mL), was added thionyl chloride (6.25 mL, 86.3 mmol). The flask was flushed with nitrogen and heated to 60 °C for 10 h until TLC analysis had indicated the consumption of starting material. After reaction cooled to room temperature, the organic

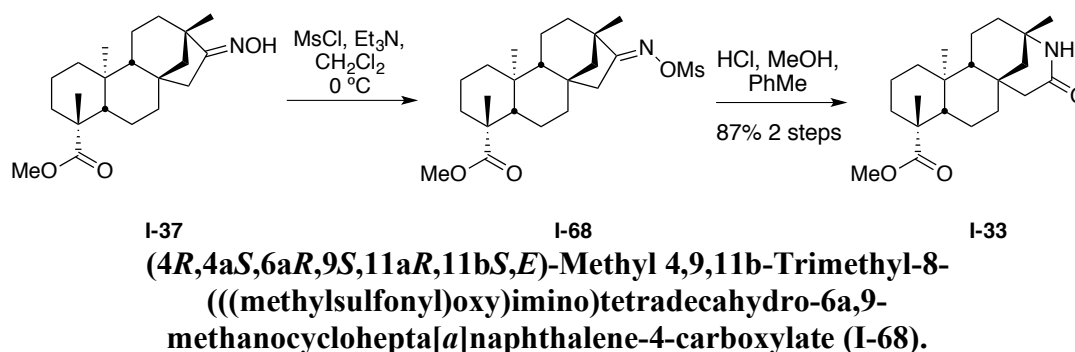
layer was then washed with 1 M NaOH (10 mL) and brine and the aqueous layers were re-extracted with EtOAc (2x20 mL). The combined organic layers were then dried over MgSO₄, filtered and the solvent removed under reduced pressure. The residue was chromatographed on silica gel (Hex:EtOAc 9:1 → CH₂Cl₂:MeOH 9:1) to give nitrile **I-35** (6.23g, 65%) as white needle-like crystals and lactam **I-33** (2.70 g, 27%) as an off-white solid.

I-33: $R_f = 0.2$ (10% MeOH: CH₂Cl₂); mp 163-165 °C; IR (film) 3193, 1723, 1657 cm⁻¹; ¹H NMR (400 MHz, CDCl₃): δ 5.59 (br s, 1H), 3.62 (s, 3H), 2.91 (dd, $J = 18.4, 2.2$ Hz, 1H), 2.17 (d, $J = 13.40$ Hz, 1H), 1.90 (d, $J = 18.4$ Hz, 1H), 1.72-1.89 (m, 4H), 1.58-1.71 (m, 3H), 1.55 (d, $J = 13.0$ Hz, 1H), 1.36-1.50 (m, 3H), 1.28-1.33 (m, 1H), 1.20-1.25 (m, 1H), 1.17 (s, 3H), 1.16 (s, 3H), 1.07 (dd, $J = 11.4, 3.2$ Hz, 1H), 1.00 (td, $J = 13.5, 13.4, 4.4$ Hz, 1H), 0.85 (ddd, $J = 17.8, 12.9, 3.8$ Hz, 2H), 0.77 (s, 3H); ¹³C NMR (100 MHz, CDCl₃): δ 177.7, 173.6, 57.4, 56.8, 51.8, 51.2, 49.4, 44.2, 43.8, 40.4, 39.9, 39.7, 38.0, 37.8, 35.2, 28.9, 28.5, 19.6, 18.9, 18.8, 13.6; HRMS (ESI) (m/z): [M+Na]⁺ calcd for C₂₁H₃₃NO₃Na requires 370.2353; found 370.2345; $[\alpha]_D^{23} -15.3^\circ$ (c 0.300, CHCl₃).

I-35: $R_f = 0.5$ (Hex:EtOAc 4:1); mp 186-187 °C; IR (film) 2949, 2242, 1720, 1451, 1150 cm⁻¹; ¹H NMR (400 MHz, CDCl₃): δ 5.36 (d, $J = 1.7$ Hz, 1H), 3.65 (s, 3H), 2.57, 2.42 (dABq, $J = 16.6, 1.9$ Hz, 2H), 2.01-2.19 (m, 4H), 1.93-1.68 (m, 6H), 1.65 (s, 3H), 1.44 (ddd, $J = 12.8, 4.8, 2.0$ Hz, 1H), 1.30 (dd, $J = 11.8, 5.4$ Hz, 1H), 1.19 (s, 3H), 1.12 (dd, $J = 12.2, 2.3$ Hz, 2H), 0.96-1.04 (m, 1H), 0.88 (td, $J = 13.2, 13.1, 4.2$ Hz, 1H), 0.65 (s, 3H); ¹³C NMR (100 MHz CDCl₃): δ 177.7, 131.2, 119.8, 119.0, 57.1, 51.7, 51.3, 45.7, 43.7, 39.8, 39.0, 37.8, 37.3, 35.2, 28.6, 23.3, 22.2, 20.0, 19.8, 18.9, 13.3; HRMS (ESI) (m/z):

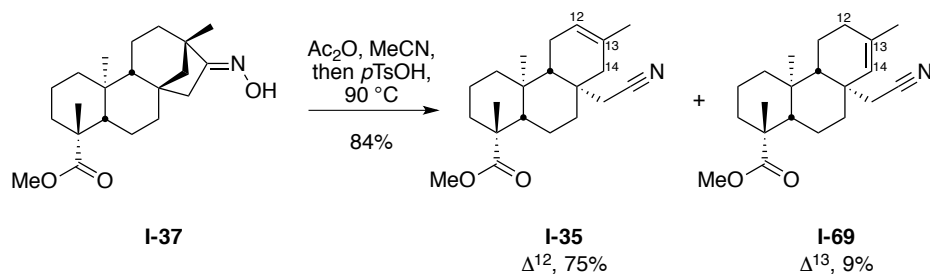
$[M+Na]^+$ calcd for $C_{21}H_{31}NO_2Na$ requires 352.2247; found 352.2241; $[\alpha]_D^{23} -86.2^\circ$ (c 1.00, $CHCl_3$).

C. Oxime Reaction Compounds



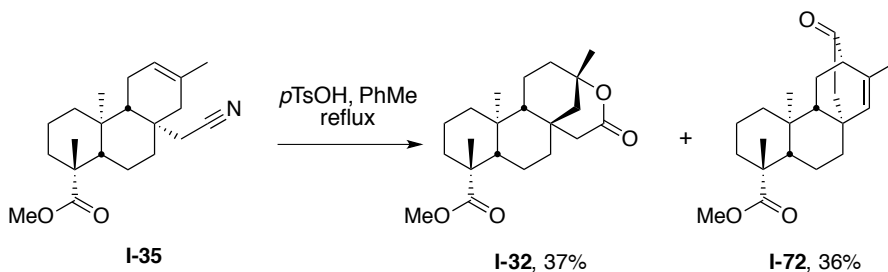
To a flame dried 100 mL round-bottomed flask was added oxime (1.00 g, 2.88 mmol) and dichloromethane (40 mL). The flask was cooled to $0^\circ C$ (ice bath) then flushed with nitrogen. Triethylamine (5.00 mL) and $MsCl$ (0.450 mL, 5.76 mmol) was added. After 30 min TLC analysis indicated that the starting material was consumed and sat. $NaHCO_3$ (10 mL) was added and the mixture stirred for 10 min. The organic layer was then washed with brine and the aqueous layers re-extracted with CH_2Cl_2 (20 mL). The combined organic layers were then dried over $MgSO_4$, filtered and the solvent removed under reduced pressure to give mesylate ester **II-68** (1.22 g, 99% crude), which was then carried on without further purification. Then, to another 100 mL flame-dried round-bottomed flask solution of mesylate ester (1.22 g, 2.86 mmol) in $MeOH$ (25 mL) and toluene (5 mL), was added concentrated HCl (416 mg, 11.4 mmol). The mixture was then heated to $60^\circ C$ and stirred overnight. The reaction was allowed to cool to room temperature then partitioned

with saturated aqueous bicarbonate and toluene. The organic phase was dried over MgSO_4 , filtered, and the solvent removed under reduced pressure to yield lactam **I-33** (870 mg, 87%).



(1*R*,4*aS*,4*bR*,8*aR*,10*aS*)-Methyl 8*a*-(Cyanomethyl)-1,4*a*,7-trimethyl-1,2,3,4,4*a*,4*b*,5,8,8*a*,9,10,10*a*-dodecahydrophenanthrene-1-carboxylate (I-35**) and (1*R*,4*aS*,4*bS*,8*aS*,10*aS*)-Methyl 8*a*-(Cyanomethyl)-1,4*a*,7-trimethyl-1,2,3,4,4*a*,4*b*,5,6,8*a*,9,10,10*a*-dodecahydrophenanthrene-1-carboxylate (**I-69**).**

To a 10 mL flame-dried round-bottomed flask was added oxime **I-37** (10 mg, .029 mmol) and MeCN (5 mL). The flask was then flushed with nitrogen and Ac_2O (6.0 μL , 0.064 mmol) added. After 10 min TLC indicated all the starting material was consumed and $p\text{TsOH}$ (5.5 mg, 0.032 mmol) was added. The reaction was stirred for 10 min after which time TLC analysis indicated that the reaction was complete. The MeCN was removed under reduced pressure and residue taken up in Et_2O (10 mL) and washed with 10% NaOH, and brine. The aqueous layers were then re-extracted with Et_2O (2x10 mL) and the combined organic layers were dried over MgSO_4 , filtered, and the solvent was removed under reduced pressure. The residue was chromatographed on silica gel (Hex:EtOAc 9:1 \rightarrow 4:1) to yield the nitriles **I-35** and **I-69** (7.9 mg, 84%) as a 8:1 mixture with nitrile **I-35** as the major alkene (7 mg, 75%). Recrystallization with EtOAc:DCM enriched the mixture to 20:1.

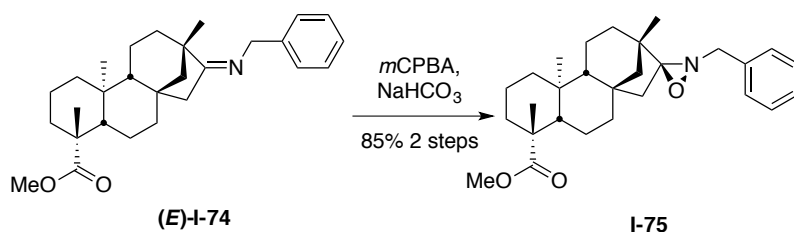


(3*S*,6*aR*,8*aS*,9*R*,12*aS*,12*bR*)-Methyl 3,9,12*a*-Trimethyl-5-oxotetradecahydro-3,6a-methanonaphtho[2,1-*d*]oxocine-9-carboxylate (I-32) and (3*S*,4*aS*,4*bS*,8*R*,8*aS*,10*aS*)-Methyl 2,4*b*,8-Trimethyl-12-oxo-4,4*a*,4*b*,5,6,7,8,8*a*,9,10-decahydro-3*H*-3,10*a*-ethanophenanthrene-8-carboxylate (I-72).

To a 50 mL flame-dried round-bottomed flask was added nitrile ester **I-35** (100 mg, 0.30 mmol) in toluene (10 mL). Then *p*TsOH (57 mg, 0.30 mmol) was added. The reaction was heated to 90 °C for 24 h. After the flask was cooled to ambient temperature, the reaction mixture was passed through a silica plug (Hex:EtOAc 9:1). The solvent was then removed under reduced pressure and the residue chromatographed on silica gel (Hex:EtOAc 9:1) to yield both the ketone **I-32** (36 mg, 36%) and lactone **I-72** (39 mg, 37%).

I-32: $R_f = 0.1$ (Hex:EtOAc 4:1); mp 194-202 °C; IR (film) 2935, 2848, 1732, 1693, 1216 cm^{-1} ; $^1\text{H NMR}$ (400 MHz, CDCl_3): δ 3.63 (s, 3H), 3.07 (dd, $J = 18.6, 2.7$ Hz, 1H), 2.16 (s, 1H), 2.02 (d, $J = 18.6$ Hz, 1H), 1.94-2.00 (m, 1H), 1.67-1.89 (m, 5H), 1.53-1.59 (m, 2H), 1.44 (d, $J = 8.2$ Hz, 1H), 1.36-1.40 (m, 1H), 1.34 (s, 3H), 1.24 (ddd, $J = 14.3, 9.5, 4.2$ Hz, 3H), 1.17 (s, 3H), 1.07 (dd, $J = 11.8, 2.7$ Hz, 1H), 1.00 (d, $J = 4.4$ Hz, 1H), 0.94 (dd, $J = 12.7, 3.1$ Hz, 1H), 0.85 (d, $J = 4.4$ Hz, 1H), 0.75 (s, 3H); $^{13}\text{C NMR}$ (100 MHz, CDCl_3): δ 117.6, 172.6, 80.3, 57.2, 55.8, 51.3, 47.7, 43.7, 43.6, 39.0, 38.7, 38.4, 37.9, 37.8, 34.9, 28.6, 28.3, 19.5, 18.8, 18.6, 13.4; HRMS (ESI) (m/z): $[\text{M}+\text{H}]^+$ calcd for $\text{C}_{21}\text{H}_{33}\text{O}_4$ requires 349.2379; found 349.2366; $[\alpha]_D^{23} -86.0^\circ$ (c 1.03, CHCl_3).

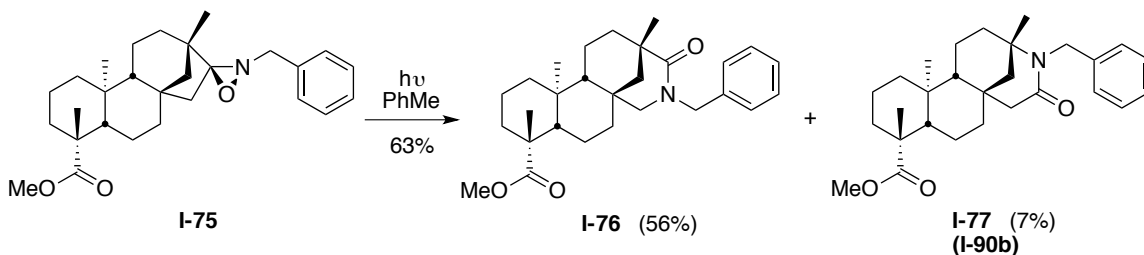
I-72: $R_f = 0.4$ (Hex:EtOAc 4:1); mp 163-165 °C; IR (film) 2947, 2848, 1721, 1466, 1444, 1235, 1164 cm^{-1} ; ^1H NMR (400 MHz, CDCl_3): δ 5.78 (t, $J = 1.46$ Hz, 1H), 3.63 (s, 3H), 2.87 (dt, $J = 3.5, 1.8, 1.8$ Hz, 1H), 2.54 (d, $J = 18.7$ Hz, 1H), 2.17 (d, $J = 14.0$ Hz, 1H), 1.99 (dt, $J = 13.3, 3.2, 3.2$ Hz, 1H), 1.86-1.90 (m, 1H), 1.78-1.85 (m, 1H), 1.77 (d, $J = 1.5$ Hz, 3H), 1.70-1.75 (m, 2H), 1.51-1.57 (m, 4H), 1.37-1.44 (m, 1H), 1.25 (ddd, $J = 11.4, 6.6, 1.7$ Hz, 1H), 1.20 (s, 3H), 1.15 (dd, $J = 12.0, 2.4$ Hz, 1H), 1.02 (td, $J = 13.5, 13.5, 4.2$ Hz, 1H), 0.92 (td, $J = 13.5, 13.4, 4.3$ Hz, 1H), 0.71 (s, 3H); ^{13}C NMR (100 MHz, CDCl_3): δ 213.9, 177.6, 138.4, 135.5, 56.6, 54.4, 51.8, 51.2, 43.6, 42.8, 40.9, 40.3, 38.1, 37.9, 36.8, 28.6, 24.8, 20.2, 19.8, 18.5, 12.5; HRMS (ESI) (m/z): $[\text{M}+\text{H}]^+$ calcd for $\text{C}_{21}\text{H}_{31}\text{O}_3$ requires 331.2273; found 331.2274; $[\alpha]_{\text{D}}^{23} -93.5^\circ$ (c 0.26, CHCl_3).



(3'S,4R,4aS,6aR,9S,11aR,11bS)-Methyl 2'-Benzyl-4,9,11b-trimethyldodecahydro-1H-spiro[6a,9-methanocyclohepta[a]naphthalene-8,3'-[1,2]oxaziridine]-4-carboxylate (I-75).

To a 100 mL round-bottomed flask was added benzylimine (**I-74**) (1.0 g, 2.35 mmol) in CH_2Cl_2 (50 mL). After cooling to 0 °C $m\text{CPBA}$ (520 mg, 2.80 mmol) and NaHCO_3 (240 mg, 2.80 mmol) were added. The mixture was allowed to stir for 10 min, at which time TLC analysis indicated that the starting material was consumed. The reaction was

quenched with an aqueous solution of NaS₂O₃ (15 mL) then washed with 1M NaOH (100 mL) and brine (100 mL). The aqueous layers were then re-extracted with CH₂Cl₂ (50 mL) and the combined organic layers dried over MgSO₄ and filtered. The solvent was then removed under reduced pressure and the residue chromatographed on silica gel (Hex:EtOAc 9:1) to yield benzyl oxaziridine **I-75** (822 mg, 80%): R_f = 0.6 (Hex:EtOAc 2:1); mp 192-198 °C; IR (film) 2949, 2906, 1741, 1719 cm⁻¹; ¹H NMR (400 MHz, CDCl₃): δ 7.36 (s, 1H), 7.27-7.35 (m, 2H), 7.18-7.26 (m, 2H), 3.87, 3.75 (ABq, J_{AB} = 13.8 Hz, 2H), 3.59 (s, 3H), 2.54 (dd, J = 15.3, 2.6 Hz, 1H), 2.11 (d, J = 13.3 Hz, 1H), 1.80 (dd, J = 14.9, 3.5 Hz, 1H), 1.50-1.74 (m, 7H), 1.30-1.43 (m, 3H), 1.16 (ddd, J = 8.4, 5.4, 2.3 Hz, 1H), 1.12 (s, 3H), 1.08 (d, J = 2.4 Hz, 1H), 0.92 (dddd, J = 35.9, 18.4, 12.7, 7.8 Hz, 4H), 0.73-0.81 (m, 1H), 0.64 (s, 3H), 0.57 (s, 3H); ¹³C NMR (100 MHz, CDCl₃): δ 177.5, 136.3, 128.06, 128.05, 127.1, 94.0, 60.9, 56.6, 54.7, 54.2, 50.8, 43.3, 41.0, 40.9, 40.7, 39.4, 37.5, 37.4, 36.1, 35.4, 28.4, 21.3, 19.5, 19.3, 18.5, 12.9; HRMS (ESI) (*m/z*): [M+H]⁺ calcd for C₂₈H₄₀NO₃ requires 438.3008; found 438.3003; [α]_D²³ -97.6° (*c* 1.00, CHCl₃).



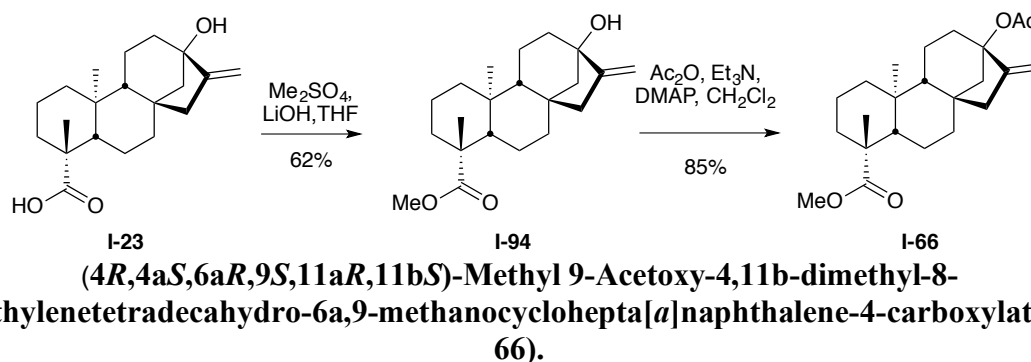
(3*S*,6*aS*,8*aS*,9*R*,12*aS*,12*bS*)-Methyl 5-Benzyl-3,9,12*a*-trimethyl-4-oxotetradecahydro-1*H*-3,6*a*-methanonaphtho[2,1-*c*]azocine-9-carboxylate (I-76**) and (3*S*,6*aR*,8*aS*,9*R*,12*aS*,12*bR*)-Methyl 4-Benzyl-3,9,12*a*-trimethyl-5-oxotetradecahydro-1*H*-3,6*a*-methanonaphtho[2,1-*d*]azocine-9-carboxylate (**I-77**/**I-90b**).**

To a 25-mL round-bottomed flask was added benzyl oxaziridine **I-75** (110 mg, 0.25 mmol) in toluene (5 mL) and was allowed to stir under an Hg lamp (254 nm) for 1.5 h, at which time TLC analysis indicated the starting material was consumed. The reaction was then chromatographed on silica gel (Hex:EtOAc 4:1) to yield benzyl lactam **I-76** (69 mg, 56%) and benzyl lactam **I-77/I-90b** (8 mg, 7%) as a yellowish solid.

I-76: $R_f = 0.21$ (Hex:EtOAc 4:1); mp 145-151 °C; IR (film) 2947, 2848, 2235, 1723, 1638, 1453, 1233, 1154 cm^{-1} ; ^1H NMR (400 MHz, CDCl_3): δ 7.29 (d, $J = 4.35$ Hz, 4H), 7.21-7.26 (m, 1H), 5.00, 4.04 (ABq, $J_{AB} = 14.0$ Hz, 2H), 3.63 (dd, $J = 12.7, 2.1$ Hz, 1H), 3.60 (s, 3H), 2.87 (d, $J = 12.7$ Hz, 1H), 2.11 (d, $J = 13.4$ Hz, 1H), 1.99 (dd, $J = 11.6, 2.4$ Hz, 1H), 1.59-1.82 (m, 5H), 1.45-1.59 (m, 3H), 1.34-1.43 (m, 1H), 1.23 (ddd, $J = 7.7, 9.4, 3.5$ Hz, 2H), 1.18 (s, 3H), 1.16 (d, $J = 3.6$ Hz, 1H), 1.13 (s, 3H), 0.93-1.10 (m, 2H), 0.89 (dd, $J = 12.4, 3.2$ Hz, 1H), 0.78 (td, $J = 13.4, 13.3, 4.3$ Hz, 1H), 0.26 (s, 3H); ^{13}C NMR (100 MHz, CDCl_3): δ 177.6, 174.9, 137.6, 128.8, 128.7, 128.4, 127.9, 127.2, 126.9, 57.5, 57.0, 55.5, 51.1, 50.0, 48.9, 43.7, 43.3, 39.7, 39.3, 39.0, 37.7, 34.2, 28.6, 25.3, 20.1, 20.0, 18.8, 12.7; HRMS (ESI) (m/z): $[\text{M}+\text{H}]^+$ calcd for $\text{C}_{28}\text{H}_{40}\text{NO}_3$ requires 438.3008; found 438.3011; $[\alpha]_D^{23} -250.0^\circ$ (c 1.00, CHCl_3);

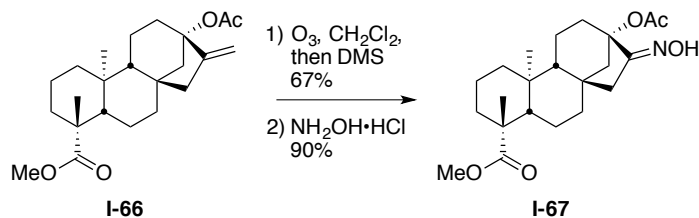
I-77/I-90b: $R_f = 0.5$ (Hex:EtOAc 4:1); mp 209-211 °C; IR (film) 2946, 2848, 1722, 1633, 145, 1399, 1151 cm^{-1} ; ^1H NMR (400 MHz, CDCl_3): δ 7.27-7.29 (m, 1H), 7.17-7.22 (m, 3H), 5.00, 4.19 (ABq, $J = 15.8$ Hz, 2H), 3.64 (s, 3H), 3.08, 2.19 (dABq, $J_{AB} = 18.4, 2.7$ Hz, 2H), 2.15-2.19 (m, 1H), 1.85-1.95 (m, 1H), 1.74-1.83 (m, 4H), 1.70 (dd, $J = 13.0, 2.7$ Hz, 1H), 1.55-1.58 (m, 3H), 1.42-1.46 (m, 1H), 1.30 (dd, $J = 13.0, 2.8$ Hz, 1H), 1.20-1.25 (m, 2H), 1.17 (s, 3H), 1.12 (s, 3H), 0.96-1.09 (m, 3H), 0.80-0.91 (m, 2H), 0.79 (s, 3H); ^{13}C

NMR (100 MHz, CDCl₃): δ 177.7, 172.4, 139.8, 128.3, 126.8, 126.5, 57.4, 56.9, 56.5, 51.6, 51.2, 44.6, 44.3, 43.7, 41.1, 39.9, 38.0, 37.8, 37.0, 34.1, 28.5, 28.0, 19.7, 18.8, 18.6, 13.6; HRMS (ESI) (m/z): $[M+H]^+$ calcd for C₂₈H₄₀NO₃ requires 438.3008; found 438.3001; $[\alpha]_D^{23}$ -53.5° (c 1.00, CHCl₃).



To a solution of steviol (**I-23**, 10 g, 32 mmol) in THF (50 mL) in a 500-mL round-bottomed flask at room temperature was added LiOH·H₂O (1.5g, 34 mmol) The reaction stirred at room temperature for 1 h under nitrogen, then Me₂SO₄ (3.3 mL, 35 mmol) was slowly added, and the reaction vessel was fitted with a reflux condenser. The reaction was refluxed for 18 h at 80 C. Once the reaction cooled to room temperature, the off-white precipitate was collected via filtration to furnish methyl ester **I-94** (7.6 g, 73%). mp 117-118 °C (Lit 113-115 °C); ¹⁶⁰ ¹H NMR (400 MHz, CDCl₃): δ 4.92 (d, J = 64.0 Hz, 2H), 3.66 (s, 3H), 2.28 – 2.04 (m, 4H), 1.93 – 1.73 (m, 7H), 1.62 – 1.40 (m, 5H), 1.33 – 1.26 (m, 1H), 1.19 (s, 3H), 1.10 – 0.93 (m, 3H), 0.85 (s, 3H), 0.82 – 0.75 (m, 1H).; ¹³C NMR (100 MHz, CDCl₃): δ 178.0, 156.0, 102.9, 80.3, 56.9, 53.8, 51.2, 47.4, 46.9, 43.8, 41.6, 41.3, 40.7, 39.4, 39.2, 38.0, 28.7, 21.9, 20.4, 19.1, 15.3. HRMS (ESI) (m/z): $[M+Na]^+$ calcd for C₂₁H₃₂O₃Na 355.2249, found 355.2080; $[\alpha]_D^{23}$ -191.3° (c 1.00, CHCl₃).

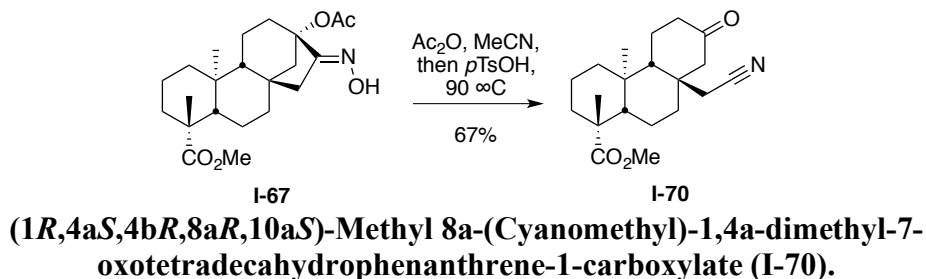
Then, the steviol methyl ester **I-94** (5.0 g, 15.0 mmol) was taken up in dry CH₂Cl₂ (200 mL) and under an atmosphere of nitrogen cooled to 0 °C. Et₃N (28 mL, 200 mmol) and Ac₂O (19 mL, 200 mmol) were added. After 30 min DMAP (200 mg) was added and the ice bath removed and the reaction was allowed to stir for 18 h. The reaction was cooled to 0 °C and H₂O (10 mL) added and the reaction was stirred for 30 minutes. The organic layer was then washed with water (100 mL), 10% HCl (100 mL), 1M NaOH (100 mL) and brine (100 mL). The aqueous layers were then re-extracted with ether (100 mL) and the combined organic layers dried over MgSO₄, filtered, and the solvent removed under reduced pressure to give an oil which was then chromatographed on silica gel (9:1 Hex:EtOAc) to provide the acetoxy methyl ester **I-66** as an oil (4.79 g, 85%): *R_f* = 0.7 (Hex:EtOAc 4:1); IR (KBr) 2948, 1726, 1447, 1366, 1236, 1149, 1047 cm⁻¹; ¹H NMR (400 MHz, CDCl₃): δ 4.90 (dd, *J* = 2.7, 2.0 Hz, 1H), 4.86 (d, *J* = 0.6 Hz, 1H), 3.63 (s, 3H), 2.57 (dd, *J* = 10.9, 2.6 Hz, 1H), 2.25 (ddd, *J* = 13.2, 4.9, 2.4 Hz, 2H), 2.14-2.20 (m, 1H), 1.98-2.05 (m, 1H), 2.02 (s, 3H), 1.85 (dd, *J* = 9.9, 7.6 Hz, 3H), 1.70-1.78 (m, 3H), 1.63 (dd, *J* = 7.5, 6.0 Hz, 1H), 1.56 (t, *J* = 3.26, 3.26, 1H), 1.44 (ddd, *J* = 15.0, 11.3, 7.6 Hz, 3H), 1.16 (s, 3H), 1.1 (ddd, *J* = 22.3, 12.6, 5.6 Hz, 3H), 0.86 (s, 3H), 0.80 (d, *J* = 4.2 Hz, 1H); ¹³C NMR (100 MHz, CDCl₃): δ 177.9, 169.9, 152.1, 103.4, 87.6, 556.9, 53.7, 51.2, 46.9, 43.8, 42.6, 42.1, 41.1, 40.7, 39.2 (x2), 38.1, 36.7, 28.7, 21.8, 20.0, 19.1, 15.1; HRMS (ESI) (*m/z*): [M+Na]⁺ calcd for C₂₃H₃₄O₄Na requires 397.2347; found 355.2356 [(M+Na)-Ac]⁺; [α]_D²³ -55.8° (*c* 1.00, CHCl₃).



(4*R*,4*aS*,6*aR*,9*S*,11*aR*,11*bS*,*E*)-Methyl 9-Acetoxy-8-(hydroxyimino)-4,11b-dimethyltetradecahydro-6*a*,9-methanocyclohepta[*a*]naphthalene-4-carboxylate (I-67).

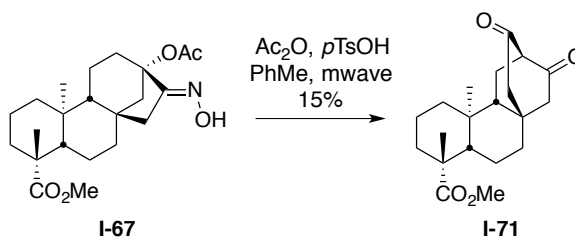
To a 50 mL flame-dried round-bottomed flask of acetoxy methyl ester **I-66** (904 mg, 2.4 mmol) in CH₂Cl₂ (30 mL) that was cooled to -78 °C, ozone was bubbled through the solution until the distinctive blue color was maintained for 30 min. The ozone line was then removed and nitrogen was bubbled through the solution until it was clear. Dimethylsulfide (703 mL, 9.6 mmol) was then added and the reaction was allowed to warm to ambient temperature and stir for 18 h. The CH₂Cl₂ was then removed under reduced pressure and residue dissolved in Et₂O (50 mL). The organic layer was washed with H₂O (10 mL) and brine (10 mL). The aqueous layers were then re-extract with Et₂O (x2, 50 mL) and the combined organic layers were then dried over MgSO₄, filtered, and the solvent removed under reduced pressure. The resulting keto-acetoxy methyl ester was chromatographed on silica gel (25:1 → 7:1) Hex:EtOAc. From there, a 50 mL round-bottomed flask of the keto-acetoxy methyl ester (437 mg, 1.2 mmol) in dry THF (25 mL) and EtOH (2 mL), was added NH₂OH·H₂O (240 mg, 3.5 mmol) and KOAc (354 mg, 3.5 mmol). The mixture was heated to 50 °C for 1 h after which time TLC analysis indicated that the starting material was consumed. The mixture was then filtered and the solvent removed under reduced pressure. The colorless residue was taken up in CH₂Cl₂ (50 mL) and the organic layer was then washed with 10% HCl (10 mL), 1M NaOH (10 mL), and brine (10 mL). The aqueous layers were then re-extracted with CH₂Cl₂ (20 mL) and the combined organic layers dried over

MgSO₄ and filtered. The solvent was then removed under reduced pressure and the residue chromatographed on silica gel (Hex:EtOAc 9:1 → 4:1) to give the 13-acetoxy oxime **I-67** (422 mg, 60% over 2 steps) as a colorless solid: $R_f = 0.44$ (Hex:EtOAc 4:1); mp 178-180 °C; IR (film) 3293, 2946, 1723, 1462, 1446, 1237 1149 cm⁻¹; ¹H NMR (400 MHz, CDCl₃): δ 8.17 (s, 1H), 3.63 (s, 3H), 2.53 (dd, $J = 11.1, 2.0$ Hz, 1H), 2.28 (d, $J = 2.2$ Hz, 1H), 2.17-2.22 (m, 2H), 2.03 (s, 3H), 1.98 (dd, $J = 11.1, 2.3$ Hz, 1H), 1.84 (ddd, $J = 13.3, 10.7, 6.9$ Hz, 5H), 1.66-1.77 (m, 2H), 1.55-1.65 (m, 2H), 1.47 (dd, $J = 39.3, 15.9$ Hz, 2H), 1.17 (s, 3H), 1.03 (ddd, $J = 20.2, 9.9, 3.2$ Hz, 3H), 0.86 (s, 3H), 0.77-0.83 (m, 1H); ¹³C NMR (100 MHz, CDCl₃): δ 177.8, 169.7, 163.3, 84.9, 56.6, 53.2, 51.3, 43.7, 42.3, 41.8, 41.7, 40.7, 40.6, 39.2, 37.9, 35.6, 28.6, 21.9, 21.4, 19.5, 18.9, 15.3; HRMS (ESI) (m/z): [M+H]⁺ calcd for C₂₂H₃₄NO₅ requires 392.2437; found 392.2439; $[\alpha]_D^{23} -47.7^\circ$ (c 0.98, CHCl₃).



To a 100 mL flame-dried round-bottomed flask containing 13-acetoxy oxime **I-67** (13 g, 39 mmol) and dry acetonitrile (100 mL) flushed with nitrogen, Ac₂O (7.4 mL, 86 mmol) was added. After 10 min TLC indicated that all the starting material was consumed and then *p*TsOH (8 g, 43 mmol) was added. The reaction was heated to reflux for 2 h and then cooled with an ice bath. NaOH (17 g, 390 mmol) dissolved in H₂O (300 mL) was then added and stirred for 5 min. The layers were then partitioned and the aqueous layer was

re-extracted with EtOAc (2x100 mL). The combined organic layers were dried over MgSO₄, filtered, and then the solvent was removed under reduced pressure. The residue was chromatographed on silica gel (400 mL) with 3 L of 9:1 Hex:EtOAc to furnish ketone nitrile **I-70** (8.66 g, 67%): *R_f* = 0.6 (Hex:EtOAc 2:1); mp 136-138 °C; IR (film) 2951, 1759, 1724, 1464, 1447, 1368, 1238, 1150 cm⁻¹; ¹H NMR (400 MHz, CDCl₃): δ 3.66 (s, 3H), 2.96 (d, *J* = 15.5 Hz, 1H), 2.47 (ddd, *J* = 16.8, 12.9, 8.3 Hz, 1H), 2.29-2.39 (m, 2H), 2.13-2.28 (m, 3H), 1.78-2.01 (m, 6H), 1.61-1.76 (m, 3H), 1.53 (d, *J* = 14.4 Hz, 1H), 1.47 (d, *J* = 7.0 Hz, 1H), 1.23 (s, 3H), 1.06 (dd, *J* = 7.4, 4.5 Hz, 2H), 0.98 (s, 3H); ¹³C NMR (100 MHz, CDCl₃): δ 211.0, 177.6, 117.1, 56.0, 51.4, 48.2, 43.7, 41.2, 39.4, 39.3, 38.3, 37.5, 31.2, 28.6, 20.8, 19.8, 19.1, 16.4; HRMS (ESI) (*m/z*): [M+H]⁺ calcd for C₂₀H₃₀NO₃ requires 332.2226; found 332.2231; [α]_D²³ -75.5° (*c* 1.24, CHCl₃).

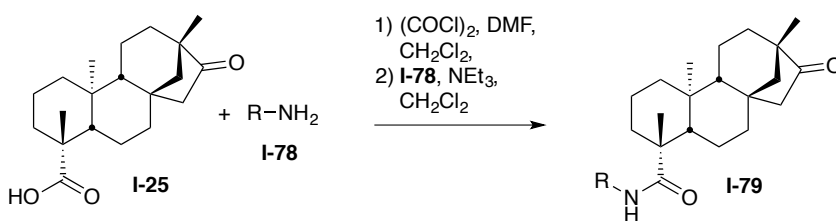


(3*S*,4*aR*,4*bS*,8*R*,8*aS*,10*aS*)-Methyl 4*b*,8-Dimethyl-2,12-dioxododecahydro-1*H*-3,10a-ethanophenanthrene-8-carboxylate (I-71**).⁸⁰**

To a 0.5-2.0 mL microwave vial of 13-acetoxy oxime **I-67** (50 mg, 0.100 mmol) and toluene (1 mL) was added Ac₂O (25 μL, 0.25 mmol). After 10 min, *p*TsOH (23 mg, 0.100 mmol, 1 equiv) was added. The vial was capped and the reaction was heated to 140 °C and stirred for 30 min in the microwave. The reaction mixture was then taken up in EtOAc (35 mL) and washed with 10% NaOH, and brine. The aqueous layers were then re-extracted with EtOAc (2x50 mL) and the combined organic layers were dried over MgSO₄, filtered,

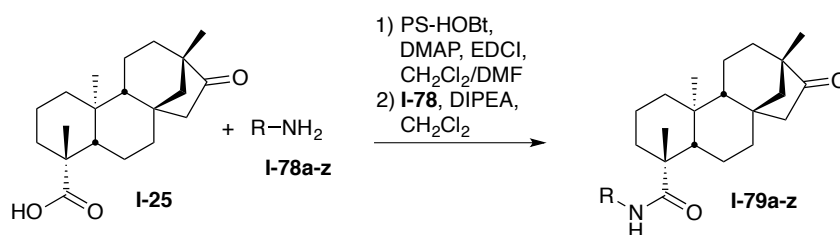
and the solvent removed under reduced pressure. The residue was chromatographed on silica gel (Hex:EtOAc 9:1) to give diketone **I-71** (13 mg, 15 %): $R_f = 0.35$ (Hex:EtOAc 2:1); mp 238-239 °C; IR (film) 2953, 1743, 1715 cm^{-1} ; ^1H NMR (400 MHz, CDCl_3): δ 3.65 (s, 3H), 3.18 (t, $J = 3.0$ Hz, 1H), 2.90 (dd, $J = 19.7, 3.5$ Hz, 1H), 2.26-2.07 (m, 4H), 1.96-1.77 (m, 6H), 1.59-1.35 (m, 4H), 1.21 (s, 3H), 1.15 (dd, $J = 11.9, 2.8$ Hz, 1H), 1.08-1.00 (m, 1H), 0.93 (d, $J = 4.3$ Hz, 1H), 0.70 (s, 3H); ^{13}C NMR (100 MHz, CDCl_3): δ 207.0, 206.9, 177.4, 64.6, 56.4, 55.5, 51.5, 50.5, 46.3, 43.8, 39.6, 38.2, 38.1, 37.9, 37.6, 28.8, 25.5, 19.9, 18.6, 12.4; HRMS (ESI) (m/z): $[\text{M}+\text{Na}]^+$ calcd for $\text{C}_{20}\text{H}_{28}\text{O}_4\text{Na}$ requires 355.1880; found 355.1891; $[\alpha]_D^{23} -65.8^\circ$ (c 0.25, CHCl_3).

D. Mono- and Bi-functional Library Compounds



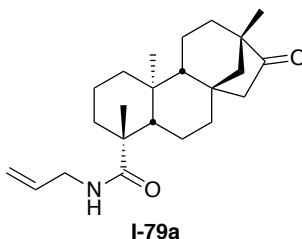
Standard procedure for the solution phase amide bond formation (Scheme I-25). To an oven-dried reaction flask under nitrogen at 0 °C (ice bath), was added DMF (37 μL , 0.47 mmol, 1.5 equiv) in DCM (1.0 mL) followed by oxalyl chloride (41 μL , 0.47 mmol, 1.5 equiv). The ice bath was removed and the mixture was allowed to stir at room temperature for 1 h. Then the reaction flask was cooled to 0 °C (ice bath) and isosteviol (**I-25**, 100 mg, 0.31 mmol) and Et_3N (130 μL , 0.47 mmol, 3 equiv) in DCM (1.0 mL) were added. After stirring for 5 min, allylamine (**I-78a**, 1 mL) was added and the mixture was stirred for 2 h.

Then the mixture was loaded onto a 20-mL silica gel plug in a 70-mL column and eluted with dry THF. The solvent was removed under vacuum, the residue was dissolved in CH₂Cl₂ (10 mL), and methylisocyanate polystyrene resin was added. The mixture was shaken for 20 h and was then loaded onto a 20-mL silica gel plug in a 70-mL column and eluted with ethyl acetate (40 mL). The solvent was removed and the residues was purified using column chromatography with 10% EtOAc:Hex as the eluent to provide the allyl amide product **I-79a** in 47% yield.



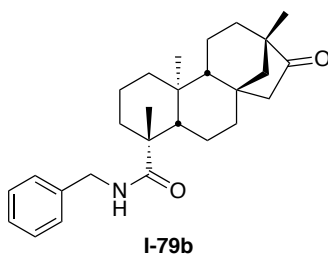
Standard procedure for solid phase amide bond formation (Schemes I-25, I-26, and I-28). To a flame-dry reaction vial of isosteviol (**I-25**, 100.0 mg, 0.318 mmol, 1.0 equiv) in CH₂Cl₂/DMF (4:1) was added PS-hydroxybenzotriazole (PS-HOBt, 1.00 mmol/g, 0.67 equiv), 4-dimethylaminopyridine (15.5 mg, 0.127 mmol, 0.40 equiv), and then 1-ethyl-3-(3-dimethylaminopropyl)carbodiimide (148 mg, 0.954 mmol, 3.0 equiv). The reaction mixture was shaken slowly for 24 h and then filtered. The resin was washed with MeOH (5 mL) and CH₂Cl₂ (5 mL) thrice to remove excess acid. Then, the resin was added to a solution of allylamine (**I-78a**, 15.5 μ L, 0.220 mmol, 0.70 equiv) and diisopropylethylamine (55.4 μ L, 0.318 mmol, 1.0 equiv) in CH₂Cl₂ and shaken slowly for another 24 h. The mixture was filtered again was washed with MeOH (5 mL) and CH₂Cl₂ (5 mL) thrice

before the solvent was removed under vacuum. Column chromatography with 20% EtOAc:Hex as the eluent gave amide product **I-79a** in 43 mg (38% yield).



(4R,4aS,6aR,9S,11aR,11bS)-N-Allyl-4,9,11b-trimethyl-8-oxotetradecahydro-6a,9-methanocyclohepta[a]naphthalene-4-carboxamide (I-79a).

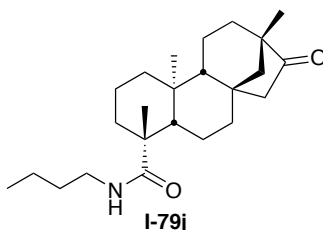
^1H NMR (400 MHz, CDCl_3): δ 5.83 – 5.70 (m, 1H), 5.62 (br s, 1H), 5.09 (dd, $J = 23.1$, 13.7 Hz, 2H), 3.79 (t, $J = 5.1$ Hz, 2H), 2.58 (dd, $J = 18.6$, 3.6 Hz, 1H), 2.01 – 1.85 (m, 3H), 1.77 – 1.25 (m, 9H), 1.19 – 1.15 (m, 2H), 1.13 (s, 3H), 1.10 – 1.05 (m, 2H), 0.91 (s, 3H), 0.89 – 0.82 (m, 2H), 0.71 (s, 3H), 0.67 – 0.63 (m, 1H). ^{13}C NMR (125 MHz, CDCl_3): δ 222.6, 176.4, 134.4, 116.6, 57.5, 57.2, 54.7, 54.2, 48.7, 48.4, 43.7, 41.9, 41.7, 40.2, 39.5, 38.1, 37.3, 30.2, 22.2, 20.3, 19.9, 19.2, 13.6;



(4R,4aS,6aR,9S,11aR,11bS)-N-Benzyl-4,9,11b-trimethyl-8-oxotetradecahydro-6a,9-methanocyclohepta[a]naphthalene-4-carboxamide (I-79b).

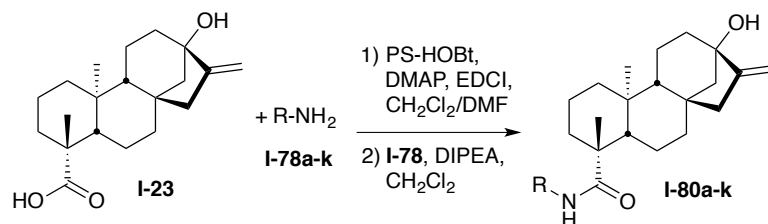
^1H NMR (400 MHz, CDCl_3): δ 7.36 – 7.25 (m, 5H), 5.86 (t, $J = 4.9$ Hz, 1H), 4.40 (d, $J = 5.4$ Hz, 2H), 2.62 (dd, $J = 18.6$, 3.6 Hz, 1H), 2.06 – 1.90 (m, 2H), 1.83 – 1.63 (m, 6H), 1.59 – 1.32 (m, 7H), 1.27 – 1.22 (m, 1H), 1.21 (s, 3H), 1.18 – 1.12 (m, 2H), 0.96 (s, 3H), 0.95

– 0.79 (m, 1H), 0.74 (s, 3H). ^{13}C NMR (125 MHz, CDCl_3): δ 222.4, 176.4, 138.5, 128.9, 128.7, 128.0, 127.5, 127.5, 57.6, 54.7, 54.3, 48.7, 48.4, 43.7, 41.7, 40.2, 39.5, 38.1, 38.1, 37.3, 30.2, 22.2, 22.2, 20.3, 19.9, 19.2, 13.6; mp 68-69 °C; LRMS (ESI) (m/z): $[\text{M}+\text{Na}]^+$ calcd for $\text{C}_{27}\text{H}_{37}\text{NO}_2\text{Na}$ 430.2824, found 430.4; $[\alpha]_{\text{D}}^{23}$ -44.0° (c 1.00, CHCl_3).

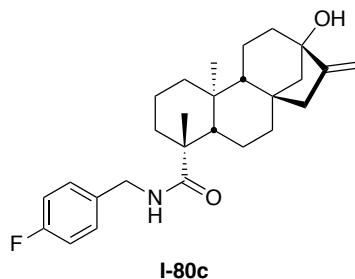


(4R,4aS,6aR,9S,11aR,11bS)-N-Butyl-4,9,11b-trimethyl-8-oxotetradecahydro-6a,9-methanocyclohepta[a]naphthalene-4-carboxamide (I-79j).

oil; ^1H NMR (400 MHz, CDCl_3): δ 5.59 (s, 1H), 3.21 (dt, $J = 11.8, 6.7$ Hz, 2H), 2.65 (dd, $J = 18.6, 3.6$ Hz, 1H), 2.01 (d, $J = 14.3$ Hz, 1H), 1.95 (d, $J = 13.3$ Hz, 1H), 1.77 (dd, $J = 19.9, 14.1$ Hz, 4H), 1.71 – 1.65 (m, 2H), 1.63 – 1.57 (m, 1H), 1.56 – 1.52 (m, 1H), 1.51 – 1.45 (m, 4H), 1.40 (dd, $J = 11.8, 3.7$ Hz, 1H), 1.37 – 1.30 (m, 3H), 1.25 – 1.18 (m, 2H), 1.17 (s, 3H), 1.16 – 1.09 (m, 2H), 0.97 (s, 3H), 0.92 (t, $J = 7.2$ Hz, 4H), 0.77 (s, 3H); ^{13}C NMR (125 MHz, CDCl_3): δ 222.4, 176.5, 57.6, 54.8, 54.3, 48.7, 48.4, 43.6, 41.8, 40.2, 39.5, 39.2, 38.2, 38.1, 37.3, 31.5, 30.2, 22.3, 20.3, 20.3, 19.9, 19.2, 13.8, 13.5; LRMS (ESI) (m/z): $[\text{M}+\text{H}]^+$ calcd for $\text{C}_{24}\text{H}_{40}\text{NO}_2$ 374.2981, found 374.3; $[\alpha]_{\text{D}}^{23}$ -32.2° (c 0.500, CHCl_3).

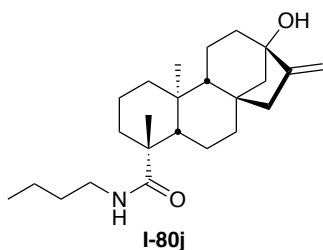


Standard procedure for solid-phase bond formation of steviol amide analogs **I-80a-k** (Scheme I-26). To a solution of steviol (**I-23**, 100 mg, 0.318 mmol, 1.00 equiv) in CH₂Cl₂/DMF (4:1) in a flame-dry reaction vial, was added PS-hydroxybenzotriazole (PS-HOBt, 1.00 mmol/g, 0.213 mmol, 0.670 equiv), 4-dimethylaminopyridine (55.4 μ L, 0.318 mmol, 0.40 equiv), and then 1-ethyl-3-(3-dimethylaminopropyl) carbodiimide (148 mg, 0.954 mmol, 3.0 equiv). The reaction mixture was shaken slowly for 24 h and then filtered. The resins were washed with MeOH (5 mL) and CH₂Cl₂ (5 mL) thrice to remove excess acid. Then, the resin was added to a solution of 4-fluorobenzylamine (**I-78c**, 27.5 mg, 0.220 mmol, 0.70 equiv) and diisopropylethylamine (55.4 μ L, 0.318 mmol, 1.0 equiv) in CH₂Cl₂ and shaken slowly for another 24 h. The mixture was filtered again was washed with MeOH (5 mL) and CH₂Cl₂ (5 mL) thrice before the solvent was removed under vacuum. The crude residue was purified by column chromatography with 20% EtOAc:Hex to furnish the amide **I-80c**.



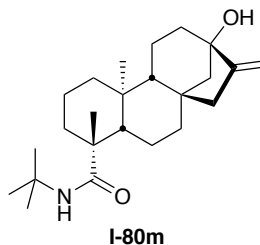
(4*R*,4*aS*,6*aR*,9*S*,11*aR*,11*bS*)-*N*-(4-Fluorobenzyl)-9-hydroxy-4,11*b*-dimethyl-8-methylenetetradecahydro-6*a*,9-methanocyclohepta[*a*]naphthalene-4-carboxamide (I-80c**).**

¹H NMR (400 MHz, CDCl₃): δ 8.27 (s, 1H), 7.70 (dd, *J* = 8.5, 5.7 Hz, 2H), 7.03 (t, *J* = 8.6 Hz, 2H), 4.82 (d, *J* = 67.5 Hz, 2H), 4.69 (s, 2H), 2.13 – 1.93 (m, 4H), 1.88 – 1.63 (m, 6H), 1.58 – 1.22 (m, 5H), 1.20 – 1.16 (m, 1H), 1.11 (s, 3H), 1.08 – 0.97 (m, 3H), 0.88 (d, *J* = 7.9 Hz, 1H), 0.79 (s, 3H), 0.75 (dd, *J* = 12.7, 3.7 Hz, 1H). ¹³C NMR (125 MHz, CDCl₃): δ 176.6, 160.6, 156.0, 130.1, 129.6, 129.4, 115.6, 115.4, 103.0, 80.2, 64.2, 57.4, 53.7, 47.4, 46.9, 43.8, 42.9, 41.7, 40.9, 39.4, 38.2, 30.1, 23.0, 22.4, 20.4, 19.3, 15.7



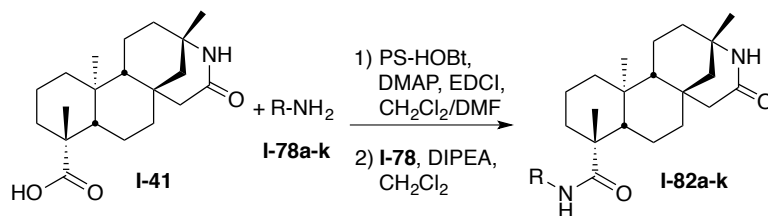
(4*R*,4*aS*,6*aR*,9*S*,11*aR*,11*bS*)-*N*-Butyl-9-hydroxy-4,11*b*-dimethyl-8-methylenetetradecahydro-6*a*,9-methanocyclohepta[*a*]naphthalene-4-carboxamide (I-80j).

¹H NMR (400 MHz, CDCl₃): δ 7.99 (s, 1H), 5.58 (s, 1H), 4.88 (d, *J* = 68.1 Hz, 2H), 3.20 (dt, *J* = 12.2, 6.8 Hz, 2H), 2.90 (d, *J* = 30.2 Hz, 1H), 2.18 (d, *J* = 17.0 Hz, 1H), 2.14 – 2.09 (m, 1H), 2.07 – 2.00 (m, 2H), 1.89 (dd, *J* = 21.7, 5.2 Hz, 3H), 1.82 – 1.71 (m, 3H), 1.63 – 1.51 (m, 2H), 1.51 – 1.43 (m, 4H), 1.42 – 1.30 (m, 3H), 1.26 (d, *J* = 10.8 Hz, 1H), 1.13 (s, 3H), 1.10 – 0.99 (m, 2H), 0.94 – 0.90 (m, 3H), 0.89 (s, 3H), 0.86 – 0.77 (m, 1H); ¹³C NMR (125 MHz, CDCl₃): δ 176.6, 156.1, 102.9, 80.2, 57.3, 53.8, 47.4, 46.9, 43.7, 41.7, 41.6, 41.1, 39.4, 39.3, 39.2, 38.3, 31.5, 30.1, 22.4, 20.5, 20.3, 19.4, 15.6, 13.8; LRMS (*m/z*): [M+H]⁺ calcd for C₂₄H₄₀NO₂ 374.2981, found 374.3; [α]_D²³ –77.5° (*c* 1.00, CHCl₃).



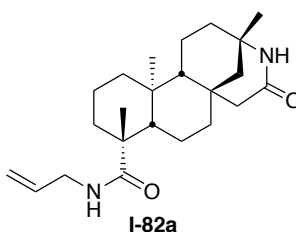
(4*R*,4*aS*,6*aR*,9*S*,11*aR*,11*bS*)-*N*-(*tert*-butyl)-9-hydroxy-4,11*b*-dimethyl-8-methylenetetradecahydro-6*a*,9-methanocyclohepta[*a*]naphthalene-4-carboxamide (I-80m).

oil; ^1H NMR (400 MHz, CDCl_3): δ 5.34 (s, 1H), 4.88 (d, $J = 66.6$ Hz, 2H), 2.94 (s, 1H), 2.18 (d, $J = 19.5$ Hz, 1H), 2.10 (d, $J = 17.2$ Hz, 1H), 1.99 (d, $J = 13.6$ Hz, 1H), 1.91 – 1.84 (m, 4H), 1.82 – 1.73 (m, 4H), 1.60 – 1.50 (m, 2H), 1.49 – 1.37 (m, 3H), 1.33 (s, 3H), 1.31 (s, 6H), 1.27 (dd, $J = 14.7, 3.6$ Hz, 1H), 1.12 (s, 3H), 1.08 – 0.98 (m, 2H), 0.95 (s, 3H), 0.82 (d, $J = 4.0$ Hz, 1H); ^{13}C NMR (125 MHz, CDCl_3): δ 175.7, 156.1, 102.9, 80.2, 77.4, 77.0, 76.7, 57.2, 53.8, 50.7, 47.4, 46.9, 44.1, 41.7, 41.6, 41.2, 39.5, 39.3, 38.5, 30.2, 28.8, 28.7, 28.7, 22.5, 20.5, 19.3, 15.9; LRMS (ESI) (m/z): $[\text{M}+\text{H}]^+$ calcd for $\text{C}_{24}\text{H}_{40}\text{NO}_2$ 374.2981, found 374.3; $[\alpha]_{\text{D}}^{23} -102.1^\circ$ (c 0.750, CHCl_3).



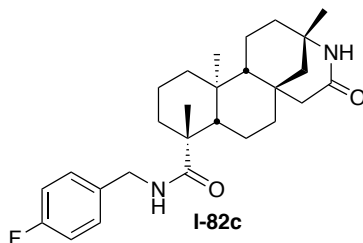
Standard procedure for solid-phase bond formation of isosteviol lactam (**I-41**) amide analogs **I-82a-k** (Scheme I-26). To a solution of lactam (**I-41**, 100 mg, 0.333 mmol, 1.00 equiv) in $\text{CH}_2\text{Cl}_2/\text{DMF}$ (4:1) in a flame-dry reaction vial, was added PS-hydroxybenzotriazole (PS-HOBt, 1.00 mmol/g, 0.223 mmol, 0.670 equiv), 4-

dimethylaminopyridine (58.0 μL , 0.333 mmol, 0.40 equiv), and then 1-ethyl-3-(3-dimethylaminopropyl) carbodiimide (155 mg, 1.00 mmol, 3.0 equiv). The reaction mixture was shaken slowly for 24 h and then filtered. The resins were washed with MeOH (5 mL) and CH_2Cl_2 (5 mL) thrice to remove excess acid. Then, the resin was added to a solution of allylamine (**I-78a**, 29.1 mg, 0.220 mmol, 0.70 equiv) and diisopropylethylamine (58.0 μL , 0.333 mmol, 1.0 equiv) in CH_2Cl_2 and shaken slowly for another 24 h. The mixture was filtered again was washed with MeOH (5 mL) and CH_2Cl_2 (5 mL) thrice before the solvent was removed under vacuum. The crude residue was purified by column chromatography with 20% EtOAc:Hex to furnish the amide **I-82a**.



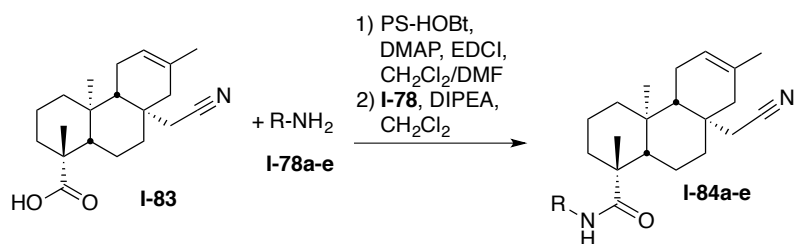
(3*S*,6*aR*,8*aS*,9*R*,12*aS*,12*bR*)-*N*-Allyl-3,9,12*a*-trimethyl-5-oxotetradecahydro-2*H*-3,6*a*-methanonaphtho[2,1-*d*]azocine-9-carboxamide (I-82a**).**

oil; ^1H NMR (400 MHz, CDCl_3): δ 5.84 – 5.70 (m, 1H), 5.60 (s, 1H), 5.18 – 5.03 (m, 2H), 3.87 – 3.71 (m, 2H), 2.82 (d, $J = 29.2$ Hz, 1H), 2.44 (ddd, $J = 52.5, 16.6, 2.1$ Hz, 1H), 2.14 – 1.62 (m, 8H), 1.52 (s, 6H), 1.49 – 1.16 (m, 4H), 1.13 (s, 3H), 1.13 – 0.99 (m, 3H), 0.84 (dd, $J = 13.6, 3.8$ Hz, 1H), 0.76 – 0.62 (m, 3H). ^{13}C NMR (125 MHz, CDCl_3): δ 176.3, 134.5, 131.4, 120.0, 116.8, 57.9, 52.0, 45.9, 43.8, 42.1, 40.3, 39.5, 38.1, 37.6, 35.4, 33.2, 30.2, 23.4, 22.4, 20.5, 20.1, 19.4, 14.0; HRMS (ESI) (m/z): $[\text{M}+\text{Na}]^+$ calcd for $\text{C}_{23}\text{H}_{36}\text{O}_2\text{N}_2\text{Na}$ 395.2777, found 395.2680; $[\alpha]_{\text{D}}^{23}$ -10.3° (c 1.20, CHCl_3).

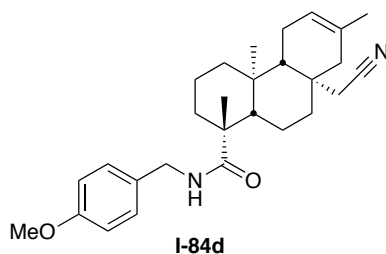


(3*S*,6*aR*,8*aS*,9*R*,12*aS*,12*bR*)-*N*-(4-fluorobenzyl)-3,9,12*a*-trimethyl-5-oxotetradecahydro-2*H*-3,6*a*-methanonaphtho[2,1-*d*]azocine-9-carboxamide(I-82c).

oil; $^1\text{H NMR}$ (400 MHz, CDCl_3): δ 7.33 – 7.29 (m, 1H), 7.25 – 7.22 (m, 1H), 7.03 – 6.97 (m, 2H), 6.51 (t, $J = 6.0$ Hz, 1H), 4.56 (dd, $J = 15.0, 6.5$ Hz, 1H), 4.49 – 4.33 (m, 2H), 2.40 (d, $J = 12.1$ Hz, 1H), 2.31 (d, $J = 17.8$ Hz, 1H), 2.17 (d, $J = 13.4$ Hz, 1H), 1.88 (dd, $J = 16.9, 2.7$ Hz, 4H), 1.78 (d, $J = 13.2$ Hz, 1H), 1.73 – 1.67 (m, 2H), 1.64 – 1.56 (m, 2H), 1.51 – 1.42 (m, 1H), 1.39 (s, 3H), 1.36 – 1.28 (m, 2H), 1.25 (s, 3H), 1.22 – 1.15 (m, 1H), 1.13 – 1.04 (m, 2H), 1.02 – 0.93 (m, 2H), 0.86 (s, 3H); $^{13}\text{C NMR}$ (125 MHz, CDCl_3): δ 183.0, 176.1, 171.0, 161.1, 129.5, 129.5, 115.7, 115.5, 77.3, 77.0, 76.7, 59.5, 57.3, 56.6, 51.2, 43.7, 43.6, 42.8, 42.0, 39.8, 38.0, 37.7, 37.5, 35.0, 28.8, 26.1, 19.5, 19.1, 18.9, 13.8; LRMS (ESI) (m/z): $[\text{M}+\text{H}]^+$ calcd for $\text{C}_{27}\text{H}_{38}\text{FN}_2\text{O}_2$ 441.2339, found 441; $[\alpha]_{\text{D}}^{23}$ 19.2° (c 1.00, CHCl_3).



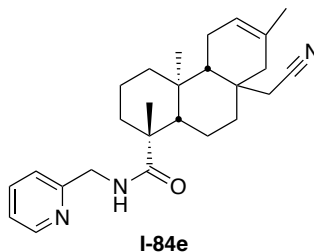
Standard procedure for direct amide bond formation from nitrile **I-83** (Scheme I-26). To a flame-dried reaction flask of the nitrile acid **I-83** (1.0 equiv) in CH₂Cl₂/DMF (4:1) in a flame-dry reaction vial, was added PS-hydroxybenzotriazole (PS-HOBt, 1.00 mmol/g, 0.67 equiv), 4-dimethylaminopyridine (55.4 μL, 0.318 mmol, 0.40 equiv), and then 1-ethyl-3-(3-dimethylaminopropyl) carbodiimide (148 mg, 0.954 mmol, 3.0 equiv). The reaction mixture was shaken slowly for 24 h and then filtered. The resins were washed with MeOH (5 mL) and CH₂Cl₂ (5 mL) thrice to remove excess acid. Then, the resin was added to a solution of amine **I-78** (0.220 mmol, 0.70 equiv) and diisopropylethylamine (55.4 μL, 0.318 mmol, 1.0 equiv) in CH₂Cl₂ and shaken slowly for another 24 h. The mixture was filtered again was washed with MeOH (5 mL) and CH₂Cl₂ (5 mL) thrice before the solvent was removed under vacuum. The crude residue was purified by column chromatography with 20% EtOAc:Hex to furnish the amide **I-84**.



(1*R*,4*aS*,4*bR*,8*aR*,10*aS*)-*N*-benzyl-8*a*-(cyanomethyl)-1,4*a*,7-trimethyl-1,2,3,4,4*a*,4*b*,5,8,8*a*,9,10,10*a*-dodecahydrophenanthrene-1-carboxamide (I-84d**).**

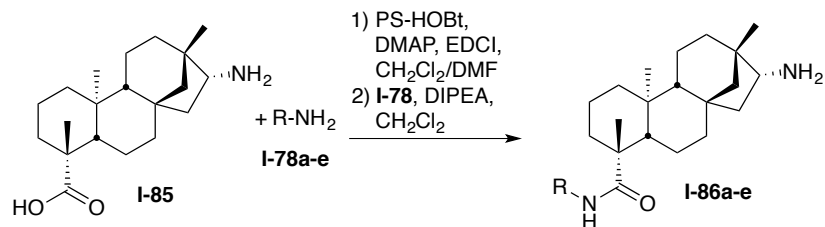
¹H NMR (400 MHz, CDCl₃): δ 7.21 (d, *J* = 8.4 Hz, 2H), 6.86 (d, *J* = 8.4 Hz, 2H), 5.69 (s, 1H), 4.36 (d, *J* = 5.6 Hz, 2H), 3.80 (s, 3H), 2.98 (dd, *J* = 19.0, 2.5 Hz, 1H), 2.17 (d, *J* = 13.1 Hz, 1H), 2.01 (s, 3H), 2.05 – 1.96 (m, 1H), 1.90 – 1.66 (m, 4H), 1.61 (d, *J* = 13.6 Hz,

2H), 1.51 – 1.38 (m, 4H), 1.28 (s, 1H), 1.23 (s, 3H), 1.09 (s, 3H), 1.01 (td, $J = 13.5, 3.8$ Hz, 1H), 0.93 – 0.87 (m, 1H), 0.85 (s, 3H)¹³C NMR (125 MHz, CDCl₃): δ 183.0, 170.6, 170.0, 159.2, 130.4, 129.4, 129.4, 114.2, 114.2, 77.5, 77.2, 76.8, 57.3, 56.4, 55.5, 55.1, 44.0, 43.7, 43.4, 40.8, 40.1, 39.6, 38.4, 37.2, 29.2, 23.4, 22.3, 21.7, 20.6, 19.1, 13.6; mp 63 – 64 °C; LRMS (ESI) (m/z): $[M+Na]^+$ calcd for C₂₈H₃₈N₂O₂ 434.2933, found 457.3; $[\alpha]_D^{23}$ 3.60° (c 0.600, CHCl₃).



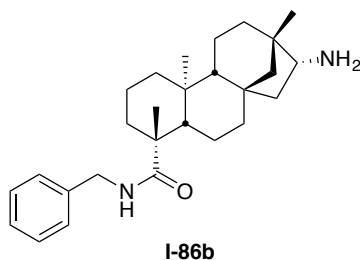
(1R,4aS,4bR,10aS)-8a-(cyanomethyl)-1,4a,7-trimethyl-N-(pyridin-2-ylmethyl)-1,2,3,4,4a,4b,5,8,8a,9,10,10a-dodecahydrophenanthrene-1-carboxamide (I-84e).

oil; ¹H NMR (400 MHz, CDCl₃): δ 8.57 (d, $J = 4.5$ Hz, 1H), 7.67 (t, $J = 7.6$ Hz, 1H), 7.27 (d, $J = 7.9$ Hz, 1H), 7.25 – 7.17 (m, 1H), 7.11 (s, 1H), 5.35 (s, 1H), 5.31 (s, 1H), 4.53 (tdd, $J = 16.5, 11.7, 4.7$ Hz, 2H), 2.78 – 2.53 (m, 1H), 2.49 – 2.29 (m, 1H), 2.26 – 2.12 (m, 2H), 2.12 – 1.92 (m, 5H), 1.87 – 1.77 (m, 1H), 1.75 – 1.69 (m, 1H), 1.66 (s, 3H), 1.58 – 1.49 (m, 1H), 1.35 – 1.27 (m, 1H), 1.23 (s, 3H), 1.22 – 1.12 (m, 3H), 0.92 (dt, $J = 16.0, 8.2$ Hz, 1H), 0.65 (s, 3H); ¹³C NMR (125 MHz, CDCl₃): δ 176.6, 156.4, 149.0, 136.7, 131.2, 122.4, 122.3, 119.9, 119.0, 77.4, 77.1, 76.8, 57.7, 51.7, 45.7, 44.4, 43.7, 40.2, 39.4, 37.9, 37.4, 35.3, 29.9, 23.3, 22.2, 20.2, 19.9, 19.1, 13.5; LRMS (m/z): $[M+Na]^+$ calcd for C₂₆H₃₅N₃ONa 428.2780, found 428.3; $[\alpha]_D^{23}$ –34.0° (c 1.00, CHCl₃).



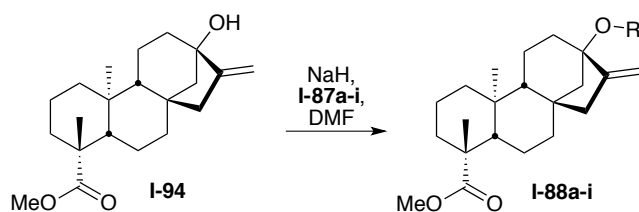
Standard procedure for direct amide bond formation from amine **I-85** (Scheme I-26).

To a flame-dried reaction flask of the amine **I-85** (1.0 equiv) in CH₂Cl₂/DMF (4:1) in a flame-dry reaction vial, was added PS-hydroxybenzotriazole (PS-HOBt, 1.00 mmol/g, 0.67 equiv), 4-dimethylaminopyridine (55.4 μL, 0.318 mmol, 0.40 equiv), and then 1-ethyl-3-(3-dimethylaminopropyl) carbodiimide (148 mg, 0.954 mmol, 3.0 equiv). The reaction mixture was shaken slowly for 24 h and then filtered. The resins were washed with MeOH (5 mL) and CH₂Cl₂ (5 mL) thrice to remove excess acid. Then, the resin was added to a solution of amine **I-78** (0.220 mmol, 0.70 equiv) and diisopropylethylamine (55.4 μL, 0.318 mmol, 1.0 equiv) in CH₂Cl₂ and shaken slowly for another 24 h. The mixture was filtered again was washed with MeOH (5 mL) and CH₂Cl₂ (5 mL) thrice before the solvent was removed under vacuum. The crude residue was purified by column chromatography with 5% MeOH:DCM to furnish the amide **I-86**.



(4*R*,4*aS*,6*aR*,8*R*,9*S*,11*aR*,11*bS*)-8-Amino-*N*-benzyl-4,9,11*b*-trimethyltetradecahydro-6*a*,9-methanocyclohepta[*a*]naphthalene-4-carboxamide (I-86b**).**

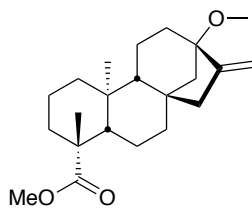
oil; ^1H NMR (400 MHz, CDCl_3): δ 7.83 (s, 1H), 7.36 (d, $J = 6.8$ Hz, 2H), 7.34 - 7.30 (m, 3H), 4.53 (d, $J = 6.2$ Hz, 2H), 2.18 (d, $J = 13.9$ Hz, 1H), 1.94 - 1.78 (m, 4H), 1.76 - 1.71 (m, 3H), 1.69 - 1.58 (m, 3H), 1.49 - 1.41 (m, 3H), 1.40 - 1.33 (m, 2H), 1.30 - 1.26 (m, 1H), 1.25 (s, 3H), 1.17 - 1.12 (m, 1H), 1.11 - 1.01 (m, 3H), 0.98 (t, $J = 7.4$ Hz, 1H), 0.93 (s, 3H), 0.92 - 0.85 (m, 1H), 0.82 (s, 3H); ^{13}C NMR (125 MHz, CDCl_3): δ 182.3, 159.9, 136.9, 128.8, 128.8, 127.9, 127.9, 57.6, 56.9, 56.0, 55.6, 43.8, 43.6, 42.6, 42.0, 41.3, 40.5, 39.9, 38.2, 37.8, 33.9, 29.0, 24.8, 21.6, 20.7, 18.8, 13.5; LRMS (m/z): $[\text{M}+\text{H}]^+$ calcd for $\text{C}_{27}\text{H}_{40}\text{N}_2\text{O}$ 408.3141, found 409; $[\alpha]_{\text{D}}^{23} -5.25^\circ$ (c 0.750, CHCl_3).



Standard procedure for *O*-alkylation of steviol ester (**I-94**) to form ethers **I-88a-i** (Scheme I-27).

To a solution of steviol ester (100 mg, 0.318 mmol, 1.0 equiv) in DMF (5 mL) in a flame-dry reaction vial was added slowly via cannula a solution of sodium hydride (38.3 mg in 60% dispersion in oil, 0.954 mmol, 3.0 equiv) in dry DMF (5 mL). Then, methyl iodide (90.3 mg, 0.636 mmol, 2.0 equiv) was added to the reaction flask and the mixture was allowed to stir for 2 h at ambient temperature. The reaction was quenched with MTBE and the organic phase was washed successively with water. The aqueous phase was extracted with MTBE and the combined organic layers were dried over MgSO_4 , filtered, and

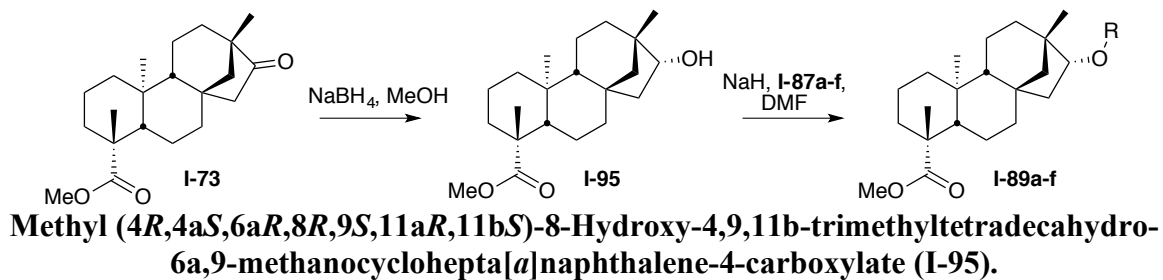
concentrated *in vacuo*. Purification by flash column chromatography with 20% EtOAc:Hex yielded the product.



I-88a

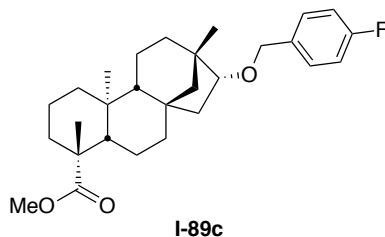
Methyl (4*R*,4*aS*,6*aR*,9*S*,11*aR*,11*bS*)-9-methoxy-4,11*b*-dimethyl-8-methylenetetradecahydro-6*a*,9-methanocyclohepta[*a*]naphthalene-4-carboxylate (I-88a).

oil; ¹H NMR (400 MHz, CDCl₃): δ 4.87 (d, *J* = 6.1 Hz, 2H), 3.64 (s, 3H), 3.22 (s, 3H), 2.18 (d, *J* = 13.2 Hz, 1H), 2.14 – 2.00 (m, 2H), 1.89 – 1.80 (m, 4H), 1.79 – 1.71 (m, 3H), 1.69 – 1.58 (m, 1H), 1.57 – 1.49 (m, 2H), 1.48 – 1.40 (m, 3H), 1.17 (s, 3H), 1.07 – 0.94 (m, 3H), 0.82 (s, 3H), 0.85 – 0.76 (m, 1H); ¹³C NMR (125 MHz, CDCl₃): δ 151.0, 103.7, 85.2, 77.3, 77.0, 76.7, 57.0, 54.0, 51.2, 50.1, 48.1, 43.8, 41.7, 41.5, 40.7, 40.0, 39.3, 38.8, 38.0, 28.7, 21.9, 20.2, 19.1, 15.3, LRMS (ES) (*m/z*): [M+CH₂O₂]⁺ calcd for C₂₂H₃₄O₃ 390.2508, found 390.3; [α]_D²³ -93.5° (*c* 0.800, CHCl₃).



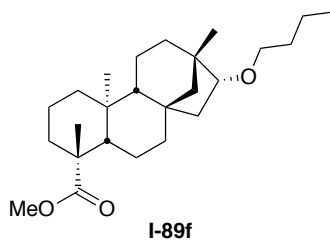
To a solution of the isosteviol ester (**I-73**, 1.00 g, 3.00 mmol) in 25 mL of MeOH at 0 °C (ice bath), was slowly added NaBH₄ (134 mg, 3.55 mmol). The reaction mixture was stirred for 1 h at 0 °C (ice bath), and then solvent was evaporated under reduced pressure. It was then diluted with water and extracted with MTBE. Evaporation of the solvent and purification of the product on a silica gel column using 10% EtOAc:Hex to give hydroxyl ester **I-95** (450 mg, 45%). ¹H NMR (400 MHz, CDCl₃): δ 3.65 (dd, J = 10.6, 4.6 Hz, 1H), 3.42 (s, 3H), 1.96 (d, J = 13.4 Hz, 1H), 1.73 (s, 1H), 1.68 – 1.47 (m, 6H), 1.45 – 1.27 (m, 4H), 1.24 – 0.97 (m, 4H), 0.96 (s, 3H), 0.86 – 0.75 (m, 4H), 0.70 (s, 3H), 0.69 – 0.61 (m, 1H), 0.52 (s, 3H); ¹³C NMR (100 MHz, CDCl₃): δ 178.1, 80.4, 57.1, 55.8, 55.2, 51.1, 43.7, 42.8, 42.0, 42.0, 41.7, 39.9, 38.0, 38.0, 33.7, 28.9, 24.9, 21.7, 20.4, 18.9, 13.1. HRMS (ESI) (*m/z*): [M+Na]⁺ calcd for C₂₁H₃₄O₃Na 357.2406, found 357.2398; [α]_D²³ -57.1° (*c* 0.833, CHCl₃).

Standard procedure for *O*-alkylation of isosteviol hydroxyl ester (**I-95**) to form ethers **I-89a-f** (Scheme I-27). To a solution of hydroxyl ester (**I-95**, 100 mg, 0.345 mmol, 1.0 equiv) in DMF (5 mL) in a flame-dry reaction vial was added slowly via cannula a solution of sodium hydride (38.3 mg in 60% dispersion in oil, 0.954 mmol, 3.0 equiv) in dry DMF (5 mL). Then, methyl iodide (90.3 mg, 0.636 mmol, 2.0 equiv) was added to the reaction flask and the mixture was allowed to stir for 2 h at ambient temperature. The reaction was quenched with MTBE and the organic phase was washed successively with water. The aqueous phase was extracted with MTBE and the combined organic layers were dried over MgSO₄, filtered, and concentrated *in vacuo*. Purification by flash column chromatography with 20% EtOAc:Hex yielded the product **I-89**.



Methyl (4*R*,4*aS*,6*aR*,8*S*,9*S*,11*aR*,11*bS*)-8-((4-Fluorobenzyl)oxy)-4,9,11b-trimethyltetradecahydro-6*a*,9-methanocyclohepta[*a*]naphthalene-4-carboxylate (I-89c).

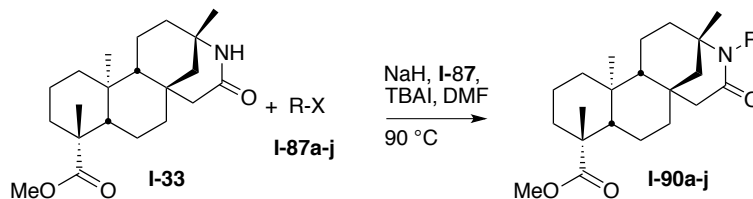
¹H NMR (400 MHz, CDCl₃): δ 7.29 (dd, *J* = 8.4, 5.7 Hz, 2H), 7.01 (t, *J* = 8.7 Hz, 2H), 4.45 (dd, 2H), 3.63 (s, 3H), 3.54 (dd, *J* = 10.3, 4.1 Hz, 1H), 2.17 (d, *J* = 13.3 Hz, 1H), 1.96 – 1.79 (m, 4H), 1.76 – 1.62 (m, 3H), 1.59 – 1.53 (m, 2H), 1.50 – 1.36 (m, 3H), 1.33 – 1.24 (m, 2H), 1.17 (s, 3H), 1.06 – 0.96 (m, 4H), 0.93 (s, 3H), 0.91 – 0.83 (m, 1H), 0.72 (s, 3H); ¹³C NMR (125 MHz, CDCl₃): δ 178.3, 132.9, 129.0, 128.9, 115.9, 115.2, 115.0, 87.0, 71.3, 57.3, 56.0, 55.5, 51.3, 43.9, 42.4, 42.2, 42.0, 40.3, 40.0, 38.2, 38.1, 34.5, 29.0, 25.6, 21.9, 20.6, 19.1, 13.3; mp 151-152 °C; HRMS (ESI) (*m/z*): [M+Na]⁺ calcd for C₂₀H₃₀O₃Na 465.2883, found 465.2795; [α]_D²³ –103.7° (*c* 0.655, CHCl₃).



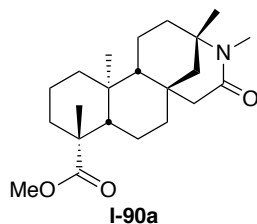
Methyl (4*R*,4*aS*,6*aR*,8*R*,9*S*,11*aR*,11*bS*)-8-Butoxy-4,9,11b-trimethyltetradecahydro-6*a*,9-methanocyclohepta[*a*]naphthalene-4-carboxylate (I-89f).

oil ; ¹H NMR (400 MHz, CDCl₃): δ 3.65 (s, 3H), 3.53 – 3.43 (m, 1H), 3.43 – 3.31 (m, 2H), 2.17 (d, *J* = 13.0 Hz, 1H), 1.89 – 1.84 (m, 2H), 1.83 – 1.77 (m, 3H), 1.72 – 1.66 (m, 2H),

1.64 – 1.56 (m, 3H), 1.51 (dd, $J = 12.2, 6.1$ Hz, 3H), 1.44 – 1.37 (m, 4H), 1.32 – 1.24 (m, 2H), 1.21 (d, $J = 4.7$ Hz, 1H), 1.18 (s, 3H), 1.12 – 1.03 (m, 2H), 1.02 – 0.97 (m, 2H), 0.94 (s, 3H), 0.92 – 0.83 (m, 2H), 0.73 (s, 3H); ^{13}C NMR (125 MHz, CDCl_3): δ 178.2, 87.3, 69.9, 57.3, 56.0, 55.5, 51.1, 43.8, 42.2, 42.0, 40.5, 39.9, 38.1, 38.0, 34.4, 32.3, 28.9, 25.6, 21.8, 21.7, 20.4, 19.5, 19.0, 14.0, 13.1; HRMS (ESI) (m/z): $[\text{M}+\text{Na}]^+$ calcd for $\text{C}_{25}\text{H}_{42}\text{O}_3\text{Na}$ 413.3134, found 413.2998; $[\alpha]_{\text{D}}^{23} -42.8^\circ$ (c 0.850, CHCl_3).



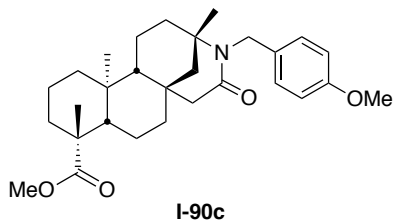
D: Standard procedure for *N*-alkylation of lactam **I-33** (Scheme I-27). To a solution of the lactam (100 mg, 0.347 mmol, 1.0 equiv) in DMF (5 mL) in a flame-dried reaction flask, was added sodium hydride (3.0 equiv, pre-washed with hexanes), alkyl halide **I-87** (5.0 equiv) and a catalytic amount of tetrabutylammonium iodide (TBAI, 10 mol%). The reaction flask was heated to 90 °C, stirred overnight and then the reaction was carefully quenched with water (2 mL). The organic layer was then washed with brine and the aqueous layers were re-extracted with Et_2O (2 x 10 mL). The combined organic layers were then dried over MgSO_4 , filtered, and the Et_2O was removed under reduced pressure, while a centrifugal evaporator was used to remove the DMF to give alkylated lactam **I-90**. Column chromatography with 5% $\text{MeOH}:\text{CH}_2\text{Cl}_2$ gave the substituted-lactam products.



(3*S*,8*aS*,9*R*,12*aS*,12*bR*)-Methyl 3,4,9,12*a*-Tetramethyl-5-oxotetradecahydro-1*H*-3,6*a*-methanonaphtho[2,1-*d*]azocine-9-carboxylate (I-90a).

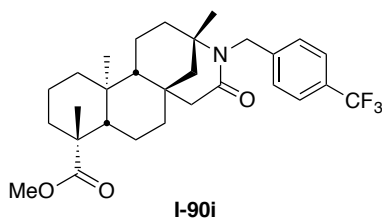
To a 50 mL flame-dried round-bottomed flask of lactam **I-33** (100 mg, 0.29 mmol) in DMF (15 mL) under nitrogen, was added sodium hydride (35 mg, 0.86 mmol, pre-washed with hexanes), methyl iodide (90 μ L, 1.44 mmol) and a catalytic amount of tetrabutylammonium iodide (11 mg, 0.029 mmol). The reaction flask was heated to 90 $^{\circ}$ C and allowed to stir overnight. At this time TLC analysis indicated the consumption of starting material and the reaction was carefully quenched with water (2 mL). The organic layer was then washed with brine and the aqueous layers were re-extracted with Et₂O (2x15 mL). The combined organic layers were then dried over MgSO₄, filtered and the Et₂O was removed under reduced pressure, while a centrifugal evaporator was used to remove the DMF to give methyl alkylated lactam **I-90a** (90 mg, 86%) as an off-white solid. R_f = 0.2 (Hex:EtOAc 4:1); mp 168-172 $^{\circ}$ C; IR (film) 2926, 1722, 1636 cm^{-1} ; ¹H NMR (400 MHz, CDCl₃): δ 3.62 (s, 3H), 2.98 (dd, J = 18.3, 2.9 Hz, 1H), 2.84 (s, 3H), 2.16 (d, J = 13.3 Hz, 1 H), 2.04 (d, J = 18.3 Hz, 1H), 1.83-1.92 (m, 2H), 1.55-1.83 (m, 6H), 1.51 (dt, J = 12.9, 3.2, 3.2 Hz, 1H), 1.40-1.47 (m, 1H), 1.30 (dd, J = 12.8, 2.9 Hz, 1H), 1.25 (s, 3H), 1.18-1.23 (m, 1H), 1.16 (s, 3H), 1.11 (dd, J = 12.8, 3.8 Hz, 1H), 1.04-1.06 (m, 1H), 1.03-0.95 (m, 1H), 0.86 (d, J = 17.65, 2H), 0.75 (s, 3H); ¹³C NMR (100 MHz, CDCl₃): δ 177.7, 171.9, 57.4, 56.8, 55.3, 51.1, 51.0, 44.3, 43.7, 41.0, 39.9, 38.0, 37.8, 35.7, 33.9, 28.5, 27.4, 26.8,

19.7, 18.8, 18.7, 13.5; HRMS (ESI) (m/z): $[M+H]^+$ calcd for $C_{22}H_{36}NO_3$ 362.2695; found 362.2677; $[\alpha]_D^{23}$ 18.9° (c 0.800, $CHCl_3$).



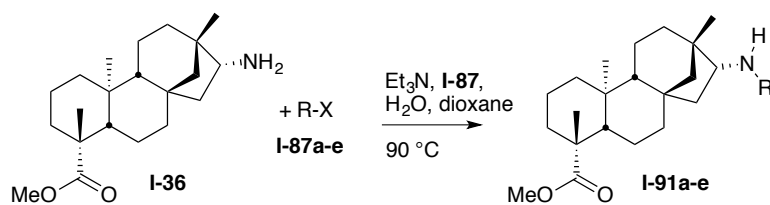
Methyl (3*S*,6*aR*,8*aS*,9*R*,12*aS*,12*bR*)-4-(4-Methoxybenzyl)-3,9,12*a*-trimethyl-5-oxotetradecahydro-2*H*-3,6*a*-methanonaphtho[2,1-*d*]azocine-9-carboxylate (I-90c).

1H NMR (400 MHz, $CDCl_3$): 7.16 (d, J = 8.7 Hz, 2H), 6.81 (d, J = 8.7 Hz, 2H), 4.86 (d, J = 15.4 Hz, 1H), 4.20 (d, J = 15.5 Hz, 1H), 3.78 (s, 3H), 3.64 (s, 3H), 3.07 (dd, J = 18.4, 2.7 Hz, 1H), 2.16 (d, J = 18.2 Hz, 2H), 1.93 – 1.82 (m, 1H), 1.81 – 1.72 (m, 4H), 1.67 (dd, J = 13.0, 2.8 Hz, 1H), 1.54 (dd, J = 12.9, 3.1 Hz, 2H), 1.48 – 1.39 (m, 1H), 1.31 – 1.19 (m, 3H), 1.17 (s, 3H), 1.14 (s, 3H), 1.12 – 0.95 (m, 3H), 0.90 – 0.79 (m, 2H), 0.78 (s, 3H); ^{13}C NMR (125 MHz, $CDCl_3$): 177.8, 172.3, 158.3, 132.1, 128.3 (2C), 113.7 (2C), 57.5, 56.9, 56.4, 55.2, 51.7, 51.2, 44.3, 44.0, 43.8, 41.2, 40.0, 38.0, 37.8, 37.1, 34.1, 28.6, 28.1, 19.8, 18.9, 18.6, 13.7; mp 151-152 °C; LRMS (ESI) (m/z): $[M+H]^+$ calcd for $C_{29}H_{42}NO_4$ 468.3036, found 468.3; $[\alpha]_D^{23}$ -15.6° (c 1.00, $CHCl_3$).



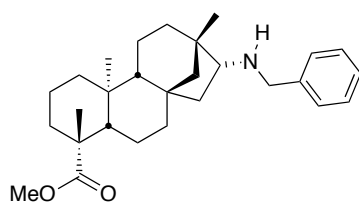
Methyl (3*S*,6*aR*,8*aS*,9*R*,12*aS*,12*bR*)-3,9,12*a*-Trimethyl-5-oxo-4-(4-(trifluoromethyl)benzyl)tetradecahydro-2*H*-3,6*a*-methanonaphtho[2,1-*d*]azocine-9-carboxylate (I-90i**).**

¹H NMR (400 MHz, CDCl₃): δ 7.53 (d, *J* = 8.1 Hz, 2H), 7.32 (d, *J* = 8.1 Hz, 2H), 5.08 (d, *J* = 16.2 Hz, 1H), 4.15 (d, *J* = 16.1 Hz, 1H), 3.64 (s, 3H), 3.09 (dd, *J* = 18.2, 2.5 Hz, 1H), 2.23 – 2.15 (m, 2H), 1.91 – 1.75 (m, 5H), 1.71 (dd, *J* = 13.1, 2.5 Hz, 1H), 1.64 – 1.55 (m, 2H), 1.45 (d, *J* = 13.7 Hz, 1H), 1.36 – 1.29 (m, 1H), 1.27 – 1.20 (m, 2H), 1.18 (s, 3H), 1.17 – 1.11 (m, 1H), 1.10 (s, 3H), 1.08 – 0.96 (m, 2H), 0.94 – 0.84 (m, 2H), 0.79 (s, 3H); ¹³C NMR (125 MHz, CDCl₃): δ 177.7, 172.7, 144.0, 127.1, 127.1, 127.1, 125.6, 125.3, 125.3, 57.4, 56.8, 56.6, 51.5, 51.2, 44.5, 44.2, 43.8, 41.1, 40.0, 38.0, 37.8, 36.9, 34.1, 28.6, 28.0, 19.7, 18.9, 18.6, 13.7; mp 151-152 °C; LRMS (ESI) (*m/z*): [M]⁺ calcd for C₂₉H₃₈F₃NO₃ 505.2814, found 506.4; [α]_D²³ –36.6° (*c* 0.905, CHCl₃).



Standard procedure for *N*-alkylation of amine **I-36** (Scheme I-27). To a flame-dried reaction flask of the amine **I-36** (100 mg, 0.333 mmol, 1.0 equiv) and trimethylamine (1.5 equiv) in a 1,4-dioxane-water mixed solvent (1:1, 6 mL), the alkyl halide (**I-87**, 1.0 equiv) was added. The reaction flask was heated to $90\text{ }^\circ\text{C}$ and allowed to stir for one day. The reaction mixture was quenched with EtOAc and the organic layer was washed with saturated aqueous NH_4Cl . The organic layer was then washed with brine and the aqueous

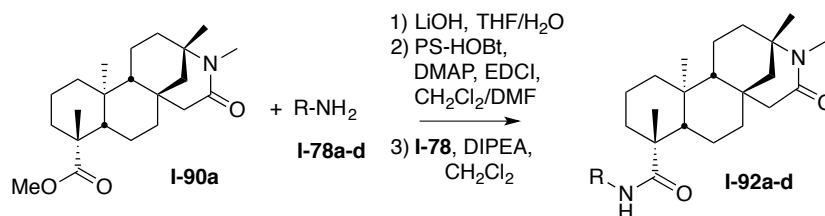
layers were extracted with EtOAc (2 x 10 mL). The combined organic layers were then dried over MgSO₄, filtered, and concentrated *in vacuo* to give the crude alkylated-amine product **I-91**. Purification was done by column chromatography with 5% MeOH:DCM.



I-91b

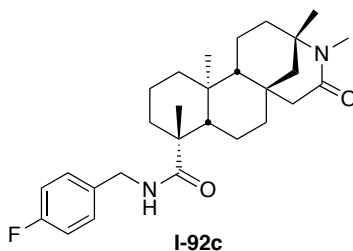
Methyl (4R,4aS,6aR,8R,9S,11aR,11bS)-8-(Benzylamino)-4,9,11b-trimethyltetradecahydro-6a,9-methanocyclohepta[a]naphthalene-4-carboxylate (I-91b).

oil; ¹H NMR (400 MHz, CDCl₃): δ 7.35 (d, *J* = 7.6 Hz, 4H), 7.29 – 7.25 (m, 1H), 3.80 (q, *J* = 46.0, 13.4, 12.4 Hz, 2H), 3.66 (s, 3H), 3.64 (s, 1H), 2.77 (dd, *J* = 10.6, 5.4 Hz, 1H), 2.19 (d, *J* = 13.3 Hz, 1H), 1.86 – 1.80 (m, 2H), 1.74 (d, *J* = 13.5 Hz, 3H), 1.64 – 1.59 (m, 3H), 1.57 – 1.51 (m, 2H), 1.46 – 1.40 (m, 1H), 1.38 – 1.31 (m, 2H), 1.19 (s, 3H), 1.10 – 1.04 (m, 2H), 1.03 – 0.98 (m, 3H), 0.92 (s, 3H), 0.90 – 0.86 (m, 1H), 0.74 (s, 3H); ¹³C NMR (125 MHz, CDCl₃): δ 178.2, 141.4, 128.3, 128.2, 128.0, 128.0, 126.7, 66.2, 57.3, 57.0, 55.9, 53.2, 51.1, 43.8, 42.4, 41.8, 41.6, 41.2, 40.0, 38.1, 38.1, 34.3, 28.9, 25.6, 21.8, 20.7, 19.0, 13.3; HRMS (ESI) (*m/z*): [M]⁺ calcd for C₂₈H₄₁NO₂ 423.3137, found 424.3; [α]_D²³ –58.5° (*c* 1.00, CHCl₃).



Standard procedure for amide bond formation from lactam ester **I-90a** (Scheme I-28).

To a solution of methyl-lactam ester **I-90** (1.00 g, 2.77 mmol) in THF/H₂O (1:1, 10 mL) in a round-bottom flask was added 1M aq. LiOH (5 mL) at room temperature. The reaction was heated to reflux and stirred overnight. Then, it was cooled to room temperature and quenched with 1M aq. HCl to pH 4. The resultant mixture was extracted with EtOAc and the combined organic layers were washed with brined and dried over MgSO₄. The acid was carried on without further purification. To a solution of acid (100 mg, 0.302 mmol, 1.0 equiv) in CH₂Cl₂/DMF (4:1) in a flame-dry reaction vial, was added PS-hydroxybenzotriazole (PS-HOBt, 1.00 mmol/g, 0.67 equiv), 4-dimethylaminopyridine (21.1 μ L, 0.121 mmol, 0.40 equiv), and then 1-ethyl-3-(3-dimethylaminopropyl) carbodiimide (140 mg, 0.905 mmol, 3.0 equiv). The reaction mixture was shaken slowly for 24 h and then filtered. The resins were washed with MeOH (5 mL) and CH₂Cl₂ (5 mL) thrice to remove excess acid. Then, the resin was added to a solution of amine **I-78** (0.211 mmol, 0.70 equiv) and diisopropylethylamine (52.6 μ L, 0.302 mmol, 1.0 equiv) in CH₂Cl₂ and shaken slowly for another 24 h. The mixture was filtered again was washed with MeOH (5 mL) and CH₂Cl₂ (5 mL) thrice before the solvent was removed under vacuum. The crude residue was purified by column chromatography with 20% EtOAc:Hex to furnish the lactam amide **I-92**.



(3*S*,6*aR*,8*aS*,9*R*,12*aS*,12*bR*)-*N*-(4-fluorobenzyl)-3,4,9,12*a*-tetramethyl-5-oxotetradecahydro-2*H*-3,6*a*-methanonaphtho[2,1-*d*]azocine-9-carboxamide(I-92c**).**

oil; ^1H NMR (400 MHz, CDCl_3): δ 7.28 – 7.23 (m, 2H), 7.03 (t, $J = 8.5$ Hz, 2H), 5.24 (d, $J = 15.4$ Hz, 1H), 4.69 (s, 1H), 4.47 (d, $J = 15.5$ Hz, 1H), 3.66 (s, 3H), 2.21 (d, $J = 13.8$ Hz, 1H), 2.15 (d, $J = 13.3$ Hz, 1H), 1.91 – 1.83 (m, 1H), 1.82 – 1.77 (m, 1H), 1.73 (s, 3H), 1.71 – 1.60 (m, 3H), 1.58 (s, 3H), 1.49 (h, 1H), 1.44 – 1.32 (m, 3H), 1.29 (d, $J = 6.8$ Hz, 2H), 1.26 – 1.21 (m, 1H), 1.19 (s, 3H), 1.08 – 0.94 (m, 4H), 0.90 (dd, $J = 13.0, 4.1$ Hz, 1H), 0.85 – 0.76 (m, 1H); LRMS (ESI) (m/z): $[\text{M}+\text{H}]^+$ calcd for $\text{C}_{28}\text{H}_{40}\text{FN}_2\text{O}_2$ 455.2996, found 455; $[\alpha]_{\text{D}}^{23} -74.3^\circ$ (c 0.450, CHCl_3).

PART II- RETINOIC ACID RECEPTOR ALPHA ANTAGONIST
DEVELOPMENT FOR MALE CONTRACEPTION

Chapter 5. Design and Synthesis of Retinoids for Non-Hormonal Male Contraceptive Development

A. Contraception Background

Contraception is the prevention of pregnancy with methods that control male or female fertility.¹⁶² The first reports of contraception date back centuries ago with the invention of the condom in 1564.¹⁶³ This form of birth control was reliant on the male counterpart of sexual relationships, but much has changed since then in terms of more effective condom development and female contraception.¹⁶³ Female birth control most notably began in the 1950s with the introduction of an oral contraception method, also known as “the pill.”¹⁶⁴ The birth control pill inhibits ovulation in normal, ovulating women by mimicking gonadal hormones: estrogen and progesterone. The first human trials were in 1956 with Food and Drug Administration (FDA) approval of the first hormonal contraception by 1960.^{164,165}

1. Unintended Pregnancies and Unmet Need for Contraception

Despite significant advances in reproductive services since then, a *Lancet* report in 2013 estimated that around 146 million women worldwide have an unmet need for contraception, or family planning.¹⁶⁶ That is to say, that millions of women, especially in developing nations, lack access to necessary contraceptive methods.

Moreover, that global estimate increases to 225 million women for women who do not use contraception or employ traditional methods, which include withdrawal or

abstinence.^{167, 168} Table II-1 below displays all the pregnancies from 2008, including the percent distribution of intended and unintended pregnancies. In that year alone, over 85 million pregnancies were unintended with over ten million of those pregnancies coming from developed regions in the world, like the United States. The Centers for Disease Control and Prevention (CDC) describe an unintended pregnancy as an undesired or mistimed pregnancy that occurs.¹⁶⁹ Furthermore, of those unintended pregnancies worldwide, 16%, or over 33 million, resulted in undesired births plus the other 25%, or 52 million, pregnancies that ended in abortion or miscarriages.

Table II-1. The number of pregnancies and percent distribution in 2008.¹⁷⁰

Region	Total # of pregnancies (millions)	% distribution of pregnancies		Unintended pregnancy outcomes (%)		
		Intended	Unintended	Births	Abortions	Miscarriages
World	208.2	59	41	16	20	5
More developed regions	22.8	53	47	15	25	6
Less developed regions	185.4	60	40	16	19	5

We can infer from the number of unintended pregnancies in Table II-1 that there is indeed a large unmet need for families all over the world for modern and effective contraception that will affect millions of women. Compounded by the number of women who experience health problems that prevent them from taking effective contraception,¹⁷¹ the unmet need has led to more research in both female and male contraception.

2. Current Forms of Male Contraception

Females have a variety of options for contraception, each with potential risks and benefits. Aside from the traditional, and at times unsuccessful, methods of natural family planning or barrier methods, women also can employ hormonal systemic contraception, injectable progestins, long-acting reversible contraception, and permanent sterilization.¹⁶⁵ Male contraceptive research, on the other hand, is underdeveloped, with only two currently available options: condoms or a vasectomy.¹⁷² Condoms provide a temporary barrier to fertilization that is reversible upon removal of its use, while vasectomies, the clamping or cutting of the vas deferens to cause male sterilization, can be permanent.¹⁷³ The following chart shows existing contraceptive methods in the developing and developed regions worldwide; the majority of the available methods depend on female fulfillment (Chart II-1).¹⁷⁴

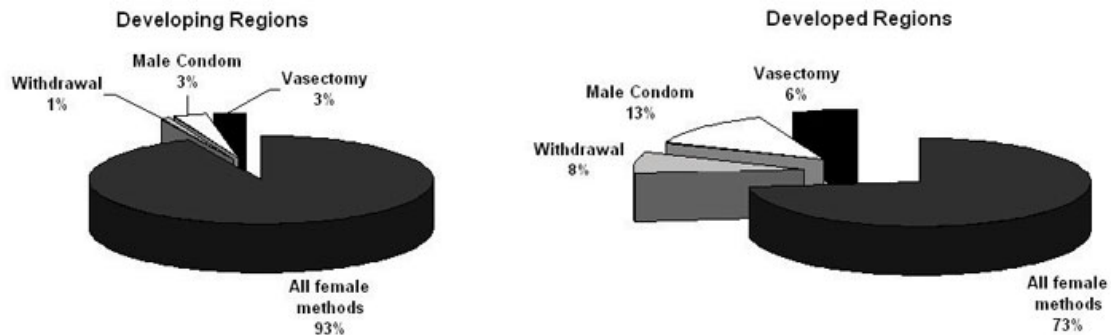


Chart II-1. Existing contraceptive methods in the developing and developed regions in the world.¹⁷⁴

Several research projects are under way intended on producing other male contraceptive options.^{172, 173, 175, 176} Potential male contraceptive methods are classified into categories based on their target of action: hindering the transport of sperm or suppressing spermatogenesis, the maturation of sperm from spermatogonia to spermatozoa.¹⁷⁴ Within

the past decade, the development of a male contraceptive agents that target spermatogenesis is becoming a pharmaceutical option.¹⁷² Understanding spermatogenesis and its mechanism is paramount for male contraceptive development¹⁷⁵ and will be discussed throughout this chapter. As noted by Giwercman *et al.*, spermatogenesis is probably a more vulnerable process than ovulation.¹⁷⁷ Spermatogenesis is the process that generates mature sperm in the testes.¹⁷⁸ This continuous process takes approximately 75 days and produces millions of mature haploid sperm.¹⁷³ Figure II-1, illustrates the spermatogenesis process.

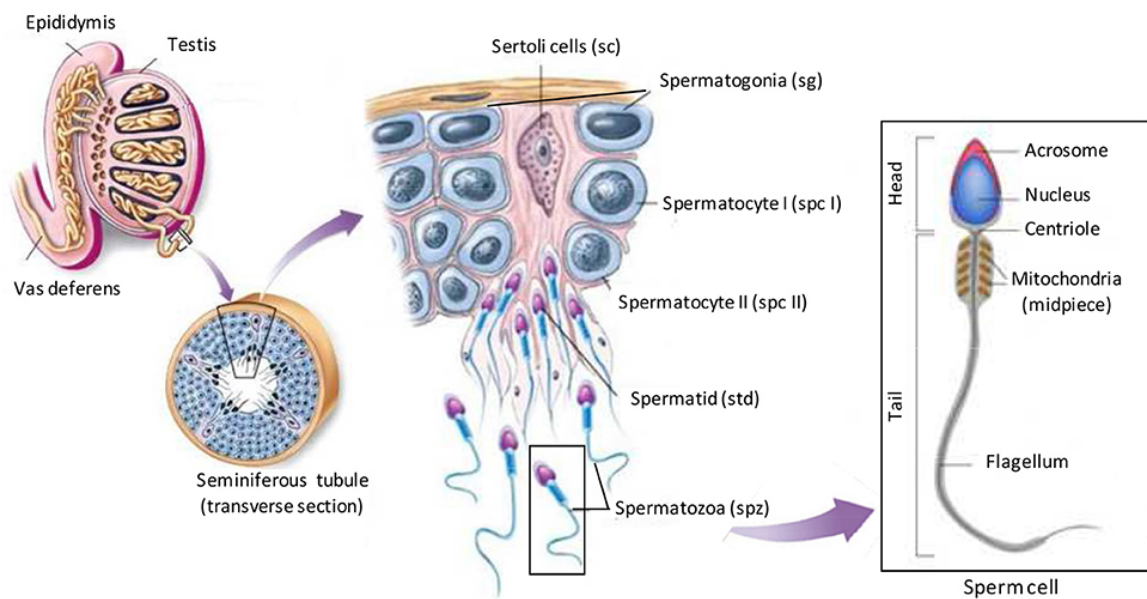


Figure II-1. The process of Spermatogenesis.¹⁷⁹

Beginning in the seminiferous tubules of the testes, diploid spermatogonia (sg) undergo mitosis to produce diploid primary spermatocytes (spc I). These spermatocytes can continue to divide mitotically or move on to the next step: meiosis I. The spc I migrate toward the lumen to undergo meiosis I and produce haploid secondary spermatocytes (spc II). The spc II continue to meiotically divide through meiosis II to generate haploid

spermatids (std). The spermatids continue to mature into spermatozoa (spz) in the lumen of the seminiferous tubules during spermiogenesis.¹⁷⁹ Spermatozoa, or mature sperm cells, consist of a head, mid-piece, and flagella tail. Research has been done to inhibit spermatogenesis through the exogenous administration of testosterone derivatives in male hormonal contraceptive development.^{180, 181} All these studies show the effects of injecting the androgens subcutaneously, because the oral administration route was not effective.¹⁷⁴ Moreover, aside from the slight pain caused by needle injection, other unwanted side effects of supernatural levels of testosterone include negative cardiovascular effects, mood changes, acne,¹⁸² weight gain,¹⁸³ and possible prostate malignancy.¹⁸⁴ Altogether, these side effects and the type of drug administration have made hormonal contraceptive development unattractive.¹⁷⁴ Herein lies the need for a non-hormonal male contraceptive agent.

3. Areas of Focus for Non-Hormonal Male Contraceptive Development

A non-hormonal male contraceptive approach can be defined as one that does not involve the administration of exogenous hormones or agents that block hormone action or secretion.¹⁸⁵ This approach will be less likely to have the adverse effects from the hormonal treatment. Non-hormonal male contraception is an unmet need and an attractive area for drug development, since this allows men to have power to control their fertility as well as take an active role in family planning. Unfortunately, pharmaceutical interest in the male contraceptive research arena has died down, probably due to the slow research; the burden to provide enough safety, efficacy, and reversibility data; and the assurance of not having deleterious effects to future offspring.^{172, 174} As a result, the NIH has taken this global

problem as a major financial contributor.¹⁷² Through the Eunice Kennedy Shriver National Institute of Child Health and Human Development (NICHD), the Male Contraceptive Development Program (MCDP) is an invaluable resource for the future of male birth control.

The MCDP conducts research that can identify mechanisms of sperm maturation regulation and new therapeutic targets.¹⁸⁶ The main areas of research focus on inhibiting spermiogenesis or spermatogenesis, *vide supra*. Our group received funding through the Contraceptive Research Branch to explore multiple areas of potential contraceptive development, such as targeting the sperm-specific Na,K-ATPase alpha 4 ($\alpha 4$), bromodomain testis-specific protein (BRDT), or retinoic acid receptor alpha (RAR α). Na,K-ATPase $\alpha 4$ is a specific isoform of a transmembrane protein that is found to control motility and hyperactivation in sperm through active sodium and potassium ion exchange.¹⁸⁷ BRDT is a tissue-restricted protein that is important in spermatogenesis.¹⁸⁸ The RAR α target will be discussed in greater detail below.

B. Retinoic Acid Receptor Alpha (RAR α)

While the Georg research group focuses on these and other targets for the development of male contraceptive agents, a subset of us (Dr. Rebecca Cuellar, Jillian Kyzer, Dr. Narsihmulu Cheryala, and Trinh Holth) have been investigating RAR α nuclear receptor antagonists. Retinoic acid receptors belong to the nuclear receptor family and are composed of three isotypes: RAR α , β , and γ .¹⁸⁹ They are involved in many significant biological processes including embryogenesis, reproduction, vision, growth, inflammation, cell differentiation, cell proliferation, and apoptosis.¹⁹⁰ Additionally, this family of nuclear

receptors also includes retinoid X receptors, which also come in three similar isoforms: α , β , and γ .¹⁹¹ RARs exist as heterodimers with RXR, forming RAR-RXR complex, which may be responsible for transducing the retinoid signal at the molecular level.¹⁹² RARs are also required for the mediation of the important vitamin A functions during human development.¹⁹³ In addition to forming heterodimer complexes with retinoic acid receptors, RXRs can also exist as homodimers.¹⁹⁴ Both RAR and RXR receptors are activated by retinoic acid (RA) in the cells.¹⁹⁵ Retinoic acid receptors can bind to either all-*trans* RA (ATRA) or 9-*cis* RA, while retinoid X receptors, only bind to 9-*cis* RA (Figure II-2).^{196, 197}

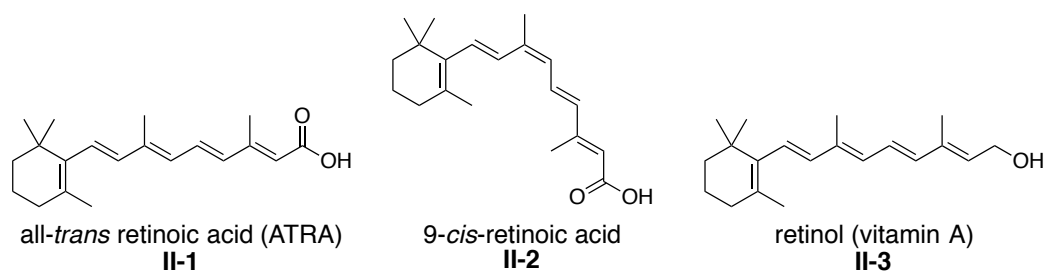


Figure II-2. Structures of all-*trans* retinoic a, 9-*cis* RA, and vitamin A.

ATRA (**II-1**) and 9-*cis*-RA (**II-2**) belong to a group of compounds called retinoids: natural or synthetic analogs of retinol (**II-3**), also known as vitamin A (Figure II-2).¹⁹⁸ Retinol (**II-3**) is converted to **II-1** through sequential oxidation steps in the body.¹⁹⁹ While many of the RAR and RXR isoforms are found in spermatocytes and at different developmental stages, RA mediates its effects through the action of the RAR α in Sertoli cells,¹⁹⁵ Sertoli cells are located in the seminiferous tubules and aid in spermatogenesis.²⁰⁰

1. Implications in Male Contraception

Previous research has shown that a knockout mouse model of RAR α exhibited disrupted spermatogenesis and infertility.²⁰¹ Additionally, defects in vitamin A-deficient (VAD) wild-type mice were reversed after administration of RAR agonists.²⁰¹ While vitamin A-deficiency does occur in humans, not enough information is known regarding the effects on reproductive capabilities.²⁰² However, there is some evidence of the effect of RA on human male germ cells.²⁰³ Reports reveal that germ cells in fetal human testes cultured with retinoic acid underwent apoptosis after they were stimulated to proliferate.²⁰⁴ Additionally, retinoic acid also induces an increase in the gene stimulated by RA *gene 8* (*STRA8*) for the expression of RA in the human embryonic ovary and testis and the postnatal testis.^{195, 205} While the research is ongoing and these processes are not well understood overall, these reports imply the importance of retinoic acid and vitamin A in spermatogonial differentiation, meiosis, and the cycle of the seminiferous epithelium.

The Wolgemuth group at Columbia University first reported on the connection between vitamin A and retinoic acid in mammalian male sterility.^{189, 206} In mouse studies, where the Rara gene is removed (Rara^{-/-}), the results showed sterile male mice with specific abnormalities in spermatogenesis, as seen in histological cross sections of the tubules.²⁰⁷ They also observed that the defects in spermatogenesis were similar to those in vitamin A deficient testes.²⁰⁸ Chung *et al.* also reported that disruptions in RAR α -mediated retinoid signaling in spermatogenesis result in a failure of sperm alignment and release into the seminiferous tubular lumen,¹⁹⁸ which is similar to the effects observed in VAD mice.¹⁸⁹ Of note, RAR α is required for spermatogenesis and its absence results in progressive breakdown of the spermatogenesis process.²⁰⁹ Figure II-3 demonstrates the histological

cross sections (A and B) of a seminiferous tubule in the testes and their illustrations below (C and D) show the effects on spermatogenesis in normal, fertile mice compared to VAD mice.²¹⁰

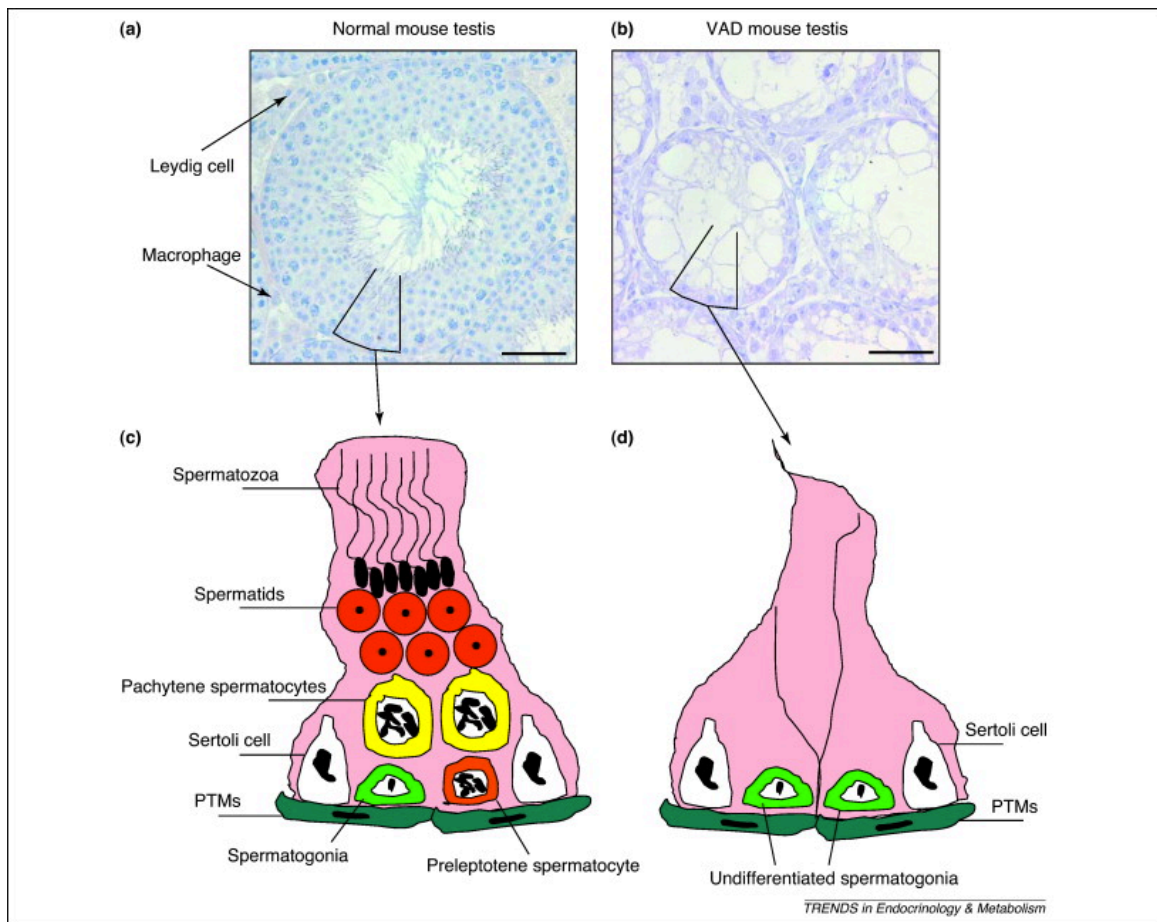


Figure II-3. Normal spermatogenesis in healthy vs vitamin A deficient mice.²¹⁰

Under normal spermatogenic conditions, spermatogonia differentiate into spermatozoa. In between the Sertoli cells, spermatogonia mature to spermatocytes then spermatids before they are released into the lumen for spermiation.^{189, 198} In VAD and $RAR\alpha$ null mice, the process is completely absent, with no spermatozoa production, which causes the sterility.

2. Previous Agonist and Antagonist Development

The reversibility of sterile effects on mice with abnormalities in vitamin A deficiency or RAR α -deficient testes,²⁰⁶ suggest an opportunity for non-hormonal contraceptive development of specific RAR α antagonists. A series of compounds have been developed that block ATRA binding and activation of transcription of RAR target genes by Bristol-Myers Squibb (BMS) (Figure II-4).²¹¹ In the 1980s, BMS 189453 (**II-4**), a non-selective RAR antagonist retinoid, acting on all isoforms (α , β , and γ), was shown to cause reversible infertility.²¹² Retinoids are derivatives of vitamin A and are composed of three general parts: a hydrophobic ring portion, a linker region, and a carboxylic acid end group (Figure II-4). For RAR α retinoids, the hydrophobic ring portion imparts antagonism with bulky groups inducing antagonistic effects over less bulky hydrophobic moieties. When a *gem*-dimethyl is in place of the phenyl ring in the hydrophobic region, the molecule exhibits agonistic activity.²¹³ An amide group in the linker region reveals the greatest RAR α selectivity. With an alkene linker, **II-4** is a pan-antagonist, while **II-5** and **II-6** are RAR α selective antagonists. Lastly, the carboxylic acid end group is essential for RAR activity.

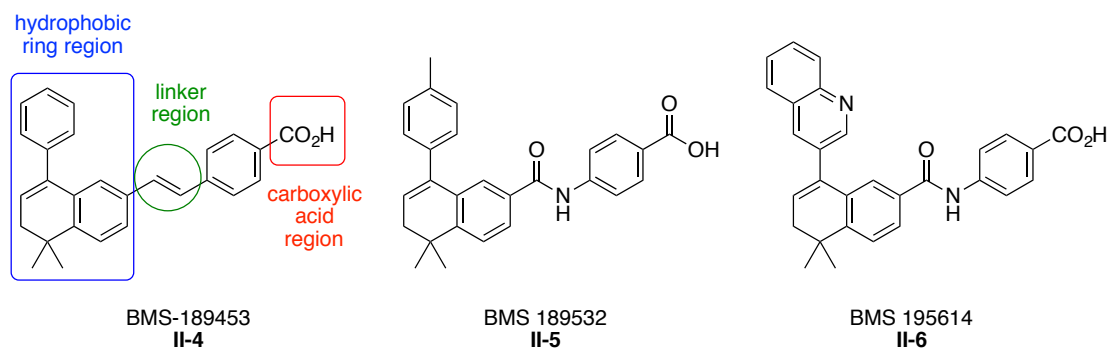


Figure II-4. BMS compounds.

Interestingly, the BMS compound BMS-189453 was originally tested on animals as a treatment for inflammatory skin diseases. Researchers in the Wolgemuth group at Columbia University reported that when doses for the BMS pan-antagonist were decreased in fertility experiments, the infertility, that was previously observed, had a reversible effect without significant toxicity.²⁰⁸ Additional studies were performed with other retinoids: BMS-189532 (**II-5**) and BMS-195614 (**II-6**) (Figure II-4).²⁰⁶ These compounds proved to be RAR α -selective antagonists through competition assays with the other RAR isoforms.²⁰⁶ While both retinoids showed great potential in *in vitro* analyses, they demonstrated poor *in vivo* effects when orally administered to mice.²⁰⁶ We submitted a sample of both **II-4**, the pan antagonist, and **II-5**, the RAR α selective antagonist to Cerep, Inc. for evaluation in a variety of assays including aqueous solubility (in phosphate buffered saline (PBS), pH 7.4), partition coefficient determination (octanol-PBS buffer, pH 7.4), cell permeability (Caco-2 cells), plasma protein binding (mouse), and metabolic stability (mouse liver microsomes), along with the reference compounds used (Table II-2). The partition coefficient (Log D) data shows that **II-4** was less favorable than **II-5**, with a value of 3.25 and 3.84, respectively. Ideally, the higher the Log D value, the more lipophilic

the compound is and the more the drug is absorbed by the cells.²¹⁴ Additionally, **II-4** had lower permeability and was considerably less soluble. However, BMS-189453 (**II-4**) did indeed have a more favorable plasma protein binding value. While BMS-189532 (**II-5**) is the more ideal candidate for our project because it is α isoform specific, the compound was ineffective *in vivo*. The Cerep data confirms this knowledge: only 0.8% of **II-5** was not bound to plasma protein and a very small portion of free compound was then metabolized at a much faster rate than the pan-antagonist.

Table II-2. Pharmacology of known RAR α antagonist and pan-antagonist.

Assay (conditions)	II-5	II-4	Reference compounds
Aqueous Solubility (PBS, pH 7.4)	136 μ M	3.1 μ M	diethylstilbestrol, haloperidol, metoprolol tartrate, phenytoin, rifampicin, simvastatin, tamoxifen
Partition Coefficient (Log D, <i>n</i> -octanol/PBS, pH 7.4, 1.0×10^{-4} M)	3.84	3.25	diethylstilbestrol, haloperidol, ketoconazole, metoprolol tartrate, phenytoin, rifampicin, simvastatin
Plasma Protein Binding (mouse, CD-1, 1.0×10^{-5} M)	99.2% bound; 99.8% recovery	95.3% bound; 93.3% recovery	acebutolol, quinidine, warfarin
A-B Permeability (TC7, pH 6.5/7.4, 1.0×10^{-5} M)	8.3×10^{-6} cm/s; 20% recovery	$<0.7 \times 10^{-6}$ cm/s; 14% recovery	colchicines, labetalol, propranolol, ranitidine
Metabolic Stability (liver microsomes, mouse, CD-1, 1.0×10^{-6} M, 60 min.)	49% parent remaining	79% parent remaining	imipramine, propranolol, terfenadine, verapamil

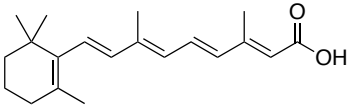
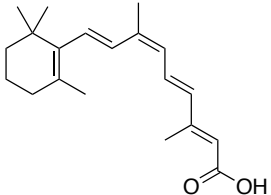
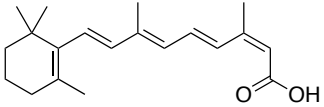
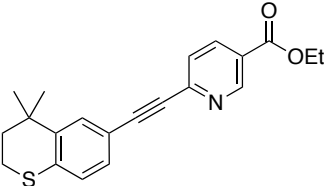
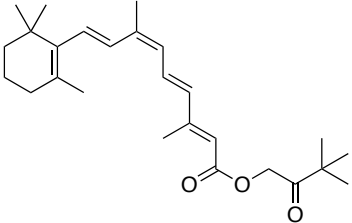
From the results of the biological screening of BMS compounds **II-4** and **II-5** in Table II-2, we determined that the amide linker of **II-5**, the α selective antagonist, has a much larger metabolic liability than the alkene linker of **II-4**, the pan antagonist. We conclude from this data that simultaneously addressing plasma protein binding and metabolic stability should yield compounds that are bioavailable in our later animal models. We determined that the cause of undesired *in vivo* effects was most likely due to poor bioavailability of the compounds and modifications to their structures could circumvent these problems. Given the importance of RAR α in sperm maturation and male reproduction, the goal of our research is to develop a reversible, non-hormonal therapeutic agent that targets and blocks RAR α . For this, we pursued the BMS retinoids as a starting place for compound development.

C. Design of Retinoids

The retinoids are made up of three general parts: a hydrophobic ring portion, a linker region, and a carboxylic acid end group (Figure II-4). These three general features tolerate a wide range of moieties: quinolone, naphthalene, or chromane heterocycles in the hydrophobic ring portion; an alkene, an amide, or a heterocyclic isostere for the linker region; and benzoic, cyclohexanoic, or naphthoic acid on the end. Table II-3 shows several examples of retinoids that are clinically approved or in clinical testing.²¹⁵ Some of these retinoids, including the natural ligands **II-1** and **II-2**, are commercially available as treatments for acne, psoriasis, and various types of cancer. All of these approved drugs contain a similar structure to our target compounds with a hydrophobic region, a linker portion, and a carboxylic end. Additionally, the compounds in Table II-3 all contain a *gem*-

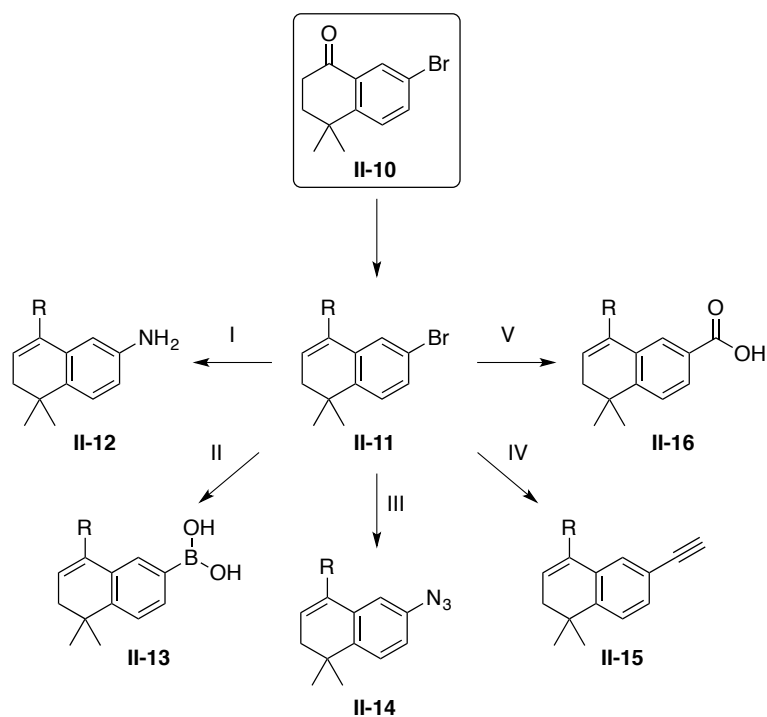
dimethyl group in the hydrophobic ring region, which has been shown to promote agonism, *vide supra*.

Table II-3. Commercially available retinoids.

Name (Trade Name)	Structure	Phase: Indication
ATRA, Tretinoin (Avita)	 <p style="text-align: center;">II-1</p>	Launched: acne, warts Phase II: breast, brain, and renal cancers
9- <i>cis</i> -RA, Aliretinoin (Panretin)	 <p style="text-align: center;">II-2</p>	Launched: Kaposi's sarcoma
Isotretinoin (Accutane)	 <p style="text-align: center;">II-7</p>	Launched: acne Phase II: T-cell malignancies Phase III: high grade glioma
Tazarotene (Tazorac)	 <p style="text-align: center;">II-8</p>	Launched: acne, psoriasis
Pinacolyl-9- <i>cis</i> -retinoate, MDI 301	 <p style="text-align: center;">II-9</p>	Preclinical: acne, cancer, psoriasis

Since we needed to generate compounds that would address our earlier problems with **II-4** and **II-5** yet also be selective for RAR α , we sought to develop compounds with

bioisosteres for the amide linker: triazoles, oxadizoles, imidazoles, pyrazoles, oxazoles, and other heterocycles.^{216,217} For the hydrophobic ring region, we initially chose to work with the same naphthalene ring as the BMS compounds because the synthesis was known and modifications at various positions were possible. From bromo-tetralone (**II-10**), a straight forward Grignard reaction followed by elimination provides access to the tetralin core of the hydrophobic ring region (Scheme II-1). The tetralin bromide serves as an excellent DOS template, *vide supra*, because many different reactions with the bromide will provide multiple different linkers for the retinoids.

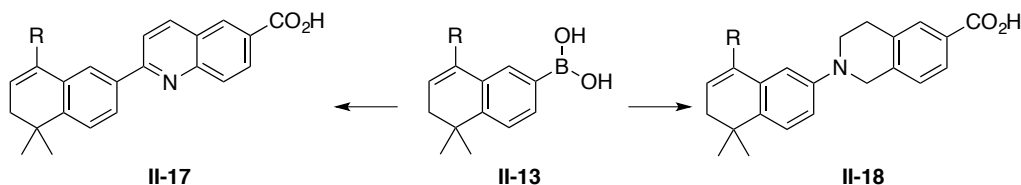


Scheme II-1. Formation of different tetralin linkers.

Path I leads to aniline **II-12** possibly through copper catalysis.²¹⁸ Path II pertains the borylation through an organometallic reagent plus a boric ester, followed by acid hydrolysis to yield boronic acid **II-13**.²¹⁹ Similarly, **II-14** and **II-15** can be produced

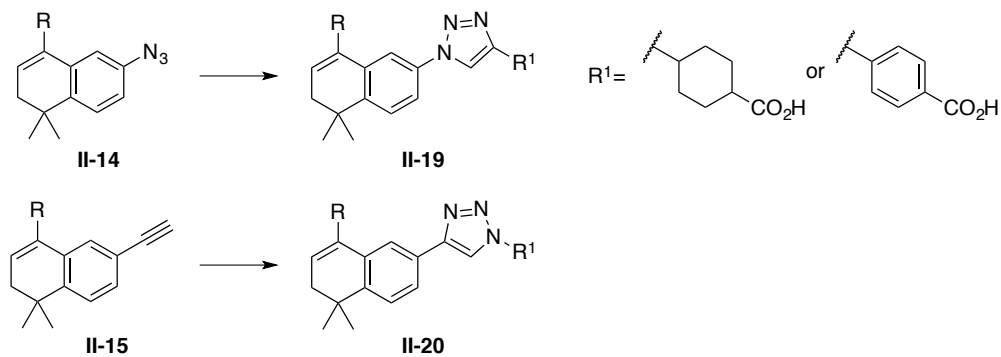
through a lithium-halogen exchange to give the corresponding aldehyde,²²⁰ followed by a sodium azide reaction to give azide **II-14** or Bestmann-Ohira reaction conditions to give alkyne **II-15**.²²¹ Hydroxycarbonylation can produce an aryl carboxylic acid **II-16** from aryl bromide **II-11**.²²²

Additionally, from the aryl boronic acid derivative **II-13**, we envisioned synthesizing the quinolone linker analogs (Scheme II-2). While quinolone is not a known bioisostere for the amide group, the robustness of the quinoline and tetrahydroisoquinoline rings could help form tighter or better binding compounds. These heterocycles encompass both the linker and carboxylic acid regions so we wanted to explore their potential in our tetralin series.



Scheme II-2. Quinoline linkers via boronic acid **II-13**.

On the other hand, we are exploring the triazole heterocycle through the synthesis of both aryl azide and aryl alkyne derivatives, **II-14** and **II-15**, respectively, as amide bond bioisosteres. Through click chemistry with the corresponding alkyne or azide, we envision the formation of triazole linker **II-19** or **II-20** (Scheme II-3).



Scheme II-3. Triazole products from azide **II-14** and alkyne **II-15**.

Additionally, my part of this work involves the synthesis of cyclohexanoic acid analogs to understand the behavior of the binding pocket and introduce some rigidity into the retinoids. The DOS approach for the tetralin core is an excellent way to access multiple substituents in the linker region.

D. Computational Modeling of Retinoids

While the synthesis was underway, we also performed *in silico* analysis of our compounds to assess their potential for a structure-based drug design approach of the retinoids. For our investigation, we fortunately had an available crystal structure of a RAR α heterodimer (PDB:1dkf) bound with a known BMS antagonist **II-6** (Figure II-5).²²³ Using the Schrodinger Molecular Modeling suite, we were able generate a grid for the binding pocket that was established from the bound **II-6**.

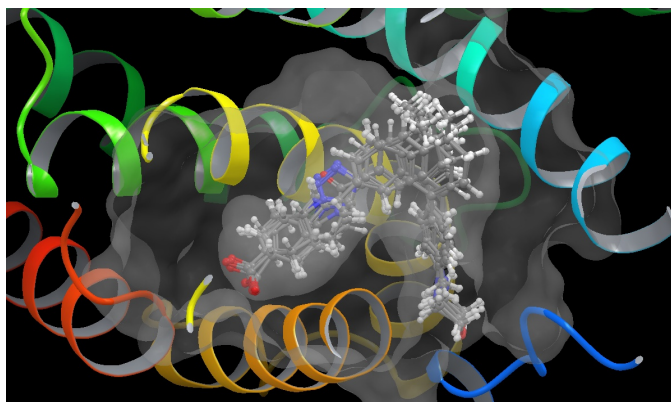
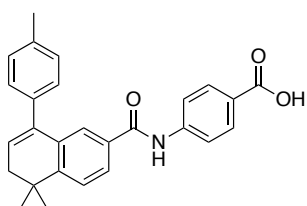
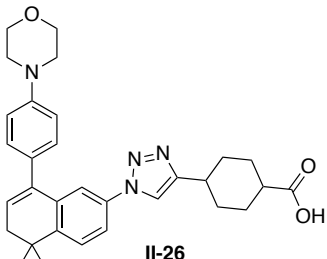
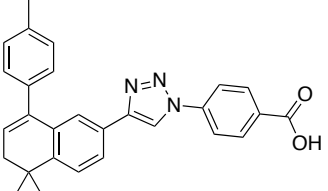
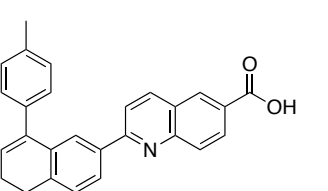
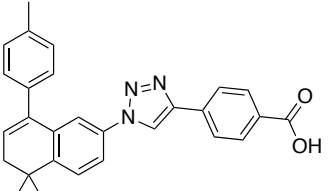
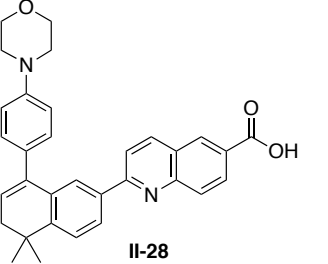
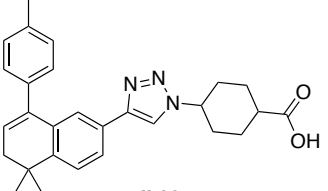
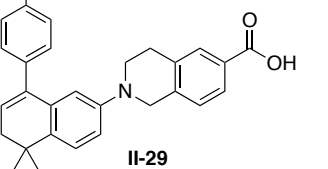
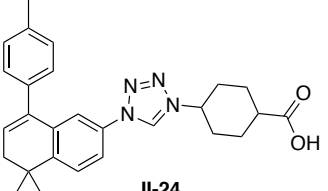
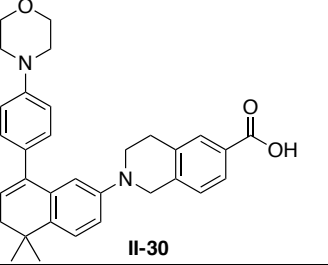
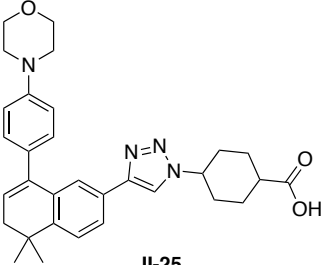


Figure II-5. 1dkf protein structure with proposed docked compounds.

With the Maestro program in the suite, docking scores were calculated for our retinoids bound within the receptor site. Table II-4 shows the lowest docking scores for a sample of our proposed structures; of note, more negative values for docking scores indicate better docking within the grid of the binding pocket. Our scores show that the RAR α selective compound **II-5** did not score as well as our retinoids. Dr. Cuellar from our group has previously synthesized RAC-I-163 (**II-21**) as a triazole analog of **II-5**, as well as its structural isomer (**II-22**). Within the table, there are Dr. Cuellar's triazole analogs with the benzoic acid moiety, cyclohexanoic acid triazole analogs **II-23-II-26**, as well as the quinoline linker analogs **II-27-II-30** (Table II-4).

Table II-4. Docking scores for proposed retinoids plus **II-5**.

Compound	Docking Score	Compound	Docking Score
 <p>BMS 189532 II-5</p>	-14.3615	 <p>II-26</p>	-14.6250

 RAC-I-163 II-21	-15.3422	 II-27	-14.6288
 II-22	-15.3401	 II-28	-15.4904
 II-23	-14.5278	 II-29	-14.9819
 II-24	-14.8753	 II-30	-15.4518
 II-25	-14.7372		

With the 1dkf crystal structure, the quinoline moiety of **II-6** computationally displayed an ability to fill the antagonist binding pocket in RAR α active site, which suggests that actual binding of our molecules could produce similar results.

From the Maestro program, we were able to calculate the binding energies of the interactions of the retinoids to the amino acids in the binding pocket. Ideally, we want to produce molecules that are more energetically favorable, or $-\Delta G$, as represented as the bars negative from the 0 axis. These proposed retinoids have the most interaction with residues 220 to 280. This analysis is helping in determining which parts of the molecules are interacting with the binding pocket in a positive or negative manner. Future work would be to adjust these parts of the molecule to produce favorably interactions.

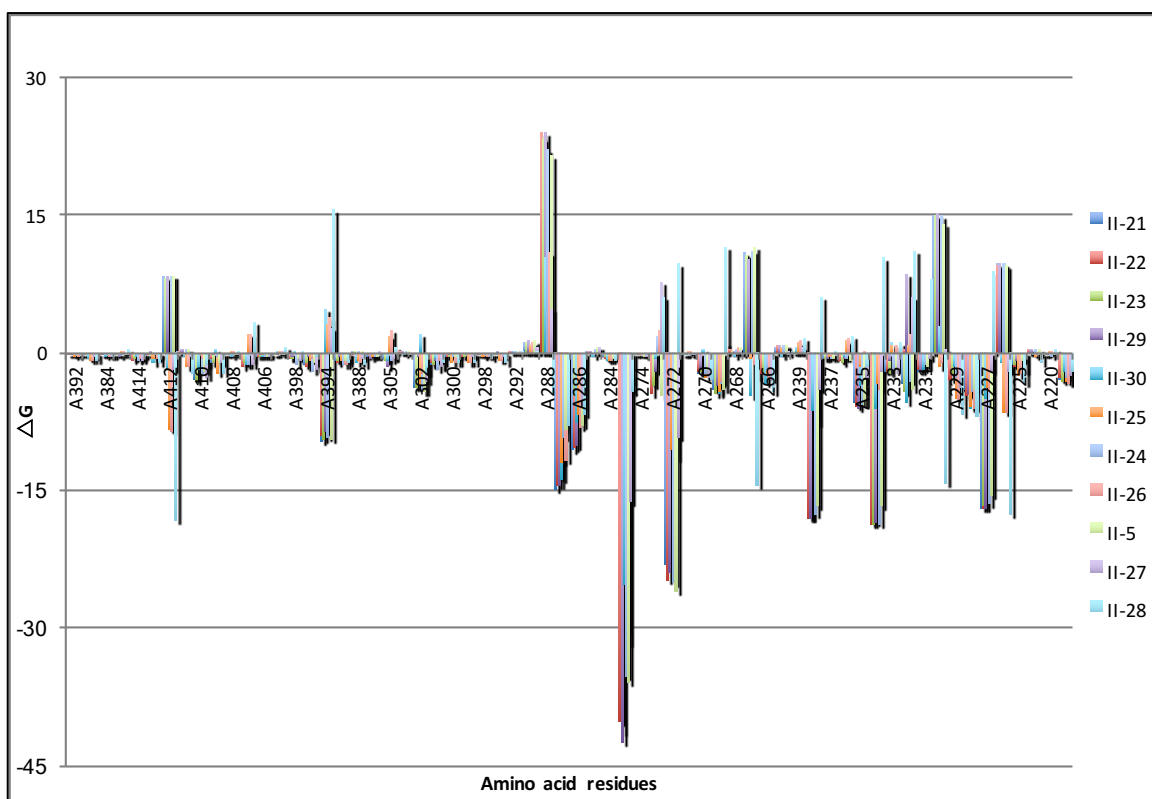


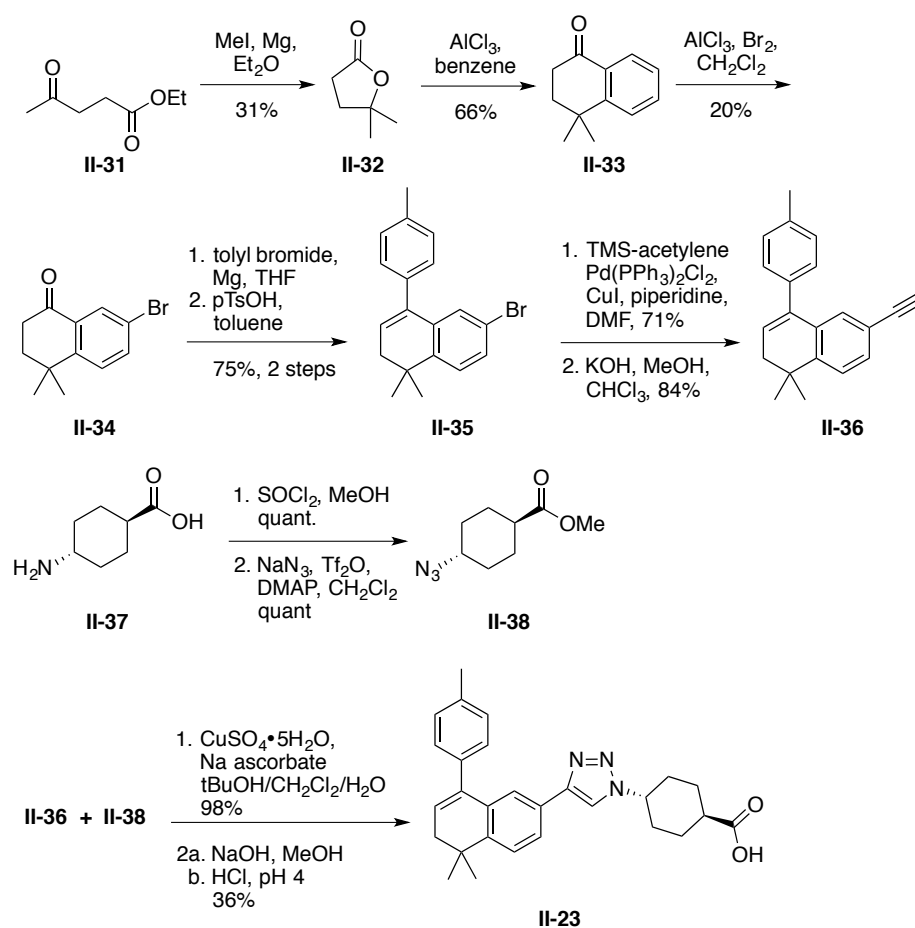
Figure II-6. Binding energies for proposed compounds.

Our computation data suggests that the cyclohexanoic acid moiety could impart some rigidity in the retinoids. Research has been ongoing to produce the BMS triazole analogs as well as a new group of Eisai Research (ER) analogs.

E. Synthesis of Retinoids

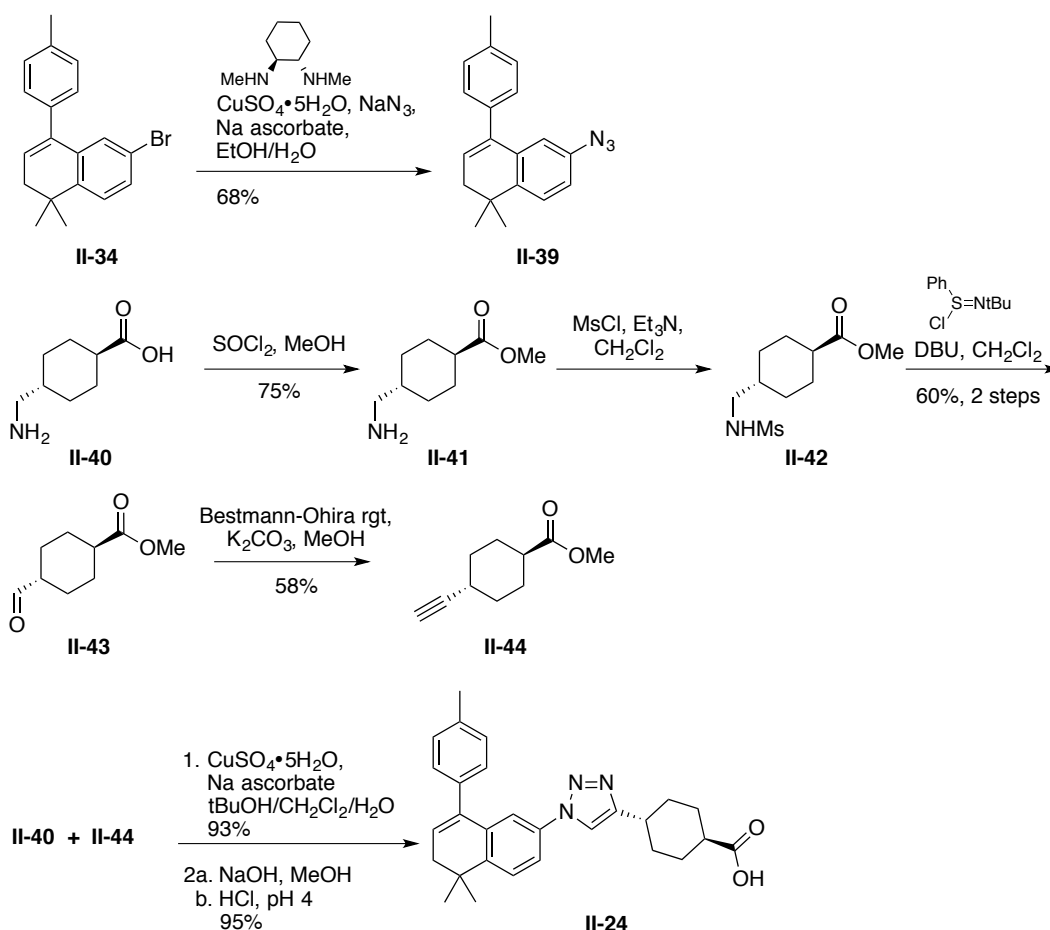
1. BMS Triazole Derivatives

For the RAR α retinoid synthesis, my work included the cyclohexanoic acid and quinolone linkers. To start, the 7-bromo tetralone **II-34** was synthesized to serve as a building block for the tetralin core (Scheme II-4). Treatment of ethyl levulinate (**II-31**) with methyl magnesium iodide afforded dimethyl furan **II-32**, which was followed by Friedel–Crafts acylation/intramolecular alkylation of benzene to give tetralone **II-33**.²²⁴ Bromination of **II-33** gave multiple side products (not shown), but the desired **II-34** was isolated in 20% yield. After attempts to optimize the reaction were unsuccessful, we went ahead and bought the commercially available **II-34**.



Scheme II-4. Synthesis of triazole **II-23**.

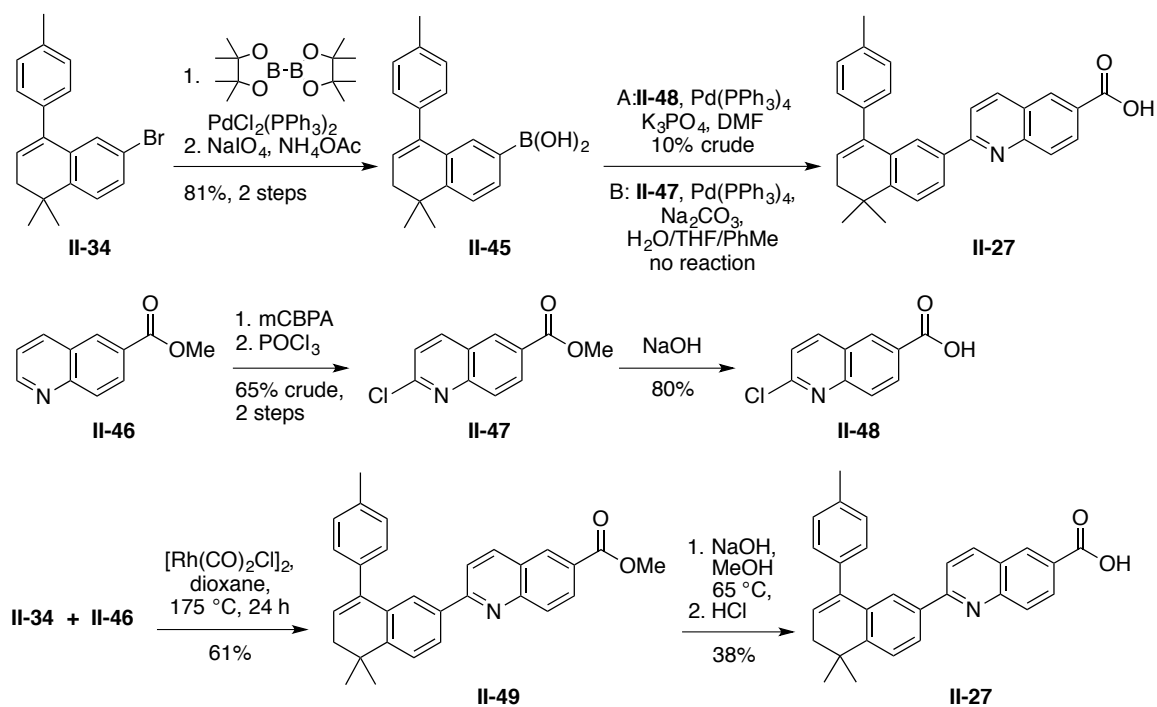
A Grignard reaction with tolyl bromide followed by elimination gave the tolyl bromide **II-35**. Sonogashira coupling with TMS acetylene and silyl deprotection produced alkyne **II-36** (Scheme II-4). The alkyne was then coupled to azide **II-38** with the Huisgen 1,3-cycloaddition reaction, or click chemistry, to give triazole **II-23** after hydrolysis. Azide **II-38** (Scheme II-4) was made by treating trans amino cyclohexanoic acid with thionyl chloride to form the ester in quantitative yield followed by azide formation with sodium azide and triflic anhydride. Triazole **II-23** was carried on to activity screening, *vide infra*.



Scheme II-5. Towards the synthesis of triazole **II-24**.

In addition to the **II-23** triazole, its structural analog **II-24** was produced. Aryl azide **II-39** was synthesized under mild conditions with a chiral diamine ligand.²²⁵ Aryl azide **II-39** then underwent another click reaction with alkyne **II-44** to produce the ester of **II-24**. Hydrolysis of the ester under normal basic conditions followed by crystallization in methylene chloride and hexanes completed the synthesis of **II-24**. To access the alkyne precursor **II-44**, we started with tranexamic acid (**II-40**) and formed its ester **II-41**. Next, the amine was treated with mesyl chloride to give the mesylated amine **II-42**, then it was oxidatively deaminated with N-tert-butylphenylsulfonimidoyl chloride to yield the corresponding aldehyde **II-43**. Lastly, dimethyl (1-diazo-2-oxopropyl) phosphonate, or Bestmann-Ohira reagent, was added under basic conditions to afford the alkyne **II-44** (Scheme II-5).

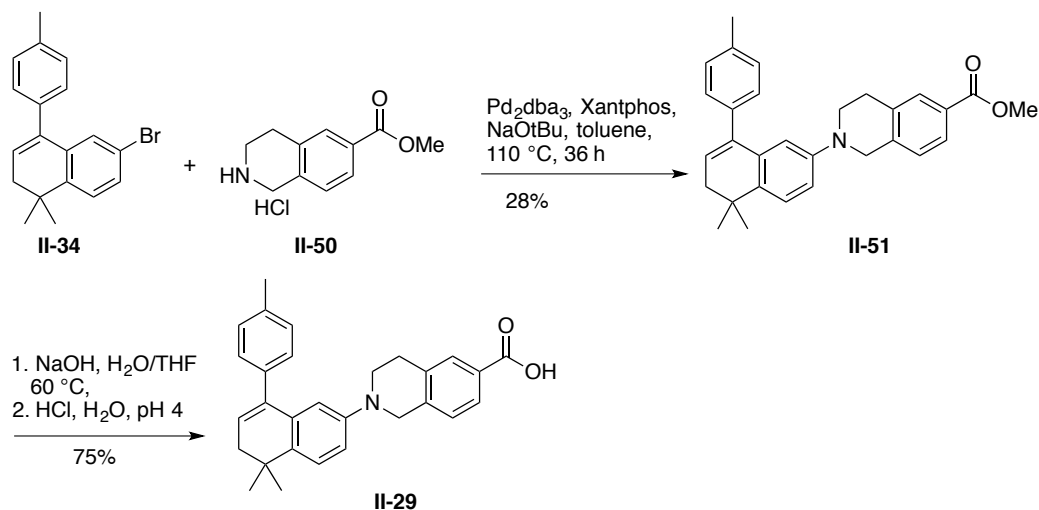
The synthesis of retinoids isoquinoline **II-27** and tetrahydroisoquinoline **II-29** were also performed (Scheme II-6 and II-7). Boronic acid **II-45** was formed from bromide **II-34** with a diboron reagent followed by hydrolysis with sodium periodate. Acid **II-45** was coupled to chloroquinoline **II-47** with a Suzuki coupling protocol.²²⁶ To generate chloroquinoline **II-47**, quinolone **II-46** was treated with *meta*-chloroperoxybenzoic acid followed by phosphoryl chloride.²²⁷ The Suzuki coupling yielded a small amount of **II-27** that was not enough to be biologically tested. We therefore tried coupling with the acid derivative **II-48** to avoid the final saponification step and potentially another low yield (route B, Scheme II-6), but after 24 hours, only starting material was detected.



Scheme II-6. Towards the synthesis of quinoline **II-27**.

Eventually, this route was abandoned when a more simple direct arylation with quinoline using the rhodium catalyst was realized.²²⁸ After optimizing the conditions, we were able to get good yields for both the coupling and saponification steps for the production of **II-27** (Scheme II-6).

Lastly, synthesis of the quinolone analog **II-29** was completed by catalytic palladium coupling of tetrahydroisoquinoline **II-50** to bromide **II-34** to give the desired ester. Reaction optimization with BINAP did not produce a yield higher than 28% but the product was carried on. Saponification under basic conditions gave quinolone acid **II-29** cleanly without further purification.



Scheme II-7. Synthesis of quinoline analog **II-29**.

2. ER Derivatives

During the synthesis of these BMS-derived retinoids, our group also explored quinoline **II-51** (ER-50891), another α selective compound (Figure II-7).²²⁹ Preliminary results from analogs made in our group showed promise, so a cyclohexanoic acid analog with a triazole linker was attempted.

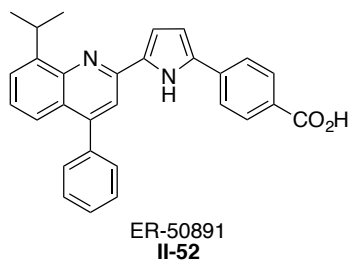
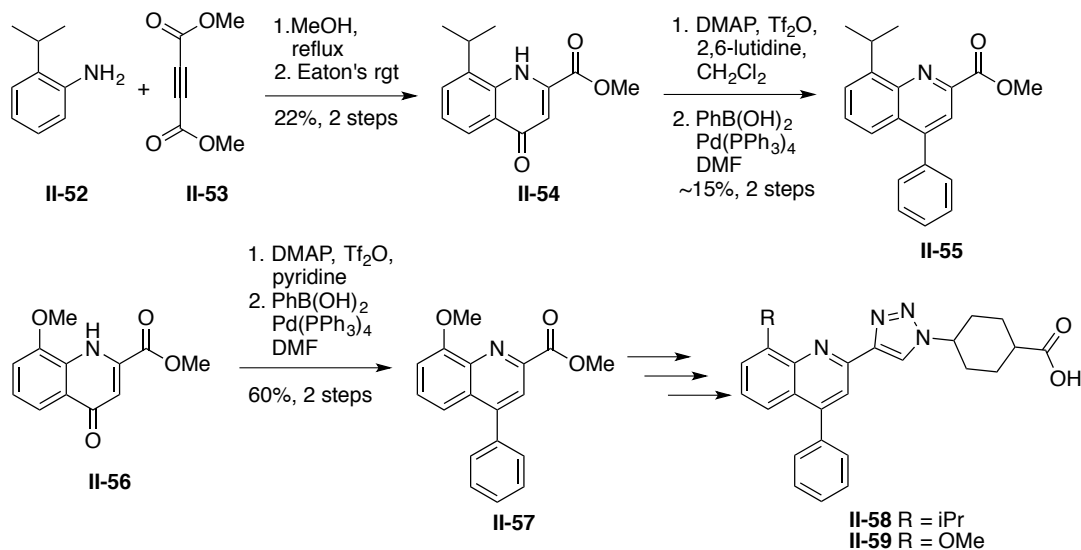


Figure II-7. ER-50891 (**II-52**).

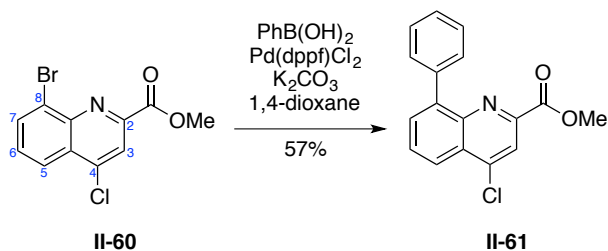
This section covers the brief work I have done towards the synthesis of ER-50891 derived retinoids. I completed the synthesis of the isopropyl and methoxy quinolone analogs **II-54** and **II-57**, respectively, with the aim to convert them to triazole cyclohexanoic acid analogs **II-58** and **II-59** (Scheme II-8).



Scheme II-8. Towards the synthesis of ER analogs.

For the synthesis of isopropyl quinoline **II-55**, isopropyl aniline **II-52** was first treated with butynedioic ester **II-53** followed by Eaton's reagent to generate the quinoline ester **II-54**.²³⁰ This underwent treatment with triflic anhydride and dimethylaminopyridine (DMAP) to yield the triflate intermediate that was then treated with phenyl boronic acid to produce **II-55** in low yield. The triflate intermediate formation followed by the Suzuki reaction was done with methoxy quinoline **II-56** to give ester **II-57** in good yield after two steps. Following the production of the esters **II-55** and **II-57**, the initial goal was to produce retinoids **II-58** and **II-59** with the triazole linker by first reducing the respective ester to its corresponding aldehyde followed by a Seyferth-Gilbert homologation to give the alkyne product that would then be coupled with azide **II-39** (from Scheme II-4) via click chemistry. However, while the syntheses of these triazole analogs were under way, others in our group tested ER analogs with the presence of the triazole linker and found them to

be inactive for RAR α . With this in mind, new routes are being explored for different linkers for the ER analogs.



Scheme II-9. Developing quinoline analogs for hydrophobic pocket exploration.

A new route for quinoline analogs are being explored by our group for selective aryl- or alkylation of the 4- and 8- positions of the quinoline ring (Scheme II-9). The aim of this work is to make different quinoline analogs at the C-4 and C-8 positions to explore the hydrophobic pocket of RAR α . With 8-bromo-4-chloroquinoline ester **II-60**, Suzuki coupling with phenylboronic acid using Pd(dppf)Cl₂ as the catalyst gave the exclusive bromo-substituted phenyl quinoline **II-61** in good yield. This leaves room to explore further substitution at the chloro- position and saves extra steps from having to form the 8-substituted quinoline exclusively, as in **II-54** or **II-56**.

F. Biological Screening of Retinoids

Once synthesis of the retinoids has been completed, the compounds were subjected to a binding assay and luciferase reporter activity assay.

1. Binding Assay

As a complement to our computational structure-based drug design approach, we have also been able to determine where to make structural modifications on our compounds to maximize binding interactions to their known targets with the help of our collaborators in the Schönbrunn group. They have produced the RAR α binding domain with a bacterial over-expression system and have used it in isothermal titration calorimetry (ITC) binding studies and crystallization screens. ITC is the gold standard technique for determining thermodynamic parameters of chemical interactions, especially binding constants. This technique is the only experimental method that simultaneously obtains thermodynamic parameters, which greatly reduces the potential errors introduced from piggybacking calculations. Of note, isothermal titration calorimetry is used for quantifying binding constants, while X-ray co-crystallization is used for qualifying those results from binding. Additionally, X-ray co-crystallization of our compounds will be used to identify possible sites of interest for further modification through structure-activity relationship (SAR) analysis. Furthermore, ITC avoids the use of reporter labels including isotopes, fluorophores, chromophores, to monitor a reaction; thus, it saves time and money.

Generally, ITC involves the titration of a ligand into a solution of protein in a closed system while monitoring the energy consumption or the generation of heat. The change in heat is then used in the Gibbs' free energy equation to determine K_d ($\Delta G = \Delta H - T\Delta S = -RT \ln K_a$ where $K_a = 1/K_d$). The K_d value, or dissociation constant, is a measurement of binding affinity. Binding affinity describes the strength of the interaction between the protein and the ligand. In general, smaller K_d values indicate tighter binding and greater binding affinity.²³¹

For the RAR project, both 9-*cis*-retinoic acid (**II-2**) and all-*trans*-retinoic acid (**II-1**) are used as controls, with all tests done in triplicate. Figure II-8 and II-9 shows ITC data for all-*trans*-retinoic acid (**II-1**) and 9-*cis*-retinoic acid (**II-2**) with analysis in both RAR and RXR proteins. As mentioned earlier, **II-1** binds to RAR but not RXR.¹⁹⁷ The K_d value of 0.80 μM for the RAR homodimer is similar to 0.82 μM found for the RAR/RXR heterodimer (Figure II-8). The similar values could account to exclusive binding to just the RAR site.

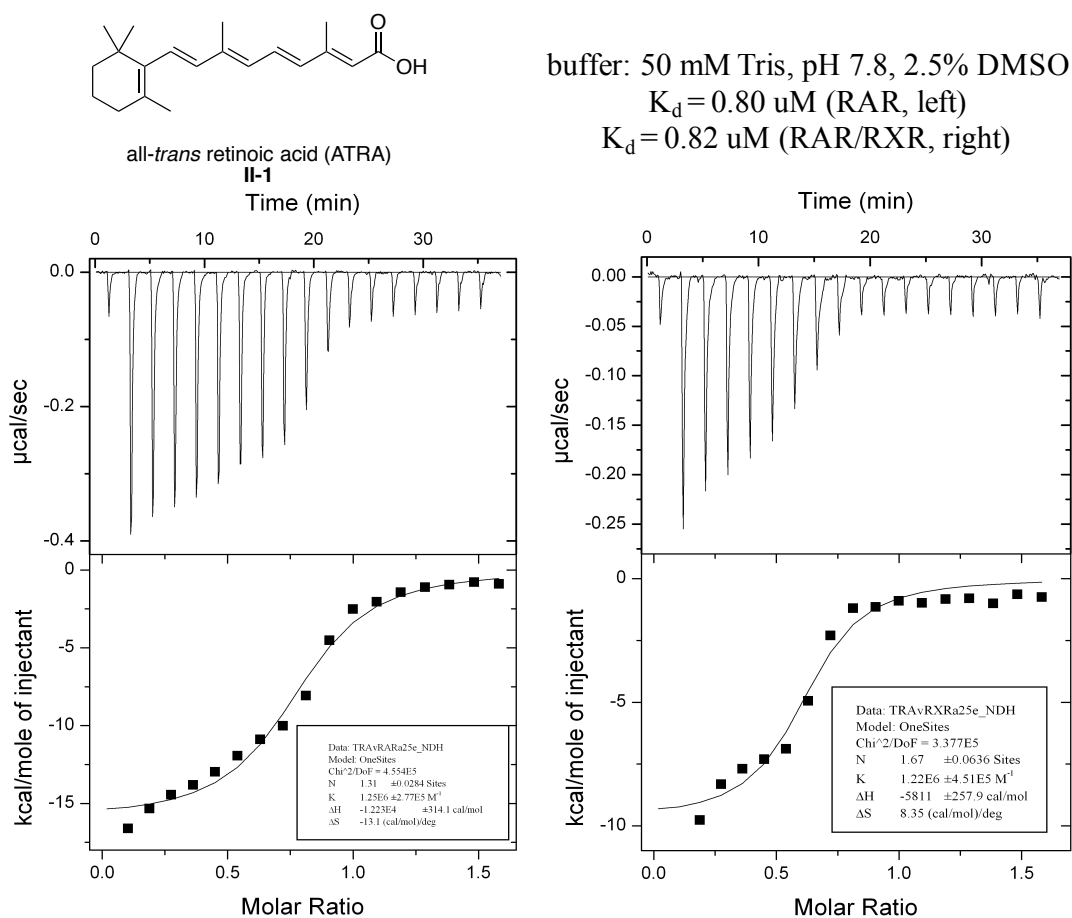


Figure II-8. ITC data for **II-1**.

On the other hand, 9-*cis*-retinoic acid (**II-2**) binds to both RAR and RXR. ITC binding assays for **II-2** show that binding is lower in RAR by almost two-fold (Figure II-

9). The K_d values for binding to RAR homodimer and RAR/RXR heterodimer are 1.02 μM and 0.63 μM , respectively. Moreover, the natural ligand for RAR is ATRA **II-2** and this data does indicate that RAR has a better affinity for ATRA vs 9-*cis*-retinoic acid.

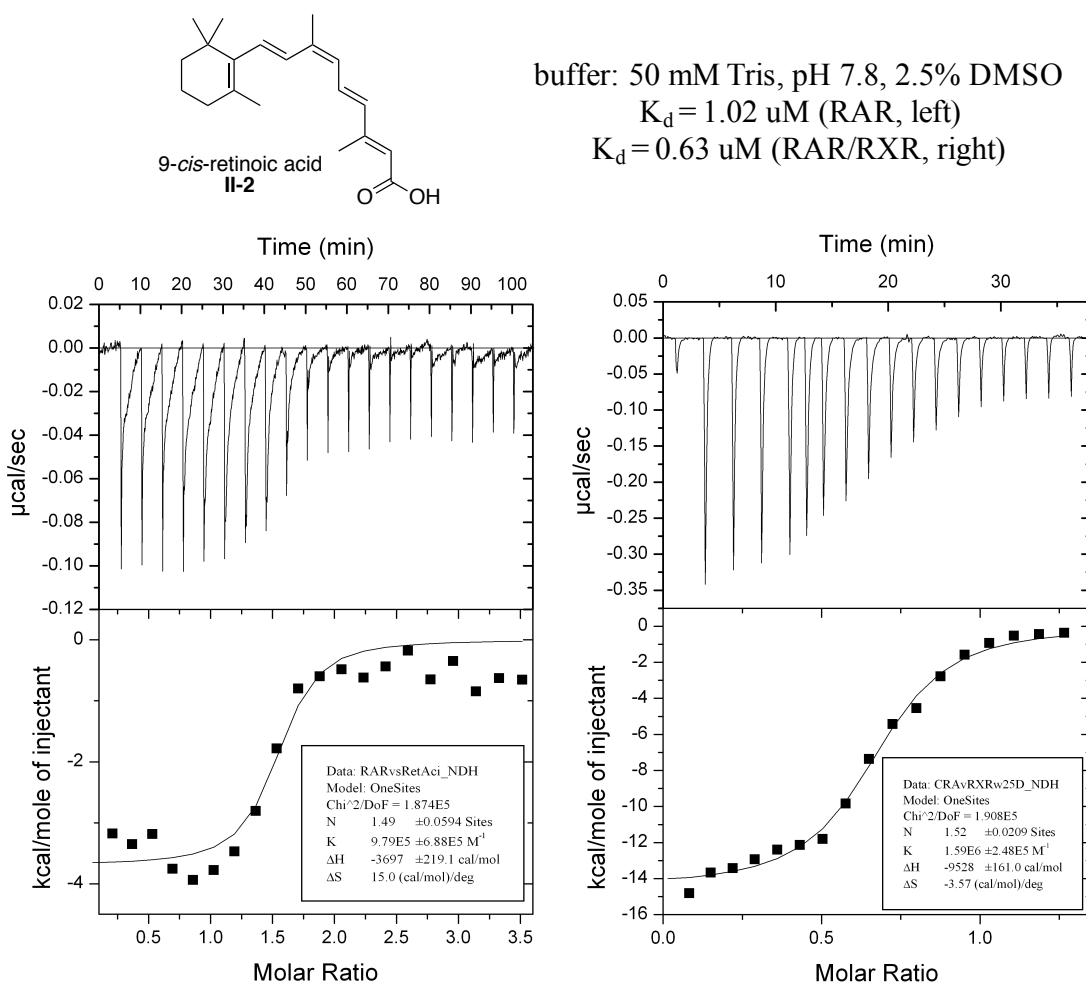
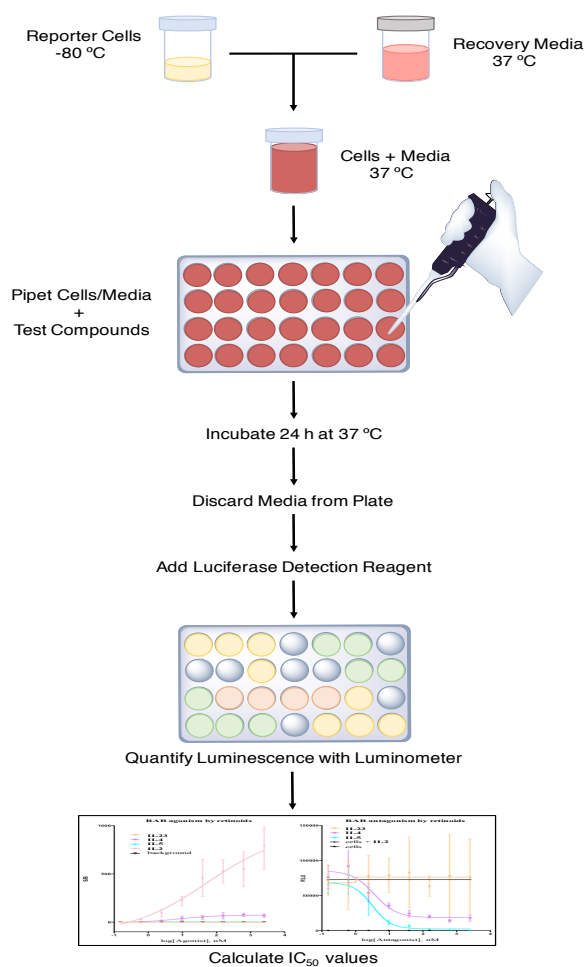


Figure II-9. ITC data for **II-2**.

Many of the compounds in our project have been tested with ITC; my compounds have been submitted for ITC analysis.

2. Luciferase Reporter Activity Assay

We also evaluated our retinoids in a luciferase reporter assay to determine what kind of activity they have in RAR α , either agonist or antagonist. Our compounds we also tested in the RAR β and RAR γ activity assays. We chose to work with INDIGO Biosciences reporter assay kits.²³² These kits are all-inclusive cell-based assay systems with RAR reporter cells, optimized media, a reference agonist, a luciferase detection reagent, and a cell culture-ready assay plate. Their assays utilize proprietary non-human mammalian cells engineered to express human RAR α (NR1B1), RAR β (NR1B2), and RAR γ (NR1B3).²³²



Scheme II-10. General process for INDIGO activity assay.²³³

The RAR reporter cells include the luciferase reporter gene functionally linked to a responsive promoter, which is able to detect small changes in activity through luciferase expression in treated reporter cells. The overall process of the assay is shown in Scheme II-10.²³³ First, report cells and the optimized media are mixed and pipetted into the cell plate, along with test compounds and controls. After 24 hours of incubation, the luciferase reagent is added and the plate is allowed to rest for 30 minutes undisturbed. Then, a luminometer is used to quantify the luminescence and the values from this data can be used to calculate the IC₅₀ values of the test compounds.

The BMS compounds: **II-23**, **II-24**, **II-27**, and **II-29** were tested for RAR α agonism and antagonism with concentrations ranging from 0.31 nM to 5000 nM (Figure II-10).

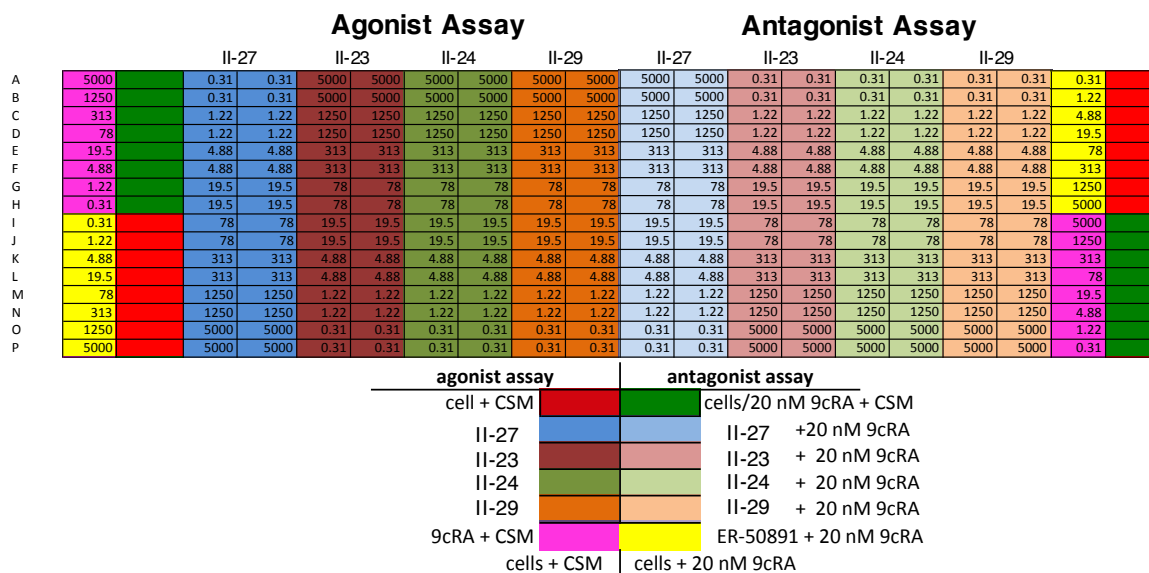


Figure II-10. Concentration map of the activity plate.

From the activity map below, the BMS analogs demonstrated low to no activity in the agonist assay represented by the violet color in the left half of the assay plate (Figure II-11). In the assay plate map, a red color indicates high activity with shades of orange, yellow, green, and blue in between to designate the decreasing levels of activity, respectively.

Compounds **II-23**, **II-24**, and **II-29** did not demonstrate any agonism. However, **II-27** showed slight agonism with 25-fold activity over the background, as compared to the control (9-cis-retinoic acid), which had greater than 750-fold activity at 2500 nM concentration. The antagonist assay showed much more color variation with boxes displaying of yellow and green activity colors (Figure II-11).

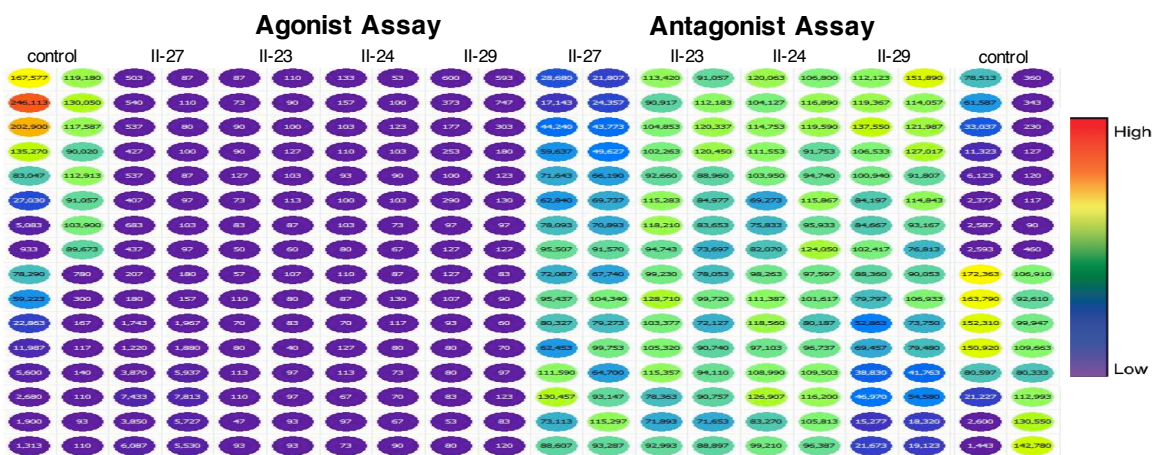


Figure II-11. Map of activity plate assay results of BMS retinoids.

The antagonism activity data was graphed to calculate the IC₅₀ values of the tested compounds (Figure II-12). For the antagonist assay analysis, **II-27** and **II-29** showed activity at 321 nm and 341 nm, respectively. Retinoids **II-23** and **II-24** did not exhibit any

antagonism as demonstrated by their non-sigmoidal, flat lines in Figure II-12. The RAR β and RAR γ activity assays of these BMS analogs will be performed in the future. There is an immediate need to test all the highly active compounds from the RAR α activity assays first.

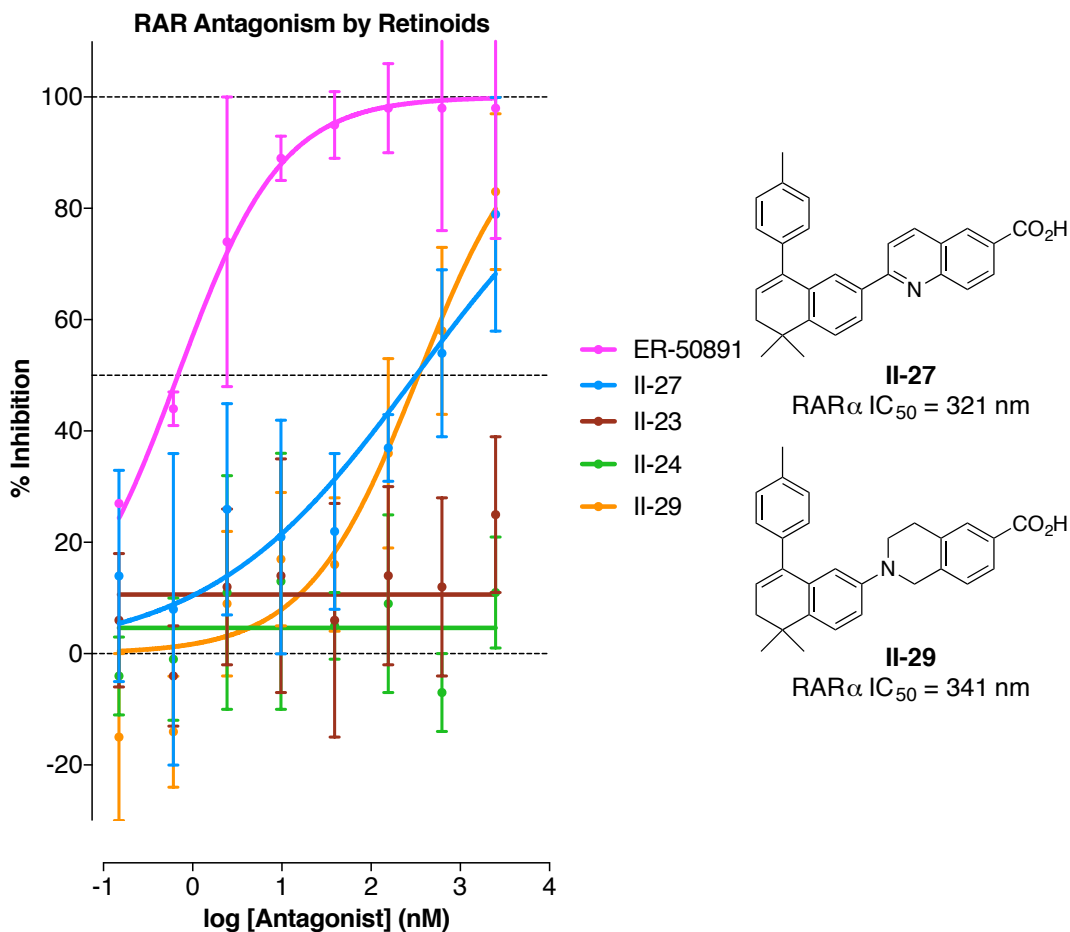


Figure II-12. Antagonistic assay of BMS RAR analogs.

G. Concluding Remarks

Male contraceptive research aims to address the unmet need of finding better alternatives for men and families to prevent pregnancy. While condoms and vasectomies are viable options, the possible ineffectiveness of condoms or the permanency of vasectomies are problematic. Additionally, hormonal contraceptive agents have been researched but have caused unwanted side effects. Our group is investigating non-hormonal male contraceptive agents as a solution to tackle these concerns with the help of the NIH NICHD. Within the Georg research group, a subset of researchers is focused on the discovery of RAR α antagonists. This nuclear receptor has been validated as a male contraceptive, non-hormonal drug target. RAR α is heavily involved in spermatogenesis since previous reports showed its gene deletion induced sterility in mice.

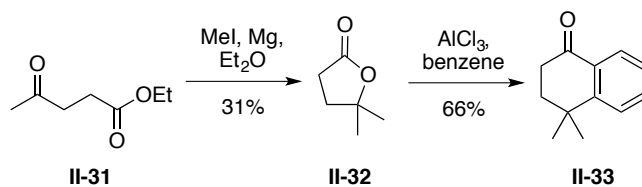
Our work revolves around the design and synthesis of selective, bioavailable RAR α antagonists based on retinoids composed of three parts: a hydrophobic ring portion, a linker region, and a carboxylic acid moiety. We used the scaffold of known BMS antagonists (**II-4**, **II-5**, **II-6**) to begin our contraceptive development and the first generation of compounds contained a tetralin core with various aryl substituents in the ring portion, amide bioisosteres in the linker region, and benzoic or cyclohexanoic acids in the carboxylic acid moiety. Our compounds were evaluated using *in silico* analysis with the Schrodinger suite, isothermal titration calorimetry, and a luciferase reporter assay. Evaluation of our first-generation retinoids determined that additional lipophilic substituents in the ring portion and fluoro- groups in the benzoic acid moiety could increase the selectivity. Hence, we are pursuing other ring structures, such as a naphthyl ring scaffold similar to ER-50891 (**II-51**), and others, for the discovery of second generation of retinoids.

Once the synthesis of our compounds is complete, they are subjected to biological activity analysis. From the luciferase reporter assay data, my BMS analogs with the cyclohexanoic acid moiety (**II-23** and **II-24**) showed no activity in the agonistic or antagonistic assays. However, the quinoline analogs (**II-27** and **II-29**) showed sub-micromolar activity in the antagonistic assay with **II-27** exhibiting very slight agonism as well.

Chapter 6. Experimental Data

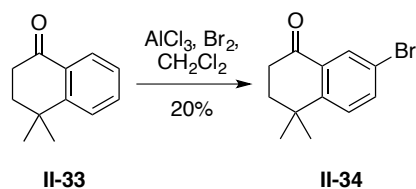
As previously stated in Chapter 4, *vide supra*, unless otherwise indicated, reactions were carried out open to air with reagent grade solvents directly from the bottle. Purified tetrahydrofuran (THF), toluene, diethyl ether (Et₂O), and dichloromethane (CH₂Cl₂) were purified by passage through a bed of activated alumina in our solvent system. Purification of reaction products was carried out by flash column chromatography using silica gel 60 (230-400 mesh). Analytical thin layer chromatography (TLC) was performed on 0.25 mm silica gel 60-F plates. Visualization was accomplished with UV light and cerium molybdate stain followed by heating. Low-resolution mass spectral data were acquired utilizing the electrospray ionization technique. ¹H NMR spectra were recorded at ambient temperature at 400 MHz and are reported in ppm using a solvent as an internal standard (CDCl₃ at 7.26 ppm or CD₃OD at 3.31 ppm). Proton-decoupled ¹³C NMR spectra were recorded at 100 MHz and are reported in ppm using a solvent as an internal standard (CDCl₃ at 77.16 ppm). The data are reported as follows: chemical shift on the δ scale, multiplicity (b = broad, s = singlet, d = doublet, dd = doublet of doublets, t = triplet, q = quartet, m = multiplet), coupling constants (Hz), and integration. Melting points were determined with

Electrothermal Digital Mel-Temp 3.0 melting point apparatus. High-resolution mass spectra were recorded with electron-spray ionization (ESI) or electron ionization (EI).



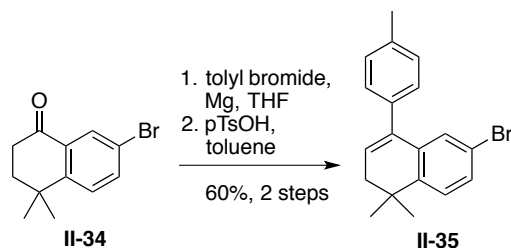
4,4-Dimethyl-3,4-dihydronaphthalen-1(2H)-one (II-33).

To a stirring solution of AlCl_3 (351 mg, 2.63 mmol) in benzene at 5 °C (dry ice/benzene bath), was added lactone (100 mg, 0.876 mmol) in benzene dropwise. The mixture was then slowly warmed to 100 °C and allowed to stir for 3 h. Then an ice-cold solution of 1N HCl quenched the reaction before workup in MTBE with dilute HCl, water, and aqueous NaHCO_3 , and brine. The combined organic layers then dried over MgSO_4 , filtered, and concentrated *in vacuo*. Flash column chromatography with 20% EtOAc/Hex gave UV active product. ^1H NMR (400 MHz, CDCl_3): δ 7.95 (dd, $J = 7.8, 1.4$ Hz, 1H), 7.47 – 7.42 (m, 1H), 7.34 (d, $J = 7.9$ Hz, 1H), 7.15 – 7.09 (m, 1H), 2.71 – 2.61 (m, 2H), 1.94 (t, $J = 6.6$ Hz, 2H), 1.32 (s, 6H); ^{13}C NMR (125 MHz, CDCl_3): δ 198.4, 152.3, 133.9, 128.3, 127.3, 126.3, 125.8, 37.1, 35.1, 33.9, 29.7, 29.7.



7-Bromo-4,4-dimethyl-3,4-dihydronaphthalen-1(2H)-one (II-34).

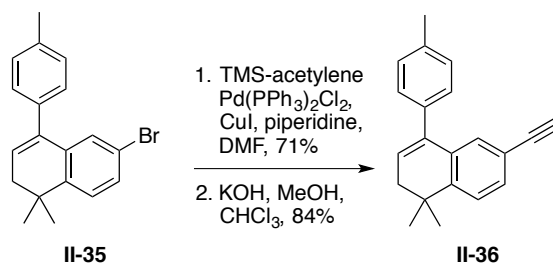
To a stirring flask of AlCl₃ (1.91 g, 14.3 mmol) in CH₂Cl₂ was added tetralone (1.0 g, 5.74 mmol), dropwise at ambient temperature. Then bromine (1.1 g, 6.90 mmol) was slowly added, and the mixture was allowed to stir for 2 h at ambient temperature. The reaction was then quenched with an ice-cold solution of 6M HCl, followed by extraction with Et₂O. Combined organic layers washed with water, aqueous NaHCO₃, and brine, then dried over MgSO₄, filtered, and concentrated *in vacuo*. TLC analysis gave several spots and flash column chromatography with 10 % EtOAc/Hex gave a few brominated products. The spectra for the desired 7-bromo tetralone is reported here. mp 92-93 °C; ¹H NMR (400 MHz, CDCl₃): 8.12 (d, J=3.0 Hz, 1H), 7.60 (dd, J=3.0, 9.0 Hz, 1H), 7.32 (d, J=9.0 Hz, 1H), 2.72 (t, J=6.0 Hz, 2H), 2.01 (t, J=6.0 Hz, 2H), 1.27 (s, 6H). ¹³C NMR (125 MHz, CDCl₃): δ 198.4, 133.9, 128.3, 127.3, 126.3, 125.8, 37.1, 35.1, 29.7, 29.7; [M+Na]⁺ calcd for C₁₂H₁₃OBrNa requires 275.0150, found 275.0044.



6-Bromo-1,1-dimethyl-4-(*p*-tolyl)-1,2-dihydronaphthalene (II-35).

To a flask of Mg (24 mg, 2.66 mmol), tolyl bromide (440 mg, 1.3 mmol) and a couple iodine crystals. The flask was heated until bubbles appeared and stirred for 1 h. The reaction is then cooled to 0 °C (ice bath) and a solution of the bromo tetralone (500mg, 1.97 mmol) in toluene was added. The reaction was allowed to stir overnight at ambient temperature. Then, it was quenched with ammonium chloride, extracted with EtOAc, washed with brine. The combined organic layers were dried over MgSO₄, filtered, and

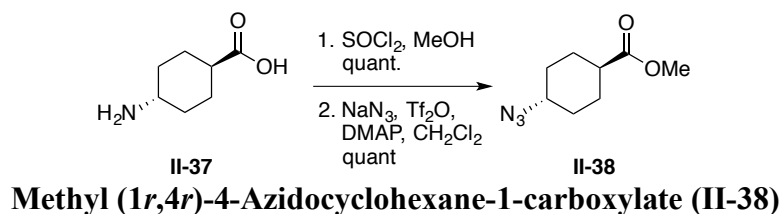
concentrated *in vacuo* before flash column chromatography with 30% EtOAc:Hex to give alcohol intermediate as a yellow oil (74%). Then, to a solution of the alcohol intermediate in toluene (10ml), was added a catalytic amount of pTsoH (1 mol%) and molecular sieves. The reaction was stirred at reflux for 2 h then worked up with water and MTBE, dried over MgSO₄, filtered, and concentrated *in vacuo* followed by flash chromatography with 1 to 10% EtOAc: Hex to give tolyl bromide. mp 107-109 °C; ¹H NMR (400 MHz, CDCl₃): δ 7.37 (dd, J = 8.2, 2.1 Hz, 1H), 7.28 – 7.23 (m, 5H), 7.20 (d, J = 2.0 Hz, 1H), 6.02 (t, J = 4.7 Hz, 1H), 2.44 (s, 3H), 2.37 (d, J = 4.7 Hz, 2H), 1.35 (s, 6H); ¹³C NMR (125 MHz, CDCl₃): δ 144.1, 138.5, 137.3, 137.0, 136.2, 130.2, 129.1, 129.1, 128.8, 128.5, 128.2, 127.3, 125.6, 119.8, 38.7, 33.5, 28.0, 28.0, 21.2; [M]⁺ calcd for C₁₉H₁₉Br requires 326.0670, found 326.0664.



6-Ethynyl-1,1-dimethyl-4-(*p*-tolyl)-1,2-dihydronaphthalene (II-36).

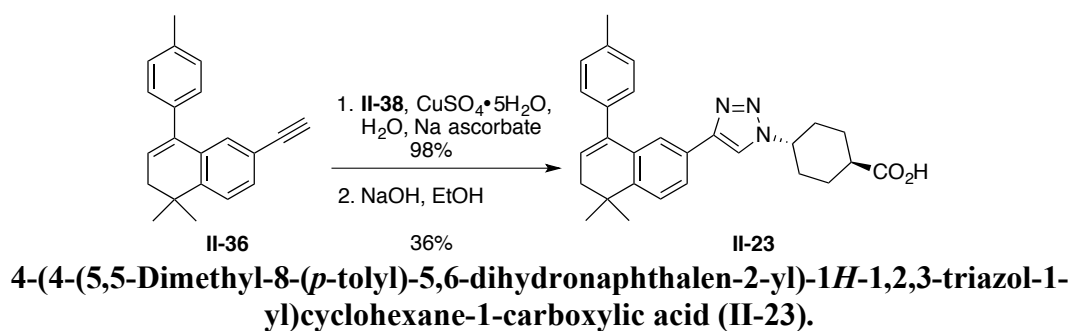
A flask of bromide (200 mg, 0.61 mmol), TMS-acetylene (78mg, 0.79 mmol), copper iodide (11 mg, 10 mol%), and palladium catalyst (21 mg, 5 mol%) in trimethylamine (2 mL) was stirred overnight at 70°C. The solvent was then evaporated and the intermediate was purified by column chromatography with 1% EtOAc:Hex to produce 71% product that was carried forward to the desilylation step. The silyl intermediate was then dissolved in a MeOH:CHCl₃ (1:1) mixture and 1N KOH was added. The solution stirred overnight at

ambient temperature before work up with DCM. The organic layers were combined, dried over MgSO₄, filtered, and then concentrated *in vacuo*. Flash column chromatography with 0 to 1% EtOAc:Hex gave pure tolyl naphthyl alkyne **II-36** in 84% yield. mp 94-95 °C; ¹H NMR (400 MHz, CDCl₃): δ 7.55 (dd, J = 7.9, 1.5 Hz, 1H), 7.50 (d, J = 7.9 Hz, 1H), 7.45 – 7.38 (m, 4H), 7.37 (d, J = 1.1 Hz, 1H), 6.17 (t, J = 4.7 Hz, 1H), 3.14 (s, 1H), 2.60 (s, 3H), 2.53 (d, J = 4.7 Hz, 2H), 1.52 (s, 6H); ¹³C NMR (125 MHz, CDCl₃): δ 146.2, 138.7, 137.5, 136.9, 134.1, 131.2, 129.5, 129.1, 129.1, 128.5, 128.5, 126.7, 123.9, 119.4, 83.9, 76.3, 38.7, 33.7, 28.0, 28.0, 21.2; GCMS (HREI) m/z calcd for C₂₁H₂₀ [M]⁺ requires 272.1565, found 272.1552.



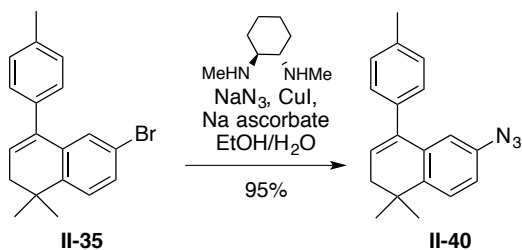
To a solution of acid **II-37** (3.00 g, 20.1 mmol) in MeOH (10 mL) was added thionyl chloride (1.82 mL, 25.1 mmol) at 0 °C (ice bath). The mixture was allowed to stir overnight at ambient temperature before concentrating *in vacuo*. Then, the residue was washed with hexanes to give the ester salt as a white solid in quantitative yield and carried on without further purification. **II-37** ester: ¹H NMR (400 MHz, CD₃OD): δ 3.69 (s, 3H), 3.33 (t, J = 1.2 Hz, 2H), 3.10 (t, J = 11.4 Hz, 1H), 2.37 (tt, J = 12.0, 2.8 Hz, 1H), 2.11 (d, J = 10.1 Hz, 4H), 1.61 – 1.38 (m, 4H); ¹³C NMR (125 MHz, CDCl₃): δ 176.7, 52.3, 50.7, 42.8, 30.8, 30.8, 28.0, 28.0. Then, the triflic azide was formed *in situ* by adding to a solution of sodium azide (1.33 g, 20.4 mmol) in 5 mL water at 0 °C (ice bath), 5 mL DCM followed by Tf₂O

(700 μ L, 4.14 mmol). The mixture was stirred for 2 h in the ice bath. The DCM phase was separated, and the aqueous phase was extracted with DCM twice. The combined DCM phase was washed with sat. NaHCO_3 and water, dried over MgSO_4 , and set aside. Next, amino ester (172 mg, 1.09 mmol) was dissolved in 5 mL dry DCM and stirred at ambient temperature. To it was added DMAP (585 mg, 4.80 mmol) and then the above-prepared triflic azide in DCM solution was added dropwise. The mixture was stirred for overnight and then concentrated *in vacuo* to give the azide ester **II-38** in quantitative yield as an oil. ^1H NMR (400 MHz, CDCl_3): δ 3.64 (s, 3H), 3.26 (tt, $J = 20.1, 5.7$ Hz, 1H), 2.26 (tt, $J = 11.7, 3.0$ Hz, 1H), 2.08 – 1.97 (m, 4H), 1.56 – 1.26 (m, 4H); ^{13}C NMR (125 MHz, CDCl_3): δ 175.5, 59.2, 51.7, 41.8, 30.6, 30.6, 27.1, 27.1.



To a suspension of alkyne **II-36** (50 mg, 0.18 mmol) and azide **II-38** (31 mg, 0.18 mmol) in a solution of $\text{H}_2\text{O}:\text{tBuOH}$ (1:1), was added sodium ascorbate (3.6 mg, 10 mol%) and copper sulfate pentahydrate (1.0 mg, 2 mol%). The mixture was vigorously stirred overnight at ambient temperature. Then the reaction was cooled to -5 $^\circ\text{C}$ (aqueous NH_4Cl and ice bath) and a precipitate formed. The precipitate was filtered, washed with ice cold water, collected, and dried *in vacuo* to give triazole ester intermediate. Then, to a round-bottom flask of the triazole ester intermediate (84 mg, 0.18 mmol) in EtOH (2 mL), was added 1M NaOH (1 mL) and the reaction was allowed to stir overnight at ambient

temperature. Then, the mixture was acidified with 1M HCl slowing at 100 μ L increments and the product was extracted with EtOAc to give desired triazole acid **II-23**. Further recrystallization in MeOH:DCM to give yellowish crystals. mp 128-130 $^{\circ}$ C; 1 H NMR (400 MHz, CDCl_3): δ 7.95 (d, J = 1.6 Hz, 1H), 7.50 – 7.38 (m, 2H), 7.30 – 7.17 (m, 4H), 5.99 (t, J = 4.7 Hz, 1H), 4.47 (tt, J = 11.9, 3.8 Hz, 1H), 3.70 (s, 1H), 2.51 – 2.40 (m, 1H), 2.39 (s, 3H), 2.36 (d, J = 4.7 Hz, 2H), 2.30 – 2.25 (m, 2H), 2.20 (d, J = 13.6 Hz, 2H), 1.92 (qd, J = 12.7, 3.1 Hz, 2H), 1.66 (qd, J = 13.3, 2.8 Hz, 2H), 1.36 (s, 6H), 1.29 (br s, 1H); 13 C NMR (125 MHz, CDCl_3): δ 187.5, 147.0, 140.5, 139.2, 138.1, 135.9, 130.3, 130.3, 129.8, 129.8, 129.0, 127.9, 126.2, 125.7, 124.6, 120.0, 60.9, 52.8, 43.1, 40.1, 34.9, 34.9, 33.4, 33.3, 29.0, 29.0, 28.9, 21.9; LRMS (ESI) m/z calcd for $\text{C}_{28}\text{H}_{32}\text{N}_3\text{O}_2$ $[\text{M}+\text{H}]^+$ 442.2, found 442.9.

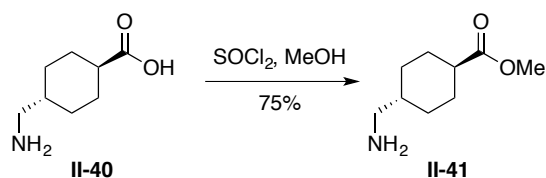


6-Azido-1,1-dimethyl-4-(*p*-tolyl)-1,2-dihydronaphthalene (II-40).

To a flask of aryl bromide (100 mg, 0.31 mmol) in a solution of EtOH:H₂O (7:3), was added sodium azide (40 mg, 0.61 mmol), sodium ascorbate (3.0 mg, 5.0 mol%), copper iodide (6.0 mg, 5.0 mol%), and diamine ligand (7.0 mg, 15 mol%). The flask was degassed with house nitrogen then stirred under reflux for 6 hours, or until consumption of starting material. The reaction was then cooled to ambient temperature before work up with EtOAc

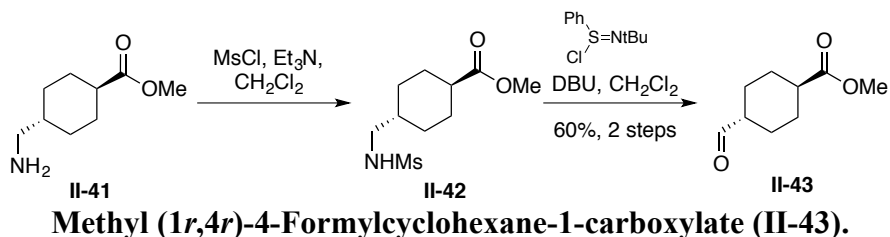
and brine. The combined organic layers were dried over MgSO₄, filtered, and purified over a short silica plug and then concentrated *in vacuo* to give a dark yellow oil.

¹H NMR (400 MHz, CDCl₃): δ 7.34 (d, J = 8.2 Hz, 1H), 7.24 – 7.17 (m, 4H), 6.90 (dd, J = 8.2, 2.4 Hz, 1H), 6.70 (d, J = 2.4 Hz, 1H), 6.00 (t, J = 4.7 Hz, 1H), 2.40 (s, 3H), 2.34 (d, J = 4.7 Hz, 2H), 1.32 (s, 6H); ¹³C NMR (125 MHz, CDCl₃): δ 142.2, 138.8, 137.7, 137.5, 137.1, 135.8, 129.2, 129.2, 128.6, 128.6, 127.5, 125.3, 117.7, 117.1, 39.0, 33.6, 28.4, 28.4, 21.3.

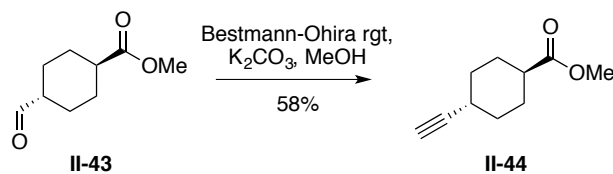


Methyl (1*r*,4*r*)-4-(Aminomethyl)cyclohexane-1-carboxylate (II-41).

To a flask of amino acid (1.00 g, 6.36 mmol) in MeOH (150 mL) was added thionyl chloride (919 μL, 12.7 mmol) slowly at 0 °C (ice bath) for 10 min. The suspension was allowed to stir at reflux and monitored with TLC. The reaction was then cooled to ambient temperature when TLC indicated consumption of starting material. The solvent was evaporated and the reaction was worked up with EtOAc and concentrated *in vacuo* to give off white crystals. mp 162-164 °C; ¹H NMR (400 MHz, CD₃OD) δ 3.68 (s, 3H), 2.81 (d, J = 6.9 Hz, 2H), 2.33 (tt, J = 12.3, 3.5 Hz, 1H), 2.12 – 1.87 (m, 4H), 1.65 (ddp, J = 11.3, 7.2, 3.7 Hz, 1H), 1.47 (qd, J = 13.1, 3.2 Hz, 2H), 1.10 (qd, J = 13.0, 3.2 Hz, 2H); ¹³C NMR (125 MHz, CD₃OD): δ 177.8, 52.4, 46.2, 43.9, 36.7, 30.3, 30.3, 29.3, 29.3; HRMS (ESI) *m/z* calcd for C₉H₁₇NO₂ [M+H]⁺ requires 172.1338, found 172.1328.

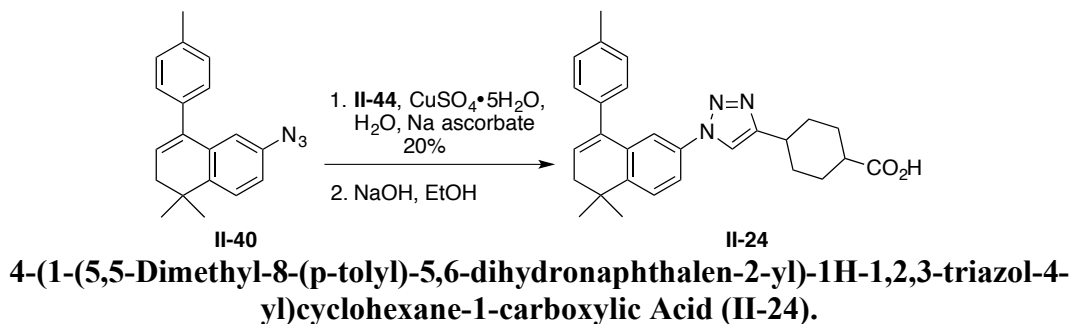


To a flask of amine ester **II-41** (1.00 g, 5.84 mmol) in DCM (10 mL) at 0 °C (ice bath), was added mesyl chloride (452 μ L, 5.84 mmol). The mixture was allowed to stir at 0 °C for 1 h. The reaction was quenched with water, washed with DCM, and then cooled to -78 °C (dry ice, iPrOH) for the next step without isolation of **II-42**. DBU (1.78 g, 11.68 mmol) was then added to the flask, followed by a solution of the sulfinimidoyl chloride (2.52 g, 11.68 mmol) in DCM. The reaction stirred at -78 °C for 2 h before warming to ambient temperature and quenching with 1M HCl. Work up was done with Et₂O, then the combined organic layers were dried over MgSO₄, filtered, and concentrated *in vacuo*. Column chromatography with 5-10% MeOH:DCM gave the desired product in 60% after two steps. ¹H NMR (400 MHz, CDCl₃): δ 3.82 (d, *J* = 7.0 Hz, 1H), 3.17 (s, 3H), 2.05 (tt, *J* = 12.3, 3.5 Hz, 1H), 1.88 – 1.80 (m, 2H), 1.74 – 1.67 (m, 2H), 1.49 – 1.37 (m, 1H), 1.29 – 1.17 (m, 2H), 0.87 (qd, *J* = 13.2, 3.4 Hz, 2H); ¹³C NMR (125 MHz, CDCl₃): δ 203.8, 175.7, 49.3, 42.5, 31.5, 27.9, 25.0, 23.3, 22.6.



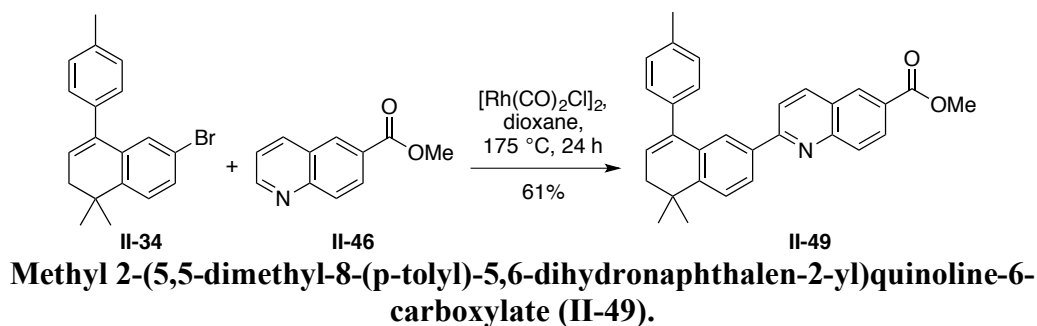
Methyl (1*r*,4*r*)-4-Ethynylcyclohexane-1-carboxylate (II-44).

To a suspension of aldehyde **II-43** (500 mg, 2.9 mmol) and K_2CO_3 (1.4 g, 10 mmol) in dry MeOH (10 mL) at ambient temperature, was added the Bestmann-Ohira reagent (790 mg, 4.1 mmol). The reaction stirred for overnight at ambient temperature and monitored with TLC. After consumption of starting material, the solvent was removed and the product was washed with DCM and water. The combined organic layers were washed with brine then dried over $MgSO_4$, filtered, and concentrated *in vacuo*. Alkyne **II-44** was obtained by column chromatography with 25% EtOAc: Hex in 58% yield. 1H NMR (400 MHz, $CDCl_3$): δ 3.68 (s, 3H), 2.35 – 2.24 (m, 2H), 2.11 – 1.97 (m, 5H), 1.45 (h, $J = 11.0, 10.6$ Hz, 4H). ^{13}C NMR (125 MHz, $CDCl_3$): δ 176.1, 88.2, 68.2, 51.7, 42.2, 31.8, 31.8, 28.7, 28.1, 28.1.



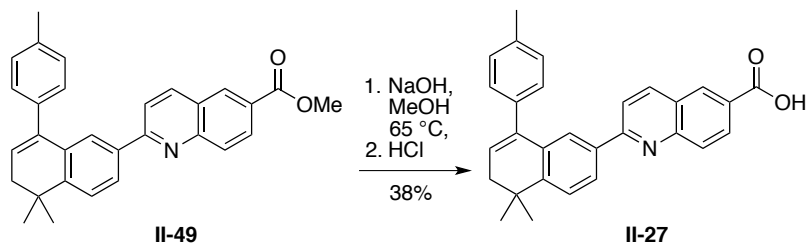
To a suspension of naphthyl azide **II-40** (52 mg, 0.18 mmol) and cyclohexyl alkyne ester **II-44** (30 mg, 0.18 mmol) in a solution of $H_2O:tBuOH$ (1:1), was added sodium ascorbate (3.6 mg, 10 mol%) and copper sulfate pentahydrate (1.0 mg, 2 mol%). The mixture was vigorously stirred overnight at ambient temperature. Then the reaction was cooled to $-5\text{ }^\circ C$ (aqueous $NHCl_4$ and ice bath) and a precipitate formed. The precipitate was filtered, washed with ice cold water, collected, and dried *in vacuo* to give the other triazole ester intermediate. Then, to a round-bottom flask of the other triazole ester intermediate (84 mg,

0.18 mmol) in EtOH (2 mL), was added 1M NaOH (1 mL) and the reaction was allowed to stir overnight at ambient temperature. Then, the mixture was acidified with 1M HCl slowing at 100 μ L increments and the product was extracted with EtOAc to give the other desired triazole acid **II-24**. Further recrystallization in MeOH:DCM to give off-white/yellow crystals. mp 235-237 $^{\circ}$ C; 1 H NMR (400 MHz, CD₃OD): δ 7.69 (s, 1H), 7.55 (d, J = 2.0 Hz, 1H), 7.50 (d, J = 8.4 Hz, 1H), 7.31 (d, J = 2.0 Hz, 1H), 7.22 (q, J = 8.1 Hz, 4H), 6.06 (t, J = 4.7 Hz, 1H), 2.76 (tt, J = 11.2, 3.1 Hz, 1H), 2.43 – 2.40 (m, 2H), 2.39 (s, 3H), 2.33 (ddt, J = 14.7, 6.5, 3.7 Hz, 2H), 2.14 (t, J = 13.7 Hz, 4H), 1.63 – 1.47 (m, 4H), 1.37 (s, 6H); 13 C NMR (125 MHz, CD₃OD): δ 179.9, 148.6, 147.6, 139.9, 138.5, 137.0, 133.9, 132.9, 130.5, 130.5, 129.8, 129.8, 129.2, 127.2, 126.6, 121.1, 120.0, 119.5, 44.0, 40.0, 35.9, 35.0, 33.1, 33.1, 30.0, 30.0, 29.2, 22.2; LRMS (ESI) m/z calcd for C₂₈H₃₂N₃O₂ [M+H]⁺ 442.2, found 442.9.



To a sealable microwave vial of tolyl bromide **II-34** (130 mg, 0.400 mmol) and quinoline ester **II-46** (450 mg, 0.240 mmol) in dioxane (2 mL) was added the Rh catalyst (8 mg, 5 mol %). The reaction was heated to 175 $^{\circ}$ C in an oil bath for 24 h and then allowed to warm temperature. The reaction was sent through a Celite plug and washed with MTBE and then the solvent was removed *in vacuo*. The product was purified by column chromatography

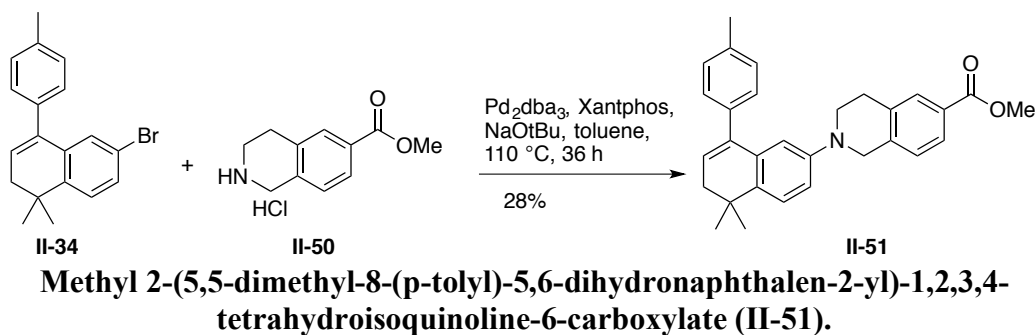
with 1-10% EtOAc:Hex and produced the coupled ester product **II-49** in 61% yield. mp 190-191 °C; ¹H NMR (400 MHz, CDCl₃): δ 8.54 (d, J = 1.5 Hz, 1H), 8.27 (dd, J = 8.9, 1.5 Hz, 1H), 8.20 (d, J = 8.6 Hz, 1H), 8.17 – 8.08 (m, 2H), 7.79 (d, J = 1.7 Hz, 1H), 7.64 (dd, J = 72.1, 8.3 Hz, 2H), 7.34 (d, J = 7.9 Hz, 2H), 7.23 (d, J = 7.9 Hz, 2H), 6.05 (t, J = 4.7 Hz, 1H), 3.99 (s, 3H), 2.42 (s, 3H), 2.39 (d, J = 4.7 Hz, 2H), 1.39 (s, 6H).; ¹³C NMR (125 MHz, CDCl₃): δ 166.8, 159.6, 150.1, 147.4, 145.9, 139.2, 137.9, 137.8, 136.9, 134.5, 130.6, 129.9, 129.1, 129.1, 129.0, 128.6, 128.6, 127.5, 127.1, 126.7, 126.2, 125.3, 124.6, 119.8, 52.4, 38.9, 33.9, 28.1, 28.1, 21.3; HRMS (ESI) m/z calcd for C₃₀H₂₇NO₂ [M+H]⁺ requires 434.2121, found 434.2132.



2-(5,5-Dimethyl-8-(p-tolyl)-5,6-dihydronaphthalen-2-yl)quinoline-6-carboxylic Acid (II-27).

To a flask of quinoline ester **II-49** (50 mg, 0.12 mmol) in MeOH (3 mL), was added 1N NaOH (1 mL). The reaction was heated to 65 °C and stirred for 2 h. Then, the flask was allowed to warm to room temperature and the solvent was removed *in vacuo*. The reaction was diluted with water and acidified to pH 4 with 1N HCl. The product precipitated and was collected via filtration and recrystallized with DCM:MeOH to give desired quinoline acid **II-27** in 38% yield after two steps. mp 268-269 °C; ¹H NMR (400 MHz, CDCl₃): δ 3.82 (d, J = 7.0 Hz, 1H), 3.17 (s, 3H), 2.05 (tt, J = 12.3, 3.5 Hz, 1H), 1.88 – 1.80 (m, 2H),

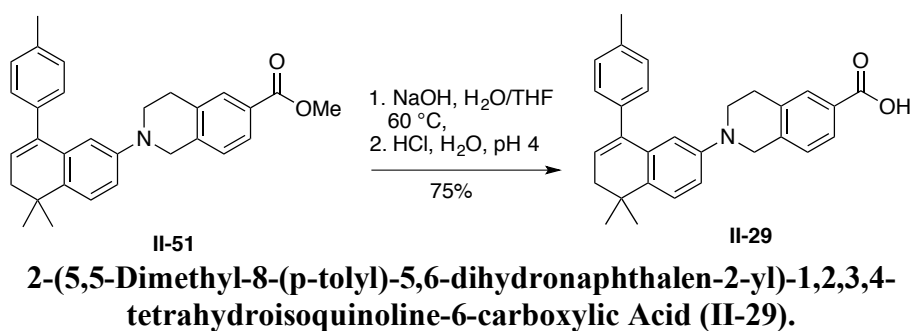
1.74 – 1.67 (m, 2H), 1.49 – 1.37 (m, 1H), 1.29 – 1.17 (m, 2H), 0.87 (qd, J = 13.2, 3.4 Hz, 2H). ¹³C NMR (125 MHz, CDCl₃): δ 176.7, 51.7, 43.3, 39.5, 28.4, 28.4, 27.1, 27.1; LRMS (ESI) m/z calcd for C₂₉H₂₆NO₂ [M+H]⁺ 420.2, found 420.8.



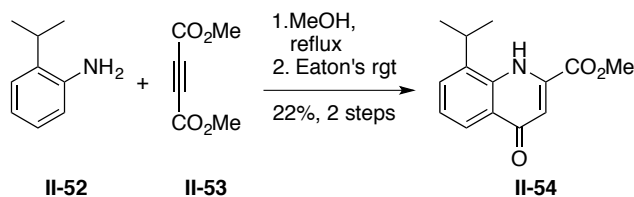
To a two-neck round-bottom flask was added Xantphos (53 mg, 0.092 mmol, 10 mol%) and Pd catalyst (42 mg, 0.046 mmol, 5 mol%) in toluene (2 mL). The reaction was purged with nitrogen for 10-15 min then heated to 110 °C for 15 min. After it reaction vessel was cooled to ambient temperature, NaOtBu (180 mg, 1.8 mmol) was added followed by the tolyl bromide **II-34** (300 mg, 0.92 mmol), then the quinoline analog **II-50** (350 mg, 1.8 mmol). The reaction was purged again with nitrogen for 10-15 min then heated to 110 °C and allowed to stir for 36 h. After the flask had cooled to ambient temperature, the reaction was filtered through a Celite plug and the solvent was removed *in vacuo*. Column chromatography with 1% EtOAc:Hex gave the desired coupled ester **II-51** in 38% yield.

*Previous attempts with *rac*-BINAP gave less than 20% product after 24 or 48 h. mp 187-190 °C; ¹H NMR (400 MHz, CDCl₃) δ 7.77 (s, 1H), 7.26 – 7.12 (m, 6H), 7.10 (d, J = 8.4 Hz, 1H), 6.83 (dd, J = 8.4, 2.6 Hz, 1H), 6.70 (d, J = 2.6 Hz, 1H), 5.94 (t, J = 4.7 Hz, 1H), 4.25 (s, 2H), 3.87 (s, 3H), 3.37 (t, J = 5.8 Hz, 2H), 2.91 (t, J = 5.7 Hz, 2H), 2.38 (s, 3H),

2.28 (d, J = 4.7 Hz, 2H), 1.28 (s, 6H); ¹³C NMR (101 MHz, CDCl₃) δ 167.2, 148.6, 140.1, 139.6, 138.3, 136.7, 136.7, 135.2, 134.8, 130.0, 129.0, 129.0, 128.7, 128.7, 128.2, 127.1, 126.8, 126.7, 124.7, 114.8, 114.6, 52.1, 51.6, 47.0, 39.3, 33.2, 29.0, 28.5, 28.5, 21.3.

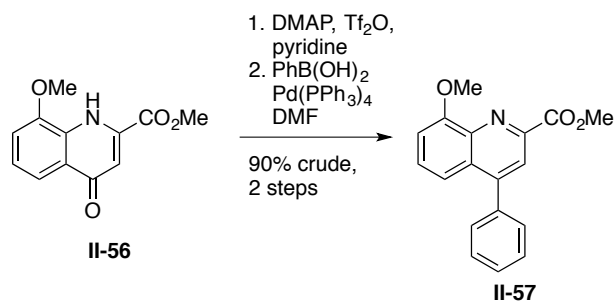


To a flask of quinoline ester **II-51** (50 mg, 0.12 mmol) in THF:H₂O (1:1, 3 mL), was added 1N NaOH (1 mL). The reaction was heated to 60 °C and stirred for 24 h. Then, the flask was allowed to warm to room temperature and the solvent was removed *in vacuo*. The reaction was diluted with water and acidified to pH 4 with 1N HCl. The product precipitated and was collected via filtration and recrystallized with DCM:MeOH to give desired tetrahydroisoquinoline acid **II-29** in 75% after two steps. mp 243-244 °C; ¹H NMR (400 MHz, CD₃OD): δ 7.87 (s, 1H), 7.84 (d, J = 8.1 Hz, 1H), 7.50 (d, J = 8.4 Hz, 1H), 7.39 (d, J = 8.4 Hz, 1H), 7.14 (d, J = 8.0 Hz, 1H), 7.08 (d, J = 2.0 Hz, 4H), 6.97 (d, J = 2.4 Hz, 1H), 6.02 (t, J = 4.6 Hz, 1H), 4.60 (s, 2H), 3.75 (t, J = 6.2 Hz, 2H), 3.19 (d, J = 5.7 Hz, 2H), 2.33 (d, J = 4.7 Hz, 2H), 2.30 (s, 3H), 1.30 (s, 6H). LRMS (ESI) m/z calcd for C₂₉H₃₀NO₂ [M+H]⁺ 424.2, found 424.9.



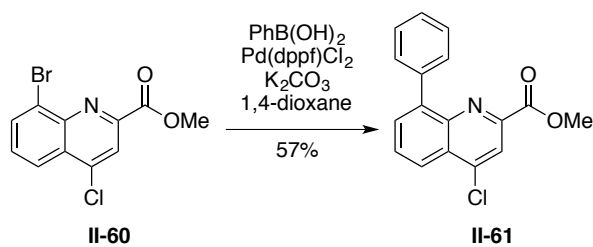
Methyl 8-isopropyl-4-oxo-1,4-dihydroquinoline-2-carboxylate (II-54).

To a flask of aniline (1.0 g, 8.1 mmol) in MeOH (5 mL) at 5 °C (ice bath), was added dicarboxylate (1.4 g, 9.7 mmol). The reaction stirred for 2 h at ambient temperature. Evaporation of solvent gave a dark yellow solid that was carried on to next step. To a flask of intermediate diester (1.8g, 6.6 mmol), was added Eaton's reagent (7 mL). The reaction was heated to 50 °C and stirred for 2-3 h, until TLC revealed consumption of starting material. Then, the reaction mixture was cooled to 5 °C (ice bath) and poured into an ice cold saturated NaHCO₃ solution, as precipitate formed. The solid was filtered and washed with water and dried *in vacuo* to give yellowish oil. ¹H NMR (400 MHz, CDCl₃): δ 9.10 (s, 1H), 8.25 (d, *J* = 8.0 Hz, 1H), 7.60 (dd, *J* = 7.4, 0.9 Hz, 1H), 7.37 (t, *J* = 7.8 Hz, 1H), 6.98 (d, *J* = 1.7 Hz, 1H), 4.07 (s, 3H), 3.30 (p, *J* = 6.8 Hz, 1H), 1.43 (d, *J* = 6.8 Hz, 6H); ¹³C NMR (125 MHz, CDCl₃): δ 180.0, 163.8, 136.4, 135.6, 135.6, 129.1, 126.7, 124.4, 124.1, 111.2, 53.9, 27.7, 22.7.



Methyl 8-methoxy-4-phenylquinoline-2-carboxylate (II-57).

To a flask of quinoline (200 mg, 0.86 mmol) dissolved in dry DCM (5 mL), was added DMAP (41 mg, 0.34 mmol) and 2,6-lutidine (303 μ L, 2.6 mmol). Then, the flask was cooled to 0 $^{\circ}$ C (ice bath) and triflic anhydride (440 μ L, 2.6 mmol) was added dropwise. The reaction was warmed to ambient temperature and allowed to stir overnight. The solvent was then evaporated the next day and the residue was washed with MeOH and concentrated *in vacuo* to give an off-white product. Then, the triflate product (100 mg, 0.27 mmol) was then dissolved in DMF (5 mL) and phenyl boronic acid (50mg, 0.41 mmol), trimethylamine (75 μ L, 0.54 mmol) was added. The flask was degassed with house argon, then palladium tetrakis (10 mg, 30 mol%) was added and the reaction stirred for 4 h at reflux. The reaction was extracted with DCM, washed with brine, and dried over MgSO₄. After filtration, the product was concentrated *in vacuo* and then purified by flash column chromatography with 30% EtOAc/Hex. ¹H NMR (400 MHz, CDCl₃): δ 8.24 (d, *J* = 7.1 Hz, 1H), 8.16 (s, 1H), 7.54-7.52 (m, 4H), 7.36 – 7.29 (m, 2H), 7.14-7.10 (m, 1H), 4.10 (s, 3H), 4.05 (s, 3H); ¹³C NMR (125 MHz, CDCl₃): δ 183.4, 155.7, 148.7, 138.3, 133.6, 132.1, 129.6, 129.5, 129.5, 128.7, 128.6, 128.5, 128.5, 128.4, 122.0, 117.7, 56.1, 53.1.



Methyl 4-chloro-8-phenylquinoline-2-carboxylate (II-61)

To a two-neck round-bottom flask was added quinoline **II-60** (500 mg, 1.66 mmol), phenylboronic acid (305 mg, 2.50 mmol, 1.50 equiv), and potassium carbonate (688 mg, 4.98, 3.00 equiv) in 1,4-dioxane (5 mL). The solution was purged with nitrogen for 5-20

min, then Pd(dddpf)Cl₂ (136 mg, 0.166 mmol) was added. The reaction was heated to 100 °C (oil bath) and allowed to stir overnight. After cooling to room temperature, the reaction was diluted with EtOAc and washed with water. The reaction was then filtered and the filtrate was washed again with water and brine. The combined organic layers were dried over MgSO₄, filtered, and concentrated *in vacuo*. Column chromatography with 0 to 10% EtOAc:Hex, gave the 4-phenyl quinoline ester **II-61** in 57% yield. ¹H NMR (400 MHz, CDCl₃) δ 8.38 – 8.25 (m, 2H), 7.92 (d, J = 7.1 Hz, 1H), 7.85 – 7.78 (m, 3H), 7.51 (t, J = 7.6 Hz, 2H), 7.45 (d, J = 7.0 Hz, 1H), 3.98 (s, 3H); ¹³C NMR (101 MHz, CDCl₃) δ 165.5, 147.3, 146.1, 144.1, 142.3, 138.3, 132.0, 131.4, 129.6, 128.9, 128.1, 128.0, 128.0, 123.7, 121.3, 77.5, 53.2; [M+Na]⁺ calcd for C₁₇H₁₂ClNO₂Na requires 320.0557, found 320.0456.

CUMULATIVE REFERENCES

1. Carakostas, M. C.; Curry, L. L.; Boileau, A. C.; Brusick, D. J. Overview: the history, technical function and safety of rebaudioside A, a naturally occurring steviol glycoside, for use in food and beverages. *Food Chem. Toxicol.* **2008**, *46 Suppl 7*, S1-S10.
2. Singh, H. P.; Dhir, S. K.; Dhir, S. Stevia. In *Compendium of Transgenic Crop Plants*, Blackwell Publishing Ltd.: **2009**; 97-116.
3. Ferrazzano, G. F.; Cantile, T.; Alcidi, B.; Coda, M.; Ingenito, A.; Zarrelli, A.; Di Fabio, G.; Pollio, A. Is Stevia rebaudiana Bertoni a Non Cariogenic Sweetener? A Review. *Molecules* **2015**, *21*, E38.
4. Kinghorn, A. D. *Stevia: The Genus Stevia*. Taylor & Francis: London, **2002**; 214.
5. Gosling, C. Miscellaneous Notes. *Bull. Misc. Inf., R. Bot. Gard.* **1901**, *1901*, 173-174.
6. Giuffré, L.; Romaniuk, R.; Ciarlo, E. Stevia, ka'a he'e, wild sweet herb from South America - An overview. *Emir. J. Food Agric.* **2013**, *25*, 746-750.
7. Soejarto, D.; Compadre, C.; Medon, P.; Kamath, S.; Kinghorn, A. D. Potential sweetening agents of plant origin. II. Field search for sweet-tasting Stevia species. *Econ. Bot.* **1983**, *37*, 71-79.
8. Kinghorn, A. D.; Soejarto, D. D.; Nanayakkara, N. P.; Compadre, C. M.; Makapugay, H. C.; Hovanec-Brown, J. M.; Medon, P. J.; Kamath, S. K. A phytochemical screening procedure for sweet ent-kaurene glycosides in the genus Stevia. *J. Nat. Prod.* **1984**, *47*, 439-444.

9. Yadav, A. K.; Singh, S.; Dhyani, D.; Ahuja, P. S. A review on the improvement of stevia [*Stevia rebaudiana* (Bertoni)]. *Can. J. Plant Sci.* **2011**, *91*, 1-27.
10. Brandle, J. E.; Telmer, P. G. Steviol glycoside biosynthesis. *Phytochemistry* **2007**, *68*, 1855-1863.
11. Julliard, J. H.; Douce, R. Biosynthesis of the thiazole moiety of thiamin (vitamin B1) in higher plant chloroplasts. *Proc. Natl. Acad. Sci. U. S. A.* **1991**, *88*, 2042-2045.
12. Qidwai, T.; Jamal, F.; Khan, M. Y.; Sharma, B. Exploring drug targets in isoprenoid biosynthetic pathway for *Plasmodium falciparum*. *Biochem. Res. Int.* **2014**, *2014*.
13. Hunter, W. N. The non-mevalonate pathway of isoprenoid precursor biosynthesis. *J. Biol. Chem.* **2007**, *282*, 21573-21577.
14. McGarvey, D. J.; Croteau, R. Terpenoid metabolism. *The Plant Cell* **1995**, *7*, 1015.
15. Richman, A. S.; Gijzen, M.; Starratt, A. N.; Yang, Z.; Brandle, J. E. Diterpene synthesis in *Stevia rebaudiana*: recruitment and up-regulation of key enzymes from the gibberellin biosynthetic pathway. *Plant J.* **1999**, *19*, 411-421.
16. Humphrey, T. V.; Richman, A. S.; Menassa, R.; Brandle, J. E. Spatial organisation of four enzymes from *Stevia rebaudiana* that are involved in steviol glycoside synthesis. *Plant Mol. Biol.* **2006**, *61*, 47-62.
17. Bennett, R. D.; Lieber, E. R.; Heftmann, E. Biosynthesis of steviol from (-)-kaurene. *Phytochemistry* **1967**, *6*, 1107-1110.

18. Kim, K. K.; Sawa, Y.; Shibata, H. Hydroxylation of ent-kaurenoic acid to steviol in *Stevia rebaudiana* Bertoni--purification and partial characterization of the enzyme. *Arch. Biochem. Biophys.* **1996**, *332*, 223-230.
19. Mosettig, E.; Beglinger, U.; Dolder, F.; Lichti, H.; Quitt, P.; Waters, J. A. The absolute configuration of steviol and isosteviol. *J. Am. Chem. Soc.* **1963**, *85*, 2305-2309.
20. Shibata, H.; Sonoke, S.; Ochiai, H.; Nishihashi, H.; Yamada, M. Glucosylation of Steviol and Steviol-Glucosides in Extracts from *Stevia rebaudiana* Bertoni. *Plant Physiol.* **1991**, *95*, 152-156.
21. Pezzuto, J. M.; Compadre, C. M.; Swanson, S. M.; Nanayakkara, D.; Kinghorn, A. D. Metabolically activated steviol, the aglycone of stevioside, is mutagenic. *Proc. Natl. Acad. Sci. U. S. A.* **1985**, *82*, 2478-2482.
22. Wolwer-Rieck, U. The leaves of *Stevia rebaudiana* (Bertoni), their constituents and the analyses thereof: a review. *J. Agric. Food Chem.* **2012**, *60*, 886-895.
23. Bridel, M.; Lavieille, R. The sweet principle in Kaa-he-e (*Stevia rebaudiana* Bertoni). II. Hydrolysis of stevioside by enzymes. III. Steviol by enzymic hydrolysis and isosteviol by acid hydrolysis. *Bull. Soc. Chim. Biol. (Paris)* **1931**, *13*, 781-796.
24. Prakash, I.; Campbell, M.; San Miguel, R. I.; Chaturvedula, V. S. Synthesis and sensory evaluation of ent-kaurane diterpene glycosides. *Molecules* **2012**, *17*, 8908-8916.
25. Puri, M.; Sharma, D.; Tiwari, A. K. Downstream processing of stevioside and its potential applications. *Biotechnol. Adv.* **2011**, *29*, 781-791.
26. Lemus-Mondaca, R.; Ah-Hen, K.; Vega-Gálvez, A.; Honores, C.; Moraga, N. O. *Stevia rebaudiana* Leaves: Effect of Drying Process Temperature on Bioactive

Components, Antioxidant Capacity and Natural Sweeteners. *Plant Foods Hum. Nutr.* **2016**, *71*, 49-56.

27. Chatsudthipong, V.; Muanprasat, C. Stevioside and related compounds: therapeutic benefits beyond sweetness. *Pharmacol. Ther.* **2009**, *121*, 41-54.
28. Brahmachari, G.; Mandal, L. C.; Roy, R.; Mondal, S.; Brahmachari, A. K. Stevioside and related compounds - molecules of pharmaceutical promise: a critical overview. *Arch. Pharm. Chem. Life Sci.* **2011**, *344*, 5-19.
29. Savita, S.; Sheela, K.; Sunanda, S.; Shankar, A.; Ramakrishna, P.; Sakey, S. Health implications of *Stevia rebaudiana*. *J. Hum. Ecol.* **2004**, *15*, 191-194.
30. Herranz-Lopez, M.; Barrajon-Catalan, E.; Beltran-Debon, R.; Joven, J.; Micol, V. *Stevia* is a source for alternative sweeteners: potential medicinal effects. *Agro Food Indus. Hi-Tech* **2010**, *21*, 38-42.
31. Gupta, E.; Purwar, S.; Sundaram, S.; Rai, G. Nutritional and therapeutic values of *Stevia rebaudiana*: A review. *J. Med. Plants Res.* **2013**, *7*, 3343-3353.
32. Jeppesen, P. B.; Gregersen, S.; Alstrup, K. K.; Hermansen, K. Stevioside induces antihyperglycaemic, insulinotropic and glucagonostatic effects in vivo: studies in the diabetic Goto-Kakizaki (GK) rats. *Phytomedicine* **2002**, *9*, 9-14.
33. Hsieh, M. H.; Chan, P.; Sue, Y. M.; Liu, J. C.; Liang, T. H.; Huang, T. Y.; Tomlinson, B.; Chow, M. S.; Kao, P. F.; Chen, Y. J. Efficacy and tolerability of oral stevioside in patients with mild essential hypertension: a two-year, randomized, placebo-controlled study. *Clin. Ther.* **2003**, *25*, 2797-2808.

34. Jayaraman, S.; Manoharan, M. S.; Illanchezian, S. In-vitro antimicrobial and antitumor activities of *Stevia rebaudiana* (Asteraceae) leaf extracts. *Trop. J. Pharm. Res.* **2008**, *7*, 1143-1149.
35. Ghosh, S.; Subudhi, E.; Nayak, S. Antimicrobial assay of *Stevia rebaudiana* Bertoni leaf extracts against 10 pathogens. *Int. J. Integr. Biol.* **2008**, *2*, 1-5.
36. Takahashi, K.; Matsuda, M.; Ohashi, K.; Taniguchi, K.; Nakagomi, O.; Abe, Y.; Mori, S.; Sato, N.; Okutani, K.; Shigeta, S. Analysis of anti-rotavirus activity of extract from *Stevia rebaudiana*. *Antiviral Res.* **2001**, *49*, 15-24.
37. Yuajit, C.; Muanprasat, C.; Gallagher, A. R.; Fedeles, S. V.; Kittayaruksakul, S.; Homvisasevongsa, S.; Somlo, S.; Chatsudthipong, V. Steviol retards renal cyst growth through reduction of CFTR expression and inhibition of epithelial cell proliferation in a mouse model of polycystic kidney disease. *Biochem. Pharmacol.* **2014**, *88*, 412-421.
38. Kedik, S.; Yartsev, E.; Stanishevskaya, I. Antiviral activity of dried extract of *Stevia*. *Pharm. Chem. J.* **2009**, *43*, 198-199.
39. Silva, P. A.; Oliveira, D. F.; Prado, N. R. T. d.; Carvalho, D. A. d.; Carvalho, G. A. d. Evaluation of the antifungal activity by plant extracts against *Colletotrichum gloeosporioides* PENZ. *Cienc. Agrotecnol.* **2008**, *32*, 420-428.
40. Takahashi, K.; Iwata, Y.; Mori, S.; Shigeta, S. In vitro anti-HIV activity of extract from *Stevia rebaudiana*. *Antiviral Res.* **1998**, *37*, 59-59.
41. Mohan, K.; Robert, J. Hepatoprotective effects of *Stevia rebaudiana* Bertoni leaf extract in CCl₄-induced liver injury in albino rats. *Med. Arom. Plant Sci. Biotechnol.* **2009**, *3*.

42. Boonkaewwan, C.; Toskulkao, C.; Vongsakul, M. Anti-Inflammatory and Immunomodulatory Activities of Stevioside and Its Metabolite Steviol on THP-1 Cells. *J. Agric. Food Chem.* **2006**, *54*, 785-789.
43. Barriocanal, L. A.; Palacios, M.; Benitez, G.; Benitez, S.; Jimenez, J. T.; Jimenez, N.; Rojas, V. Apparent lack of pharmacological effect of steviol glycosides used as sweeteners in humans. A pilot study of repeated exposures in some normotensive and hypotensive individuals and in Type 1 and Type 2 diabetics. *Regul. Toxicol. Pharmacol.* **2008**, *51*, 37-41.
44. Geuns, J. M.; Buyse, J.; Vankeirsbilck, A.; Temme, E. H.; Compennolle, F.; Toppet, S. Identification of steviol glucuronide in human urine. *J. Agric. Food Chem.* **2006**, *54*, 2794-2798.
45. Gardana, C.; Simonetti, P.; Canzi, E.; Zanchi, R.; Pietta, P. Metabolism of stevioside and rebaudioside A from *Stevia rebaudiana* extracts by human microflora. *J. Agric. Food Chem.* **2003**, *51*, 6618-6622.
46. Geuns, J. M.; Buyse, J.; Vankeirsbilck, A.; Temme, E. H. Metabolism of stevioside by healthy subjects. *Exp. Biol. Med. (Maywood)* **2007**, *232*, 164-173.
47. Geuns, J. M.; Augustijns, P.; Mols, R.; Buyse, J. G.; Driessen, B. Metabolism of stevioside in pigs and intestinal absorption characteristics of stevioside, rebaudioside A and steviol. *Food Chem. Toxicol.* **2003**, *41*, 1599-1607.
48. Austin, C. P.; Brady, L. S.; Insel, T. R.; Collins, F. S. NIH Molecular Libraries Initiative. *Science* **2004**, *306*, 1138-1139.
49. Probe Reports from the NIH Molecular Libraries Program.
<https://www.ncbi.nlm.nih.gov/books/NBK47352/>

50. Hanson, J. R.; De Oliveira, B. H. Stevioside and related sweet diterpenoid glycosides. *Nat. Prod. Rep.* **1993**, *10*, 301-309.
51. Hutt, O. E.; Doan, T. L.; Georg, G. I. Synthesis of skeletally diverse and stereochemically complex library templates derived from isosteviol and steviol. *Org. Lett.* **2013**, *15*, 1602-1605.
52. Wu, Y.; Dai, G. F.; Yang, J. H.; Zhang, Y. X.; Zhu, Y.; Tao, J. C. Stereoselective synthesis of 15- and 16-substituted isosteviol derivatives and their cytotoxic activities. *Bioorg. Med. Chem. Lett.* **2009**, *19*, 1818-1821.
53. Moons, N.; De Borggraeve, W.; Dehaen, W. Stevioside and Steviol as Starting Materials in Organic Synthesis. *Curr. Org. Chem.* **2012**, *16*, 1986-1995.
54. Zhang, J. I.; Li, X.; Ouyang, Z.; Cooks, R. G. Direct analysis of steviol glycosides from Stevia leaves by ambient ionization mass spectrometry performed on whole leaves. *Analyst* **2012**, *137*, 3091-3098.
55. Zhou, G. B.; Zhang, J.; Wang, Z. Y.; Chen, S. J.; Chen, Z. Treatment of acute promyelocytic leukaemia with all-trans retinoic acid and arsenic trioxide: a paradigm of synergistic molecular targeting therapy. *Philos. Trans. R. Soc. Lond. B Biol. Sci.* **2007**, *362*, 959-971.
56. Mokarram, P.; Mohammadi, Z.; Khazayel, S.; Dayong, Z. Induction of Epigenetic Alteration by CPUK02, An Ent- kaurenoid Derivative of Stevioside. *Avicenna J. Med. Biotechnol.* **2017**, *9*, 13-18.
57. Tan, D. S. Diversity-oriented synthesis: exploring the intersections between chemistry and biology. *Nat. Chem. Biol.* **2005**, *1*, 74-84.

58. Lachance, H.; Wetzel, S.; Kumar, K.; Waldmann, H. Charting, navigating, and populating natural product chemical space for drug discovery. *J. Med. Chem.* **2012**, *55*, 5989-6001.
59. Rosen, J.; Gottfries, J.; Muresan, S.; Backlund, A.; Oprea, T. I. Novel chemical space exploration via natural products. *J. Med. Chem.* **2009**, *52*, 1953-1962.
60. Newman, D. J.; Cragg, G. M. Natural products as sources of new drugs from 1981 to 2014. *J. Nat. Prod.* **2016**, *79*, 629-661.
61. Newman, D. J. Natural Products as Leads to Potential Drugs: An Old Process or the New Hope for Drug Discovery? *J. Med. Chem.* **2008**, *51*, 2589-2599.
62. Breinbauer, R.; Vetter, I. R.; Waldmann, H. From protein domains to drug candidates: Natural products as guiding principles in the design and synthesis of compound libraries. *Angew. Chem. Int. Ed.* **2002**, *41*, 2878-2890.
63. Dobson, C. M. Chemical space and biology. *Nature* **2004**, *432*, 824-828.
64. Feher, M.; Schmidt, J. M. Property distributions: differences between drugs, natural products, and molecules from combinatorial chemistry. *J. Chem. Inf. Comput. Sci.* **2003**, *43*, 218-227.
65. Burke, M. D.; Berger, E. M.; Schreiber, S. L. Generating Diverse Skeletons of Small Molecules Combinatorially. *Science* **2003**, *302*, 613-618.
66. Thomas, G. L.; Wyatt, E. E.; Spring, D. R. Enriching chemical space with diversity-oriented synthesis. *Curr. Opin. Drug Discov. Devel.* **2006**, *9*, 700-712.

67. Mao, S.; Probst, D.; Werner, S.; Chen, J.; Xie, X.; Brummond, K. M. Diverging Rh(I)-Catalyzed Carbocyclization Strategy to Prepare a Library of Unique Cyclic Ethers. *J. Comb. Chem.* **2008**, *10*, 235-246.
68. Lachance, H.; Wetzel, S.; Kumar, K.; Waldmann, H. Charting, navigating, and populating natural product chemical space for drug discovery. *J. Med. Chem.* **2012**, *55*, 5989-6001.
69. Larsson, J.; Gottfries, J.; Muresan, S.; Backlund, A. ChemGPS-NP: tuned for navigation in biologically relevant chemical space. *J. Nat. Prod.* **2007**, *70*, 789-794.
70. Rosén, J.; Gottfries, J.; Muresan, S.; Backlund, A.; Oprea, T. I. Novel chemical space exploration via natural products. *J. Med. Chem.* **2009**, *52*, 1953-1962.
71. Medina-Franco, J. L. Interrogating novel areas of chemical space for drug discovery using chemoinformatics. *Drug Dev. Res.* **2012**, *73*, 430-438.
72. Reymond, J.-L. The chemical space project. *Acc. Chem. Res.* **2015**, *48*, 722-730.
73. Wang, C.; Rath, N. P.; Covey, D. F. Abnormal Beckmann fragmentation/ring closing metathesis route for preparation of 18-nor-Delta-androgens and their 18-nor-13,17-epoxide derivatives. *Tetrahedron Lett.* **2006**, *47*, 7837-7839.
74. Titov, D. V.; Gilman, B.; He, Q. L.; Bhat, S.; Low, W. K.; Dang, Y.; Smeaton, M.; Demain, A. L.; Miller, P. S.; Kugel, J. F.; Goodrich, J. A.; Liu, J. O. XPB, a subunit of TFIIF, is a target of the natural product triptolide. *Nat. Chem. Biol.* **2011**, *7*, 182-188.

75. Chen, C. C.; Shiao, Y. J.; Lin, R. D.; Shao, Y. Y.; Lai, M. N.; Lin, C. C.; Ng, L. T.; Kuo, Y. H. Neuroprotective Diterpenes from the Fruiting Body of *Antrodia camphorata*. *J. Nat. Prod.* **2006**, *69*, 689-691.
76. Ogawa, T.; Nozaki, M.; Matsui, M. Total synthesis of stevioside. *Tetrahedron* **1980**, *36*, 2641-2648.
77. Cook, I. F.; Knox, J. R. Synthesis of steviol. *Tetrahedron Lett.* **1970**, 4091-4093.
78. Mori, K.; Nakahara, Y.; Matsui, M. Diterpenoid total synthesis. XIV. Total synthesis of (+)-steviol. *Tetrahedron Lett.* **1970**, 2411-2414.
79. Nakahara, Y.; Mori, K.; Matsui, M. Diterpenoid total synthesis. XVI. Alternative synthetic routes to (+)-steviol and (+)-kaur-16-en-19-oic acid. *Agric. Biol. Chem.* **1971**, *35*, 918-928.
80. Mori, K.; Nakahara, Y.; Matsui, M. Diterpenoid total synthesis. XIX. (+)-Steviol and erythroxydiol A. Rearrangements in bicyclooctane compounds. *Tetrahedron* **1972**, *28*, 3217-3226.
81. Ziegler, F. E.; Kloek, J. A. The stereocontrolled photoaddition of allene to cyclopent-1-ene-1-carboxaldehydes. A total synthesis of (+)-steviol methyl ester and isosteviol methyl ester. *Tetrahedron* **1977**, *33*, 373-380.
82. Coates, R. M.; Bertram, E. F. Biogenetic-like rearrangements of isosteviol derivatives. A partial synthesis of trachylobane. *Tetrahedron Lett.* **1968**, 5145-5148.
83. Coates, R. M.; Bertram, E. F. Structural modifications of isosteviol. Partial synthesis of atiserene and isoatiserene. *J. Org. Chem.* **1971**, *36*, 2625-2631.

84. Terauchi, T.; Asai, N.; Doko, T.; Taguchi, R.; Takenaka, O.; Sakurai, H.; Yonaga, M.; Kimura, T.; Kajiwara, A.; Niidome, T.; Kume, T.; Akaike, A.; Sugimoto, H. Synthesis and pharmacological profile of serofendic acids A and B. *Biorg. Med. Chem.* **2007**, *15*, 7098-7107.
85. Wang, F.-P.; Liang, X.-T. C20-diterpenoid alkaloids. *Alkaloids Chem. Biol.* **2002**, *59*, 1-280.
86. Mander, L. N. Twenty years of gibberellin research. *Nat. Prod. Rep.* **2003**, *20*, 49-69.
87. Hanson, J. R. Diterpenoids. *Nat. Prod. Rep.* **2007**, *24*, 1332-1341.
88. Schreiber, S. L. Target-oriented and diversity-oriented organic synthesis in drug discovery. *Science* **2000**, *287*, 1964-1969.
89. Spring, D. R. Diversity-oriented synthesis; a challenge for synthetic chemists. *Org. Biomol. Chem.* **2003**, *1*, 3867-3870.
90. O' Connor, C. J.; Beckmann, H. S.; Spring, D. R. Diversity-oriented synthesis: producing chemical tools for dissecting biology. *Chem. Soc. Rev.* **2012**, *41*, 4444-4456.
91. Burke, M. D.; Berger, E. M.; Schreiber, S. L. A synthesis strategy yielding skeletally diverse small molecules combinatorially. *J. Am. Chem. Soc.* **2004**, *126*, 14095-14104.
92. van Herwerden, E. F.; Süßmuth, R. D. Sources for leads: Natural products and libraries. In *New Approaches to Drug Discovery*, Springer: **2015**; 91-123.

93. Wu, Y.; Yang, J. H.; Dai, G. F.; Liu, C. J.; Tian, G. Q.; Ma, W. Y.; Tao, J. C. Stereoselective synthesis of bioactive isosteviol derivatives as alpha-glucosidase inhibitors. *Bioorg. Med. Chem.* **2009**, *17*, 1464-1473.
94. Ma, C.; Lazo, J. S.; Xie, X. Q. Compound acquisition and prioritization algorithm for constructing structurally diverse compound libraries. *ACS Comb. Sci.* **2011**, *13*, 223-231.
95. Lin, S. J.; Su, T. C.; Chu, C. N.; Chang, Y. C.; Yang, L. M.; Kuo, Y. C.; Huang, T. J. Synthesis of C-4-Substituted Steviol Derivatives and Their Inhibitory Effects against Hepatitis B Virus. *J. Nat. Prod.* **2016**, *79*, 3057-3064.
96. Avent, A. G.; Hanson, J. R.; De Oliviera, B. H. Hydrolysis of the diterpenoid glycoside, stevioside. *Phytochemistry* **1990**, *29*, 2712-2715.
97. Zhu, C.-Z.; Wang, K.; Zhang, M.-h.; Zhang, D.-Y.; Wu, Y.-C.; Wu, X.-M.; Hua, W.-Y. Efficient Synthesis of Jolkinolides A and B from Steviol. *Synthesis* **2014**, *46*, 2574-2578.
98. Młochowski, J.; Wójtowicz-Młochowska, H. Developments in synthetic application of selenium (IV) oxide and organoselenium compounds as oxygen donors and oxygen-transfer agents. *Molecules* **2015**, *20*, 10205-10243.
99. Lin, Z.; Guo, Y.; Gao, Y.; Wang, S.; Wang, X.; Xie, Z.; Niu, H.; Chang, W.; Liu, L.; Yuan, H. ent-Kaurane diterpenoids from Chinese liverworts and their antitumor activities through Michael Addition as detected in situ by a Fluorescence Probe. *J. Med. Chem.* **2015**, *58*, 3944-3956.
100. Wang, T.-t.; Liu, Y.; Chen, L. Synthesis and cytotoxic activity of nitric oxide-releasing isosteviol derivatives. *Biorg. Med. Chem. Lett.* **2014**, *24*, 2202-2205.

101. Liu, C. J.; Yu, S. L.; Liu, Y. P.; Dai, X. J.; Wu, Y.; Li, R. J.; Tao, J. C. Synthesis, cytotoxic activity evaluation and HQSAR study of novel isosteviol derivatives as potential anticancer agents. *Eur. J. Med. Chem.* **2016**, *115*, 26-40.
102. Holth, T. A.; Hutt, O. E.; Georg, G. I. Beckmann rearrangements and fragmentations in organic synthesis. In *Molecular Rearrangements in Organic Synthesis*, **2015**; 111-150.
103. Beckmann, E. Zur Kenntniss der Isonitrosoverbindungen. *Ber. Dtsch. Chem. Ges.* **1886**, *19*, 988-993.
104. Wang, Z. Beckmann Rearrangement and Beckmann Fragmentation. In *Comprehensive Organic Name Reactions and Reagents*, John Wiley & Sons, Inc.: **2010**; 288-295.
105. Pereira, M. M. A.; Santos, P. P. Rearrangements of hydroxylamines, oximes, and hydroxamic acids. In *The Chemistry of Hydroxylamines, Oximes and Hydroxamic Acids*, Rappoport, Z.; Liebman, J. F., Eds. John Wiley & Sons, Ltd: **2009**; 343-498.
106. Gawley, R. E. The Beckmann Reactions: Rearrangements, Elimination-Additions, Fragmentations, and Rearrangement-Cyclizations. In *Organic Reactions*, Kende, A. S., Ed. John Wiley & Sons, Inc: New York, **2004**; *Vol. 35*, 1-420.
107. Craig, D. The Beckmann and Related Reactions. In *Comprehensive Organic Synthesis*, Trost, B. M.; Fleming, I., Eds. Oxford: **1991**; *Vol. 7*, 689-702.
108. Conley, R. T.; Ghosh, S. Abnormal Beckmann rearrangements. In *Mechanisms of Molecular Migration*, Thyagarajan, S., Ed. Wiley-Interscience: New York, **1971**; *Vol. 4*, 197-308.

109. Drahl, M. A.; Manpadi, M.; Williams, L. J. C-C Fragmentation: Origins and Recent Applications. *Angew. Chem., Int. Ed.* **2013**, *52*, 11222-11251.
110. Rojas, C. M. *Molecular Rearrangements in Organic Synthesis*. John Wiley & Sons: **2015**.
111. Kaur, G.; Rajput, J. K.; Arora, P.; Devi, N. Keggin-type Bronsted dodecatungstophosphoric acid: a quasi homogenous and reusable catalyst system for liquid phase Beckmann rearrangement. *Tetrahedron Lett.* **2014**, *55*, 1136-1140.
112. Peng, J. J.; Deng, Y. Q. Catalytic Beckmann rearrangement of ketoximes in ionic liquids. *Tetrahedron Lett.* **2001**, *42*, 403-405.
113. Furuya, Y.; Ishihara, K.; Yamamoto, H. Cyanuric chloride as a mild and active Beckmann rearrangement catalyst. *J. Am. Chem. Soc.* **2005**, *127*, 11240-11241.
114. Yamamoto, Y.; Hasegawa, H.; Yamataka, H. Dynamic path bifurcation in the Beckmann reaction: support from kinetic analyses. *J. Org. Chem.* **2011**, *76*, 4652-4660.
115. Clayden, J.; Greeves, N.; Warren, S. *Organic Chemistry*. OUP Oxford: **2012**.
116. Montgomery, R.; Dougherty, G. The Interconversion and Beckman Rearrangement of Some α , β -Unsaturated Cyclic Oximes. *J. Org. Chem.* **1952**, *17*, 823-826.
117. Kenyon, J.; Young, D. P. Retention of Asymmetry during the Curtius and the Beckmann Change. *J. Chem. Soc.* **1941**, 263-267.

118. Porter, J. R.; Traverse, J. F.; Hoveyda, A. H.; Snapper, M. L. Three-component catalytic asymmetric synthesis of aliphatic amines. *J. Am. Chem. Soc.* **2001**, *123*, 10409-10410.
119. Hill, R. K.; Conley, R. T.; Chortyk, O. T. A Fragmentation-Recombination Mechanism for the Beckmann Rearrangement in Strong Acid. *J. Am. Chem. Soc.* **1965**, *87*, 5646-5651.
120. Campbell, A.; Kenyon, J. Retention of Asymmetry During Beckmann, Lossen, and Curtius Changes. *J. Chem. Soc.* **1946**, 25-27.
121. An, N.; Tian, B. X.; Pi, H. J.; Eriksson, L. A.; Deng, W. P. Mechanistic insight into self-propagation of organo-mediated Beckmann rearrangement: a combined experimental and computational study. *J. Org. Chem.* **2013**, *78*, 4297-4302.
122. Vanos, C. M.; Lambert, T. H. Cyclopropenium-activated Beckmann rearrangement. Catalysis versus self-propagation in reported organocatalytic Beckmann rearrangements. *Chem. Sci.* **2010**, *1*, 705-708.
123. Amin, J. H.; Mayo, P. D. The irradiation of aryl aldoximes. *Tetrahedron Lett.* **1963**, *4*, 1585-1589.
124. Izawa, H.; De Mayo, P.; Tabata, T. The photochemical Beckmann rearrangement. *Can. J. Chem.* **1969**, *47*, 51-62.
125. Ogata, Y.; Takagi, K.; Mizuno, K. Photochemical Beckmann Rearrangements - Correspondence between Substituent Effects in Oximes and Oxaziridines. *J. Org. Chem.* **1982**, *47*, 3684-3687.

126. Suginome, H. E,Z-Isomerization and Accompanying Photoreactions of Oximes, Oxime Ethers, Nitrones, Hydrazones, Imines, Azo- and Azoxy Compounds, and Various Applications. In *CRC Handbook of Organic Photochemistry and Photobiology*, Horspool, W. M.; Lenci, F., Eds. CRC Press: Boca Raton, FL, **2004**.
127. Lattes, A.; Oliveros, E.; Riviere, M.; Belzecki, C.; Mostowicz, D.; Abramskj, W.; Piccinnileopardi, C.; Germain, G.; Vanmeerssche, M. Photochemical and Thermal Rearrangement of Oxaziridines - Experimental-Evidence in Support of the Stereoelectronic Control-Theory. *J. Am. Chem. Soc.* **1982**, *104*, 3929-3934.
128. White, J. D.; Hrcniar, P.; Stappenbeck, F. Asymmetric synthesis of (+)-morphine. The phenanthrene route revisited. *J. Org. Chem.* **1997**, *62*, 5250-5251.
129. Roy, A.; Roberts, F. G.; Wilderman, P. R.; Zhou, K.; Peters, R. J.; Coates, R. M. 16-Aza-ent-beyerane and 16-Aza-ent-trachylobane: potent mechanism-based inhibitors of recombinant ent-kaurene synthase from *Arabidopsis thaliana*. *J. Am. Chem. Soc.* **2007**, *129*, 12453-12460.
130. White, J. D.; Hrcniar, P.; Stappenbeck, F. Asymmetric Total Synthesis of (+)-Codeine via Intramolecular Carbenoid Insertion. *J. Org. Chem.* **1999**, *64*, 7871-7884.
131. Gawley, R. E. The Beckmann Reactions: Rearrangements, Elimination-Additions, Fragmentations, and Rearrangement-Cyclizations. In *Organic Reactions*, **1988**; Vol. 35, 1-420.
132. Judd, W. R.; Katz, C. E.; Aube, J. Synthesis of amides by rearrangement. *Science of Synthesis* **2005**, *21*, 133-178.
133. Al'fonsov, V. A.; Andreeva, O. V.; Bakaleinik, G. A.; Beskrovnyi, D. V.; Gubaidullin, A. T.; Kataev, V. E.; Kovylyaeva, G. I.; Konovalov, A. I.; Korochkina, M.

G.; Litvinov, I. A.; Militsina, O. I.; Strobykina, I. Y. Chemistry and Structure of Diterpene Compounds of the Kaurane Series: VIII. Azomethines Derived from Isosteviol. *Russ. J. Gen. Chem.* **2003**, *73*, 1255-1260.

134. Hook, B. D.; Dohle, W.; Hirst, P. R.; Pickworth, M.; Berry, M. B.; Booker-Milburn, K. I. A practical flow reactor for continuous organic photochemistry. *J. Org. Chem.* **2005**, *70*, 7558-7564.

135. Aube, J. Oxaziridine rearrangements in asymmetric synthesis. *Chem. Soc. Rev.* **1997**, *26*, 269-277.

136. Biddlecom, A.; Awusabo-Asare, K.; Bankole, A. Role of parents in adolescent sexual activity and contraceptive use in four African countries. *Int. Perspect. Sex. Reprod. Health* **2009**, *35*, 72-81.

137. Corson, T. W.; Aberle, N.; Crews, C. M. Design and applications of bifunctional small molecules: why two heads are better than one. *ACS Chem. Biol.* **2008**, *3*, 677-692.

138. Leriche, G.; Chisholm, L.; Wagner, A. Cleavable linkers in chemical biology. *Biorg. Med. Chem.* **2012**, *20*, 571-582.

139. McCombs, J. R.; Owen, S. C. Antibody drug conjugates: design and selection of linker, payload and conjugation chemistry. *AAPS J.* **2015**, *17*, 339-351.

140. Ho, S.; Sackett, D. L.; Leighton, J. L. A "Methyl Extension" Strategy for Polyketide Natural Product Linker Site Validation and Its Application to Dictyostatin. *J. Am. Chem. Soc.* **2015**, *137*, 14047-14050.

141. Grabowski, K.; Baringhaus, K.-H.; Schneider, G. Scaffold diversity of natural products: inspiration for combinatorial library design. *Nat. Prod. Rep.* **2008**, *25*, 892-904

142. Kim, S.; Thiessen, P. A.; Bolton, E. E.; Chen, J.; Fu, G.; Gindulyte, A.; Han, L.; He, J.; He, S.; Shoemaker, B. A.; Wang, J.; Yu, B.; Zhang, J.; Bryant, S. H. PubChem Substance and Compound databases. *Nucleic Acids Res.* **2016**, *44*, D1202-1213.
143. Wang, Y.; Suzek, T.; Zhang, J.; Wang, J.; He, S.; Cheng, T.; Shoemaker, B. A.; Gindulyte, A.; Bryant, S. H. PubChem BioAssay: 2014 update. *Nucleic Acids Res.* **2014**, *42*, D1075-1082.
144. Chaudhary, B.; Khaled, Y. S.; Ammori, B. J.; Elkord, E. Neuropilin 1: function and therapeutic potential in cancer. *Cancer Immunol. Immunother.* **2014**, *63*, 81-99.
145. Ellis, L. M. The role of neuropilins in cancer. *Mol. Cancer Ther.* **2006**, *5*, 1099-1107.
146. Comeaux, E. Q.; van Waardenburg, R. C. Tyrosyl-DNA phosphodiesterase I resolves both naturally and chemically induced DNA adducts and its potential as a therapeutic target. *Drug Metab. Rev.* **2014**, *46*, 494-507.
147. Campbell, L.; Raheem, I.; Malemud, C. J.; Askari, A. D. The Relationship between NALP3 and Autoinflammatory Syndromes. *Int. J. Mol. Sci.* **2016**, *17*.
148. Leung, Y. Y.; Yao Hui, L. L.; Kraus, V. B. Colchicine--Update on mechanisms of action and therapeutic uses. *Semin. Arthritis Rheum.* **2015**, *45*, 341-350.
149. Trucchi, C.; Orsi, A.; Alicino, C.; Sticchi, L.; Icardi, G.; Ansaldi, F. State of the Art, Unresolved Issues, and Future Research Directions in the Fight against Hepatitis C Virus: Perspectives for Screening, Diagnostics of Resistances, and Immunization. *J. Immunol. Res.* **2016**, *2016*, 1412840.

150. Morris, A. Obesity: 5-HT_{2A} in GLP1-mediated weight loss. *Nat. Rev. Endocrinol.* **2017**, *13*, 127.
151. Beller, M.; Thomas, C.; Shen, M.; Auld, D. Identification of lipid storage modulators. In *Probe Reports from the NIH Molecular Libraries Program*, Bethesda (MD), **2010**.
152. Lipinski, C. A.; Lombardo, F.; Dominy, B. W.; Feeney, P. J. Experimental and computational approaches to estimate solubility and permeability in drug discovery and development settings. *Adv. Drug Delivery Rev.* **2001**, *46*, 3-26.
153. Walters, W.; Green, J.; Weiss, J.; Murcko, M. What Do Medicinal Chemists Actually Make? A 50-Year Retrospective. *J. Med. Chem.* **2011**, *54*, 6405-6416.
154. Huigens, R.; Morrison, K.; Hicklin, R.; Flood, T.; Richter, M.; Hergenrother, P. A ring-distortion strategy to construct stereochemically complex and structurally diverse compounds from natural products. *Nat. Chem.* **2013**, *5*, 195-202.
155. Lovering, F.; Bikker, J.; Humblet, C. Escape from flatland: increasing saturation as an approach to improving clinical success. *J. Med. Chem.* **2009**, *52*, 6752-6756.
156. Beswick, P. Not all LogP's are calculated equal: CLogP and other short stories. In *Sussex Drug Discovery Centre*, **2015**.
157. Souza, E. S.; Zaramello, L.; Kuhnen, C. A.; Junkes Bda, S.; Yunes, R. A.; Heinzen, V. E. Estimating the octanol/water partition coefficient for aliphatic organic compounds using semi-empirical electrotopological index. *Int. J. Mol. Sci.* **2011**, *12*, 7250-7264.

158. Nicolaou, K. C. Organic synthesis: the art and science of replicating the molecules of living nature and creating others like them in the laboratory. *Proc. R. Soc. London, Ser. A* **2014**, *470*, 20130690.
159. Mizukami, H.; Shiiba, K.; Ohashi, H. Enzymatic Determination of Stevioside in Stevia-Rebaudiana. *Phytochemistry* **1982**, *21*, 1927-1930.
160. Terai, T.; Ren, H.; Mori, G.; Yamaguchi, Y.; Hayashi, T. Mutagenicity of steviol and its oxidative derivatives in Salmonella typhimurium TM677. *Chem. Pharm. Bull.* **2002**, *50*, 1007-1010.
161. Wood, H. B., Jr.; Allerton, R.; Diehl, H. W.; Fletcher, H. G., Jr. Stevioside. I. The structure of the glucose moieties. *J. Org. Chem.* **1955**, *20*, 875-883.
162. Eunice Kennedy Shriver National Institute of Child Health and Human Development, N., HHS. Contraception and Birth Control.
<https://www.nichd.nih.gov/health/topics/contraception/Pages/default.aspx>
163. Bernstein, G. S. Conventional methods of contraception: condom, diaphragm, and vaginal foam. *Clin. Obstet. Gynecol.* **1974**, *17*, 21-33.
164. Tyler, E. T. Current status of oral contraception. *JAMA, J. Am. Med. Assoc.* **1964**, *187*, 562-565.
165. Tracy, E. E. Contraception: Menarche to Menopause. *Obstet. Gynecol. Clin. North Am.* **2017**, *44*, 143-158.
166. Alkema, L.; Kantorova, V.; Menozzi, C.; Biddlecom, A. National, regional, and global rates and trends in contraceptive prevalence and unmet need for family planning

between 1990 and 2015: a systematic and comprehensive analysis. *The Lancet* **2013**, *381*, 1642-1652.

167. Sedgh, G.; Ashford, L. S.; Hussain, R. *Unmet need for contraception in developing countries: Examining women's reasons for not using a method*; Guttmacher Institute: <http://www.guttmacher.org/report/unmet-need-for-contraception-in-developingcountries>, **2016**.

168. Singh, S.; Darroch, J. *Adding it up: costs and benefits of contraceptive services—estimates for 2012*; Guttmacher Institute and United Nations Population Fund: New York, **2012**.

169. Santelli, J.; Rochat, R.; Hatfield-Timajchy, K.; Gilbert, B. C.; Curtis, K.; Cabral, R.; Hirsch, J. S.; Schieve, L. The Measurement and Meaning of Unintended Pregnancy. *Perspect. Sex. Reprod. Health* **2003**, *35*, 94-101.

170. Singh, S.; Sedgh, G.; Hussain, R. Unintended pregnancy: worldwide levels, trends, and outcomes. *Stud. Family Plann.* **2010**, *41*, 241-250.

171. Mosher, W. D.; Jones, J.; Abma, J. C. Intended and unintended births in the United States: 1982-2010. In US Department of Health and Human Services, Centers for Disease Control and Prevention, National Center for Health Statistics: **2012**.

172. Murdoch, F. E.; Goldberg, E. Male contraception: another Holy Grail. *Bioorg. Med. Chem. Lett.* **2014**, *24*, 419-424.

173. Anderson, R. A.; Baird, D. T. Male contraception. *Endocr. Rev.* **2002**, *23*, 735-762.

174. Kanakis, G. A.; Goulis, D. G. Male contraception: a clinically-oriented review. *Hormones (Athens)* **2015**, *14*, 598-614.
175. Comhaire, F. H. Male contraception: hormonal, mechanical and other. *Hum. Reprod.* **1994**, *9*, 586-590.
176. Ringheim, K. Factors that determine prevalence of use of contraceptive methods for men. *Stud. Fam. Plan.* **1993**, 87-99.
177. Giwercman, A.; Skakkebaek, N. The human testis—an organ at risk? *Int. J. Androl.* **1992**, *15*, 373-375.
178. Griswold, M. D. Spermatogenesis: the commitment to meiosis. *Physiol. Rev.* **2016**, *96*, 1-17.
179. Allais-Bonnet, A.; Pailhoux, E. Role of the prion protein family in the gonads. *Frontiers Cell Dev. Biol.* **2014**, *2*, 1-9.
180. Aaltonen, P.; Amory, J. K.; Anderson, R. A.; Behre, H. M.; Bialy, G.; Blithe, D.; Bone, W.; Bremner, W. J.; Colvard, D.; Cooper, T. G. 10th Summit Meeting consensus: recommendations for regulatory approval for hormonal male contraception. *J. Androl.* **2007**, *28*, 362-363.
181. Gu, Y.-Q.; Wang, X.-H.; Xu, D.; Peng, L.; Cheng, L.-F.; Huang, M.-K.; Huang, Z.-J.; Zhang, G.-Y. A multicenter contraceptive efficacy study of injectable testosterone undecanoate in healthy Chinese men. *J. Clin. Endocrinol. Metab.* **2003**, *88*, 562-568.
182. Liu, P. Y.; Swerdloff, R. S.; Christenson, P. D.; Handelsman, D. J.; Wang, C. Rate, extent, and modifiers of spermatogenic recovery after hormonal male contraception: an integrated analysis. *The Lancet* **2006**, *367*, 1412-1420.

183. Bhasin, S.; Woodhouse, L.; Storer, T. Proof of the effect of testosterone on skeletal muscle. *J. Endocrinol.* **2001**, *170*, 27-38.
184. Raynaud, J.-P. Prostate cancer risk in testosterone-treated men. *J. Steroid Biochem. Mol. Biol.* **2006**, *102*, 261-266.
185. Nya-Ngatchou, J. J.; Amory, J. K. New approaches to male non-hormonal contraception. *Contraception* **2013**, *87*, 296-299.
186. Eunice Kennedy Shriver National Institute of Child Health and Human Development, N., HHS. Male Contraceptive Development Program (MCDP). <https://www.nichd.nih.gov/research/supported/Pages/mcdp.aspx>
187. Jimenez, T.; McDermott, J. P.; Sánchez, G.; Blanco, G. Na, K-ATPase $\alpha 4$ isoform is essential for sperm fertility. *Proc. Natl. Acad. Sci. U. S. A.* **2011**, *108*, 644-649.
188. Matzuk, M. M.; McKeown, M. R.; Filippakopoulos, P.; Li, Q.; Ma, L.; Agno, J. E.; Lemieux, M. E.; Picaud, S.; Yu, R. N.; Qi, J.; Knapp, S.; Bradner, J. E. Small-molecule inhibition of BRDT for male contraception. *Cell* **2012**, *150*, 673-684.
189. Chung, S. S.; Wolgemuth, D. J. Role of retinoid signaling in the regulation of spermatogenesis. *Cytogenet. Genome Res.* **2004**, *105*, 189-202.
190. Mukherjee, S.; Date, A.; Patravale, V.; Korting, H. C.; Roeder, A.; Weindl, G. Retinoids in the treatment of skin aging: an overview of clinical efficacy and safety. *Clin. Interv. Aging* **2006**, *1*, 327.
191. Chambon, P. The retinoid signaling pathway: molecular and genetic analyses. *Semin. Cell Biol.* **1994**, *5*, 115-125.

192. Kastner, P.; Mark, M.; Ghyselinck, N.; Krezel, W.; Dupé, V.; Grondona, J. M.; Chambon, P. Genetic evidence that the retinoid signal is transduced by heterodimeric RXR/RAR functional units during mouse development. *Development* **1997**, *124*, 313-326.
193. Kastner, P.; Messaddeq, N.; Mark, M.; Wendling, O.; Grondona, J. M.; Ward, S.; Ghyselinck, N.; Chambon, P. Vitamin A deficiency and mutations of RXRalpha, RXRbeta and RARalpha lead to early differentiation of embryonic ventricular cardiomyocytes. *Development* **1997**, *124*, 4749-4758.
194. Zhang, X.-k.; Lehmann, J.; Hoffmann, B.; Dawson, M. I.; Cameron, J.; Graupner, G.; Hermann, T.; Tran, P.; Pfahl, M. Homodimer formation of retinoid X receptor induced by 9-cis retinoic acid. *Nature* **1992**, *358*, 587.
195. Hogarth, C. A.; Griswold, M. D. The key role of vitamin A in spermatogenesis. *J. Clin. Invest.* **2010**, *120*, 956-962.
196. Mark, M.; Ghyselinck, N. B.; Wendling, O.; Dupé, V.; Mascrez, B.; Kastner, P.; Chambon, P. A genetic dissection of the retinoid signalling pathway in the mouse. *Proc. Nutr. Soc.* **1999**, *58*, 609-613.
197. Allenby, G.; Bocquel, M. T.; Saunders, M.; Kazmer, S.; Speck, J.; Rosenberger, M.; Lovey, A.; Kastner, P.; Grippo, J. F.; Chambon, P.; et al. Retinoic acid receptors and retinoid X receptors: interactions with endogenous retinoic acids. *Proc. Natl. Acad. Sci. U. S. A.* **1993**, *90*, 30-34.
198. Wolgemuth, D.; Chung, S. Retinoid signaling during spermatogenesis as revealed by genetic and metabolic manipulations of retinoic acid receptor alpha. *Soc. Reprod. Fertil. Suppl.* **2007**, *63*, 11.

199. Duester, G. Alcohol dehydrogenase as a critical mediator of retinoic acid synthesis from vitamin A in the mouse embryo. *J. Nutr.* **1998**, *128*, 459S-462S.
200. Kerr, J.; Loveland, K.; O'bryan, M.; De Kretser, D. Cytology of the testis and intrinsic control mechanisms. In *Knobil and Neill's Physiology of Reproduction*, Plant, T. M.; Zeleznik, A. J., Eds. **2006**; *Vol. 1*, 827-947.
201. Chung, S. S.; Wang, X.; Wolgemuth, D. J. Expression of retinoic acid receptor alpha in the germline is essential for proper cellular association and spermiogenesis during spermatogenesis. *Development* **2009**, *136*, 2091-2100.
202. Sommer, A. The continuing challenge of vitamin A deficiency. *Ophthalmic Epidemiol.* **2009**, *16*, 1.
203. Bowles, J.; Koopman, P. Retinoic acid, meiosis and germ cell fate in mammals. *Development* **2007**, *134*, 3401-3411.
204. Lambrot, R.; Coffigny, H.; Pairault, C.; Donnadieu, A.-C.; Frydman, R.; Habert, R.; Rouiller-Fabre, V. Use of organ culture to study the human fetal testis development: effect of retinoic acid. *J. Clin. Endocrinol. Metab.* **2006**, *91*, 2696-2703.
205. Childs, A. J.; Cowan, G.; Kinnell, H. L.; Anderson, R. A.; Saunders, P. T. Retinoic Acid signalling and the control of meiotic entry in the human fetal gonad. *PLoS One* **2011**, *6*, e20249.
206. Chung, S. S.; Cuellar, R. A.; Wang, X.; Reczek, P. R.; Georg, G. I.; Wolgemuth, D. J. Pharmacological activity of retinoic acid receptor alpha-selective antagonists in vitro and in vivo. *ACS Med. Chem. Lett.* **2013**, *4*, 446-450.

207. Chung, S. S.; Wang, X.; Wolgemuth, D. J. Male sterility in mice lacking retinoic acid receptor alpha involves specific abnormalities in spermiogenesis. *Differentiation* **2005**, *73*, 188-198.
208. Chung, S. S.; Wang, X.; Roberts, S. S.; Griffey, S. M.; Reczek, P. R.; Wolgemuth, D. J. Oral administration of a retinoic acid receptor antagonist reversibly inhibits spermatogenesis in mice. *Endocrinology* **2011**, *152*, 2492-2502.
209. Chung, S. S.; Sung, W.; Wang, X.; Wolgemuth, D. J. Retinoic acid receptor alpha is required for synchronization of spermatogenic cycles and its absence results in progressive breakdown of the spermatogenic process. *Dev. Dyn.* **2004**, *230*, 754-766.
210. Hogarth, C. A.; Amory, J. K.; Griswold, M. D. Inhibiting vitamin A metabolism as an approach to male contraception. *Trends Endocrinol. Metab.* **2011**, *22*, 136-144.
211. Chen, J. Y.; Penco, S.; Ostrowski, J.; Balaguer, P.; Pons, M.; Starrett, J. E.; Reczek, P.; Chambon, P.; Gronemeyer, H. RAR-specific agonist/antagonists which dissociate transactivation and AP1 transrepression inhibit anchorage-independent cell proliferation. *EMBO J.* **1995**, *14*, 1187-1197.
212. Schulze, G. E.; Clay, R. J.; Mezza, L. E.; Bregman, C. L.; Buroker, R. A.; Frantz, J. D. BMS-189453, a novel retinoid receptor antagonist, is a potent testicular toxin. *Toxicol. Sci.* **2001**, *59*, 297-308.
213. Martinez, C.; Lieb, M.; Alvarez, S.; Rodriguez-Barrios, F.; Alvarez, R.; Khanwalkar, H.; Gronemeyer, H.; de Lera, A. R. Dual RXR Agonists and RAR Antagonists Based on the Stilbene Retinoid Scaffold. *ACS Med. Chem. Lett.* **2014**, *5*, 533-537.

214. Cerep. Partition Coefficient - Log D. In Cerep, Ed. Cerep: [http://www.cerep.fr/cerep/users/pages/downloads/Documents/Marketing/Pharmacology & ADME/Application notes/2013/Partition coefficient-LogD.pdf](http://www.cerep.fr/cerep/users/pages/downloads/Documents/Marketing/Pharmacology&ADME/Application%20notes/2013/Partition%20coefficient-LogD.pdf), **2013**.
215. Altucci, L.; Leibowitz, M. D.; Ogilvie, K. M.; De Lera, A. R.; Gronemeyer, H. RAR and RXR modulation in cancer and metabolic disease. *Nat. Rev. Drug Discovery* **2007**, *6*, 793-810.
216. Patani, G. A.; LaVoie, E. J. Bioisosterism: a rational approach in drug design. *Chem. Rev.* **1996**, *96*, 3147-3176.
217. Sun, S.; Zhang, Z.; Kodumuru, V.; Pokrovskaja, N.; Fonarev, J.; Jia, Q.; Leung, P.-Y.; Tran, J.; Ratkay, L. G.; McLaren, D. G. Systematic evaluation of amide bioisosteres leading to the discovery of novel and potent thiazolyimidazolidinone inhibitors of SCD1 for the treatment of metabolic diseases. *Biorg. Med. Chem. Lett.* **2014**, *24*, 520-525.
218. Jiang, L.; Lu, X.; Zhang, H.; Jiang, Y.; Ma, D. CuI/4-Hydro-L-proline as a More Effective Catalytic System for Coupling of Aryl Bromides with N-Boc Hydrazine and Aqueous Ammonia. *J. Org. Chem.* **2009**, *74*, 4542-4546.
219. Lennox, A. J.; Lloyd-Jones, G. C. Selection of boron reagents for Suzuki–Miyaura coupling. *Chem. Soc. Rev.* **2014**, *43*, 412-443.
220. Kagechika, H.; Himi, T.; Kawachi, E.; Shudo, K. Retinobenzoic acids. 4. Conformation of aromatic amides with retinoidal activity. Importance of trans-amide structure for the activity. *J. Med. Chem.* **1989**, *32*, 2292-2296.
221. Müller, S.; Liepold, B.; Roth, G. J.; Bestmann, H. J. An improved one-pot procedure for the synthesis of alkynes from aldehydes. *Synlett* **1996**, *1996*, 521-522.

222. Han, W.; Jin, F.; Zhou, Q. Ligand-Free Palladium-Catalyzed Hydroxycarbonylation of Aryl Halides under Ambient Conditions: Synthesis of Aromatic Carboxylic Acids and Aromatic Esters. *Synthesis* **2015**, *47*, 1861-1868.
223. Bourguet, W.; Vivat, V.; Wurtz, J. M.; Chambon, P.; Gronemeyer, H.; Moras, D. Crystal structure of a heterodimeric complex of RAR and RXR ligand-binding domains. *Mol. Cell* **2000**, *5*, 289-298.
224. Alvarez, S.; Khanwalkar, H.; Alvarez, R.; Erb, C.; Martínez, C.; Rodríguez-Barrios, F.; Germain, P.; Gronemeyer, H.; de Lera, A. R. C3 halogen and c8'' substituents on stilbene arotinoids modulate retinoic acid receptor subtype function. *ChemMedChem* **2009**, *4*, 1630-1640.
225. Andersen, J.; Madsen, U.; Björkling, F.; Liang, X. Rapid synthesis of aryl azides from aryl halides under mild conditions. *Synlett* **2005**, *2005*, 2209-2213.
226. Shen, A.; Hu, Y.-C.; Liu, T.-T.; Ni, C.; Luo, Y.; Cao, Y.-C. Supporting ligand-assisted N-heterocyclic carbene palladium complexes: characterization, computation, and catalytic activity in Suzuki–Miyaura cross coupling between aryl and heteroaromatic chlorides and various boronic acids. *Tetrahedron Lett.* **2016**, *57*, 2055-2058.
227. Gore, V. K.; Ma, V. V.; Yin, R.; Ligutti, J.; Immke, D.; Doherty, E. M.; Norman, M. H. Structure–activity relationship (SAR) investigations of tetrahydroquinolines as BKCa agonists. *Biorg. Med. Chem. Lett.* **2010**, *20*, 3573-3578.
228. Berman, A. M.; Bergman, R. G.; Ellman, J. A. Rh (I)-Catalyzed Direct Arylation of Azines. *J. Org. Chem.* **2010**, *75*, 7863-7868.

229. Somenzi, G.; Sala, G.; Rossetti, S.; Ren, M.; Ghidoni, R.; Sacchi, N. Disruption of retinoic acid receptor alpha reveals the growth promoter face of retinoic acid. *PLoS One* **2007**, *2*, e836.
230. Zewge, D.; Chen, C.-y.; Deer, C.; Dormer, P. G.; Hughes, D. L. A mild and efficient synthesis of 4-quinolones and quinolone heterocycles. *J. Org. Chem.* **2007**, *72*, 4276-4279.
231. Sanders, C. R. *Biomolecular Ligand-Receptor Binding Studies: Theory, Practice, and Analysis*; Vanderbilt University: **2010**; 1-42.
232. INDIGOBiosciences. Human Retinoic Acid Receptor Reporter Assays. In *Biosciences*, I., Ed. INDIGO Biosciences: State College, PA.
233. INDIGOBiosciences. Assay Kit Platform & Formats.
<http://indigobiosciences.com/assay-kit-platform-formats/>

